

**EGE UNIVERSITY GRADUATE SCHOOL OF
NATURAL AND APPLIED SCIENCE**

(PhD THESIS)

**PREPARATION AND APPLICATIONS OF MODIFIED
ELECTRODES WITH REDOX MEDIATORS FOR
PHOTOELECTROCATALYTIC SYSTEMS**

Didem GİRAY DİLGİN

Supervisor: Prof. Dr. H. İsmet GÖKÇEL

Department of Chemistry

Scientific Department Code: 405.03.01

Presentation Date: 17.02.2014

Bornova - İZMİR

2014

Didem GİRAY DİLGİN tarafından **Doktora** tezi olarak sunulan “**Preparation and Applications of Modified Electrodes with Redox Mediators for Photoelectrocatalytic Systems** ” başlıklı bu çalışma E.Ü. Lisansüstü Eğitim ve Öğretim Yönetmeliği ile E.Ü. Fen Bilimleri Enstitüsü Eğitim ve Öğretim Yönergesi'nin ilgili hükümleri uyarınca tarafımızdan değerlendirilerek savunmaya değer bulunmuş ve 17.02.2014 tarihinde yapılan tez savunma sınavında aday oybirliği ile başarılı bulunmuştur.

Jüri Üyeleri:

İmza

Jüri Başkanı : Prof. Dr. H. İsmet GÖKÇEL

Raportör Üye : Prof. Dr. Zekerya DURSUN

Üye : Prof. Dr. F. Nil ERTAŞ

Üye : Prof. Dr. Nuri NAKİBOĞLU

Üye : Doç. Dr. Şenol ALPAT

ÖZET**FOTOELEKTROKATALİTİK SİSTEMLER İÇİN REDOKS
MEDİYATÖRLERİYLE MODİFİYE ELEKTROTLARIN
HAZIRLANMASI VE UYGULAMALARI**

GİRAY DİLGİN, Didem

Doktora Tezi, Kimya Anabilim Dalı
Tez Danışmanı: Prof. Dr. H. İsmet GÖKÇEL
Şubat 2014, 156 sayfa

Bu çalışmada hematoksilin (HT), metilen yeşili (MY), nötral kırmızısı (NK) ve meldola mavisi (Mm) olmak üzere 4 farklı redoks mediyatörüyle elektropolimerizasyon yöntemi kullanılarak hazırlanan ve elektrokimyasal davranışları incelenen modifiye camımsı karbon elektrotlarla (glassy carbon electrode, GCE) elektrokimyasal ve fotoelektrokimyasal sensörlere yönelik çalışmalar gerçekleştirilmiştir. Elektrot yüzeyinin ışıklandırılmasının NADH'nin elektrokatalitik yükseltgenmesine ve NAD^+/NADH redoks çifti-dehidrogenaz enzimine bağlı glukoz biyosensörüne etkisi hem döngüsel voltametri ve amperometri için geleneksel voltammetrik hücrede hem de akışa enjeksiyon analiz (Flow Injection Analysis, FIA) sistemi için akış geçişli fotoelektrokimyasal hücrede gerçekleştirilmiştir. Mm hariç, diğer modifiye elektrotlar, NADH'nin elektrokatalitik yükseltgenmesine iyi yanıt vermiştir. Işıksız ortamla karşılaştırıldığında, ışık altında NADH'nin elektrokatalitik yükseltgenme akımı yaklaşık iki kat artmıştır. Bu çalışmanın en önemli kısmı PAMAM-glukoz dehidrogenaz (GDH) tutturulmuş poli-HT/GCE kullanılarak glukoz için fotoelektrokimyasal biyosensör tasarlamaktır. Işıksız ortamla karşılaştırıldığında, duyarlık ve belirtme alt sınırı (limit of detection, LOD) sırasıyla yaklaşık 2,5 ve 2 kat artmıştır. FIA sisteminde ışıksız ortamda doğrusal aralık 1×10^{-5} M ile 1×10^{-3} M arasında, duyarlık $0,76 \mu\text{A mM}^{-1}$ ve LOD $3,0 \mu\text{M}$ dır. Işıklılandırılmadan sonra ise doğrusal aralık 5×10^{-6} M ile 1×10^{-3} M arasında, duyarlık $1,90 \mu\text{A mM}^{-1}$ ve LOD $1,5 \mu\text{M}$ olarak bulunmuştur. Bu tezdten elde edilen sonuçların gelecekte bu konu üzerine yapılacak çalışmalara bir temel oluşturacağı sonucuna varılmıştır.

Anahtar sözcükler: Fotoelektrokimyasal sensör, biyosensör, akışa enjeksiyon analizi, hematoksilin, NADH, glukoz, elektrokatalitik ve fotoelektrokatalitik yükseltgenme, elektropolimerizasyon, glukoz dehidrogenaz.

ABSTRACT

**PREPARATION AND APPLICATIONS OF MODIFIED
ELECTRODES WITH REDOX MEDIATORS FOR
PHOTOELECTROCATALYTIC SYSTEMS**

GİRAY DİLGİN, Didem

PhD in Chemistry
Supervisor: Prof. Dr. H. İsmet GÖKÇEL
February, 2014, 156 pages

In this thesis, modified glassy carbon electrodes (GCE) were prepared by electropolymerization of four different redox mediators (hematoxylin (HT) methylene green (MG), neutral red (NR) and meldola blue (MdB)) and investigated their electrochemical behavior. The studies on electrochemical and photoelectrochemical sensors were performed using these modified electrodes. The effect of irradiation of electrode surface on the electrocatalytic oxidation of NADH, and biosensing of glucose dependent on NAD^+/NADH redox couple-dehydrogenase enzyme was investigated by using both traditional voltammetric cell for cyclic voltammetry and amperometry and photo electrochemical cell for flow injection analysis (FIA) system. Apart from MdB, the other modified electrodes have a good response towards electrocatalytic oxidation of NADH. The peak current NADH with irradiation at these modified electrodes increased about two times compared with the reaction without irradiation. An important part of this study is the construction of photoelectrochemical biosensor for glucose using PAMAM-Glucose dehydrogenase (GDH) immobilized poly-HT/GCE which shows best response to electrocatalysis of NADH. Compared with the reaction without irradiation, the sensitivity and the detection limit increased around 2.5 and 2.0 folds, respectively. The linear range was from 1×10^{-5} M to 1×10^{-3} M with the sensitivity of $0.76 \mu\text{A mM}^{-1}$ and a detection limit of $3.0 \mu\text{M}$ without irradiation in FIA system. After the irradiation, the linear range was from 5×10^{-6} M to 1×10^{-3} M with the sensitivity of $1.90 \mu\text{A mM}^{-1}$ and a detection limit of $1.5 \mu\text{M}$. It was concluded that the results obtained from this thesis will provide a basis on this topic for future studies.

Keywords: Photoelectrochemical sensor, biosensor, flow injection analysis, hematoxylin, NADH, glucose, electrocatalytic and photoelectrocatalytic oxidation, electropolymerization, glucose dehydrogenase.

ACKNOWLEDGEMENT

I would like to present my sincere gratitude to my supervisor Prof. Dr. H. İsmet GÖKÇEL, for her kind supervision and great contributions the whole study. I am very thankful to Prof Dr. F. Nil ERTAŞ and Prof. Dr. Nuri NAKİBOĞLU, members of PhD thesis committee for their valuable suggestions during my studies.

I also thank to all of the members of the Chemistry Department and especially to the members of Analytical Chemistry Division of Science Faculty, Ege University for providing the conditions and support throughout my studies. I would like to thank to my friends who have encouraged and helped me throughout my work.

I would like to thank PhD student Bensu ERTEK, MS student Özlem SAĞLAM from Çanakkale Onsekiz Mart University and Dr. İpek ÜRKMEZ from Ege University for their continuous support and encouragement.

A part of this study was supported by the Scientific and Technological Research Council of Turkey (TUBITAK). I acknowledge TUBITAK (Project No. 107T572) and The National Authority for Scientific Research of Romania ANCS (Project no. 75CB/18.07.2008) for financial support. I would like to thank to project members, Prof. Dr. Yusuf DİLGİN (supervisor in Turkey), Prof. Dr. Zekerya DURSUN (researcher), Prof. Dr. H. İsmet GÖKÇEL (researcher) and Dr. Delia Maira GLIGOR (supervisor in Romania) for their valuable contributions. I also thank to Biga Vocational College and Department of Chemistry, Science and Art Faculty, Çanakkale Onsekiz Mart University.

Finally, I would like to thank and present my gratitude to my family and especially my dear husband Prof. Dr. Yusuf DİLGİN, my dear son Arda DİLGİN, my father, my mother, my sister for their encouragement, understanding, support and patience during the study.

Didem GİRAY DİLGİN

2014, İZMİR

CONTENTS

	<u>Page</u>
ÖZET.....	v
ABSTRACT.....	vii
ACKNOWLEDGEMENT.....	ix
LIST OF FIGURES.....	xv
LIST OF TABLES.....	xxvii
LIST OF SYMBOLS AND ABBREVIATIONS.....	xxviii
1. INTRODUCTION.....	1
1.1. Chemically Modified Electrodes (CMEs).....	5
1.1.1. Preparation methods for modified electrodes.....	7
1.2. Pyridine Dinucleotides (NAD(P)H and NAD(P) ⁺).....	11
1.2.1. Physical and chemical properties.....	11
1.2.2. The role of NAD ⁺ /NADH in living system.....	14
1.2.3. Electrocatalytic oxidation of NADH.....	16
1.3. Construction of Biosensor Dependent on Dehydrogenase Enzyme and NAD ⁺ /NADH Redox Couple.....	28
1.4. Photoelectrochemistry and Photoelectrochemical Sensors.....	33
1.5. Flow Injection Analysis System.....	36

CONTENTS (continued)

	<u>Page</u>
1.6. Cyclic Voltammetry.....	39
1.7. Chronoamperometry.....	41
1.8. The Importance of Thesis.....	43
2. MATERIALS AND METHODS.....	44
2.1. Apparatus.....	44
2.2. Reagents and Solutions.....	46
2.2.1. Chemicals.....	46
2.2.2. Preparation of Solutions.....	46
2.3. Procedures.....	49
2.3.1. Preparation of modified electrodes.....	49
2.3.2. Characterization of modified electrodes.....	53
2.3.3. Electrocatalytic and photoelectrocatalytic oxidation of NADH using modified electrodes.....	53
2.3.4. Flow injection analysis procedure.....	54
2.3.5. Construction of biosensor and photoelectrochemical biosensor.....	55
3. RESULTS AND DISCUSSION.....	59

CONTENTS (continued)

	<u>Page</u>
3.1. Preparation of Modified Electrodes and Their Response towards	
Oxidation of NADH.....	59
3.1.1. Poly-Hematoxylin modified glassy carbon electrode (Poly-HT/GCE).....	59
3.1.2. Poly-Methylene Green modified glassy carbon electrode	
(Poly-MG/GCE).....	66
3.1.3. Poly-Neutral Red modified glassy carbon electrode (Poly-NR/GCE).....	71
3.1.4. Poly-Meldola Blue modified glassy carbon electrode (Poly-MdB/GCE)....	77
3.2. Electrochemical Characterization of Prepared Modified Electrodes.....	78
3.2.1. Electrochemical behaviour of poly-HT/GCE.....	78
3.2.2. Electrochemical behaviour of poly-MG/GCE.....	80
3.2.3. Electrochemical behaviour of poly-NR/GCE.....	82
3.3. Photoelectrocatalytic Studies.....	83
3.3.1. Photoelectrocatalytic oxidation of NADH using poly-HT/GCE.....	83
3.3.2. Photoelectrocatalytic oxidation of NADH using poly-MG/GCE.....	87
3.3.3. Photoelectrocatalytic oxidation of NADH using poly-NR/GCE.....	90
3.4. Photoelectrocatalytic Studies in Flow Injection Analysis System.....	93
3.4.1. Photoamperometric detection of NADH using poly-HT/GCE in FIA.....	93

CONTENTS (continued)

	<u>Page</u>
3.4.2. Photoamperometric detection of NADH using poly-MG/GCE in FIA.....	98
3.5. Biosensor and Photoelectrochemical Biosensor Studies.....	103
3.5.1. Cyclic voltammetric studies.....	103
3.5.2. Amperometric studies in FIA system.....	110
4. CONCLUSION.....	118
REFERENCES.....	125
CIRRICULUM VITAE.....	151
APPENDICES.....	

LIST OF FIGURES

<u>Figure</u>	<u>Page</u>
1.1. Schematic representation for the oxidation reaction of $A \rightarrow B$ on bare (A) and mediated conditions (B, C); NHE normal hydrogen electrode (Zen et al., 2003).....	7
1.2. Schematic presentation for various kinds of CME preparation routes (Zen et al., 2003).....	8
1.3. Chemical structure of NAD^+ and $NADP^+$	12
1.4. The Redox reaction of NAD^+	13
1.5. UV-Vis adsorption spectra of NAD^+ and $NADH$	13
1.6. Enzymatic reaction of malic acid (Gözükara, 2001).....	15
1.7. Schematic illustration of the hydride-acceptor and -donor pyridine nucleotide moiety proposed ECE-mechanism (Radoi and Compagnone, 2009).....	17
1.8. Oxidation of $NADH$ by a homogenous mediator (Simon and Bartlett, 2003)	19
1.9. Oxidation of $NADH$ at a modified electrode (Simon and Bartlett, 2003).....	20
1.10. Reaction scheme for an amperometric ethanol biosensor based on the use of alcohol dehydrogenase enzyme (Yang and Liu, 2009).....	30
1.11. A representation of photoelectrochemical biosensor for glucose (Deng et al., 2008).....	36
1.12. General description of FIA (GlobalFIA, 2013).....	37

LIST OF FIGURES (continued)

<u>Figure</u>	<u>Page</u>
1.13. Schematic diagram of a typical FIA manifold (top) its components (bottom) P is a pump, C and R are carrier and reagent lines respectively, S is sample injection, MC's are mixing coils, D is a flow through detector, and W is the waste line (McKelvie, 1999).....	38
1.14. Chronoamperometric method: (a) potential–time waveform; (b) change in concentration profiles as time progresses; (c) the resulting current–time response (Wang, 2006).....	42
2.1. A) Electrochemical cell with three electrode system WE: working electrode (GCE or modified GCE), CE: counter electrode (Pt wire), RE: reference electrode (Ag/AgCl (sat. KCl). B) Home-made photoelectrochemical cell (Dilgin, 2004).....	45
2.2. A) Schematic diagram of the FIA manifold, C: carrier stream, P: peristaltic pump, S: sampling valve, L: light source, W: waste, R: recorder, WE: working electrode, AE: auxiliary electrode, RE: reference electrode. B) Schematic diagram of photoelectrochemical flow cell, T: Teflon block, L: light source, TT: transmission tube, QW: quartz window (Dilgin, 2004) and C) Its images in different perspectives....	45
2.3. Schematic representation of enzyme immobilization procedure.....	56
2.4. Schematic representation of the photoelectrochemical biosensor.....	57

LIST OF FIGURES (continued)

<u>Figure</u>	<u>Page</u>
3.1. Repetitive cyclic voltammograms (10 cycles) of 0.3 mM HT at GCE in 0.1 M PBS with pH 7.0 (A) and pH 2.0 (C) containing 0.1 M NaNO ₃ at 100 mVs ⁻¹ , in the potential range of -0.5 to +2.0 V vs. Ag/AgCl. B) and D) Cyclic voltammograms of poly-HT/GCE obtained from A and C respectively, in the absence (a) and in the presence (b) of 0.8 mM NADH c) the cyclic voltammograms of 0.8 mM NADH at bare GCE. Supporting electrolyte: 0.1 M PBS (pH 7.0); scan rate: 50 mVs ⁻¹	60
3.2. The effect of A) pH of supporting electrolyte B) anodic potential limit C) monomer concentration, and D) cycle number during the preparation of modified electrodes on the electrocatalytic oxidation of 0.8 mM NADH.....	62
3.3. Repetitive cyclic voltammograms (10 cycles) of 0.3 mM HT at GCE in 0.1 M PBS (pH 7.0) containing 0.1 M NaNO ₃ at 100 mVs ⁻¹ in the potential range A) of -0.5 to 1.0 V and C) of -0.5 to 1.75 V. B) and D) Cyclic voltammograms of a poly-HT/GCE obtained from A and C, respectively, in the absence (a) and in the presence (b) of 0.8 mM NADH, (c) cyclic voltammogram of 0.8 mM NADH at a bare GCE. Supporting electrolyte: 0.1 M PBS (pH 7.0); scan rate: 50 mVs ⁻¹	63
3.4. Electropolymerization mechanism of HT.....	66
3.5. Repetitive cyclic voltammograms (10 cycles) of 0.5 mM MG at GCE in 0.1 M H ₃ PO ₄ (A), and 0.1 M phosphate solutions with pH 7.0 (C) and pH 10.0 (E) containing 0.1 M NaNO ₃ at 100 mVs ⁻¹ , in the range of -0.7 to +1.1 V vs. Ag/AgCl. B), D) and F) Cyclic voltammograms of poly-MG/GCE obtained from A, C and E respectively, in the absence (a) and in the presence (b) of 0.4 mM NADH c) the cyclic voltammograms of 0.4 mM NADH at bare GCE. Supporting electrolyte: 0.1 M PBS (pH 7.0); scan rate: 50 mVs ⁻¹	67

LIST OF FIGURES (continued)

<u>Figure</u>	<u>Page</u>
3.6. The effect of A) pH of supporting electrolyte B) anodic potential limit C) monomer concentration and D) cycle number during the preparation of modified electrodes on the electrocatalytic oxidation of 0.4 mM NADH.....	69
3.7. Repetitive cyclic voltammograms (10 cycles) of 0.5 mM MG at GCE in 0.1 M H ₃ PO ₄ + 0.1 M NaNO ₃ at 100 mVs ⁻¹ in the range of A) -0.7 to 0.6 V and C) -0.7 to 1.6 V. B) and D): Cyclic voltammograms of a poly-MG/GCE obtained from A and C, respectively, in the absence (a) and in the presence (b) of 0.4 mM NADH, (c) cyclic voltammogram of 0.4 mM NADH at a bare GCE. Supporting electrolyte: 0.1 M PBS (pH 7.0) scan rate: 50 mVs ⁻¹	70
3.8. Electropolymerization mechanism of MG (Barsan et al., 2008).....	71
3.9. Repetitive cyclic voltammograms (10 cycles) of 0.05 mM NR at GCE in 0.1 M H ₂ SO ₄ (A) and 0.1 M phosphate solutions with pH 4.0 (C) and pH 7.0 (E) containing 0.1 M NaNO ₃ at 100 mVs ⁻¹ , in the range of -0.7 to +1.2 V vs. Ag/AgCl. B), D) and F) Cyclic voltammograms of poly-NR/GCE obtained from A, B and C respectively, in the absence (a) and in the presence (b) of 0.4 mM NADH c) the cyclic voltammograms of 0.4 mM NADH at bare GCE. Supporting electrolyte: 0.1 M PBS (pH 7.0) scan rate: 50 mVs ⁻¹	73
3.10. The effect of A) pH of supporting electrolyte B) anodic potential limit C) monomer concentration and D) cycle number during the preparation of modified electrodes on the electrocatalytic oxidation of 0.4 mM NADH.....	74

LIST OF FIGURES (continued)

<u>Figure</u>	<u>Page</u>
3.11. Repetitive cyclic voltammograms (10 cycles) of 0.01 mM NR at GCE in 0.1 M H ₂ SO ₄ + 0.1 M NaNO ₃ at 100 mVs ⁻¹ in the range of A) -0.6 to 0.6 V and C) -0.6 to 1.6 V B) and D) Cyclic voltammograms of a poly-NR/GCE obtained from A and C, respectively, in the absence (a) and in the presence (b) of 0.4 mM NADH, (c) cyclic voltammogram of 0.4 mM NADH at a bare GCE. Supporting electrolyte: 0.1 M PBS (pH 7.0); scan rate: 50 mVs ⁻¹	76
3.12. A) Repetitive cyclic voltammograms (10 cycles) of 0.01 mM MdB at GCE in 0.1 M phosphate solution with pH 10 containing 0.1 M NaNO ₃ at 100 mVs ⁻¹ , in the range of -0.7 to + 1.2 V vs. Ag/AgCl. B) Cyclic voltammograms of poly-MdB/GCE obtained from A in the absence (a) and in the presence (b) of 0.4 mM NADH c) the cyclic voltammograms of 0.4 mM NADH at bare GCE. Supporting electrolyte: 0.1 M PBS (pH 7.0); scan rate: 50 mVs ⁻¹	78
3.13. A) Cyclic voltammograms of poly-HT/GCE in 0.1 M PBS (pH 7.0) at a scan rates of 50, 100, 160, 200, 400, 640, 800, 1280, 1600, 2560, 3200 mVs ⁻¹ . B) The plot of the anodic (<i>i</i> _{pa}) and cathodic (<i>i</i> _{pc}) peak currents versus the scan rates for redox couple II. C) The plot of formal potential versus pH which was calculated from cyclic voltammograms of poly-HT/GCE recorded at 50 mVs ⁻¹ in the potential range of -0.8 to +0.8 V vs. Ag/AgCl. D) Repetitive cyclic voltammograms of poly-HT/GCE with 300 cycles in 0.1 M PBS (pH 7.0) at scan rate of 50 mVs ⁻¹	80

LIST OF FIGURES (continued)

<u>Figure</u>	<u>Page</u>
3.14. A) Cyclic voltammograms of poly-MG/GCE in 0.1 M PBS (pH 7.0) at a scan rates of I: 20, 50, 100, 160, 200, 400, 640; II: 800, 1280, 1600, 2560, 3200, 5120, 6400 mVs ⁻¹ B) The plot of the anodic (<i>i_{pa}</i>) and cathodic (<i>i_{pc}</i>) peak currents versus the scan rates for redox couple II. C) The plot of formal potential versus pH which was calculated from cyclic voltammograms of poly-MG/GCE recorded at 50 mVs ⁻¹ in the potential range of -0.8 to +0.8 V vs. Ag/AgCl. D) Repetitive cyclic voltammograms of poly-MG/GCE with 250 cycles in 0.1 M PBS (pH 7.0) at scan rate of 50 mVs ⁻¹	81
3.15. A) Cyclic voltammograms of poly-NR/GCE in 0.1 M PBS (pH 7.0) at a scan rates of I: 20, 50, 100, 160, 200, 400, 640; II: 800, 1280, 1600, 2560, 3200, 5120, 6400 mVs ⁻¹ . B) The plot of the anodic (<i>i_{pa}</i>) and cathodic (<i>i_{pc}</i>) peak currents versus the scan rates for redox couple II. C) The plot of formal potential versus pH which was calculated from cyclic voltammograms of poly-NR/GCE recorded at 50 mVs ⁻¹ in the potential range of -0.8 to +0.8 V vs Ag/AgCl. D) Repetitive cyclic voltammograms of poly-NR/GCE with 200 cycles in 0.1 M PBS (pH 7.0) at scan rate of 50 mVs ⁻¹	82
3.16. Cyclic voltammograms of poly-HT/GCE in the absence (a, b) and in the presence (c, d) of 0.8 mM NADH without (a, c) and with (b, d) irradiation of the electrode surface (in 0.1 M PBS (pH 7.0) scan rate: 50 mVs ⁻¹). c ₁ and d ₁ : first cycle; c ₂ and d ₂ : second cycle.....	84
3.17. A) The plot of current for 0.2 mM NADH versus applied potential and B) the plot of current response versus the concentration of NADH at +150 mV applied potential in 0.1 M PBS (pH 7.0) using bare GCE with/without irradiation conditions.....	86

LIST OF FIGURES (continued)

<u>Figure</u>	<u>Page</u>
3.18. A) The plot of electrocatalytic and photoelectrocatalytic current for 0.2 mM NADH versus applied potential, B) Current versus time curve of a poly-HT/GCE in the absence (a, b) and in the presence (c, d) of 0.2 mM NADH without (a, c) and with (b, d) irradiation of the electrode surface in 0.1 M PBS (pH 7.0). Applied potential: +200 mV C) Plot of electrocatalytic and photoelectrocatalytic current response vs. the concentration of NADH at +200 mV applied potential in 0.1 M PBS (pH 7.0) using poly-HT/GCE.....	87
3.19. Cyclic voltammograms of a poly-MG/GCE in the absence (a, b) and in the presence (c, d) of 0.4 mM NADH without (a, c) and with (b, d) irradiation of the electrode surface. Supporting electrolyte: 0.1 M PBS (pH 7.0); scan rate: 50 mVs ⁻¹	88
3.20. A) The plot of electrocatalytic and photoelectrocatalytic current for 0.2 mM NADH versus applied potential, B) Current versus time curve of a poly-MG/GCE in the absence (a, b) and in the presence (c, d) of 0.2 mM NADH without (a, c) and with (b, d) irradiation of the electrode surface in 0.1 M PBS (pH 7.0). Applied potential: +100 mV C) Plot of electrocatalytic and photoelectrocatalytic current response vs. the concentration of NADH at +100 mV applied potential in 0.1 M PBS (pH 7.0) using polyMG/GCE.....	89
3.21. Cyclic voltammograms of a poly-NR/GCE in the absence (a, b) and in the presence (c, d) of 0.4 mM NADH without (a, c) and with (b, d) irradiation of the electrode surface. Supporting electrolyte: 0.1 M PBS (pH 7.0); scan rate: 50 mVs ⁻¹	91

LIST OF FIGURES (continued)

<u>Figure</u>	<u>Page</u>
3.22. A) Plot of electrocatalytic and photoelectrocatalytic current for 0.2 mM NADH versus applied potential, B) Current versus time curve of a poly-NR/GCE in the absence (a, b) and in the presence (c, d) of 0.2 mM NADH without (a, c) and with (b, d) irradiation of the electrode surface in 0.1 M PBS (pH 7.0). Applied potential: +150 mV C) Plot of electrocatalytic and photoelectrocatalytic current response vs. the concentration of NADH at +150 mV applied potential in 0.1 M PBS (pH 7.0) using poly-NR/GCE.....	92
3.23. The fiagrams of 0.1 mM NADH at various applied potential using Poly-HT/GCE.....	94
3.24. The fiagrams of 0.1 mM NADH at various applied potential using bare GCE.....	95
3.25. The effect of applied potential on a) amperometric and b) photoamperometric peak currents obtained fiagrams using bare GCE and c) amperometric and d) photoamperometric peak currents obtained fiagrams using poly-HT/GCE. Injected: 0.1 mM NADH solution.....	95
3.26. The effect of flow rate on a) amperometric, and b) photoamperometric peak currents of 0.1 mM NADH obtained fiagrams using poly-HT/GCE.....	96
3.27. Current- time curves of NADH with different concentrations a) 10 b) 40 c)100 d) 400 e) 1000 μ M NADH using poly-HT/GCE in FIA system (Carrier stream: 0.1 M PBS (pH 7.0) containing 0.1 M KCl, Applied potential: +300 mV; Flow rate: 1.3 mL min ⁻¹ , sample loop: 100 μ L; transmission tubing length: 10 cm).....	97

LIST OF FIGURES (continued)

<u>Figure</u>	<u>Page</u>
3.28. Dependence of the catalytic currents on NADH concentration for a) amperometric and b) photoamperometric analysis of NADH using poly-HT/GCE in FIA system. (Carrier stream: 0.1 M PBS (pH 7.0) containing 0.1 M KCl, applied potential: +300 mV; flow rate: 1.3 mLmin ⁻¹ ; sample loop: 100 μL; transmission tubing length: 10 cm	98
3.29. The fiagrams of 0.1 mM NADH at various applied potential using poly-MG/GCE.....	99
3.30. The effect of applied potential on a) amperometric and b) photoamperometric peak currents obtained fiagrams using poly-MG/GCE. Injected: 0.1 mM NADH solution.....	100
3.31. The effect of flow rate on a) amperometric b) photoamperometric peak currents of 0.1 mM NADH obtained fiagrams using poly-MG/GCE.....	101
3.32. Current- time curves of NADH with different concentrations a) 10 b) 50 c)100 d) 500 e) 1000 μM NADH using poly-MG/GCE in FIA system (Carrier stream: 0.1 M PBS (pH 7.0) containing 0.1 M KCl, Applied potential: +150 mV; Flow rate: 1.3 mL min ⁻¹ , sample loop: 100 μL; transmission tubing length: 10 cm).....	102
3.33. Dependence of the catalytic currents on NADH concentration for a) amperometric and b) photoamperometric analysis of NADH using poly-MG/GCE in FIA system. (Carrier stream: 0.1 M PBS (pH 7.0) containing 0.1 M KCl, applied potential: +150 mV; flow rate: 1.3 mLmin ⁻¹ ; sample loop: 100 μL; transmission tubing length: 10 cm....	103

LIST OF FIGURES (continued)

<u>Figure</u>	<u>Page</u>
3.34. Cyclic voltammograms of GDH/GCE in the presence of 10 mM NAD ⁺ and a) in the absence, b) in the presence of 10 mM glucose without irradiation and c) b with irradiation. Supporting electrolyte: 0.1 M PBS (pH 7.0) scan rate: 5 mVs ⁻¹	104
3.35. Cyclic voltammograms of GDH/PAMAM/GCE in the presence of 10 mM NAD ⁺ and a) in the absence, b) in the presence of 10 mM glucose without irradiation and c) b with irradiation. Supporting electrolyte: 0.1 M PBS (pH 7.0) scan rate: 5 mVs ⁻¹	104
3.36. Cyclic voltammograms of GDH/poly-HT/PAMAM/GCE, which obtained from electropolymerization of HT on PAMAM/GCE using 10,cycles, in the presence of 10 mM NAD ⁺ and 10 mM glucose without irradiation (1) and with irradiation (2) at various scan rates A) 5 B) 10, C) 20 and D)50 mV s ⁻¹ . Supporting electrolyte: 0.1 M PBS (pH 7.0).....	106
3.37. Cyclic voltammograms of GDH/poly-HT/PAMAM/GCE, which obtained from electropolymerization of HT on PAMAM/GCE using 10, 20 and 30 cycles, in the presence of 10 mM NAD ⁺ and 10 mM glucose without (1) and with (2) irradiation. Supporting electrolyte: 0.1 M PBS (pH 7.0); scan rate: 5 mVs ⁻¹	106
3.38. Repetitive cyclic voltammograms (20 cycles) of 0.3 mM HT at GCE in 0.1 M PBS (pH 7.0) containing 0.1 M NaNO ₃ at 100 mVs ⁻¹ , in the range of -0.5 to + 2.1 V vs. Ag/AgCl.....	107
3.39. Repetitive cyclic voltammograms (20 cycles) of 0.3 mM HT at PAMAM/GCE in 0.1 M PBS (pH 7.0) containing 0.1 M NaNO ₃ at 100 mVs ⁻¹ , in the range of -0.5 to + 2.1 V vs. Ag/AgCl.....	107

LIST OF FIGURES (continued)

<u>Figure</u>	<u>Page</u>
3.40. Cyclic voltammograms of GDH/poly-HT/GCE in the presence of 10 mM NAD ⁺ and a) in the absence, b) in the presence of 10 mM glucose without irradiation and c) b with irradiation. Supporting electrolyte: 0.1 M PBS (pH 7.0); scan rate: 5 mVs ⁻¹	108
3.41. Cyclic voltammograms of GDH/poly-HT/PAMAM/GCE in the presence of 10 mM NAD ⁺ and a) in the absence, b) in the presence of 10 mM glucose without irradiation and c) b with irradiation. Supporting electrolyte: 0.1 M PBS (pH 7.0); scan rate: 5 mVs ⁻¹	108
3.42. Current-time curves of 0.8 mM glucose containing 10 mM NAD ⁺ at various applied potential using GDH/Poly-HT/PAMAM/GCE. (Carrier stream: 0.1 M PBS (pH 7.0) containnig 0.1 M KCl; flow rate: 1.1 mL min ⁻¹ ; sample loop:100 μL; tubing length:10 cm).....	110
3.43. The effect of applied potential on ■) amperometric and ●) photoamperometric peak currents obtained fiagrams using GDH/Poly-HT/PAMAM/GCE. Injected: 0.8 mM glucose containing 10 mM NAD ⁺	111
3.44. The fiagrams of 0.8 mM glucose containing 10 mM NAD ⁺ at various flow rate using GDH/Poly-HT/PAMAM/GCE. (Carrier stream: 0.1 M PBS (pH 7.0) containnig 0.1 M KCl; applied potential: 300 mV; sample loop: 100 μL; tubing length: 10 cm).....	112
3.45. The effect of flow rate on ■) amperometric and ●) photoamperometric peak currents obtained fiagrams using GDH/Poly-HT/PAMAM/GCE. Injected: 0.8 mM glucose containing 10 mM NAD ⁺	112

LIST OF FIGURES (continued)

<u>Figure</u>	<u>Page</u>
3.46. Current-time curves of glucose with different concentrations in the range from 0.005 mM to 10 mM glucose containing 10 mM NAD ⁺ using GDH/Poly-HT/PAMAM/GCE in FIA system (Carrier stream: 0.1 M PBS (pH 7.0) containing 0.1 M KCl, Applied potential: +300 mV; Flow rate: 0.125 mL min ⁻¹ , sample loop: 100 μL; transmission tubing length: 10 cm).....	113
3.47. Current- time curves of glucose with various concentrations containing 10 mM NAD ⁺ using GDH/PAMAM/GCE in FIA system (Carrier stream: 0.1 M PBS (pH 7.0) containing 0.1 M KCl, applied potential: +300 mV; flow rate: 0.125 mL min ⁻¹ , sample loop: 100 μL; transmission tubing length: 10 cm).....	114
3.48. A) Dependence of the catalytic currents on glucose concentration B) calibration curve for ■) amperometric and ●) photoamperometric analysis of glucose using GDH/Poly-HT/PAMAM/GCE in FIA system. (Carrier stream: 0.1 M PBS (pH 7.0) containing 0.1 M KCl, applied potential: +300 mV; flow rate: 0.125 mL min ⁻¹ ; sample loop: 100 μL; transmission tubing length: 10 cm)	115
3.49. Repeat injections of 3x10 ⁻⁴ and 1x10 ⁻³ M glucose using the proposed biosensor with and without irradiation (Carrier stream: 0.1 M PBS (pH 7.0) containing 0.1 M KCl, applied potential: +300 mV; flow rate: 0.125 mL min ⁻¹ ; sample loop: 100 μL; transmission tubing length: 10 cm).....	116
3.50. Electrochemical biosensing of 3x10 ⁻⁴ M glucose (a) in the presence of 3x10 ⁻⁴ M fructose (b), galactose (c), saccharose (d); 3x10 ⁻² M fructose (e), galactose (f), saccharose (g) and 3x10 ⁻⁴ M ascorbic acid (h), dopamine (i), uric acid (j) and L.cystein (k) (Carrier stream: 0.1 M PBS (pH 7.0) containing 0.1 M KCl, applied potential: +300 mV; flow rate: 0.125 mL min ⁻¹ ; sample loop: 100 μL; transmission tubing length: 10 cm).....	117

LIST OF TABLES

<u>Table</u>	<u>Page</u>
1.1. Electrode modification schemes (Murray et al., 1987).....	8
1.2. Studies on electrocatalytic oxidation of NADH using CME prepared with widely used redox mediators.....	22
1.3. Some studies on biosensor dependent on NADH and dehydrogenase enzymes.....	31
2.1. Optimized parameters for electropolymerization of each mediator.....	52
3.1. Equations obtained from current-scan rate and formal potential-pH curves.....	119
3.2. Analytical characteristics of modified electrodes for amperometric and photoamperometric determination of NADH.....	120
3.3. Analytical characteristics of poly-HT/GCE and poly-MG/GCE for amperometric and photoamperometric detection of NADH in FIA system.....	121
3.4. Comparison of analytical parameters obtained from GDH/poly-HT/PAMAM/GCE with different electrodes in the literature for electrochemical biosensing of glucose dependent on NAD ⁺ /NADH redox couple and dehydrogenase enzyme.....	123

LIST OF SYMBOLS AND ABBREVIATIONS

<u>Symbols</u>	<u>Explanation</u>
A	Surface area of the electrode
d	Density
D	Diffusion coefficient
E^0	Standard electrode potential for the redox couple
E_p	Peak potential
E_{pa}	Anodic peak potential
E_{pc}	Cathodic peak potential
F	Faraday constant
i_p	Peak current
i_{pa}	Anodic peak current
i_{pc}	Cathodic peak current
k	Rate constant
M	Molar
mL	Mililiter
<i>mM</i>	<i>milimolar</i>
mV	Milivolt
MW	Molecular weight

n	Number of electrons transferred
nm	Nanometer
s	Standard deviation
T	The absolute temperature
t	Time
V	Volt
W	Watt
α	Charge transfer coefficient
η	Overpotential
v	Scan rate
μA	Microamper
μL	Microliter
μM	Micromolar

Abbreviations

AA	Ascorbic Acid
ADH	Alcohol Dehydrogenase
ADP	Adenosine Diphosphate
Al-HCl	Allylamine Hydrochloride
Amp	Amperometry

An	Aniline
AP	Aminophenol
ATP	Adenosine Triphosphate
Au NPs	Gold nanoparticles
AzA	Azure A
AzB	Azure B
BCB	Brilliant Cresyl Blue
BPG	Basal Plane Graphite
BQ	Benzoquinone
BSA	Bovine Serum Albumin
CA	Chlorogenic acid
CFA	Caffeic acid
CMEs	Chemically Modified Electrodes
CMT	Coumestan
CNTP	Carbon nanotube paste
CPE	Carbon paste electrode
CT	Catechol (1-2 dihydroxybenzene)
CTC	Catechin
CV	Cyclic Voltammetry

DA	Dopamine
DHB	Dihydroxybenzaldehyde ()
DMTD	6,7-dihydroxy-3-methyl-9-thia-4,4a-diazafluoren-2-one
DNA	Deoxyribonucleic Acid
DP	Detection potential
DPV	Differential Puls Voltammetry
ECE	Electrode-Chemical-Electrode
FAD	Flavin Adenine Dinucleotide
FePhenTPy	5-[2,5-di (thiophen-2-yl)-1H-pyrrol-1-yl]-1,10-phenanthroline iron(III) chloride
FIA	Flow Injection Analysis
FMN	Flavin Mononucleotide
FT	Fisetin
G	Graphite
GA	Glutaraldehyde
GCE	Glassy carbon electrode
GDH	Glucose Dehydrogenase
GIDH	Glutamate Dehydrogenase
GSH	Glutathione
GSSG	Glutathione Disulfide

H ⁻	Hydride ion
H ⁺	Proton
HT	Hematoxylin
IL	Ionic liquid
ITO	Indium Tin Oxide
IUPAC	International Union of Pure and Applied Chemistry
L-Cyst	L-Cysteine
LDH	Lactate Dehydrogenase
LOD	Limit of Detection
LOQ	Limit of Quantification
LR	Linearity Range
MB	Methylene Blue
MdB	Meldola Blue
<i>Med</i> _{ox}	Oxidized Mediator
<i>Med</i> _{red}	Redox Mediator
MG	Methylene
MMT	Metacrylate
MWCNT	Multi-Walled Carbon Nanotube
NAD ⁺	Nicotinamide adenine dinucleotide

NADP ⁺	Nicotinamide adenine dinucleotide phosphate
NB	Nile Blue
NFR	Nitrofluorenone
NHE	Normal hydrogen electrode
NQ	Naphtoquinone
NR	Neutral Red
OPG	Ordinary pyrolytic graphite
PAMAM	Poly(amidoamin)
PBS	Phosphate Buffer Solution
PEC	Photoelectrochemistry
Phnt	1,10-phenanthroline-5,6-dione
Poly-HT	Poly-Hematoxylin
Poly-MB	Poly-Methylene Blue
Poly-MdB	Poly-Meldola Blue
Poly-MG	Poly-Methylene Green
Poly-NR	Poly-Neutral Red
Poly-TB	Poly-Toluidine Blue
PPF	Plasmon polymerized film
Py	Pyrole
QT	Quercetin

RDE	Rotating Disc Electrode
RF	Radio frequency
RSD	Relative Standard Deviation
RT	Rutin
S	Substrate
SCE	Saturated Calomel Electrode
SH ₂	Reduced form of substrate
SPCE	Screen printed carbon electrode
SPE	Screen printed electrode
SPGE	Screen printed graphite electrode
SWCNT	Single-Walled Carbon Nanotube
TB	Toluidine Blue
Th	Thionine
ThP	Thiophen
TTP	Tryptophan
UA	Uric Acid
UV	Ultraviolet
VC	Vitreous Carbon
Xa	Xanthurenic acid
ZrP	Zirconium Phosphate

1. INTRODUCTION

One of the most interesting areas of electrochemistry is to develop new electrochemical sensors and biosensors with higher sensitivity, selectivity and stability, as well as being fast and low-cost. Chemically Modified Electrodes (CMEs) have attracted considerable attention in the development of new electrochemical sensors and biosensors, because CMEs offer advantages such as high sensitivity, selectivity, reduced interference effect, preconcentration of target species, etc. (Mousty, 2004, 2010; Yogeswaran and Chen, 2008; Zen et al., 2003; Walcarius, 1999, 1998; Cox et al., 1996; Gorton, 1995; Wring and Hart, 1992). In combination with CMEs, electrochemical techniques can also be turned into important applications in electrosynthetic organic chemistry, material characterization, fuel cells, etc. Moreover, one of the distinguishing features of CMEs is their application to electroanalysis because of their own electrocatalytic properties and/or their capabilities to immobilize electrocatalytic or biocatalytic reagents (enzymes) that improve the sensitivity and selectivity of the detection step (Zen et al., 2003; Mousty, 2004).

An important application area of CMEs is investigation of electrocatalytic oxidation of Reduced Dihydronicotinamide adenine dinucleotide (NADH) and construction of biosensors for some biologically important compounds that depend on NAD^+/NADH redox couple and dehydrogenase enzymes (Gorton and Dominguez, 2002a; 2002b; Simon and Bartlett, 2003; Kumar and Chen, 2008; Radoi and Compagnone, 2009; Lobo et al., 1997; Katakis and Dominguez, 1997). The pyridine nucleotides, NAD^+ (nicotinamide adenine dinucleotide) and NADP^+ (nicotinamide adenine dinucleotide phosphate), are ubiquitous in all living systems as they are required for the reactions of more than 400 oxido-reductase denoted dehydrogenases (250 of these depend on NAD^+ and around 150 on NADP^+) (Gorton and Dominguez, 2002a). In addition, the redox turnover of NAD^+/NADH coupled has been extensively used for the construction of electrochemical biosensors for many biologically important molecules based on dehydrogenase enzymes (Katakis and Dominguez, 1997; Yan et al., 2007). The biosensing of molecules using dehydrogenases requires a highly sensitive NADH transducer, because the transformed signal of the biosensor is based on the detection of enzymatically generated NADH. NAD^+/NADH redox couple is also useful for the development of biofuel cells with cheap fuels. NAD^+ -dependent dehydrogenases in biofuel cells allow the use of various fuels such as

carbohydrates and alcohols (Yan et al., 2007; Miyake et al., 2009). Therefore, electrochemical oxidation of NADH has received considerable attention due to the important functions mentioned above.

However, the oxidation of NADH at bare electrodes takes place at high overvoltage ranging from 450 to 1100 mV depending on the material of the electrode. It was early recognized that the reaction is highly irreversible and suffers from interference from other oxidizable species at such high potentials. For concentrations higher than 0.1 mM NADH, the reaction also involves radical intermediates resulting in electrode fouling and passivation of the electrode surface which causes poor sensitivity, poor selectivity and unstable analytical signals. As a result, it can be said that the major product NAD^+ is an inhibitor of the direct electrode process. (Florou et al., 1998; Gorton and Dominguez, 2002a; 2002b; Moiroux and Elving, 1978; Jaegfeldt, 1980; Blaedel and Jenkins, 1975; Simon and Bartlett, 2003).

In order to overcome these problems, modification of the electrode surface with redox mediators has been extensively used. Various modified electrodes have been prepared with many redox mediators such as azine type dyes (phenothiazine, phenoxazine, phenazine), quinolic compounds (flavonoids, phenolic acids, catecholic compounds), nitrofluorenones, flavine and adenine derivatives, some transition metal complexes and some conducting polymers (Gorton and Dominguez, 2002a; 2002b; Simon and Bartlett, 2003; Katakis and Dominguez, 1997; Kumar and Chen, 2008). These mediators have been modified onto various electrode surfaces such as glassy carbon (GC), carbon paste (CP), ordered mesoporous carbon (OMC), carbon nanotube (CNT), graphite (G), pencil graphite (PG), carbon films with ordered cylindrical, gold (Au), platinum (Pt), gold nanoparticle (Au NPs) and nanocomposite electrodes and then successfully used for the electrocatalytic oxidation of NADH. These modified electrodes have also been used for the construction of electrochemical biosensors for many biologically important molecules based on dehydrogenase enzymes (Katakis and Dominguez, 1997; Yan et al., 2007; Li et al., 2013a; Aydogdu et al., 2013; Meredith et al., 2012; Al-Jawadi et al., 2012; Liu et al., 2010; Yang and Liu, 2009; Meng et al., 2009; Arvinte et al., 2008; Manesh et al., 2008; Dai et al., 2008; Ricci et al., 2007; Bartlett et al., 2002). The substrate detection dependent on dehydrogenases requires a highly sensitive NADH detection, because the obtained signal of the biosensor is based on the detection of enzymatically generated NADH.

Recently, many scientists have focused on photoelectrochemical sensors, which are a newly developed analytical device based on the photoelectrochemical properties of electrode or mediators. Because the combination of CMEs and photoelectrochemistry exhibits more sensitive results than that of CMEs without irradiation electrode surface. Poly-Toluidine Blue (poly-TB) (Dilgin et al., 2007), poly-Methylene Blue (poly-MB) (Dilgin et al., 2011), poly-Hematoxylin (Poly-HT), (Dilgin Giray et al., 2010) poly-Neutral Red (Poly-NR) (Dilgin Giray et al., 2011) modified glassy carbon electrodes (GCE), a new polymeric phenothiazine modified graphite electrode (Gligor et al., 2009), Graphene-TiO₂ nanohybrids modified GCE (Wang et al., 2012a), Dopamine/nanoporous TiO₂ modified Indium Tin Oxide (ITO) electrode (Wang, et al., 2009a), and poly(4,4' diaminodiphenyl sulfone)/nanoTiO₂ composite film ITO electrode (Ho et al., 2011) have been used for the photoelectrocatalytic oxidation of NADH. In these studies, a significant enhancement in the current for the oxidation of NADH was observed when the working electrode surface was irradiated by a light source. In addition, a photoelectrochemical glucose biosensor based on NAD⁺/NADH redox couple and glucose dehydrogenase enzyme has been constructed by using the Quantum dot modified Au electrode (Schubert et al., 2010) and Thionine (Th) cross-linked multi-walled carbon nanotubes (MWNTs) and Au nanoparticles (Au NPs) multilayer functionalized ITO electrode (Deng et al., 2008). Photoelectrochemistry has been used not only for the electrocatalytic oxidation of NADH and biosensors that depend on NAD⁺/NADH redox couple but also for the electrocatalytic oxidation of ascorbic acid (Cooper et al., 1998, 1999; Dilgin et al., 2003, 2005, 2006), sulphide (Dilgin, et al., 2012a), detection of some pesticides (Wang, et al., 2013a; Shi et al., 2011; Gong et al., 2012), DNA biosensor (Liang et al., 2006; Zhang et al., 2012) and construction of biosensors dependent on oxidase enzymes (Sun et al., 2009; Zheng et al., 2011; Wang et al., 2012b; Ren et al. 2009). All of these studies showed that the sensitivity of a photoelectrochemical sensor was better than an electrochemical sensor. As a result, photoelectrochemistry has been widely used in electrochemical sensors and biosensors with higher sensitivity.

Another useful approach in electrochemical sensors and biosensors is the usage of Flow Injection Analysis (FIA) with CMEs in electrochemical techniques (Hansen, 1996; Van Staden and Van Staden, 2012; Wang, et al., 1991; Mayer and Ruzicka, 1996). Because FIA has some advantages for routine analytical determinations such as very limited sample consumption, short analysis time based on a transient signal measurement in a flow-through detector, and an on-line

carrying out difficult operations of separation, physicochemical conversion of analyses into detectable species (Parikh et al., 2010). Electrocatalytic oxidation of NADH and biosensors that depend on NAD^+/NADH redox couple-dehydrogenase enzymes has also been investigated in FIA with redox mediator-modified electrodes (Baskar et al., 2012; Dilgin et al., 2011; Hasebe et al., 2011; Chen et al., 2004; Sha et al., 2004; Gao et al., 2003, 2004; Piano et al., 2010a, 2010b; Lobo et al., 1996a, 1996b; Prieto-Simon et al., 2007; Ramirez-Molina et al., 2003; Florou et al., 1998; Jaraba et al., 1998; De Lucca et al., 2002).

It is concluded that the combination of CMEs, photoelectrochemistry and FIA can be useful for electrocatalytic oxidation of NADH and biosensor dependent on NAD^+/NADH redox couple-dehydrogenase enzyme. When we take into consideration the advantages of this combination, the developed photoelectrochemical sensor and biosensor offers advantages such as i) good selectivity (CMEs have good selectivity properties), ii) good sensitivity (the sensitivity of photoelectrochemical sensors is generally better than electrochemical sensors), and iii) fast and economical analysis (FIA exhibits fast analysis and lower cost due to less consumption of reactive). Therefore, in order to construct more sensitive, selective and fast electrochemical sensors and biosensors, an investigation on photoelectrocatalytic oxidation of NADH and the construction of the glucose biosensor dependent on NAD^+/NADH redox couple-glucose dehydrogenase enzyme in the FIA system have been proposed in this thesis. As presented below, this thesis was planned as a four-stage

1. Preparation of CMEs: Electropolymerization of some redox mediators (HT, NR, Methylene Green (MG), Meldola Blue (MdB) onto GCE.
2. Characterization of modified electrodes: The recording cyclic voltammograms dependent on scan rate and supporting electrolyte pH.
3. Electrocatalytic and photoelectrocatalytic oxidation of NADH:
 - a. With cyclic voltammetry
 - b. With chronoamperometry
 - c. With amperometry in FIA system
4. Construction of photoelectrochemical biosensor: Glucose biosensor has been proposed as a model.

Although the photoelectrocatalytic oxidation of NADH (Dilgin et al., 2007, 2011; Dilgin Giray, et al., 2010, 2011; Wang et al., 2012a; Wang, et al., 2009a; Ho et al., 2011) and photoelectrochemical biosensor dependent on NAD^+/NADH

redox couple-dehydrogenase enzymes (Deng et al., 2008; Schubert et al., 2009) has been reported, these have been performed in the FIA system for the first time in this thesis (Dilgin Giray et al., 2010) and our a previous study (Dilgin et al., 2011).

In the following section, information on CMEs, pyridine dinucleotides, biosensors, photoelectrochemistry and photoelectrochemical sensors, FIA, and some electroanalytical techniques used in this thesis will be presented together with previous published studies.

1.1. Chemically Modified Electrodes (CMEs)

Electrochemical methods offer increased degrees of accuracy and detection limits, often involving dramatically lower costs than other techniques. Therefore, electrochemical methods have found wide applications in analysis, construction of sensors, organic and inorganic synthesis, etc. C, Au, Hg and Pt were used as electrode materials until the mid 1970's. However, there is fouling at these bare electrodes by unwanted precipitation or adsorption processes which cause low sensitivity and slow electrochemical reaction rates in some species. In order to overcome these problems, modifications of the electrode surface have been used in the electroanalysis. In general, the modification aims to effect: (i) transport properties to the electrode surface (barriers to exclude interferants, means of preconcentrating the analyte, e.g. ion exchange); (ii) chemical reactions at the electrode surface (e.g. preconcentration reactions by attaching ligands, enzyme reactions); (iii) electron transfer properties (electrocatalysts to improve electron transfer) (Smyth and Vos, 1992).

CMEs were defined by IUPAC recommendations in 1997 as “an electrode made of a conducting or semiconducting material that is coated with a selective monomolecular, ionic or polymeric film of a chemical modifier and that by means of faradaic reactions or interfacial potential differences (no net charge transfer) exhibits chemical, electrochemical and/or optical properties of the film” (IUPAC, 1997).

Study of CMEs was initiated in the mid-1970s and it was achieved the covalently binding of several ligands (amine, pyridine, and ethylenediamine) onto the surface of a SnO₂ electrode via silanization reaction (Moses et al., 1975).

This pioneering work was the starting point for the development of an extraordinarily wide area of research which is still continuously growing in various fields of chemistry (Walcarius, 1998). The interest in modified electrodes has increased day by day. Some studies on modified electrodes and their applications in electroanalysis have been reported in review articles (Gorton, 1995; Gilmartin and Hart, 1995; Navratilova and Kula, 2003; Walcarius, 1998, 1999; Mousty, 2004, 2010; Zen et al., 2003). The numerous important applications of CMEs have been found for example, solar energy conversion and storage, selective electro-organic synthesis, molecular electronics, electrochromic display devices, corrosion protection, and electroanalysis. Because CMEs provide some useful approaches in the electroanalysis, which were summarized by Murray (Murray et al., 1987) as five main ideas: electrocatalysis, preconcentration, membrane barriers, electroreleasing and microstructure.

An important and distinguishing feature of CMEs is electrocatalysis of the electrode reaction of analytically desired substrate. It is often observed that the electrode kinetics of an analyte at a bare electrode surface are slow, so that oxidation or reduction occurs at a potential that is much more positive or negative, respectively, than the expected thermodynamic potential (i.e., an activation overpotential (η) exists) (Murray et al., 1987). A schematic representation of an electrocatalytic process at a CME with decrease in η was given in Figure 1.1 (Zen et al., 2003). The reversible redox mediator P/Q with a standard potential of $E_{P/Q}^0$ was modified on a functionalized electrode to promote the irreversible oxidation reaction of $A \rightarrow B^+ + e^-$. A relatively high η was observed at a bare electrode while in the presence of P/Q the reaction was promoted by redox mediation at $E_{P/Q}^0$ with a low η . This type of heterogeneous CMEs is not only selective and sensitive but also fast and reusable in analytical measurements (Zen et al., 2003). There are three important characteristics of mediated electrocatalysis. Firstly, the catalyzed reaction occurs near the formal potential of the mediator catalyst couple (P/Q) unless a catalyst-substrate (S) adduct is formed, in which case reaction occurs at the potential for the adduct. Secondly, the mediator catalyst and substrate formal potentials should be similar. Because this lowers the P + S reaction free energy, however, the choice is also subject to maintaining a satisfactorily fast reaction rate. Finally, a successfully catalyzed reaction of S occurs at less negative or positive potential for reduction or oxidation, respectively, than the bare electrode reaction of S would require (Murray et al., 1987).

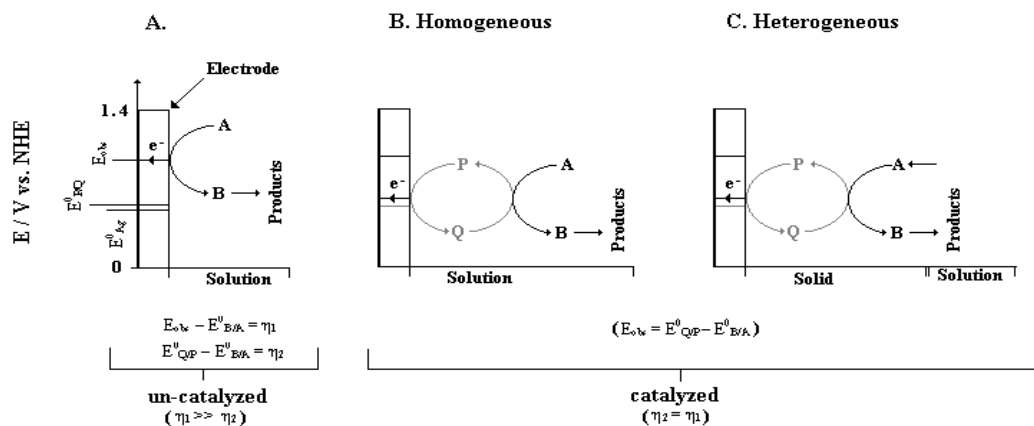


Figure 1.1. Schematic representation for the oxidation reaction of $A \rightarrow B$ on bare (A) and mediated conditions (B, C); NHE normal hydrogen electrode (Zen et al., 2003).

The terms P and Q correspond to the reversible mediator of reduced and oxidized states, respectively. The E_{obs} , $E_{P/Q}^0$, $E_{A/B}^0$ and η correspond to uncatalyzed, P/Q mediated, standard and over potentials, respectively, for the above mentioned reaction. In homogenous catalyzed reaction, the P/Q mediator and reactant are in solution phase; while for heterogeneous catalyzed reaction, the P/Q is bonded on the electrode surface (Zen et al., 2003).

Another wide application of CMEs is the preconcentration of trace analytes. In trace analysis, general stripping techniques were used. CMEs preconcentrate the analyte into a small volume on the electrode surface during the accumulation process, which allows lower concentrations to be measured than possible in the absence of preconcentrated step (Mousty, 2004).

Electroanalytical applications of modified electrodes are mostly based on achieving a certain degree of selectivity, which can then be coupled with the high sensitivity achievable from instrumental analysis. This selectivity can be obtained by either an analyte specific preconcentration effect or by selecting the properties of the layer so as to catalyse a specific reaction (Smyth and Vos, 1992). Therefore, two important features of CMEs (preconcentration and electrocatalysis) improve sensitivity and selectivity of a detection step.

1.1.1. Preparation methods for modified electrodes

Preparation methods of CMEs are classified into four main categories, depending on the nature of the modifying process (Murray et al., 1987). These procedures are defined as: i) sorption, ii) covalent attachment, iii) polymer film

coatings, iv) heterogeneous multimolecular (Table 1.1). In addition, a schematic representation of preparation methods of CMEs was proposed by Zen et al. (2003) and is given in Figure 1.2.

Table 1.1. Electrode modification schemes (Murray et al., 1987).

Monomolecular layers Chemisorption of reagent On platinum surface On carbon surface On mercury surface Au surface
Formation of covalent bond between electrode and electroactive reagent At metal oxide surfaces At carbon surfaces At semiconductors Of electroinactive, chiral substances
Multimolecular layers, polymer film coatings on electrodes Redox polymers Ion exchange-electrostatically trapped Electronically conducting polymers Ionically conducting polymers Crown ether or complexing agent Electroinactive chiral polymers
Heterogeneous multimolecular layers Modifying agent mixed with carbon paste Clay modified Zeolite modified Electroactive particles in electroinactive polymer

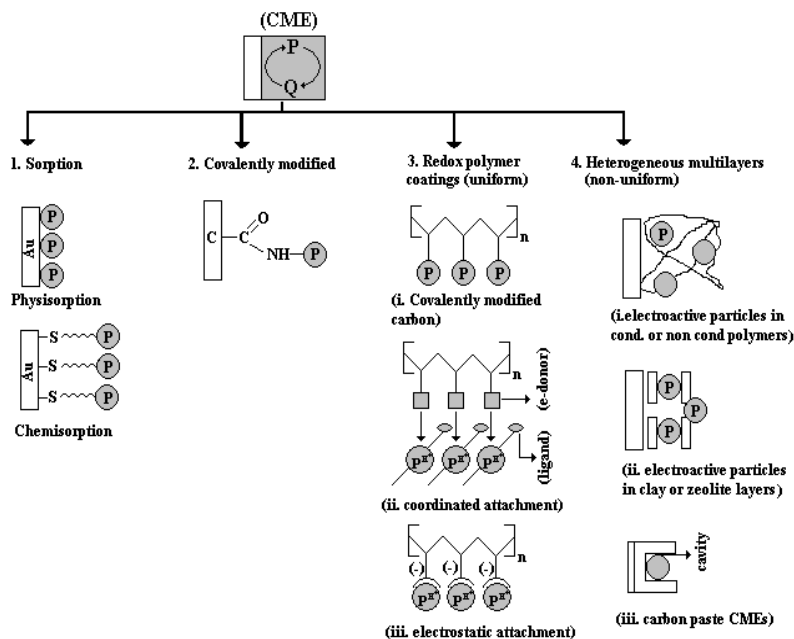


Figure 1.2. Schematic presentation for various kinds of CME preparation routes (Zen et al., 2003).

1.1.1.1. Sorption based CMEs

The earliest attachment research involved irreversibly adsorbing monolayers or submonolayers of electroactive reagents onto the electrode material. This procedure was first reported by Lane and Hubbard (1973). They showed the existence of Pt-C bonds when olefins are adsorbed onto Pt. The adsorption processes can be physisorption or chemisorption. To prepare sorption based CMEs, pure organic or organometallic complexes can be physisorbed on porous carbon bases like Vitreous Carbon (VC), graphite (G), ordinary pyrolytic graphite (OPG) and basal plane graphite (BPG) by simple coating with nonaqueous solution followed by droplet evaporation. Even though the physisorbed systems are useful for analytical applications, stability is always a critical problem for such electrodes. The stability problem, however, can be solved by a chemisorbed route (Zen, et al., 2003). This process gives a thin film, which is strongly and irreversibly adsorbed onto the electrode surface and usually yields a monolayer. In the usual method, the electrode is simply soaked for a period of time into the solution of the modifier substance. Subsequently the electrode is washed with pure water then the adsorption occurrence is controlled using voltammetry. Although this electrode modification seems to be easy and simple, it has some drawbacks. The most important drawback is that electroinactive components competing for the adsorption sites of the electrode surface can influence the electrode processes (Dursun and Nişli, 2001).

1.1.1.2. Covalently bonded CMEs

Covalent modification of the electrode surface, using a specific functional group, is also of particular interest in the preparation of CME. Covalent binding leads to a maximum of monolayer coverage of the electrode surface as in adsorptive electrode modification. This approach offers substantial synthetic diversity and has been extensively developed for attaching monomolecular and multimolecular layers of electroactive substances to semiconductor, metal oxide and carbon electrodes (Murray et al., 1987). There are two kinds of covalent bonds, silanization and direct bonding. Silanization is historically the first surface modifying technique to be utilized. It involves formation of surface hydroxyl or oxide groups, which react with trialkoxy or trichlorosilanes to form one to three bonds to the underlying electrode material. These modification methods typically give rise to monolayer modifications, although the preparation of multilayers is possible (Symth and Vos, 1992). In an alternative approach, surface carboxylic acid

groupings have been generated using a number of approaches, but the most popular include thermal and radio frequency (RF) plasma pretreatment of the electrode surface. Such reactive groups offer useful synthetic pathways for the preparation of CMEs, either directly or after conversion to acid chlorides. The immobilized acid chloride group can be used for condensation with amine groups, thus permitting amine groups containing transition metal complexes such as tetrakis (p-aminophenyl) porphyrins to be attached to the electrode surface. In direct bonding, by exposing the underlying bulk material of carbon and platinum various materials can be directly bound to the electrode surface (Symth and Vos, 1992).

1.1.1.3. Homogeneous multilayer (uniform) CMEs

Homogenous multimolecular layers and polymer film coatings on electrodes are popular nowadays because they are technically easier to apply to electrodes than a covalently bounded monolayer. In addition, they contain up to 10^5 monomolecular layers of electroactive sites so that their electrochemistry is more easily observed (Murray et al., 1987). Polymer films can be deposited on the electrode surface by a variety of methods. These methods can be classified as i) Dip coating; ii) Droplet evaporation; iii) Oxidative or Reductive deposition; iv) Spin coating; v) Binding a monolayer of polymer; vi) Electrochemical polymerization or electropolymerization which refers to the application of electrochemical methods in the cathode or anode during the electropolymerization reaction process; vii) Organosilanes and viii) RF Plasma polymerization.

Among these methods, electropolymerization has found extensive application in constructing simple design, high stable, rapid response and enhanced selectivity sensors. Because, the electropolymerization methods have important advantages over the conventional techniques for the modification and preparation of microelectrodes, permitting the regulation of the spatial location and selective control of the film properties. For example, i) the film thickness and composition can be achieved easily by controlling the electrochemical parameters during the electrochemical process, ii) polymerization can make raw monomer aggregate directly onto the substrate film to avoid the use of a large number of volatile organic solvents to achieve the aim of clean production, iii) selective immobilization of biomolecules in an array of microelectrodes can be implanted in biological tissues for the simultaneous detection of several compounds, iv) minimization arrays, fast responding electrochemical sensors and on-line detection are the developing trend of electropolymerized films in sensor areas (Qin et al., 2011).

The importance of electropolymerization was summarized by Cosnier and Karyakin (2010) as: i) electropolymerization provides simplicity of targeting in the selective modification of multielectrode structures. Indeed, even by exposing the whole structure to the precursor solution, one can target polymer formation on the electrode of interest, applying to it the required current or potential, ii) the electropolymerized films are usually much more stable on electrode surfaces compared to both adsorbed and covalently linked modifiers such as low-molecular-weight organic compounds or chemically synthesized polymers, iii) the electropolymerized materials usually possess some unique properties that are not included in those of the corresponding monomers. These properties mainly concern electroactive polymers, which demonstrate new sets of peaks in cyclic voltammograms due to the appearance of new conjugative chains or modification of the existing ones in their structure (Cosnier and Karyakin, 2010). Electropolymerized modified electrodes were therefore prepared in this thesis due to their useful properties.

1.1.1.4. Composite formation heterogeneous multilayer CMEs

Carbon based electrodes especially modified carbon paste electrode (CPE) are best suited for the determination of compounds in biological fluids. These electrodes show electrocatalytic properties for either the oxidation or reduction of compounds. CPE is a good example for composite electrodes, a mixture of components, mainly electron transfer mediator combined with carbon particles. Carbon paste electrode is one of the convenient matrixes to prepare the CME by simple mixing of graphite/binder paste and redox mediator. Enzymatic clay and zeolite modified electrodes can also be prepared by this procedure (Walcarius, 1998, 1999; Nauratilova and Kula, 2003; Zen et al., 2003).

1.2. Pyridine Dinucleotides (NAD(P)H and NAD(P)⁺)

1.2.1. Physical and chemical properties

NADH is the reduced form of NAD⁺ and NAD⁺ is the oxidized form of NADH. The molecular formula of NADH is C₂₁H₂₇N₇O₁₄P₂ and its molecular weight is about 663.43 g mol⁻¹. Generally, it is widely found in nature and is involved in numerous enzymatic reactions in which it serves as an electron carrier by being alternately oxidized (NAD⁺) and reduced (NADH). NADH like all *dinucleotides* consists of two nucleotides joined by a pair of bridging phosphate groups.

The nucleotides consist of ribose rings, one with adenine attached to the first carbon atom (the 1' position) and the other with nicotinamide at this position. It forms NADP with the addition of a phosphate group to the 2' position of the adenosyl nucleotide through an ester linkage. The structures of NAD^+ and NADP^+ are shown in Figure 1.3. The nicotinamide moiety can be attached in two orientations to this anomeric carbon atom. Because of these two possible structures, the compound exists as two diastereomers. It is the β -nicotinamide diastereomer of NAD^+ that is found in organisms. These nucleotides are joined together by a bridge of two phosphate groups through the 5' carbons (Pollak et al., 2007).

In appearance, all forms of this coenzyme are white amorphous powders that are hygroscopic and highly water-soluble (Windholz, 1983). The solids are stable if stored dry and in the dark. Solutions of NAD^+ are colorless and stable for about a week at 4°C and neutral pH, but decompose rapidly in acids or alkalis. Upon decomposition, they form products that are enzyme inhibitors (Biellmann et al., 1979).

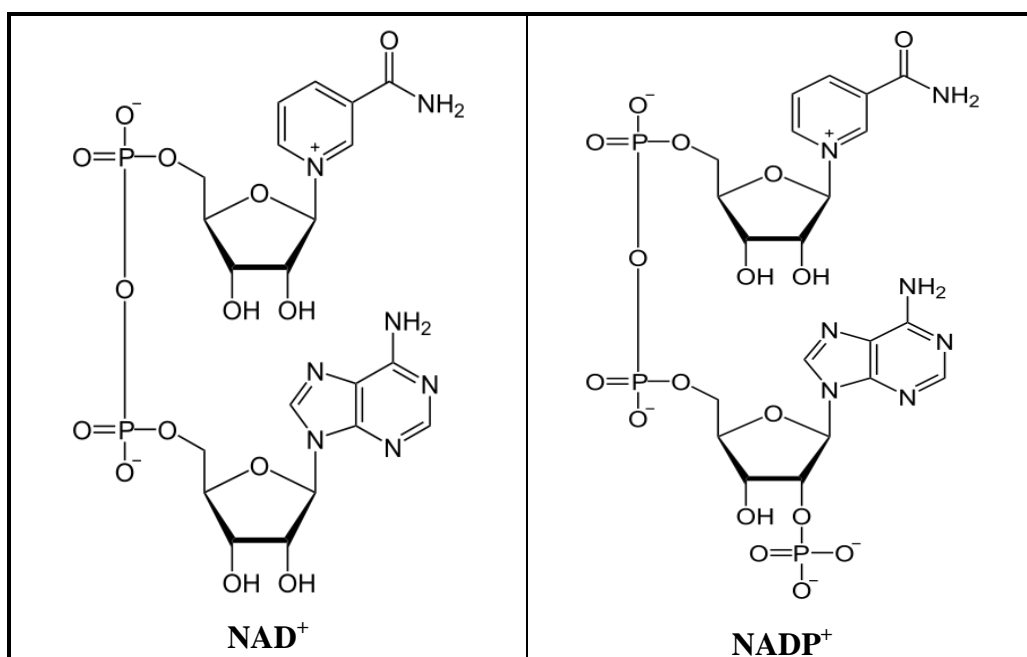


Figure 1.3. Chemical structure of NAD^+ and NADP^+ .

NAD^+ reduces to NADH by receiving 2 electrons and 1 proton. The reduction of NAD^+ is shown in Figure 1.4. From the hydride electron pair, one electron is transferred to the positively charged nitrogen of the nicotinamide ring of NAD^+ , and the second hydrogen atom transferred to the C_4 carbon atom

opposite this nitrogen. The midpoint potential of the NAD^+/NADH redox pair is -0.32 volts, which makes NADH a strong reducing agent (Uden and Bongaerts, 1997). The reaction is easily reversible, when NADH reduces another molecule and is re-oxidized to NAD^+ . This means that the coenzyme can continuously cycle between the NAD^+ and NADH forms without being consumed (Pollak et al., 2007).

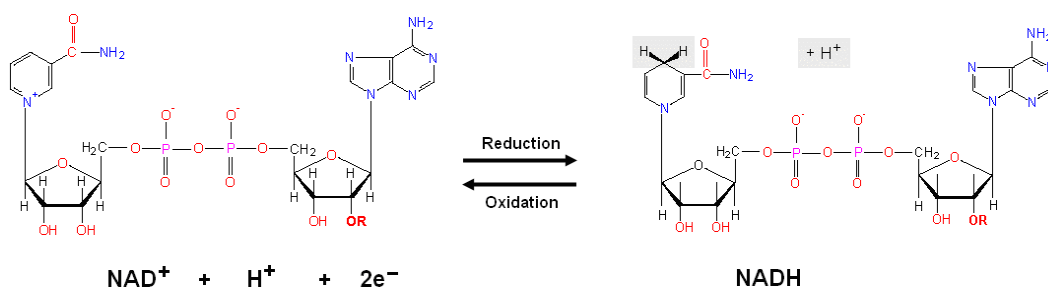


Figure 1.4. The redox reaction of NAD^+ .

When we look at the spectroscopic behavior of this coenzyme, both the oxidized form (NAD^+) and reduced form (NADH) strongly absorb ultraviolet light because of the adenine. For example, peak absorption of NAD^+ is at a wavelength of 259 nm, with an extinction coefficient of $16900 \text{ M}^{-1}\text{cm}^{-1}$. NADH also absorbs at higher wavelengths, with a second peak in UV absorption at 339 nm with an extinction coefficient of $6220 \text{ M}^{-1}\text{cm}^{-1}$ (Dawson, 1985). The spectra of these compounds are shown in Figure 1.5. This difference in the ultraviolet spectra between the oxidized and reduced forms of the coenzymes at higher wavelengths makes it simple to measure the conversion of one to another in enzyme assays – by measuring the amount of UV absorption at 340 nm using a spectrophotometer (Dawson, 1985).

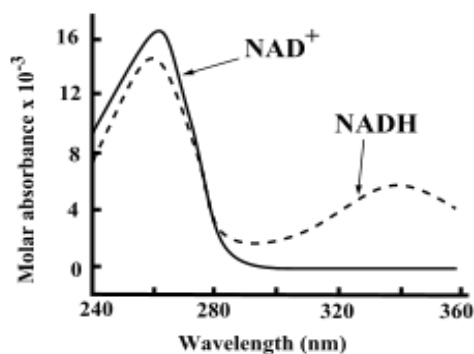


Figure 1.5. UV-Vis adsorption spectra of NAD^+ and NADH.

NAD⁺ and NADH also differ in their fluorescence. NADH in solution has an emission peak at 460 nm and a fluorescence lifetime of 0.4 nanoseconds, while the oxidized form of the coenzyme does not fluoresce (Lakowicz et al., 1992). The properties of the fluorescence signal change when NADH binds to proteins, so these changes can be used to measure dissociation, which are useful in the study of enzyme kinetics (Lakowicz et al., 1992; Jameson et al., 1989). These changes in fluorescence are also used to measure changes in the redox state of living cells, through fluorescence microscopy (Kasimova et al., 2006).

1.2.2. The role of NAD⁺/NADH in living system

Enzymes are powerful catalysts. Many of them can turn over more than 10000 reactant molecules every second. They are also very specific in the type of reaction and they catalyse the reactant molecules (or substrates) with which they react. Redox enzymes (that is, enzymes which catalyze oxidation and reduction reactions) exist to catalyse both simple electron-transfer reactions and the transfer of atoms, or small groups of atoms, to or from a range of substrates. Some redox enzymes need a small molecule, a co-enzyme, in order to be active. The co-enzyme acts as an acceptor, donor of small groups, atoms or electrons and provides the driving force for the reduction, or oxidation, of the substrate (Simon and Bartlett, 2003).

The pyridine nucleotides, NAD⁺ and NADP⁺, are ubiquitous in all living systems as they are required for the reactions of more than 400 oxidoreductase denoted dehydrogenases. This number represents 17% of all classified enzymes and consequently, these nucleotides are responsible for more enzymatic reactions than any other coenzyme (Gorton and Dominguez, 2002a). In metabolism, NAD⁺ is involved in redox reactions, carrying electrons from one reaction to another. The coenzyme is therefore found in two forms in cells: NAD⁺ is an oxidizing agent– it accepts electrons from other molecules and becomes reduced. This reaction forms NADH, which can then be used as a reducing agent to donate electrons. These electron transfer reactions are the main function of NAD⁺ (Pollak et al., 2007; Belenky et al., 2007). Such reactions (summarized in the formula below) involve the removal of two hydrogen atoms from the substrate (S), in the form of a hydride ion (H⁻), and a proton (H⁺). The proton is released into solution, while the reduced form of substrate (SH₂) is oxidized (S) and NAD⁺ reduced to NADH by transfer of the hydride to the nicotinamide ring (Reaction 1.1).



In cells, the $NAD(P)^+/NAD(P)H$ co-enzymes act as electron carriers and participate in oxidation-reduction reactions. Dehydrogenase enzymes are redox enzymes which transfer hydrogen atoms and electrons from a substrate to an electron acceptor, $NAD(P)^+$. Finally, the electron acceptor is reduced by two electrons and one proton, becoming $NAD(P)H$. These molecules can also be considered as hydride carriers (transfer of $2e^-$ and $1H^+$ or H^-).

For example, malic acid turns into oxaloacetic acid in the presence of NAD^+ and the malate dehydrogenase enzyme. In this reaction, the substrate (malic acid) gives two electrons and one hydrogen atom in its second carbon atom to dehydrogenase enzyme which transfers these electrons and hydrogen ion to the electron acceptor (NAD^+). At the end of this reaction, malic acid is oxidized to oxaloacetic acid and NAD^+ reduced to $NADH$ while one hydrogen atom is released to medium. A schematic representation is given in Figure 1.6 for all of these processes (Gözükara, 2001)

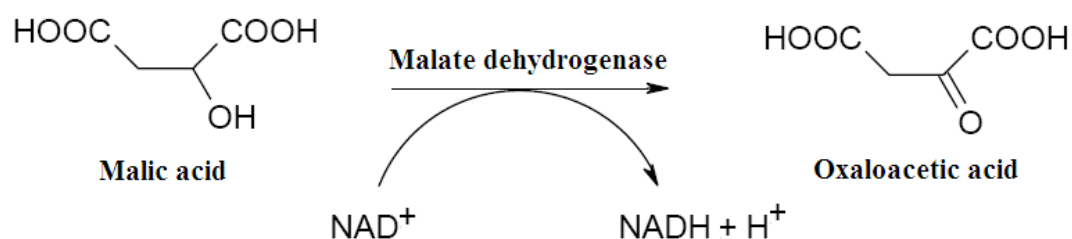


Figure 1.6. Enzymatic reaction of malic acid (Gözükara, 2001).

In organisms, NAD^+ can be synthesized from simple building-blocks (*de novo*) from the amino acids tryptophan or aspartic acid. In an alternative fashion, more complex components of the coenzymes are taken up from food as the vitamin called niacin. Some NAD^+ is also converted into $NADP^+$ the chemistry of this related coenzyme is similar to that of NAD^+ , but it has different roles in metabolism (Belenky, 2007). $NAD(P)H$ works with enzymes that catalyze anabolic reactions, supplying electrons needed to synthesize energy-rich biological molecules. In contrast, $NADH$ plays an important role as an intermediate in the system that generates ATP through the oxidation of foodstuffs (metabolism) in the mitochondria within the cell. Within the mitochondria, 42% of the energy released by the oxidation of foodstuffs is stored in molecules of ATP.

NADH is found in large amounts in mitochondria, where it is essential for the conversion of ADP to ATP. The oxidation of one molecule of NADH by oxygen releases enough energy to synthesize several molecules of ATP from ADP and inorganic phosphate (Simon and Bartlett, 2003). Apart from these important functions, NAD^+/NADH have the following benefits (Forsyth et al., 1999; Birkmayer et al., 2002, 2004; Pelzmann et al., 2003)

- Energy: Increases production of ATP energy.
- Alertness: Improves sense of wakefulness and lessens feelings of fatigue.
- Jet Lag: Improves symptoms of jet lag.
- Mood/Well-being: NADH increases the production of neurotransmitters that influence good mood, such as dopamine and epinephrine.
- Memory/Cognition: NADH indirectly increases the neurotransmitters that positively affect thinking and memory.
- Cellular Health: NADH stimulates the body's DNA repair mechanisms and works as an antioxidant. It refurbishes important body compounds. As one example, when the antioxidant glutathione is spent and oxidized it becomes glutathione disulfide (GSSG). NADH acts as a hydride and refurbishes the compound back into the healthy form of glutathione (GSH).
- Circulation: Increases blood flow to brain, augmenting blood flow in both resting and working tissues.

1.2.3. Electrocatalytic oxidation of NADH

1.2.3.1. Direct electrochemical oxidation of NADH

The electrochemical oxidation of NADH to NAD^+ has received considerable attention due to the important functions aforementioned. Studies on electrochemical oxidation of NADH have been carried out using cyclic voltammetry, chronoamperometry, potentiostatic coulometry and rotating disk electrode methodology. The solid electrodes such as glassy carbon, carbon paste, Pt and Au have been extensively used with this aim. The direct electrochemical oxidation of NADH is highly irreversible with a great overpotential at these bare,

untreated and unmodified classical electrodes. The electrode material has a significant effect on overpotential. The oxidation of NADH in an aqueous solution, seen as a single peak on cyclic voltammogram, takes place at potentials of 0,4; 0,7 and 1,0 V at C, Pt and Au electrodes, respectively (Gorton and Dominguez, 2002a).

The mechanism of the NADH oxidation at the bare electrodes has been proposed with a multi-step ECE mechanism (Figure 1.7 and Reaction 1.2,) (Gorton and Dominguez, 2002a; Radoi and Compagnone, 2009). According to this mechanism, firstly NADH gives one electron and oxidizes to its radicalic form ($\text{NADH}^{\bullet+}$) with an electrochemical reaction; secondly this radicalic form participates in a chemical reaction and converts to neutral radicalic form (NAD^{\bullet}) by giving one proton, finally NAD^{\bullet} gives one electron and oxidizes to NAD^+ with an electrochemical reaction. When oxidizing NADH in aqueous solutions, only a single wave is observed. No waves due to the re-reduction of intermediates have been observed in cyclic voltammograms even at fast sweeps, indicating a high chemical irreversibility of the reaction. As a result, the oxidation reaction of NADH was occurred as irreversible with two electrons and one H^+ (Gorton and Dominguez, 2002a).

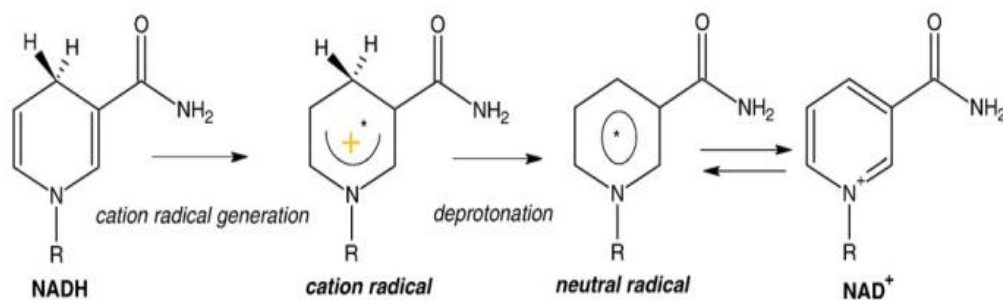
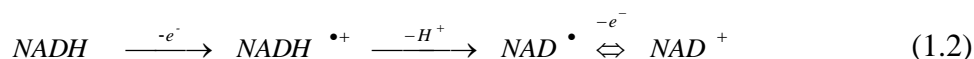
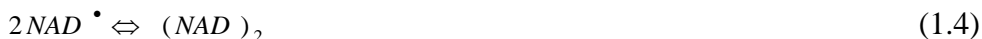


Figure 1.7. Schematic illustration of the hydride-acceptor and -donor pyridine nucleotide moiety proposed ECE-mechanism (Radoi and Compagnone, 2009).



In addition, a disproportionate reaction between the cationic radical ($\text{NADH}^{\bullet+}$) and neutral radical (NAD^{\bullet}), and dimerization reaction of neutral radicals (NAD^{\bullet}), are also possible homogeneously (Reactions 1.3 and 1.4, Katakis and Dominguez, 1997; ^bGorton and Dominguez, 2002).



The oxidized products of NADH, radicals, intermediates and NAD^+ , can be adsorbed on the electrode surface and can result in the fouling and passivation of electrode surface which cause poor sensitivity, poor selectivity and unstable analytical signals. On the other hand, this phenomena causes a decrease in the reproducibility of biosensors dependent on NADH (Gorton and Dominguez, 2002a; Simon and Bartlett, 2003).

Thus, research toward the realization of the “ideal” NADH probe has been directed from the beginning to the reduction of the oxidation overpotential and the improvement of the electron transfer rate; long term stability of the probe and selectivity being secondary tasks but not less important targets for the realization of probes working in real samples. The easiest way to achieve NADH electrooxidation at low overpotentials is historically represented by the use of redox mediators, the working applied potential necessary for NADH oxidation being reduced to the formal redox potential of the mediator, with relatively improved efficiency of the electrocatalytic oxidation process. Therefore, modification of electrode surface with redox mediators has been extensively used for electrocatalytic oxidation of NADH (Radoi and Compagnone, 2009).

1.2.3.2. The role of redox mediators in the electrocatalytic oxidation of NADH

Mediators are small molecules which catalyze the electrode reactions, because they shuttle electrons between the substrate and the electrode. Requirements for good redox mediator for the efficient electrocatalytic oxidation of NADH include the following (i) it should be electrochemically active, (ii) formal potential of the redox mediator should be smaller than the oxidation potential of NADH, (iii) higher electron transfer rate should be constant, (iv) formation of enzymatically active NAD^+ , (v) anti-fouling effect, (vi) long-term stability, (vii) reduction of considerable overpotential (Kumar and Chen, 2008).

In the first step of electrocatalytic oxidation of NADH using a mediator, the oxidized form of mediator reacts rapidly with NAD(P)H to give NAD(P)⁺ and it converts to reduced form. In the second step, the mediator reoxidizes at the electrode surface at some potential less positive than that required for the direct oxidation of NADH, yet at the same time positive E⁰ for the NAD(P)H/NAD(P)⁺ couple. The net effect is then to generate an electrocatalytic current (Figure 1.8). The electrocatalytic oxidation can be explained by ECE mechanism and, expressed by the reactions between 1.5 and 1.8 (Gorton and Dominguez, 2002a; Simon and Bartlett, 2003).

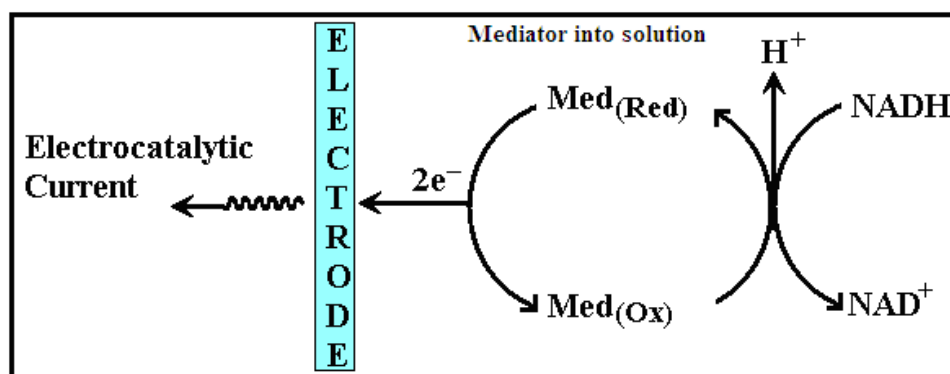
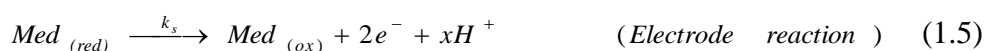


Figure 1.8. Oxidation of NADH by a homogenous mediator (Simon and Bartlett, 2003).

According to this mechanism, initially, the mediator was electrochemically kept in its reduced state ($Med_{(red)}$). When a positive scan was applied, approaching and beyond the E⁰ value of the surface-bound mediator, the mediator was transferred into catalytically active, oxidized form ($Med_{(ox)}$) (Reaction 1.5), where k_s is the electron transfer rate constant between the immobilized mediator and the electrode. The reaction in 1.5 is given here because the number of electrons and

protons (x) may differ between 1 and 2, depending on the nature of the mediator and the pH, respectively. Catalysis is then a result of the diffusion of NADH to the electrode surface, where it reduces $Med_{(ox)}$ to form NAD^+ and $Med_{(red)}$ (Reaction 1.6), where k_{obs} is the second order rate constant. The equation 1.7 is given here for a $2e^- xH^+$ -acceptor, and is in turn followed by the electrochemical reoxidation of $Med_{(red)}$, closing the ECE cycle (Gorton and Dominguez, 2002b).

The disadvantage of using soluble redox mediators is that they can diffuse away from the electrode surface and are thus no longer available to catalyze the electrode reaction. The simplest way to confine the mediator species at the electrode surface is if it is part of the electrode surface itself. For, example it has been shown that a pretreatment of the electrode can lead to the mediation of NADH oxidation. Deliberate chemical modification of electrodes is an interesting and more flexible way to catalyze NADH oxidation. Therefore, CMEs have been widely used for catalysis of NADH oxidation. Figure 1.9 shows the general scheme for the electrocatalytic oxidation of NADH at a modified electrode (Simon and Bartlett, 2003).

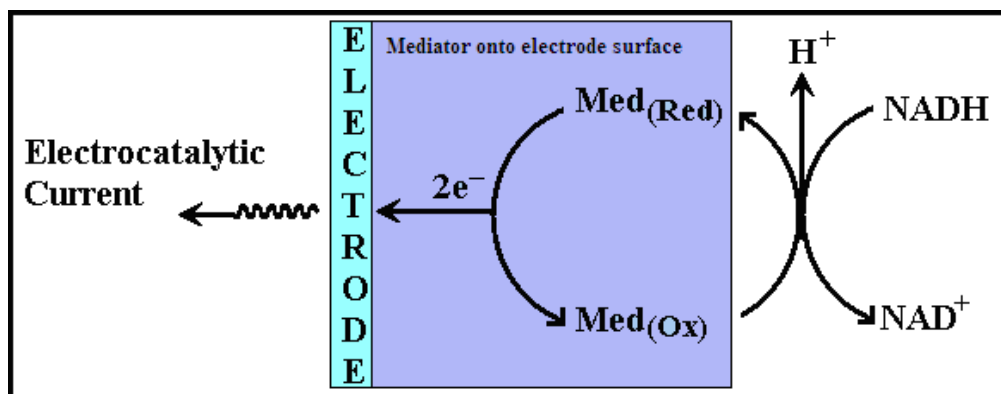


Figure 1.9. Oxidation of NADH at a modified electrode (Simon and Bartlett, 2003).

1.2.3.3. Chemically modified electrodes used in the electrocatalytic oxidation of NADH

The first paper on a CME for electrocatalytic NADH oxidation (Tse and Kuwana, 1978) was based on the immobilization of either two primary amines containing o-quinone derivatives, dopamine or 3,4-dihydroxybenzylamine, onto the surface of cyanuric chloride-activated GCEs, forming a monolayer on the

electrode surface. When these redox compounds immobilized onto electrode surface, cyclic voltammograms revealed that E^0 value of modified electrode was found to be approximately +0.16 V vs. a saturated calomel electrode (SCE) at pH 7, while an anodic peak current at approximately +0.20 V increased in the presence of NADH. Thus, the overvoltage could be reduced by some 0.4 V compared with the anodic peak potential registered for a bare GCE. Since then, this topic has been focus of many reports, summarized in a number of review papers (Gorton and Dominguez, 2002a; 2002b; Simon and Bartlett, 2003; Katakis and Dominguez, 1997; Kumar and Chen, 2008).

With this aim, various modified electrodes have been prepared with many redox mediators such as **azine type dyes (phenothiazine, phenoxazine, phenazine)** (Gorton et al., 1984; Karyakin et al., 1995, 1999a; 1999b; Zhu et al., 2009; Lawrence and Wang, 2006; Kubota and Gorton, 1999; Dilgin et al., 2011; Arechederra et al., 2010, 2011; Dilgin Giray, et al., 2011; Lin et al., 2012; Chen and Lin, 2001; Malinauskas et al., 2000, 2001; Lu et al., 2010; Barsan et al., 2008; Li et al., 2012; Meredith 2012); **quinolic compounds (flavonoids, phenolic acids, catecholic compounds)** (Dicu et al., 2003; Pariente et al., 1996; Zare et al., 2006a; Tu et al., 2007; Dilgin et al., 2012b, 2013; Maleki et al., 2012; Dilgin Giray et al., 2010); **nitrofluorenones** (Munteanu et al., 2004; Mano and Kuhn, 2001, 1999a; 1999b); **flavine and adenine derivatives** (Alvarez et al., 2001; Karyakin et al., 2004); and **some transition metal complexes** (Wu et al., 1996; Pinczewska et al., 2012; Popescu et al., 1999; Santiago et al., 2006) and **some conducting polymers** (Kumar and Chen, 2008; Bartlett and Simon, 2000), which have been successfully used for the electrocatalytic oxidation of NADH. A few excellent reviews on the uses of these redox mediators were reported by pioneer author Gorton (Gorton and Dominguez, 2002a; 2002b) and other research groups (Simon and Bartlett, 2003; Kumar and Chen, 2008; Katakis and Dominguez, 1997; Radoi and Compagnone, 2009). Some studies on electrocatalytic oxidation of NADH are summarized in Table 1.2 for modified electrodes prepared with widely used redox mediators.

Table 1.2. Studies on electrocatalytic oxidation of NADH using CME prepared with widely used redox mediators.

Mediators	Modified electrode type	Method	Explanation	References
PHENOXAZINES				
Meldola Blue (MdB)	MdB/OMC composite modified GCE	CV, AMP	A: upto 800 μM ; B: 0.21 μM C: 1 V (acc. to bare GCE) vs. Ag/AgCl	Jiang et al., 2009.
	Adsorption of MdB on $\text{SiO}_2/\text{SnO}_2/\text{Sb}_2\text{O}_5/\text{GE}$	CV, AMP	A: 8×10^{-5} - 9.0×10^{-4} M; B: 1.5×10^{-7} M	Canevari et al., 2011.
	SPE containing MdB Reinecke salt (RS)	CV, AMP, FIA	A: 0.01-1 mM C: 508 mV (acc. to SPE) vs. Ag/AgCl	Piano et al., 2010a.
	Adsorption of MdB on $\text{SiO}_2/\text{TiO}_2/\text{GE}$ prepared with sol-gel	CV, AMP	A: 0.018 - 7.29 mM; B: 0.008 mM	Maroneze et al., 2008.
	Electropolymerization of MdB on SPGE	CV, AMP	A: 8 - 500 μM ; B: 2.5 μM	Vasilescu et al., 2003a.
	Modified CPE with adsorbed MdB Silikajel/Titanium phosphate	CV, AMP	A: 1.0×10^{-5} - 5.0×10^{-5} M	Kubota et al., 1996.
	a) Electropolymerization on GE, b) adsorption on GE in SP ink, c) immobilization on GE after precipitation with Reinecke salt	CV, AMP	a) A: 8×10^{-6} - 5×10^{-4} M; B: 2×10^{-6} M b) A: 2×10^{-5} - 7.5×10^{-4} M; B: 1×10^{-5} M c) A: 2×10^{-5} - 7.5×10^{-4} M; B: 5×10^{-6} M	Vasilescu et al., 2003b.
	Adsorption on $\text{SiO}_2/\text{TiO}_2/\text{Sb}_2\text{O}_5/\text{GE}$ prepared with sol-gel	CV, AMP	A: 0.9 - 7290 mM; B: 0.003 mM C: 1V (acc. to $\text{SiO}_2/\text{TiO}_2/\text{Sb}_2\text{O}_5/\text{GE}$) vs. SCE	Maroneze et al., 2010.
	Immobilization of MdB adsorbed SWCNT on GCE	CV, AMP	A: 0.02 - 2.54 mM; B: 0.4 μM C: 305 mV (acc. to bare GCE) vs. Ag/AgCl	Arvinte et al., 2009.
	Formation of MdM/ZnO hybride film on GCE	CV, AMP	A: 50 - 300 μM ; B: 10 μM C: 600 mV (acc. to bare GCE) vs. Ag/AgCl	Kumar and Chen, 2007.
	Adsorption on SWCNT immobilized GCE	CV, AMP	A: Linear to 0.5 mM; B: 0.048 μM C: 1000 mV (acc. to bare GCE) vs. Ag/AgCl	Zhu et al., 2007.
	MdB/graphitized mesoporous carbons (GMC)/chitosan (CS) nanobiocomposite SPE	CV, AMP	A: 10 μM to 410 μM ; B: 0.186 μM C: 0.51 V (acc. to GMC/CS/SPE) and 0.94 V (acc. to bare SPE) vs. Ag pseudo RE.	Hua et al., 2013.
	MdB immobilized silver nanoparticle-PEDOT GCE	CV, AMP,	A: 10 - 560 μM ; B: 0.1 μM C: 650 mV (acc. to bare GCE) vs. Ag/AgCl	Balamurugan et al., 2010.

Table 1.2. Continued.

Nil Blue (NB)	Electropolymerization of NB on GCE	CV, RDE	C: 660 mV (acc. to bare GCE) vs. SCE	Cai and Xue, 1997a.
	Adsorption of NB on OMC composite immobilized GCE	CV, AMP	A: Linear to 350 μ M; B: 1.2 μ M	Zhu et al., 2009.
	Electropolymerization of NB on SWCNT immobilized GCE	CV	C: 700 mV (acc. to bare GCE) vs. SCE	Du et al., 2007.
	Modified CPE with NB adsorbed ZrP	CV, AMP	A: 1×10^{-5} - 5.2×10^{-4} M	Santos et al., 2002a.
	Modified CPE with NB adsorbed ZrP	CV	A: 1×10^{-4} - 2×10^{-3} M; B: 5 μ M	Pessoa et al., 1997.
	NB covalently assembled on the surface of functionalized SWCNTs modified GCE	CV, AMP	A: 0.2-200 μ M; B: 0.18 μ M	Saleh et al., 2011.
Brilliant Cresyl Blue (BCB)	Electropolymerization of BCB on SWCNT immobilized GCE	CV, AMP	A: 3 - 104.2 μ M; B: 1 μ M	Yang and Liu, 2009.
	Modified carbon ceramic electrode with exfoliated graphite adsorbed BCB	CV, AMP	A: 0.02 - 1 mM (for AMP); B: 20 μ M	Ramesh et al., 2003.
PHENOTHIAZINES				
Metilen Blue (MB)	Electropolymerization of MB on GCE	CV, FIA PhotoAMP,	A: 1.0×10^{-7} - 2.0×10^{-4} M; B: 4×10^{-8} M C: 420 V ((acc. to bare GCE) vs. Ag/AgCl	Dilgin et al., 2011.
	Coelectropolymerization of pyrrol and MB on GCE	CV, FIA	A: 0.1 - 2000 μ M; B: 0.025 μ M (NADPH) A: 0.1 - 1300 μ M; B: 0.04 μ M (NADH) C: 400 mV(acc. to bare GCE) vs. Ag/AgCl.	Chi and Dong, 1994.
Metilen Blue (MB)	Ion exchange with cellulose acetate/ZrP immobilized on Pt electrode	CV, AMP	A: Linear to 0.3 mM	Borgo et al., 2002.
	Modified CPE with MB on ZrP	CV	A: 1×10^{-4} - 2×10^{-3} M; B: 10 μ M	Pessoa et al., 1997.
	Mmodified CPE with MB on $\text{SiO}_2/\text{ZrO}_2/\text{Sb}_2\text{O}_5$	CV, AMP	B: 36 μ M; C: 500 mV(acc. to bare CPE) vs. SCE	Zaitseva et al., 2002.
Azure A (AzA)	Electropolymerization of AzA on SPCE	CV, FIA	A: 0.5 - 100 μ M; B: 0.2 μ M (for FIA) C: 500 mV(acc. to bare SPCE) vs. Ag/AgCl	Gao et al., 2004.
	Electropolymerization of AzA on GCE immobilized Polydiallyldimethylammoniumchloride and MWCNT	CV, AMP	A: 0.6 - 600 μ M; B: 0.2 μ M	Gao et al., 2010.
	Electropolymerization of AzA on GCE	CV, AMP	A: 1×10^{-5} - 8×10^{-3} M; B: 5×10^{-6} M C: 410 mV(acc. to bare GCE) vs. SCE	Li et al., 2003.

Table 1.2. Continued.

Azure B (AzB)	The electropolymerization on SPCE	CV, FIA	A: 0.5 - 100 μM ; B: 0.2 μM (for FIA) C: 400 mV (acc. to bare SPCE) vs. Ag/AgCl	Sha et al., 2004
	Electropolymerization of AzB on OMC modified GCE	CV, AMP	A: 3.0 to 1000 μM ; B: 0.1 μM C: 145 mV (acc. to OMC/GCE) vs. Ag/AgCl	Fang et al., 2010
	Electropolymerization of AzB on GCE immobilized Polydiallyldimethylammoniumchloride and MWCNT	CV, AMP	A: 0.2 - 650 μM ; B: 0.07 μM	Gao et al., 2010.
	Electropolymerization of AzB on GCE	CV	C: 460 mV (acc. to bare GCE),	Cai and Xue, 1997b.
Thionine (Th)	Electropolymerization of Th on SPCE	CV, FIA	A: 5 - 100 μM ; B: 3 μM (for FIA) C: 300 mV (acc. to bare SPCE) vs. Ag/AgCl	Gao et al., 2003.
	Chemically modified gold electrodes by Th covalently bond to self-assembled cysteamine monolayer (SAM)	CV, AMP	A: 2.0×10^{-5} to 1.0×10^{-2} M C: 600 mV (acc. to bare Au electrode) vs. SCE	Chen et al., 1997.
	Magnetic Chitosan Microspheres – Poly-Th Modified GCE	CV, AMP	A: 2 – 10 μM and 10 – 100 μM ; B: 0.51 μM C: 650 mV (acc. to GCE) vs. SCE	Liu et al., 2010.
	Electropolymerization of Th on SPCE	CV, AMP, FIA	A: 20-1000 μM ; B: 1.74 μM C: 400 mV (acc. to bare GCE) vs. Ag/AgCl	Baskar et al., 2012.
	Electropolymerization of Th on GCE immobilized polydiallyldimethyl ammoniumchloride and MWCNT	CV, AMP	A: 0.7 - 700 μM ; B: 0.2 μM	Gao et al., 2010.
	Electropolymerization of Th on MWCNT immobilized carbon ionic liquid electrode	CV, AMP	A: 0.8 - 422 μM ; B: 0.26 μM C: 190 mV (acc. to carbon ionic liquid electrode)	Mai et al., 2010.
	Electropolymerization of Th on OMC modified GCE	CV, AMP	A: 3.4×10^{-6} - 8.5×10^{-4} M; B: 5.1×10^{-8} M C: 592 mV (acc. to bare GCE)	Qi et al., 2009.
	Electroreduced graphene oxide–poly-Th nanocomposite film modified GCE	CV, AMP	A: 0.01-3.9 mM; B: 0.1 μM C: 340 mV (acc. to bare GCE) vs. SCE	Li et al., 2013a.
Methylene Green (MG)	Electropolymerization of MG on GCE	CV, AMP	A: 0.5 - 10 mM; B: 1.0×10^{-3} M C: 400 mV (acc. to bare GCE)	Zhou, 1996.
	Electropolymerization of MG on GCE	CV, AMP	A: 5.6 - 420 μM ; B: 3.8 μM C: 650 mV (acc. to bare GCE)	Dai et al., 2008.
	Preparation of CPE with silica gel-MG adsorbed niobium oxide	CV, AMP, FIA	A: 5×10^{-4} - 4×10^{-3} M (for AMP) A: 6×10^{-5} - 1×10^{-3} M; B: 8.2×10^{-6} M (FIA)	De Lucca et al., 2002.

Table 1.2. Continued

QUINOLIC COMPOUNDS (FLAVONOIDS, PHENOLIC ACIDS, CATECHOLIC COMPOUNDS)				
Hematoxylin (HT)	Adsorption of HT on PGE	CV, AMP	A: 0.5 - 10 μ M and 10 - 300 μ M; B: 0.2 μ M C: 250 mV (acc. to bare PGE) vs. Ag/AgCl	Dilgin et al., 2012b.
	Electropolymerization of HT on GCE (from this thesis)	CV, PhotoAMP, FIA	A: 1.0×10^{-7} - 2.5×10^{-4} M; B: 3×10^{-8} M C: 320 mV (acc. to bare GCE) vs. Ag/AgCl	Dilgin Giray et al., 2010.
	Preparation of CPE with mixed HT, graphite powder and nujol.	CV, DPV	A: 0.4 - 600.0 μ M NADH; B: 0.08 μ M C: 280 mV (acc. to bare CPE) vs. SCE	Zare et al., 2006a.
Xanthurenic acid (Xa)	Electropolymerization of Xa on MWCNT modified GCE	CV, AMP	A: 0.5 - 10 μ M; B: 0.1 μ M; C: 550 mV (at bare GCE) and 350 mV (acc. to MWCNT/GCE) vs. Ag/AgCl	Dos Santos Silva et al., 2010.
	Codeposited of Xa and Flavin adenin dinucleotide on MWCNT modified GCE	CV, AMP	A: 5×10^{-6} - 1.7×10^{-4} M; B: 1 μ M	Lin et al., 2013.
Chlorogenic acid (CA)	CA modified carbon ceramic electrode prepared with sol-gel technique	CV, AMP	A: 1 - 120 μ M; B: 0.2 μ M	Salimi et al., 2005.
	CA modified GCE	CV	A: 0.1 to 1.0 mM; C: 430 mV (acc. to bare GCE)	Zare and Golabi, 1999.
Catechol (1-2 dihydroxybenzene) (CT)	Electrodeposition of CT on GCE	CV	A: 0.02 - 0.34 mM	Maleki et al., 2012.
	Electropolymerization of CT on OMC modified GCE	CV, AMP	B: 0.2 μ M	Bai et al., 2010.
	Quinone (CT)-amine (o-phenylenediamine) polymer-MWCNT nanocomposite modified Au electrode	CV, AMP	A: 0.04 - 300 μ M; B: 6.4 nM C: 470 mV (acc. to bare Au) vs. SCE	Tu et al., 2007.
Caffeic acid (CFA)	CFA modified GCE	CV	A: 0.05 to 1.0 mM C: 450 mV (acc. to bare GCE) vs. Ag/AgCl	Zare and Golabi, 2000.
Coumestan (CMT)	Preparation of CPE with mixed CMT graphite powder and nujol.	CV, DPV, AMP	A: 1 - 1000 μ M; B: 0.1 μ M (for DPV) C: 240 mV (acc. to bare CPE) vs. Ag/AgCl	Zare et al., 2006b.
Fisetin (FT)	FT modified GCE	CV, AMP, RDE	B: 2.4 μ M (for AMP) C: 375 mV (acc. to bare GCE) vs. Ag/AgCl	Golabi and Irannejad, 2005.
Catechin (CTC)	Adsorption of a CTC on GCE coated with poly(3,4-ethylenedioxythiophene	CV, AMP, RDE	A: 10 - 100 μ M; B: 0.5 μ M C: 250 mV (acc. to bare GCE) vs. Ag/AgCl	Vasantha and Chen, 2006.

Table 1.2. Continued.

Quercetin (QT)	Adsorption of QT on PGE	CV, AMP	A: 0.5 to 100 μM ; B: 0.15 μM C: 200 mV (acc. to bare PGE) vs. Ag/AgCl	Dilgin et al., 2013.
Rutin (RT)	RT modified GCE	CV, DPV	A: 8.3 - 151.5 μM and 151.5 - 833.3 μM B: 1.6 μM ; C: 450 mV (acc. to GCE) vs. Ag/AgCl	Zare et al., 2010.
Dopamine (DP)	Chitosan–DP–MWCNT modified Au electrode	CV, AMP	A: 0.1 - 600 μM ; B: 12 nM C: 450 mV (acc. to Au electrode)	Ge et al., 2009.
Tryptophan (TTP)	Adsorption of 5-Hydroxy TTP on GE	CV, AMP	A: 5×10^{-8} - 6×10^{-6} M; B: 27 nM	Alvarez et al., 2005.
Dihydroxybenzaldehyd (DHB)	Electrodeposition of DHB (3,4 dihydroxy benzaldehyde (3,4 DHB) ve 2,3 DHB) and its derivatives on GCE	CV, AMP, RDE	A: 0.01 – 1.2 mM (3,4-DHB), 0.01-0.9 mM (2,3-DHB); B: 10 μM	Pariante et al., 1996.
Naphtoquinone (NQ)	Electropolymerization of 1,2-NQ to the surface of MWCNT modified electrode	CV, AMP	A: 1.0 μM to 0.14 mM; B: 1×10^{-7} M	Liu et al., 2012.
6,7-dihydroxy-3-methyl-9-thia-4,4a-diazafloren-2-one (DMTD)	DMTD/MWCNT film- CPE	CV, DPV	A: 1 - 10 nM and 10 - 80 nM; B: 0.7 nM C: 333 mV (acc. to bare GCE) vs. Ag/AgCl	Fotouhi et al., 2010
1,10-phenanthroline-5,6-dione (Phnt)	Phnt /MWCNT modified GCE	CV, AMP	A: up to 500 μM ; B: 1.8 μM	Mao et al., 2011.
Nitrofluorenone (NFR)	The adsorption of NFR derivatives on GCE	CV, RDE	A: 5 μM – 2 mM	Mano and Kuhn, 1999a.
	2,4,7-trinitro-9-fluorenone (C_1) and 2,5,7-trinitro-9-fluorenone-4-carboxylic acid (C_2) adsorbed ZrP modified CPE	CV, FIA	A: 5 - 260 μM for C_1 and 5 - 120 μM and 5 - 170 μM for C_2 B: 0.4 μM for C_1 and 0.6 and 0.07 μM for C_2	Munteanu et al., 2004.
Benzoquinone (BQ)	2,3,5,6-tetrachloro-1,4-benzoquinone (TCBQ)/MWCNT immobilized on an edge plane pyrolytic graphite electrode	CV, AMP	A: 0.5 up to 2160 μM ; B: 0.15 μM C: 300 mV (acc. to bare electrode) vs. Ag/AgCl	Silva Luz et al., 2008.
	Electropolymerization of 2,3-Dimethoxy-5-ethyl-6-vinyl-1,4-benzoquinone on GCE and ITO	CV, DPV	A: 10 - 100 μM B: 1 μM C: 380 mV (acc. to bare GCE) vs. SCE	Li et al., 2011.
CONDUCTING POLYMERS				
Aminophenol (AP)	Deposition of o-AP on GCE	CV, AMP, RDE	A: 7.5×10^{-7} – 2.5×10^{-6} M; B: 1.5×10^{-7} M C: 350 mV (acc. to bare GCE)	Nassef et al., 2006.
Thiophene (ThP)	Electropolymerization of 3-methyl ThP e on cylindrical carbon fiber microelectrode	CV, AMP, FIA	A: 1×10^{-6} - 1×10^{-4} M (for AMP and FIA) B: 7.6×10^{-7} M (for AMP), 3.8×10^{-7} M (for FIA) C: 320 mV (acc. to bare GCE)	Jaraba et al., 1998.

Table 1.2. Continued.

Aniline (An)	Preparation of nano structure poly(aniline-co-2-amino-4-hydroxybenzenesulphonic acid) on GCE	CV	C: 240 mV (electrode was prepared at 0.75 V) C: 290 mV (electrode was prepared at 0.80 V)	Mu et al., 2009.
Pyrole (Py)	Electropolymerization 3,4-ethylenedioxy pyrrole (PEDOP) MWCNTs-Pd nanoparticles modified GCE	AMP	A: 1 μ M - 13 mM; B: 0.18 μ M	You and Jeon, 2011.
Methacrylate (MMT)	Preparation of CPE with mixed poly-MMT, graphite powder and nujol.	AMP	A: 4.0 μ M to 5.6 mM	Dai et al., 2009.
Allylamine Hydrochloride (Al-HCl)	Poly-Al-HCl modified SPE	CV, DPV	A: 0.01 to 5 mM; B: 0.22 μ M	Rotariu et al., 2014.
TRANSITION METAL COMPLEXES				
Ru, Os, Re, Fe etc. complexes.	Immobilization of Os-Redox polymer on carbon nanotube paste electrode	CV	A: Linear to 8×10^{-4} M; B: 5 μ M	Antiochia and Gorton, 2007.
	Bis(1,10-phenanthroline-5,6-dione) (2,2'-bipyridine)ruthenium(II)-Exchanged ZrP Modified CPE	CV	Electrocatalytic oxidation of NADH was observed at 50 mV vs. Ag/AgCl	Santiago et al., 2006.
	Os(4,4'-dimethyl, 2,2'-bipyridine) ₂ (1,10-phenanthroline 5,6-dione) complex, adsorbed on spectrographic graphite rod electrode	CV	C: 400 mV (acc. to bare graphite electrode) vs. SCE	Popescu et al., 1999.
	Deposition of cobalt hexacyanoferrate (COHCF) on the surface of a microband gold electrode.	CV	A: 0.5 - 6.0 mM; B: 310 - 370 mV (acc. to microband Au electrode) vs. Ag/AgCl	Cai et al., 1995.
	Electroactive self-assembled monolayers SAMs of macrocyclic Ni II complex (dinickel II 2,2-bis 1,3,5,8,12-pentaazacyclotetradec-3-yl -diethyl disulfide perchlorate) on gold electrode.	CV	C: 210 mV acc. to bare Au electrode) vs Ag/AgCl.	Raj et al., 2000.

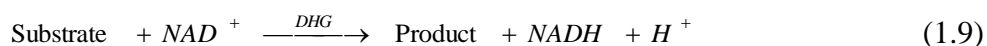
A: Linear range, AMP: Amperometry, B: Limit of detection, C: Amount of potential shifting of electrocatalytic oxidation of NADH according to (acc. to) bare electrodes, CPE: Carbon paste electrode, CV: Cyclic voltammetry, DPV: Differential pulsed voltammetry, FIA: Flow injection analysis, GCE: Glassy carbon electrode, ITO: Indium tin oxide, MWCNT: Multi-walled carbon nanotube, OMC: Ordered mesoporous carbon, RDE: Rotating disc electrode, RE: Reference electrode, SPCE: Screen printed carbon electrode; SPE: Screen printed electrode, SPGE: Screen printed graphite electrode; SWCNT: Single-walled carbon nanotube, ZrP: Zirconium phosphate.

1.3. Construction of Biosensor Dependent on Dehydrogenase Enzyme and NAD^+ / $NADH$ Redox Couple

A chemical sensor is a device that transforms chemical information, ranging from the concentration of a specific sample component to total composition analysis, into an analytically useful signal. Chemical sensors contain usually two basic components connected in series: a chemical (molecular) recognition system (receptor) and a physicochemical transducer. Biosensors are chemical sensors in which the recognition system utilizes a biochemical mechanism.

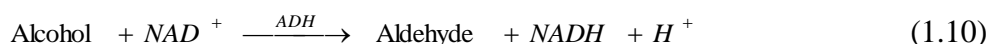
The biological recognition system translates information from the biochemical domain, usually an analyte concentration, into a chemical or physical output signal with a defined sensitivity. The main purpose of the recognition system is to provide the sensor with a high degree of selectivity for the analyte to be measured. While all biosensors are more or less selective (non-specific) for a particular analyte, some are, by design and construction, only class-specific, since they use class enzymes, e.g., phenolic compound biosensors, or whole cells, e.g., used to measure biological oxygen demand. Because in sensing systems present in living organisms/systems, such as olfaction, and taste, as well as neurotransmission pathways, the actual recognition is performed by the cell receptor, the word “receptor” or “bioreceptor” is also often used for the recognition system of a chemical biosensor. The transducer part of the sensor serves to transfer the signal from the output domain of the recognition system to, mostly, the electrical domain. Because of the general significance of the word, a “transducer” provides bidirectional signal transfer (non-electrical to electrical and vice versa); the transducer part of a sensor is also called a detector, sensor or electrode, but the term transducer is preferred to avoid confusion (Thevenot et al., 2001). Some studies on amperometric biosensor dependent on NAD^+ / $NADH$ redox couple have been made using CMEs (Katakis and Dominguez, 1997; Lobo et al., 1997).

The first biosensor that depended on $NADH$ was constructed by the direct oxidation of $NADH$, which was formed by the enzymatic reaction between substrate and NAD^+ in the presence of dehydrogenase enzyme, at clean or pretreated electrodes (Reaction 1.9).



These sensors belong to the first-generation biosensor group since the electrode was merely used to measure the concentration of one of the enzymatic reaction products (NADH). This kind of biosensor has a number of disadvantages, which are the same as those associated with the direct electrochemical oxidation of NADH. As a consequence of the high overpotentials required for the electrochemical oxidation of the reduced coenzymes, high applied potentials are needed. Under these conditions, high background currents are obtained, restricting the sensitivity of the sensor. Furthermore, the analytical system is exposed to many interferences from other species present in the sample than can contribute to the response. These biosensors show poor stability in general. This fact can be related to the poor stability of the immobilized enzyme or with passivation and fouling of the electrode surface due to the accumulation of high-molecular-weight compounds produced in the cofactor oxidation side-reactions.

In order to overcome these disadvantages, the second generation biosensor dependent on NADH was developed. In this type of biosensor, the coupling of the electrocatalytic oxidation of NADH by some of the previously mentioned mediators to the reaction catalyzed by any of the NAD-dependent dehydrogenase enzymes, allows the construction of amperometric biosensors for a large variety of substrates. This biosensor can be expressed by reactions of 1.9 and 1.5 - 1.8, respectively and a simple schematic illustration is given in Figure 1.10 for alcohol biosensor (Yang and Liu, 2009). All redox enzymes rely on a cofactor as the redox active compound for their activity. In flavoenzymes (i.e., flavin adenine dinucleotide (FAD) and flavin mononucleotide (FMN) centered enzymes) the cofactor is strongly bound within the enzyme structure. However, NAD^+ -dependent dehydrogenase enzymes are characterized by their need for a soluble cofactor for their activity. For biosensors based on flavoenzymes it has become usual to term "third generation biosensors", a kind of device in which a direct electron transfer between the active center of the enzyme and the electrode is achieved (Lobo et al., 1997). Among the biosensor types, the second generation biosensors have been widely used. Especially alcohol, carbohydrate and glutamate biosensors have been constructed using modified electrodes prepared with azine type redox dyes (Table 1.3). The mechanism for alcohol biosensor dependent on NADH can be explained thus. Firstly, an enzymatic reaction between alcohol and cofactor (NAD^+) in the presence of alcohol dehydrogenase or alcohol oxidase, which has been immobilized onto the electrode surface is performed, and aldehyde and the reduced form of NAD^+ (NADH) are formed (Reaction 1.10) (Yang and Liu, 2009).



Then formed NADH is oxidized to NAD^+ and the oxidized form of the mediator convert to its reduced form by a chemical reaction between NADH and the oxidized form of the redox mediator which was immobilized onto the electrode surface. Finally, the reduced form of mediator reoxidizes and an electrocatalytic current forms, which is recorded for indirect determination of alcohol. Similar biosensors have been also constructed for glucose, lactose and glutamate by glucose dehydrogenase, lactate dehydrogenase and glutamate dehydrogenase were used as an enzyme, respectively.

For example, Yang and Liu (2009) fabricated a SWNT modified with poly-BCB/GCE. The prepared modified electrode firstly was used for the electrocatalytic oxidation of NADH. Then an ethanol biosensor also was developed using this nanocomposite modified electrode, by immobilizing ethanol dehydrogenase onto the electrode surface. It was reported that a linear ethanol concentration response was achieved in the range from 0.4 to 2.4 mM and the detection limit was estimated to be 0.1 mM ($S/N=3$). It was concluded that the analytical performance achieved with the lead to Poly-BCB/SWNT nanocomposite electrode was expected to the development of novel biosensors, biofuel cells, and other bioelectrochemical devices.

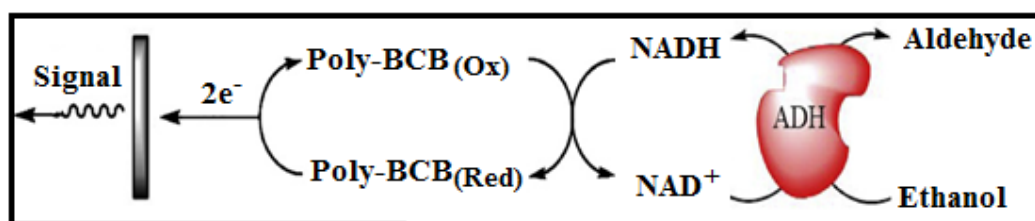


Figure 1.10. Reaction scheme for an amperometric ethanol biosensor based on the use of alcohol dehydrogenase enzyme (Yang and Liu, 2009).

As a result, many biosensors dependent on NADH using CMEs have been extensively developed for the determination of biological important molecules such as glucose, lactose, alcohol, glutamate, etc. Some studies are summarized in Table 1.3.

Table 1.3. Some studies on biosensor dependent on NADH and dehydrogenase enzymes.

Modified electrode type	Enzyme	Analyte	Explanation	References
Electropolymerization of BCB on GCE immobilized SWCNT	ADH	Ethanol	A: 0.4 - 2.4 mM; B: 0.1 mM	Yang and Liu, 2009.
Electropolymerization of MB on GCE immobilized laponite gel	ADH, LDH	Ethanol and lactate	B: 1 mM (for lactate) and 25 mM (for ethanol)	Cosnier and Lous, 1996.
Immobilization of Th adsorbed SWCNT on GCE	GIDH	Glutamate	A: 0.5 - 400 mM; B: 0.1 mM	Meng et al., 2009.
Preparation of modified CPE with MdB adsorbed SWCNT	ADH	Ethanol	A: 0.05 - 10 mM; B: 5×10^{-6} M	Santos et al., 2006.
Electropolymerization of MB on Au	GDH	Glucose	A: 1 - 4 mM	Silber et al., 1996.
Adsorption of TB on pyrolytic graphite electrode	LDH	Lactate	A: 1×10^{-6} - 6×10^{-5} M; B: 4×10^{-7} M	Villamil et al., 1997.
Immobilization of Os-redox polymer on carbon nanotube paste electrode	GDH	Glucose	A: linear to 8×10^{-4} M; B: 10 mM	Antiochia and Gorton, 2007.
Electropolymerization of NB on SWCNT immobilized GCE	ADH	Ethanol	A: 0.1 - 3 mM; B: 50 mM	Du et al., 2007.
Electropolymerization of TB on graphite electrode	GDH	Glucose	A: 5×10^{-5} - 3×10^{-3} M	Zhou et al., 1998.
Immobilization of MdB adsorbed and Chitosan MWCNT on GCE	GIDH	Glutamate	B: 2 μ M	Chakraborty and Raj, 2007.
Poly-vinyl ferrocene modified CPE	ADH	Ethanol	A: 4×10^{-4} - 4.5×10^{-3} M; B: 3.9×10^{-4} M	Koyuncu et al., 2007.
Phenothiazine (TB) and phenoxazine (MdB, NB, BCB) modified CPE	ADH	Ethanol	A: 10 - 100 μ M; B: 5×10^{-6} M	Lobo et al., 1996a.
MdB/ordered mesoporous Carbon composite modified GCE	ADH	Alcohol	A: upto 6 mM; B: 19.1 μ M	Jiang et al., 2009.

Table 1.3. Continued.

NB covalently assembled on the surface of functionalized SWCNTs modified GCE	GDH	Glucose	A:100 - 1700 μ M; B:0.3 μ M	Saleh et al., 2011.
SPCE containing MdB Reinecke salt	GDH	Glucose	A:0.075 - 30 mM	Piano et al., 2010a.
Electroreduced graphene oxide-poly-Th nanocomposite film modified GCE	ADH	Ethanol	A: 0.05 - 1.0 mM; B: 0.3 μ M	Li et al., 2013a.
Graphene-Au nanorods modified GCE	ADH	Ethanol	A: 5 to 377 μ M; B: 1.5 μ M	Li et al., 2013b.
ADH/NAD ⁺ /MdB/graphitized mesoporous carbons/chitosan nanobiocomposite	ADH	Ethanol	A: 0.5 to 15 mM; B: 80 μ M	Hua et al., 2013.
D-sorbitol dehydrogenase (DSDH) immobilized in a sol-gel carbon nanotubes-poly/MG composite GCE	DSDH	D-sorbitol	A: 0.2 - 12 mM; B:0.11 mM	Wang, et al., 2013b.
Nickel oxide nanoparticles (NiOxNPs) modified GCE	ADH	Ethanol	A: 0.2 - 6 mM; B: 6.4 μ M	Sharifi et al., 2013.
NiO nanoparticles-modified CPE	ADH	Ethanol	A: 1.6 - 38 mM	Aydođdu et al., 2013.
ZnO nanorods modified Au electrode	LDH	Lactate	A: 0.2 - 0.8 μ M; B: 4.73 nM	Nesakumar et al., 2014.
Nano CeO ₂ modified GCE	LDH	Lactate	A: 0.2 - 2 mM; B:50 μ M	Nesakumar et al., 2013.
Fe ₃ O ₄ nanoparticles/MWCNT composite modified GCE	LDH	Lactate	A: 50 - 500 μ M; B:5 μ M	Teymourian et al., 2012.
1,10-phenanthroline-5,6-dione/MWCNT modified GCE	ADH	Ethanol	A: upto 7 mM; B:0.3 mM	Mao et al., 2011.

A: Linear range, ADH: Alcohol dehydrogenase, B: Limit of detection, CPE: Carbon paste electrode, GCE: Glassy carbon electrode, GDH: Glucose dehydrogenase, GIDH: Glutamate dehydrogenase, LDH: Lactate dehydrogenase, MWCNT: Multi-walled carbon nanotube, SWCNT: Single-walled carbon nanotube.

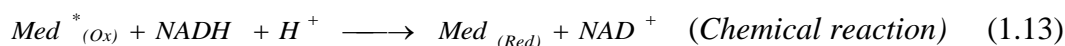
1.4. Photoelectrochemistry and Photoelectrochemical Sensors

Photoelectrochemistry (PEC), also known as photocurrent spectroscopy, is the science of measuring and interpreting the electric current which is generated by irradiation of a metal, or electrode, in an electrolyte (Dilgin, 2004). PEC is the combination of photochemistry with electrochemistry. Not only does the electrode interact with light but also the electrolyte in the near of electrode interacts as a photolytic. In this phenomenon, the light absorbed by the electrode or electrolyte is generated as a photocurrent. This photocurrent is altered by wavelength, electrode potential, and composition of electrolyte. This change gives information about the nature, kinetic and energy level of the photo process. In the application to analysis of PEC, semiconductor, modified and composite electrodes have often been used.

The photoelectrochemical sensor is a new kind of improved device which has great application potential for analytical chemistry due to its remarkable sensitivity, easy miniaturization and integration, good selectivity, simple equipment and portability (Wang et al., 2009b; Zhang and Zhao, 2013). A molecule, ion or semiconductor materials on the electrode surface absorb photons when the electrode surface is irradiated by a light source. Then, outer layer electrons of species transited to excited states from the ground state during photoelectrochemical process, which results in charge transfer and energy transfer from light to electrical (Zhang and Zhao, 2013). Because the excited molecules exhibit strong activity, these molecules can transfer to the conduction band or other electrodes with low energy by an electronic adjusting mechanism directly or indirectly. The generation of the photocurrent has been explained with two mechanisms by Zhang and Zhao, (i) as the existence of reducing agent in the solution, the species excited states are reduced to the ground state, and then the photoelectrochemical reaction is triggered again, resulting in a continuous photocurrent; (ii) when electron donor or acceptor molecule exist, electron transfer reactions take place between the excited molecules and the quenching agent molecules. The resulting molecule in oxidized or reduced state could further obtain or lose electrons from the electrode surface and generate photocurrent. The photoactive material returns to the ground state for the next round of reaction (Dong, et al., 2004; Zhang and Zhao, 2013). The magnitude of photocurrent is related to the wavelength and intensity of exciting light, property of photoelectric materials, type and shape of electrode, amplitude of bias voltage, and composition of electrolyte.

Investigations on the photoelectrocatalytic oxidation and determination of some biologically important molecules such as ascorbic acid and NADH have been performed using CMEs. In the first study on photoelectrocatalytic oxidation of NADH, a phenothiazine dye, TB, electropolymerized on the GCE surface, and the cyclic voltammograms of obtained poly-TB modified GCE, were recorded by irradiation of modified electrode surface in the presence of NADH. It was reported that the electrocatalytic peak current for NADH was increased by irradiation of electrode surface. The amperometric and photoamperometric determination of NADH was performed using this modified electrode. It was found that although the steady state current increased with an increase in the NADH concentration for the amperometric and the photoamperometric method, the slope of the current-NADH concentration curve of the photoelectrocatalytic procedure improved by about 2.2 times compared with that obtained without irradiation. As a result, it was emphasized that the photoelectrocatalytic method has better sensitivity than the electrocatalytic method for the determination of NADH (Dilgin et al., 2007).

The mechanism of photoelectrochemical oxidation of NADH with poly-TB modified GCE was explained by the fact that initially the oxidised redox mediator was excited by light, followed by the fact that the excited redox mediator rapidly reacted with NADH, and finally the formed leuco form of the mediator was reoxidized at the electrode surface (Dilgin et al., 2007). This mechanism was firstly reported by Compton's research group for electrocatalytic oxidation of ascorbic acid with TB and MB (Cooper et al., 1998, 1999). This mechanism is shown in reactions between 1.11 and 1.15.



Recently, semiconductor nanoparticles such as TiO₂ nanomaterial and quantum dots (CdSe/ZnS nanocrystals) have been the focus of considerable interest in photoelectrochemical sensing of NADH due to their high photosensitivity, large specific surface area, high surface adsorption capacity, good chemical stability and environmental safety of the photoelectrocatalytic oxidation of NADH (Ho et al., 2011; Wang, et al., 2009a; Wang et al., 2012a; Schubert et al., 2010). For example, Wang et al., prepared dopamine coordinated photoactive TiO₂ nanoporous films on ITO electrode and used this electrode for photoelectrochemical detection of NADH under visible light excitation (Wang et al., 2009a). They reported that this modified electrode displayed a linear range of $5.0 \times 10^{-7} - 1.2 \times 10^{-4}$ and a low detection limit of 1.4×10^{-7} M for NADH determination. In another study, photoelectrochemical determination of NADH was investigated by using Graphene-TiO₂ nanohybrids modified by GCE under visible light irradiation (Wang et al., 2012a). It was reported that photocurrent of Graphene-TiO₂ for NADH was enhanced about 5 times more than that of pure TiO₂. Furthermore, a wide linear range from 1.0×10^{-8} to 2.0×10^{-3} M and a low detection limit of 3.0×10^{-9} M were obtained.

Although, photoelectrocatalytic oxidation of NADH has been widely studied by using redox mediator or semiconductor nanoparticles modified electrodes, a few studies have been reported for the construction of photoelectrochemical biosensor dependent on NAD⁺/NADH redox couple and dehydrogenase enzyme (Deng et al., 2008). In one of these studies, thionine (Th) cross-linked MWCNT and Au nanoparticles multilayer functionalized ITO electrode was used for photoelectrocatalytic oxidation of NADH and also glucose photoelectrochemical biosensor after glucose dehydrogenase was immobilized onto modified electrode (Deng et al., 2008). In the proposed mechanism of this photoelectrochemical biosensor (Figure 1.11), firstly the oxidized form of mediator (Th⁺) was excited by absorption of light via irradiation of electrode surface. Secondly, enzymatic reaction takes place in which glucose oxidized gluconolacton by glucose dehydrogenase enzyme and NAD⁺ reduced to NADH. Then the excited form of mediator (Th^{*+}) chemically reacts with NADH in which Th^{*+} easily returns to its reduced form and NADH reoxidizes again to NAD⁺. Finally, the reduced form of mediator gives electrons to electrode and reoxidizes again to its oxidized to Th⁺. Therefore, the irradiation of electrode surface provides excitation of mediator which facilitates electron transfer between

electrode and mediator. In this study, it was reported that the sensitivity during irradiation of electrode surface increased nearly two fold, and the detection limit lowered 7 fold for glucose detection compared with that without irradiation.

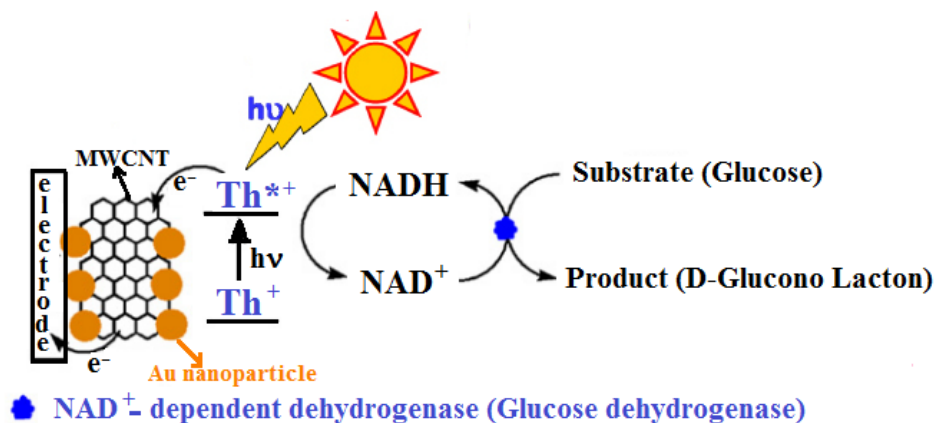


Figure 1.11. A representation of photoelectrochemical biosensor for glucose (Deng et al., 2008).

In another important study, the colloidal semiconductive CdSe/ZnS nanocrystals (quantum dots) were attached to gold by chemisorption via benzenedithiol and used for photoelectrocatalytic oxidation of NADH and the construction of glucose photoelectrochemical biosensor dependent on NAD^+/NADH redox couple and glucose dehydrogenase enzyme (Schubert et al., 2010). Although photoelectrochemical biosensor studies for glucose have been proposed in the literature (Schubert et al., 2010; Deng et al., 2008), photoelectrochemical biosensor studies dependent on NAD^+/NADH redox couple and dehydrogenase enzyme have not been carried out in FIA system. Therefore, one of the aims of this thesis was the construction of photoelectrochemical biosensors in FIA.

1.5. Flow Injection Analysis System

FIA is an approach to chemical analysis that is a continuous flow technique for chemical analysis accomplished by injecting a plug of sample into a flowing carrier stream. The technique was defined by Ruzicka and Hansen in 1975 (Ruzicka and Hansen, 1975). Simultaneous patents by Ruzicka and Hansen in Denmark and Stewart in the USA launched a new technology that has subsequently been rapid and widespread. FIA has attracted attention in modern analytical chemistry as a powerful analytical concept (Ruzicka and Hansen, 1988).

FIA is described as “a simple and versatile analytical technology for automating wet chemical analysis, based on the physical and chemical manipulation of a dispersed sample zone formed from the injection of the sample into a flowing carrier stream and detection downstream” (GlobalFIA, 2013). A schematic representation for general description of FIA is given in Figure 1.12. The schematic groups the FIA process into three stages to help visualize how the technique performs a method or analysis. The first stage of FIA is sampling, where the sample is measured out and injected into the flowing carrier stream. This step is generally performed with a sample injection valve. The second stage is sample processing, its purpose is to transform the analyte into a species that can be measured by the detector and manipulate its concentration into a range that is compatible with the detector, using one or more of the indicated processes. The third stage is detection, where the analyte or its derivative generates a signal peak that is used to quantify the compound being determined. As indicated in Figure 1.12., a large variety of detectors can be used in FIA.

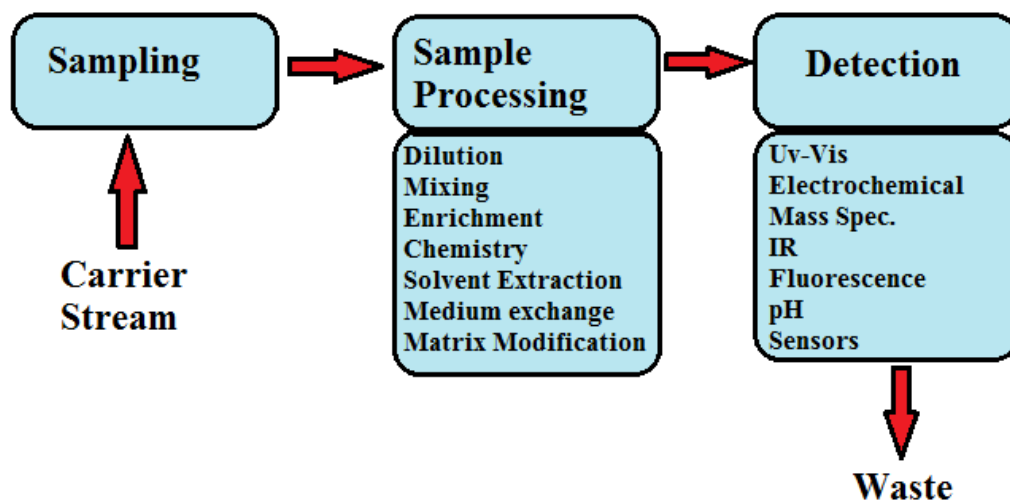


Figure 1.12. General description of FIA (GlobalFIA, 2013).

FIA system usually consists of a high quality multichannel peristaltic pump, an injection valve, a coiled reactor and a detector such as photometric or amperometric flow cells. The most common manifold configurations can be single-stream, two stream, and three stream manifolds. A simple two-line manifold is shown in Figure 1.13 (McKelvie, 1999).

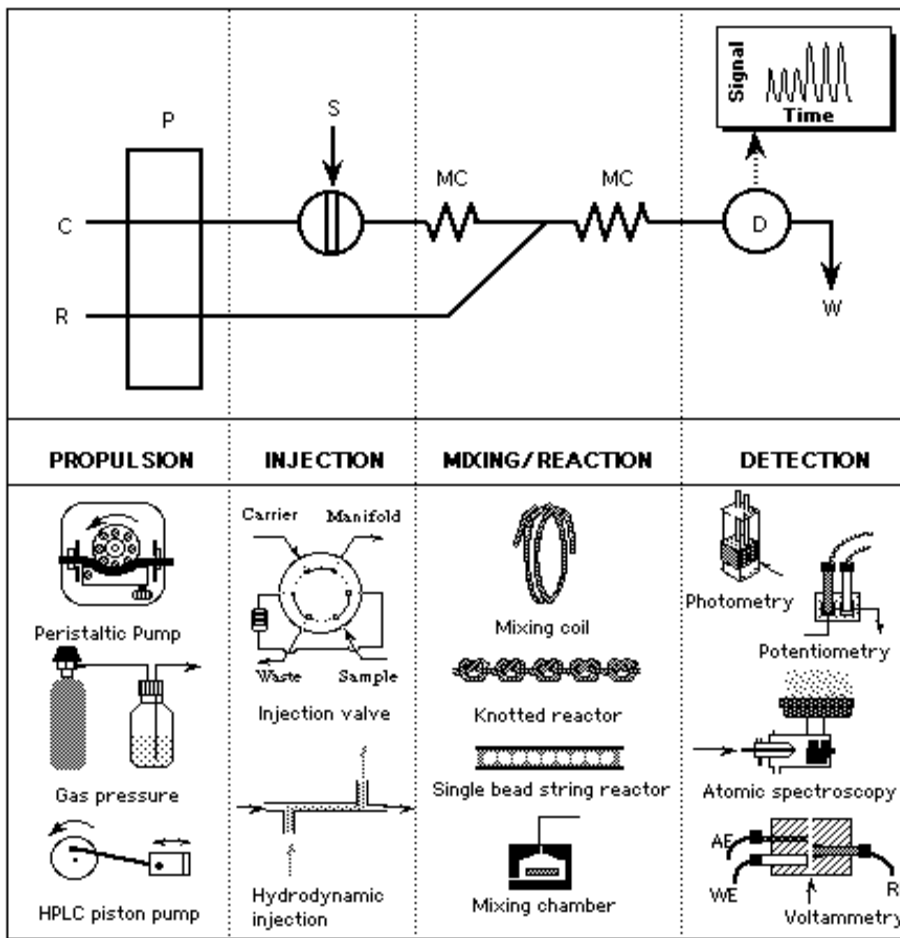


Figure 1.13. Schematic diagram of a typical FIA manifold (top) and its components (bottom). P is a pump, C and R are carrier and reagent lines respectively, S is sample injection, MC's are mixing coils, D is a flow through detector, and W is the waste line (McKelvie, 1999).

FIA has many advantages over conventional manual techniques. These advantages were described by Ruzicka and Hansen as follows (Ruzicka and Hansen, 2000)

1. Automated sample processing which provides high sample throughput (50 to 300 samples per hour) and reduced residence times (reading time is about 3 to 40 s),
2. High repeatability and great precision due to mechanical performance of the assays,
3. Adaptability to microminiaturization,
4. Containment of chemicals,

5. Reagent economy (considerable decrease in sample (normally using 10 to 50 μL) and reagent consumption) and waste reduction,
6. Controlling the timing (kinetic advantage) allows us to exploit reaction rates of different chemical reactions to increase the selectivity of the assay,
7. Simplicity and low cost instrumentation,
8. Availability of instrumentation in almost all laboratories,
9. Reproducibility (usually less than 2% RSD), reliability, low carry over, high degree of flexibility, and ease of automation.

Due to these important advantages in chemical analysis, many researchers have focused on FIA. This is not only reflected in the large number of FIA articles which over the years have appeared in international Journals, but also in the scope, utility and applications of FIA in a variety of areas (Hansen, 1996). Electrocatalytic and photoelectrocatalytic oxidation of NADH have also been studied in FIA system. However, according to our search of the literature, photoelectrochemical biosensors dependent on NAD^+/NADH and dehydrogenase enzyme has not been studied yet. One of the aims of this thesis is the construction of photoelectrochemical biosensors in the FIA system.

1.6. Cyclic Voltammetry

Cyclic Voltammetry (CV) is one of the most frequently used and perhaps the most versatile electroanalytical technique for the study of electroactive compounds, because CV has ability to rapidly provide considerable information on the thermodynamics of redox processes, on the kinetics of heterogeneous electron-transfer reactions, and on coupled chemical reactions or adsorption processes. Therefore, the first performed experiment in electroanalytical studies is often CV. In the CV, the potential of a stationary electrode in unstirred solution is scanned linearly using a triangular potential wave form (Wang, 2006). So, the electrode potential is ramped linearly to a more negative potential, and then ramped in reverse back to the starting voltage. The forward scan produces a current peak for any analytes that can be reduced through the range of the potential scan. The current will increase as the potential reaches the reduction potential of the analyte, then falls off as the concentration of the analyte is depleted close to the electrode surface. As the applied potential is reversed, it will reach a potential that will reoxidize the product formed in the first reduction

reaction, and produce a current of reverse polarity from the forward scan. This oxidation peak will usually have a similar shape to the reduction peak. During the potential sweep, the potentiostat measures the current resulting from the applied potential. The resulting current-potential plot is termed a *cyclic voltammogram*. The cyclic voltammogram is a complicated, time-dependent function of a large number of physical and chemical parameters (Wang, 2006).

The important parameters in a cyclic voltammogram are the peak potentials (E_{pc} , E_{pa}) and peak currents (i_{pc} , i_{pa}) of the cathodic and anodic peaks, respectively. The value of the peak potential (E_p) is an important diagnostic to characterize the electrode reaction. When the rate of electron transfer is fast, the E_p value will be independent of the scan rate. Such a reaction is said to be “reversible”. At 25°C, the peak current for a reversible couple is given by Randles-Sevcik equation;

$$i_p = 2.686 \times 10^{-5} n^{3/2} A C D^{1/2} \nu^{1/2} \quad (1.16)$$

where, i_p is the peak current (A), A is the electrode area (cm^2), D is the diffusion coefficient ($\text{cm}^2 \text{s}^{-1}$), C is the bulk concentration in mol cm^{-3} and ν is the scan rate of applied potential. The current is directly proportional to the concentration of electroactive species and increases with the square root of the scan rate. The ratio of the reverse-forward peak currents, i_{pr}/i_{pf} , is unity for a simple reversible couple. This peak ratio can be strongly used by chemical reactions of the peaks on the potential axis (E_p), which is related to the formal potential of the redox process. The potential difference between the peaks (peak separation) (ΔE_p , 1.17) can be used to determine the number of electrons transferred.

$$\Delta E_p = |E_{pa} - E_{pc}| = 2.303 RT / nF \quad (1.17)$$

For a reversible redox reaction at 25°C with n electrons, ΔE_p should be $59.2/n$ mV or about 60 mV for one electron. In practice this value is difficult to attain because of such factors as cell resistance. Irreversibility due to a slow electron transfer rate results in $\Delta E_p > 59.2/n$ mV, greater, say, than 70 mV for a one-electron reaction. The formal reduction potential (E°) for a reversible couple is given by:

$$E^\circ = \frac{E_{pc} + E_{pa}}{2} \quad (1.18)$$

In the irreversibility, the rate of electron transfer is sufficiently slow so that the potential no longer reflects the equilibrium activity of the redox couple of the electrode surface for irreversible processes; the individual peaks are reduced in size and widely separated. Totally irreversible systems are characterized by a shift of the peak potential with the scan rate. The peak potential and half potential at 25°C will differ by $48/\alpha n$ mV. The peak current, given by

$$i_p = (2,99 \times 10^{-5}) n(\alpha n_a)^{1/2} ACD^{1/2} \nu^{1/2} \quad (1.19)$$

is proportional to the bulk concentration, but will be lower in height. Where α is the transfer coefficient and n_a is the number of electrons involved in the charge-transfer step (Greef et al., 1985)

As a result, CV helps us to determine the rates of many oxidation-reduction reactions and allows us to study electrode surface and how they are affected by these reactions. It is useful in determining electroactivity of compounds. Moreover, CV gives very useful information for the study of redox process, for understanding reaction intermediates and for obtaining stability of reaction products. Therefore, electrochemical studies generally include cyclic voltammograms. Cyclic voltammetric technique was used in the some steps of this thesis, such as electropolymerization of mediators on GCE, voltammetric characterization of modified electrodes and photoelectrocatalytic study of NADH with these modified electrodes, etc.

1.7. Chronoamperometry

Chronoamperometry is an electrochemical technique in which the potential of the working electrode is stepped and the resulting current from faradic processes occurring at the electrode (caused by the potential step) is monitored as a function of time. Chronoamperometry involves stepping the potential of the working electrode from a value at which no faradaic reaction occurs to a potential at which the surface concentration of the electroactive species is effectively zero (Figure 1.14a). A stationary working electrode and unstirred (quiescent) solution are used. The resulting current–time dependence is monitored. As mass transport under these conditions is solely by diffusion, the current–time curve reflects the change in the concentration gradient in the vicinity of the surface. This involves a gradual expansion of the diffusion layer associated with the depletion of the reactant, and hence decreased slope of the concentration profile as time progresses (Figure 1.14b).

Chronoamperometry is often used for measuring the diffusion coefficient of electroactive species or the surface area of the working electrode. Some analytical applications of chronoamperometry (e.g., in vivo bioanalysis) rely on pulsing of the potential of the working electrode repetitively at fixed time intervals. Chronoamperometry can also be applied to the study of mechanisms of electrode processes (Wang, 2006).

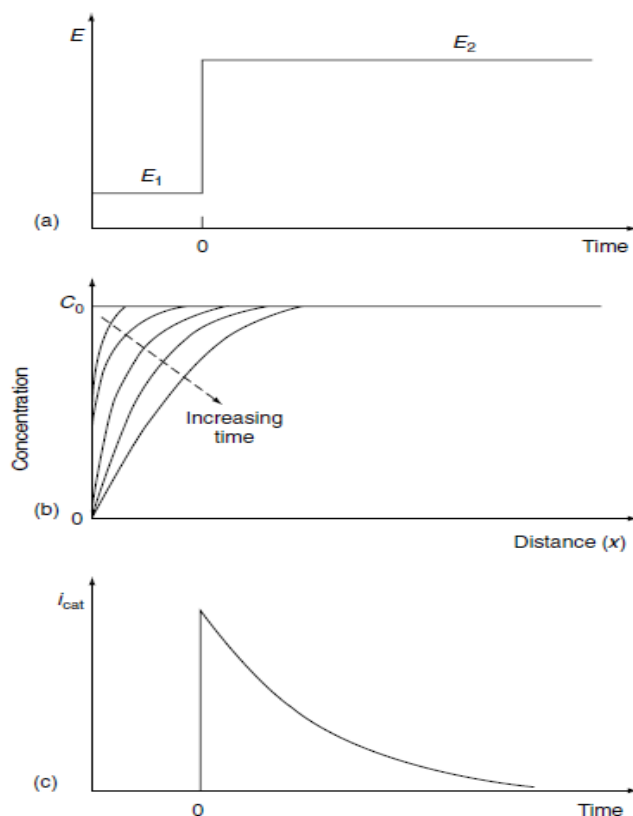


Figure 1.14. Chronoamperometric method: (a) potential–time waveform; (b) change in concentration profiles as time progresses; (c) the resulting current–time response (Wang, 2006).

Chronoamperometry experiments are most commonly either single potential step, in which only the current resulting from the forward step (as described above) is recorded, or double potential step, in which the potential is returned to a final value (E_f) following a time period, usually designated as τ , at the step potential (E_s). The most useful equation in chronoamperometry is the Cottrell equation (1.20), which describes the observed current (at a planar electrode) at any time following a large forward potential step in a reversible redox reaction (or to large overpotential) as a function of time, t (Figure 1.14c).

$$i(t) = \frac{n F A C D^{1/2}}{\pi^{1/2} t^{1/2}} = k t^{-1/2} \quad (1.20)$$

where n is the stoichiometric number of electrons involved in the reaction, F is the Faraday's constant (96485 Coulombeq⁻¹), A is the electrode area (cm²), C is the concentration of electroactive species (mol cm⁻³), and D is the diffusion constant for electroactive species (cm²s⁻¹).

In this thesis, a single potential step was used with FIA system for photoelectrochemical analysis.

1.8. The Importance of Thesis

It can be concluded that photoelectrochemistry offers a great advantage for the improvement of sensitivity. Thus we considered that, photoelectrocatalytic oxidation of NADH and photoelectrochemical biosensor dependent on NADH can be also constructed using CMEs with some redox mediators such as azine type dyes, catechol or quinone compounds. Our literature search demonstrated that there are a few papers on photoelectrocatalytic oxidation of NADH and photoelectrochemical biosensors dependent on NADH with modified electrodes. However, there is no report on photoelectrochemical biosensor studies in FIA system. In this context, the present work aimed at the photoelectrocatalytic determination of NADH in FIA system using a photoelectrochemical flow cell with a suitable transparent window for the irradiation of the electrode surface and construction of photoelectrochemical biosensors using modified electrodes. In order to perform this research, HT (a catechol compound), NR (a phenazine dye), MdB (a phenoxazine dye) and MG (a phenothiazine dye) were selected as redox mediators due to their good electrocatalytic effect on the NADH oxidation. Thus the experimental studies can be summarized in the four steps below:

1. The preparation of modified electrodes
2. The characterization of modified electrodes
3. Electrocatalytic and photoelectrocatalytic oxidation of NADH
 - a. with cyclic voltammetry
 - b. with chronoamperometry
 - c. in FIA system
4. Construction of photoelectrochemical biosensor and application to FIA system.

2. MATERIALS AND METHODS

2.1. Apparatus

Cyclic voltammetric and chronoamperometric measurements were performed at room temperature in a traditional three electrode system (Figure 2.1A). A platinum wire was used as the counter electrode, an home-made Ag/AgCl (saturated KCl) electrode as the reference electrode and a PTFE-shrouded GCE (MF2040 Bioanalytical system, 3 mm diameter) as the working electrode. However, an Ag/AgCl (0.1 M KCl) was used as reference electrode for the chronamperometric measurements in FIA system.

All electrochemical experiments were carried out using two voltammetric instruments, Compactstat Electrochemical Interface (Ivium Technologies, Eindhoven, Netherlands) and Autolab PGSTAT302N Potentiostat/Galvanostat. The pH of the solutions was measured using a Hanna HI 221 pH-meter with a combined glass electrode (Hanna HI 1332). The system was adjusted with standard buffer solutions. In order to record cyclic voltammograms during photoelectrochemical experiments, a fiberoptic illuminator 250 W halogen bulb with Foi-5 Light Guide (Titan Tool Supply Inc., USA) was used to irradiate the electrode surface and a home-made photoelectrochemical cell, which was constructed of Teflon, shown in Figure 2.1B (Dilgin, 2004).

A Perkin Elmer Lambda 35 Uv-Vis Spectrometer was used for measuring the absorbance of the NADH solutions at 340 nm. A Bandelin Sonorex RK 100H Ultrasonic bath was used for cleaning procedure of the GCEs before their modification. Deionized water was supplied by a Milli-Q device (Millipore, Bedford, USA) for the preparation of solutions and cleaning of glasses.

In order to perform FIA experiments, an eight-channel Ismatec, Ecoline peristaltic pump with polyethylene tubing (0.75mm i.d.), and a Rheodyne 8125 sample injection valve were used. A new home-made photoelectrochemical flow cell was constructed from Teflon and the schematic diagram of FIA is given in Figure 2.2 (Dilgin, 2004).

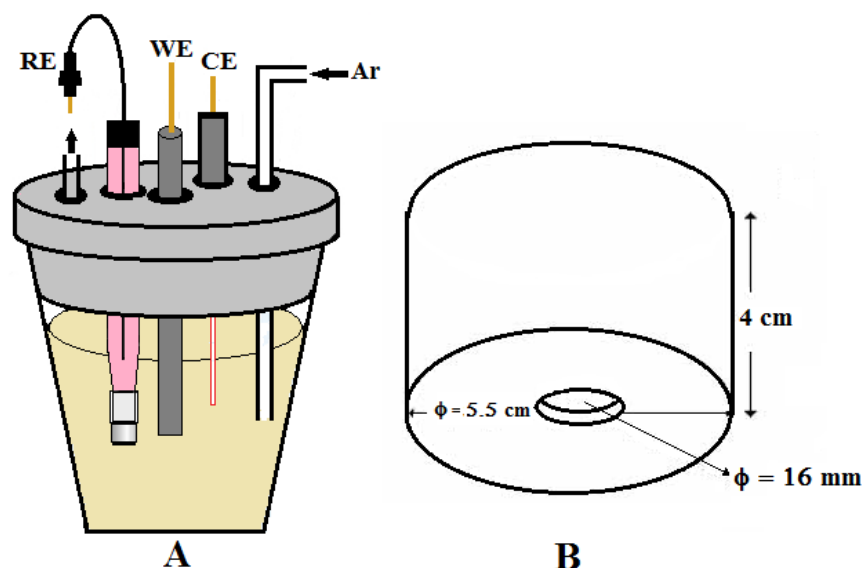


Figure 2.1. A) Electrochemical cell with three electrode system WE: working electrode (GCE or modified GCE), CE: counter electrode (Pt wire), RE: reference electrode (Ag/AgCl(sat. KCl)). B) Home-made photoelectrochemical cell (Dilgin, 2004).

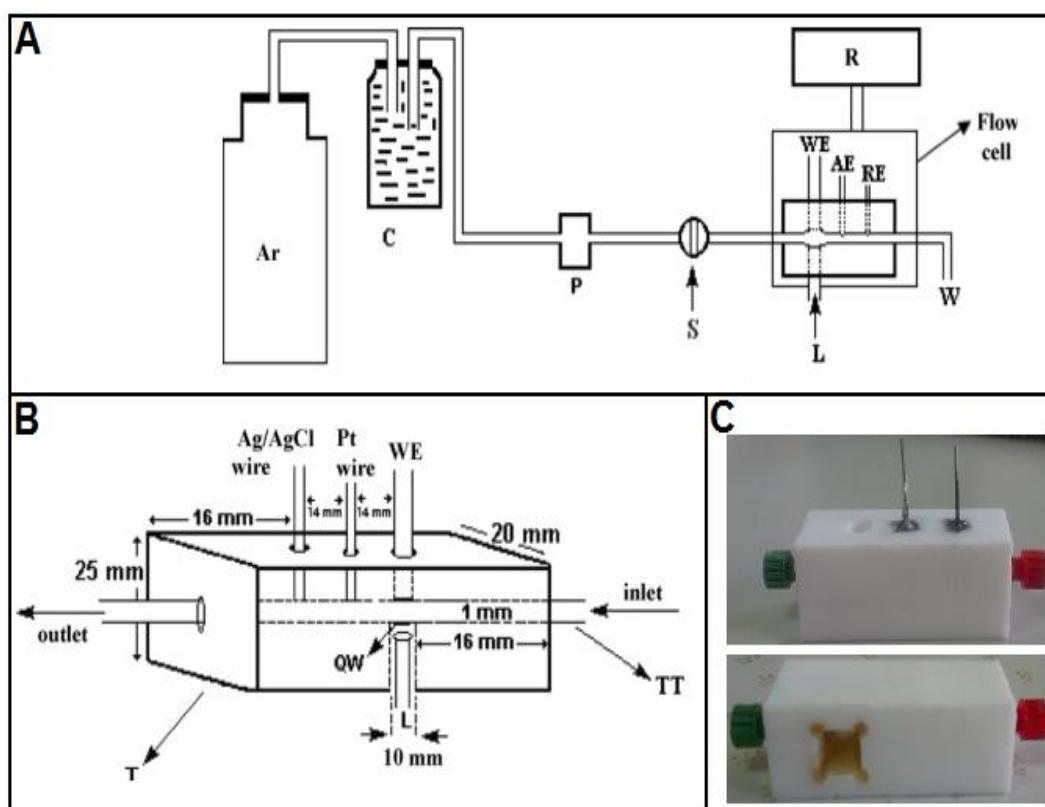


Figure 2.2. A) Schematic diagram of the FIA manifold, C: carrier stream, P: peristaltic pump, S: sampling valve, L: light source, W: waste, R: recorder, WE: working electrode, AE: auxiliary electrode, RE: reference electrode. B) Schematic diagram of photoelectrochemical flow cell, T: Teflon block, L: light source, TT: transmission tube, QW: quartz window (Dilgin, 2004) and C) Its images in different perspectives.

2.2. Reagents and Solutions

2.2.1. Chemicals

Glucose dehydrogenase enzyme from *Pseudomonas* sp. (GDH, 338.7 U mg⁻¹), β -Nicotinamide adenine dinucleotide sodium salt from *Saccharomyces cerevisiae* (C₂₁H₂₆N₇NaO₁₄P₂, NaNAD⁺, MW: 685.41 g mol⁻¹), Bovine serum albumin (BSA), glutaraldehyde (GA, d: 1.061 g mL⁻¹, MW: 100.12 g mol⁻¹, 25% w/w in water) and PAMAM Dendrimer, ethylenediamine core, generation 4.0 (d: 0.813 g mL⁻¹, MW: 14214.17 g mol⁻¹, 10% w/w in methanol) were supplied from Sigma-Aldrich (St. Louis, USA). D-Glucose, β -Nicotinamide adenine dinucleotide, reduced disodium salt (MW: 709.40 g mol⁻¹ C₂₁H₂₇N₇Na₂O₁₄P₂, NADHNa₂), Hematoxyline, (HT, C₆H₁₄O₆), Methylene green (MG, C₁₆H₁₇ClN₄O₂S.1/2ZnCl₂), and Neutral red (NR, C₁₅H₁₇ClN₄) were supplied from Merck (Steinheim, Germany). Other used chemicals such as HNO₃ (65%, 1.39 g mL⁻¹), HCl (30%, 1.15 g mL⁻¹), H₃PO₄ (85%, 1.71 g mL⁻¹) KCl, NaH₂PO₄.2H₂O, Na₂HPO₄.2H₂O, NaOH, NaNO₃, methanol and ethanol were purchased from Merck or Sigma-Aldrich Companies and they were also of analytical reagent grade. Deionized water supplied by a Milli-Q device (Millipore, Bedford, USA) throughout all experiments.

2.2.2. Preparation of solutions

2.2.2.1. Stock solutions

i. Stock solution of Na₂NADH (5.0x10⁻² M): Stock solution of NADH was freshly prepared in phosphate buffer solution (PBS) (pH 7.0) and kept in the refrigerator at 4°C. For this, an appropriate amount of Na₂NADH was dissolved in 500 μ L pH 7.0 PBS (pH 7.0) in an eppendorf tube (1 mL). The concentration of NADH in the diluted solutions was checked monitoring the absorbance of the solution at 340 nm and considering a molar extinction coefficient of 6600 cm⁻¹M⁻¹ (Kubota and Gorton, 1999).

ii. Stock solution of HT (1.0x10⁻² M): Stock solution of HT was freshly prepared in absolute ethanol. For this, an appropriate amount of HT was dissolved in a few mL of ethanol and diluted to 10 mL.

iii. Stock solution of MG (1.0×10^{-2} M): Stock solution of MG was freshly prepared in 0.1 M H_3PO_4 containing 0.1 M NaNO_3 . For this, an appropriate amount of MG was dissolved in a few mL of 0.1 M H_3PO_4 containing 0.1 M NaNO_3 and diluted to 10 mL.

iv. Stock solution of NR (1.0×10^{-2} M): Stock solution of NR was freshly prepared in 0.1 M H_2SO_4 containing 0.1 M NaNO_3 . For this, an appropriate amount of NR was dissolved in a few mL of 0.1 M H_2SO_4 containing 0.1 M NaNO_3 and diluted to 10 mL.

v. Stock solution of Glucose (1.0 M): Stock solution of glucose was freshly prepared in PBS (pH 7.0). For this, an appropriate amount of glucose was dissolved in a few mL of buffer solution and diluted to 10 mL.

vi. Stock solution of NAD^+ (1.0 M): Stock solution of NaNAD^+ was freshly prepared in PBS (pH 7.0). For this, an appropriate amount of NaNAD^+ was dissolved in a few mL of buffer solution and diluted to 10 mL.

2.2.2.2. Supporting electrolyte solutions

i) Solutions used during electropolymerization:

i₁. 0.1 M H_3PO_4 containing 0.1 M NaNO_3 : A mixture of 6.74 mL concentrated H_3PO_4 and 8.4990 g NaNO_3 was dissolved and then was diluted to 1.0 L with deionized water.

i₂. 0.1 M H_2SO_4 containing 0.1 M NaNO_3 : A mixture of 5.58 mL concentrated H_2SO_4 and 8.4990 g NaNO_3 was dissolved and then was diluted to 1.0 L with deionized water.

i₃. 0.1 M HCl containing 0.1 M NaNO_3 : A mixture of 8.29 mL concentrated HCl and 8.4990 g NaNO_3 was dissolved and then was diluted to 1.0 L with deionized water.

i₄. Phosphate buffer and phosphate solutions: Phosphate buffer and phosphate solutions (0.1 M) of one liter with various pH values (2-10) were prepared by proper mixing stock standard solutions of $\text{NaH}_2\text{PO}_4 \cdot 2\text{H}_2\text{O}$, $\text{Na}_2\text{HPO}_4 \cdot 2\text{H}_2\text{O}$, H_3PO_4 and NaOH containing 0.1 M NaNO_3 by controlling the pH meter. These stock solutions were defined at below:

0.1 M H_3PO_4 containing 0.1 M $NaNO_3$: Defined in i_1 procedure.

0.1 M $NaOH$ containing 0.1 M $NaNO_3$: A mixture of 4.0000 g $NaOH$ and 8.499 g $NaNO_3$ was dissolved in deionized water and then was diluted to 1.0 L.

0.1 M NaH_2PO_4 containing 0.1 M $NaNO_3$: A mixture of 15.6200 g $NaH_2PO_4 \cdot 2H_2O$ and 8.4490 g $NaNO_3$ was dissolved in deionized water and then was diluted to 1.0 L.

0.1 M Na_2HPO_4 containing 0.1 M $NaNO_3$: A mixture of 17.7990 g $Na_2HPO_4 \cdot 2H_2O$ and 8.4490 g $NaNO_3$ was dissolved in deionized water and then was diluted to 1.0 L.

The procedure of electropolymerization of HT, MG and NR was always carried out in supporting electrolyte containing 0.1 M $NaNO_3$.

ii. Solutions used during electrocatalytic and photoelectrocatalytic oxidation of NADH:

0.1 M phosphate buffer (pH 7.0) 0.1 M PBS (pH 7.0) of one liter was prepared by proper mixing stock standard solutions of $NaH_2PO_4 \cdot 2H_2O$ and $Na_2HPO_4 \cdot 2H_2O$ not containing 0.1 M $NaNO_3$ by controlling the pH meter.

0.1 M NaH_2PO_4 : 15.6200 g $NaH_2PO_4 \cdot 2H_2O$ was dissolved in deionized water and then was diluted to 1.0 L

0.1 M Na_2HPO_4 : 17.7990 g $Na_2HPO_4 \cdot 2H_2O$ was dissolved in deionized water and then was diluted to 1.0 L.

iii. Solutions used in FIA system :

0.1 M phosphate buffer (pH 7.0) containing 0.1 M KCl : 7.4550 g KCl was dissolved and then was diluted to 1.0 L with 0.1 M PBS (pH 7.0) not containing 0.1 M $NaNO_3$.

2.2.2.3. Solutions used in immobilization of enzyme

All used solutions in this step were freshly prepared.

i. 5 $mg mL^{-1}$ GDH enzyme solution: 1 mg of GDH enzyme was dissolved in 200 μL of 0.1 M PBS (pH 7.0).

ii. %1 BSA solution: 10 mg BSA was dissolved in 100 μL of 0.1 M PBS (pH 7.0).

iii. 100 mM GA stock solution: 189 μL GA solution (d: 1.061 g/mL, MW: 100.12 g/mol, 25% w/w about 2.7 M) was diluted to 5 mL with 0.1 M PBS (pH 7.0).

iv. 20 mM GA solution: 200 μL GA stock solution (100 mM) was diluted to 1 mL with 0.1 M PBS (pH 7.0).

v. 2 mg mL⁻¹ PAMAM solution: 24.6 μL PAMAM (d: 0.813 g mL⁻¹, 10% w/w in methanol) was diluted to 1 mL with methanol.

2.3. Procedures

2.3.1. Preparation of modified electrodes

Prior to electropolymerization of mediators onto GCE, GCEs were mechanically polished using a BAS-polishing kit with aqueous 1.0, 0.3 and 0.05 μm alumina (Al_2O_3) slurry on a polishing cloth for three min to a mirror-like surface. After they were washed with deionized water, they were cleaned by sonication in ethanol and deionized water for 5 min, respectively.

Clean GCEs were modified with HT (catechol group), MG (phenothiazine group), MB (phenoxazin group) and NR (phenazine group) by electropolymerization procedure which includes recording successive cyclic voltammograms of each mediator onto GCE.

In order to obtain the best electrocatalytic response of modified electrodes towards oxidation of NADH, the influence of the supporting electrolyte, monomer concentration, cycle number and anodic potential limit during the electropolymerization of HT, MG, MB and NR was examined and optimized. These modified electrodes were used for the investigation of electrocatalytic and photoelectrocatalytic oxidation of NADH after rinsing with deionized water.

All supporting electrolytes were deaerated by allowing highly pure argon to pass through for 5 min before the electrochemical experiments.

2.3.1.1. Optimization of supporting electrolyte

Electropolymerization of mediators (0.3, 0.5, 0.05 and 0.01 mM for HT, MG, NR and MB, respectively) was carried out on the GCE in the various supporting electrolyte such as 0.1 M H₂SO₄, 0.1 M H₃PO₄, 0.1 M HCl, 0.1 M PBS and 0.1 M phosphate solutions (pH between 2 and 10) containing 0.1 M NaNO₃. Optimization steps are given below item.

i. Recording cyclic voltammograms of supporting electrolyte: Cyclic voltammograms of GCE were recorded in each supporting electrolyte (10 mL) in the potential range between -0.5 and +2.0 V for HT and -0.7 and +1.2 V for other mediators at 100 mVs⁻¹ scan rate.

ii. Electropolymerization process: The electropolymerization of each mediator onto GCE was carried out by recording 10 successive cyclic voltammograms in the potential range between -0.5 and +2.0 V for HT and -0.7 and +1.2 V for other mediators at 100 mVs⁻¹ scan in above mentioned each supporting electrolyte. After electropolymerization, modified GCEs were washed with deionized water.

iii. Electrochemical behavior of NADH at these modified electrodes: Cyclic voltammograms of all modified electrodes prepared in the each supporting electrolyte were recorded in the absence and also presence of 0.8 mM NADH for poly-HT modified GCE and 0.4 mM NADH for other modified electrodes (Poly-MG; Poly-MdB and Poly-NR modified GCEs) in 0.1 M PBS (pH 7.0) and at 50 mV/s scan rate in the potential range between -0.8 and + 0.8 V vs. Ag/AgCl. Cyclic voltammograms of bare electrode were also recorded in the same condition, and electrochemical behavior of NADH at modified electrodes was compared to bare electrodes.

2.3.1.2. Optimization of monomer concentration

Electropolymerization of various concentrations of mediators was carried out on the GCE in the most suitable supporting electrolyte, above mentioned, supporting electrolyte optimization step for each mediator. Optimization steps are given below item.

i. Recording cyclic voltammograms of supporting electrolyte: Cyclic voltammograms of GCE were recorded in the optimized supporting electrolyte (10 mL) and in the potential range between -0.5 and +2.0 V for HT and -0.7 and +1.2 V for other mediators at 100 mVs^{-1} scan rate.

ii. Electropolymerization process: Firstly, a proper amount of stock solution of mediators was added to most suitable supporting (10 mL) electrolyte, which was optimized for each mediator. Then, 10 successive cyclic voltammograms of each monomeric mediator with various concentrations were recorded in the potential range between -0.5 and +2.0 V for HT and -0.7 and +1.2 V vs. Ag/AgCl for other mediators at 100 mVs^{-1} scan rate. After electropolymerization, modified GCEs were washed with deionized water.

iii. The third step mentioned in supporting electrolyte optimization procedure was repeated by using all obtained electrodes from monomer optimization step.

2.3.1.3. Optimization of cycle number

The effect of the cycle number was investigated on electropolymerization of each mediator by recording cyclic voltammograms with different cycle numbers in the most suitable supporting electrolyte and in the presence of most suitable monomer concentration of mediator, which was defined above mentioned supporting electrolyte and monomer concentration optimization steps for each mediator. Optimization steps are given below item.

i. Recording cyclic voltammograms of supporting electrolyte: The same procedure mentioned in the first step of optimization of monomer concentration procedure was repeated for each mediator.

ii. Stock Electropolymerization process: Modified electrodes were obtained in optimized most suitable concentration of mediator at the previous step at different cycle numbers in the potential range between -0.5 and +2.0 V for HT and -0.7 and +1.2 V vs. Ag/AgCl for other mediators at 100 mVs^{-1} scan rate by cyclic voltammetry. After electropolymerization, modified GCEs were washed with deionized water.

iii. The third step mentioned in supporting electrolyte optimization procedure was repeated by using all obtained electrodes from cycle number optimization step.

2.3.1.4. Optimization of potential range

The potential range is very important for the electropolymerization. Particularly, the upper potential values of the anodic potential have a major effect on polymerization. Thus, the effect of anodic upper potential value during electropolymerization step on the electrocatalytic oxidation of NADH at all modified electrodes was investigated. Optimization steps are given below item.

i. Recording cyclic voltammograms of supporting electrolyte: The same procedure mentioned in the first step of optimization of monomer concentration procedure was repeated for each mediator in each studied potential range.

ii. Electropolymerization process: The electropolymerization of each mediator onto GCE was carried out by recording cyclic voltammograms in the different potential ranges at 100 mVs^{-1} scan rate by using above mentioned optimized parameters such as supporting electrolyte; monomer concentration and cycle number for each mediator (Table 2.1). After electropolymerization, modified GCEs were washed with deionized water.

iii. The third step mentioned in supporting electrolyte optimization procedure was repeated by using all obtained electrodes from potential range optimization step.

All optimized parameters are shown in Table 2.1 for each mediator.

Table 2.1. Optimized parameters for electropolymerization of each mediator.

Modified electrode	Supporting electrolyte	Monomer concentration	Cycle Number	Potential range
Poly-HT/GCE	0.1 M pH 7.0 PBS containing 0,1 M NaNO ₃	0.30 mM	10	(-0.5)-(+2.0) V
Poly-MG/GCE	0.1 M H ₃ PO ₄ solution containing 0,1 M NaNO ₃	0.50 mM	10	(-0.7)-(+1.1) V
Poly-NR/GCE	0.1 M H ₂ SO ₄ solution containing 0,1 M NaNO ₃	0.01 mM	8	(-0.6)-(+1.1) V
Poly-MdB/GCE	Electropolymerization of MdB was not succesfull for all parameters.			

2.3.2. Characterization of modified electrodes

After all modified electrodes were obtained, their electrochemical characterization was investigated by recording their cyclic voltammogram in 0.1 M PBS (pH 7.0) in the potential range between -0.8 and $+0.8$ V vs. Ag/AgCl.

The effect of pH on the peak currents and the formal standard potentials ($E^{0'}$) of all modified electrodes was investigated by recording cyclic voltammograms of each modified electrode in phosphate buffers or phosphate solutions in the pH range between 2 and 9 at a 50 mVs^{-1} scan rate.

The effect of scan rate on voltammetric behavior of each modified electrode was investigated by recording cyclic voltammograms of each modified electrodes in phosphate buffers or phosphate solutions of pH values 3, 5, 7, 8 and 9 at the scan rate range between 20 and 6400 mVs^{-1} .

In order to determine the stability of each modified electrode, 200-300 successive cyclic voltammograms of each modified electrode were recorded in 0.1 M PBS (pH 7.0) at a 50 mVs^{-1} scan rate.

2.3.3. Electrocatalytic and photoelectrocatalytic oxidation of NADH using modified electrodes

After all modified electrodes were characterized by electrochemical methods, the electrocatalytic and photoelectrocatalytic oxidation of NADH was investigated by using these modified electrodes. For this, both cyclic voltammetric and amperometric techniques were used.

i. With cyclic voltammetry

Firstly, cyclic voltammograms of each modified electrode were recorded in 0.1 M PBS (pH 7.0) in the potential range between -0.8 and $+0.8$ V vs. Ag/AgCl at a scan rate of 50 mVs^{-1} in the absence of NADH. In order to see electrocatalytic effect of modified electrodes towards NADH oxidation, cyclic voltammograms of modified electrodes were recorded in the same conditions but in the presence of 0.8 mM for poly-HT/GCE and 0.4 mM for other modified electrodes. The cyclic voltammograms in the same conditions were also recorded for bare GCE.

Finally, photoelectrocatalytic oxidation of NADH was investigated by using a home-made photoelectrochemical cell as shown in Fig 2.1B, in which the working electrode surface was irradiated by the light source. In the photoelectrocatalytic experiments, the cyclic voltammograms of each modified electrode were recorded under the above mentioned same conditions (supporting electrolyte: 0.1 M PBS (pH 7.0), scan rate: 50 mVs⁻¹, potential range from -0.8 to +0.8 V) in the absence and presence of NADH, but under irradiation of the working electrode surface by the fiberoptic illuminator with 250 W halogen bulb.

ii. With Amperometric Method

In order to perform amperometric studies, firstly the optimum applied potential of each modified electrode for electrocatalytic oxidation of NADH was determined. With this aim, the current-time curves of each modified electrode were recorded at various applied potential between -100 and +600 mV in the absence and presence of 0.2 mM NADH with and without irradiation of electrode surface in the 0.1 M PBS (pH 7.0). Same procedure was repeated for bare electrode at various applied potentials between 0 and +800 mV for comparison.

To obtain calibration curve, the electrocatalytic and photoelectrocatalytic oxidation currents dependent on NADH concentration were monitored by recording amperometric curves of each modified electrode. For this, current-time curves of each modified electrode were recorded in 0.1 M PBS (pH 7.0) solution at obtained optimum potential. After obtaining a steady state background, proper amounts of stock NADH solution were successively added to supporting electrolyte in the range between 1x10⁻⁶ and 1x10⁻³ M NADH and the current-time curves dependent on NADH concentration were recorded before and after irradiation of the electrode surface. Calibration graph was obtained for both photoelectrocatalytic and electrocatalytic methods using these values.

2.3.4. Flow injection analysis procedure

In order to perform the studies of electrocatalytic and photoelectrocatalytic oxidation of NADH in FIA system, the home-made photoelectrochemical flow cell, which includes the traditional three electrodes system, as shown in Figure 2.2B, was used. In the photoelectrocatalytic flow injection study, only the working electrode surface was irradiated (Drop Sens). The used FIA system is demonstrated in Figure 2.2A.

In all FIA experiments, 0.1 M PBS (pH 7.0) containing 0.1 M KCl was used as carrier solution. AgCl-coated Ag wire diameter of 1 mm and Pt wire diameter of 1 mm was mounted directly onto the flow cell. Therefore the reference electrode was used as Ag/AgCl (0.1 M KCl). After each modified electrode had been inserted into a flow cell, some parameters such as applied potential, flow rate, column size and the sample loading volume were optimized. For this, the electrocatalytic and photoelectrocatalytic oxidation currents of a known standard solution of NADH were monitored for each modified electrodes dependent on above mentioned parameters. Injected standard NADH solution into FIA system was prepared in 0.1 M PBS (pH 7.0) containing 0.1 M KCl.

After all conditions for each electrode were optimized, electrocatalytic and photoelectrocatalytic oxidation currents of NADH were monitored dependent on NADH concentration. Thus, analytical figures of merits such as linearity range, limit of detection (LOD), limit of quantification (LOQ), etc. were determined. For this, after a steady-state background current of supporting electrolyte in the optimum conditions (for example, a sample loop of 100 μL , a flow rate of 1.3 mL min^{-1} , an applied potential of +300 mV vs. Ag/AgCl and a length of tubing of 10 cm was found to be the optimum values for poly-HT/GCE) was obtained, the various concentrations of NADH were injected into the system and the current–time curves were recorded. The current–time curves were also recorded for the photoamperometric FIA study by irradiation of electrode surface throughout experiment. In all FIA experiments, three injections were made for each NADH standard solution. Same experiments were also repeated for bare GCE. All supporting electrolytes were deaerated by allowing highly pure argon to pass through for 5 min before the electrochemical experiments commenced.

2.3.5. Construction of biosensor and photoelectrochemical biosensor

2.3.5.1. Immobilization of enzyme

Poly(amidoamine) (PAMAM) dendrimers have attracted increasing attention in recent years because of their unique structure and interesting properties. A highly branched dendritic macromolecule, PAMAM, possesses a unique surface with multiple chain ends, and the number of surface groups can be precisely controlled by choosing the appropriate synthetic generation. For

example, the fourth-generation (G4) PAMAM with a particle size of ca 5 nm possesses 64 surface amine groups per particle with excellent solubility in water (Zeng et al., 2007). In addition, the PAMAM dendrimer represents a friendly environment for the immobilization of enzymes, and it is stable and capable of generating high power density compared to other immobilization methods. Thus, in the enzyme immobilization procedure, G4-PAMAM was used.

In the enzyme immobilization procedure, firstly an aliquot of 4 μL 2 mg mL^{-1} PAMAM was cast onto the polished and cleaned bare GCE. After PAMAM was dried at room temperature for about 10 min, a polymer film of HT, which was selected as the best mediator for the electrocatalytic and photoelectrocatalytic oxidation of NADH, was prepared by recording successive cyclic voltammograms of HT on GCE in the potential range between -0.5 and $+2.0$ V in the 0.1 M PBS (pH 7.0) containing 0.1 M NaNO_3 at 100 mVs^{-1} . Then Poly-HT/PAMAM/GCE washed with deionized water and dried under Ar atmosphere and the glucose dehydrogenase (GDH) enzyme were immobilized directly on poly-HT/PAMAM/GCE by the cross-linking method using glutaraldehyde (GA) 20 mM. For this aim, firstly 5 mg mL^{-1} GDH and 1% BSA was mixed in a ratio 1:1 and then 5 μL of the mixture and 4 μL of GA were cast on poly-HT/GCE, respectively (Du et al., 2007; Saleh et al., 2011). Finally, this electrode was dried at 4°C in a refrigerator for at least 4 h. A schematic representation of the preparation of enzyme modified electrodes is given in Figure 2.3.

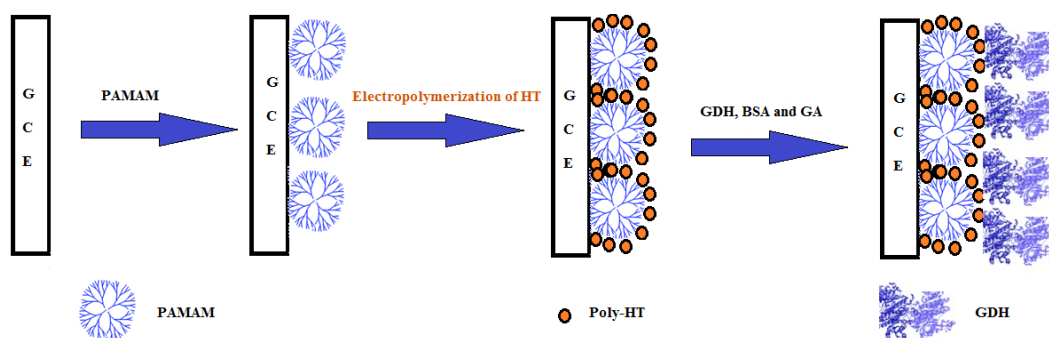


Figure 2.3. Schematic representation of enzyme immobilization procedure.

2.3.5.2. Biosensor and photoelectrochemical biosensor studies

Electrocatalytic and photoelectrocatalytic oxidation of glucose at this GDH based poly-HT/GCE was investigated using cyclic voltammetric techniques. Firstly, cyclic voltammogram of GDH-poly-HT/PAMAM/GCE was recorded in 0.1 M PBS (pH 7.0) containing 10 mM NAD^+ in the potential range between -0.8 and $+0.8$ V vs. Ag/AgCl at a scan rate of 5 mVs^{-1} in the absence of glucose. In order to see response of biosensor towards glucose, cyclic voltammograms of modified electrodes were recorded in the same conditions but in the presence of 10 mM glucose. The cyclic voltammograms in the same conditions were also recorded for bare GCE, poly-HT/GCE, poly-HT/PAMAM/GCE.

Finally, photoelectrochemical biosensor studies were performed by using the home-made photoelectrochemical cell as shown in Fig 2.1B. In the photoelectrocatalytic experiments, the cyclic voltammograms of GDH/poly-HT/PAMAM/GCE were recorded under the above mentioned same conditions (supporting electrolyte: 0.1 M PBS (pH 7.0), scan rate: 5 mVs^{-1} , potential range: from -0.8 to $+0.8$ V) in the absence and presence of glucose, but under irradiation of the working electrode surface by the fiberoptic illuminator with 250 W halogen bulb. The constructed biosensor and photobiosensor for glucose detection at GDH/poly-HT/PAMAM/GCE is schematically shown in Figure 2.4.

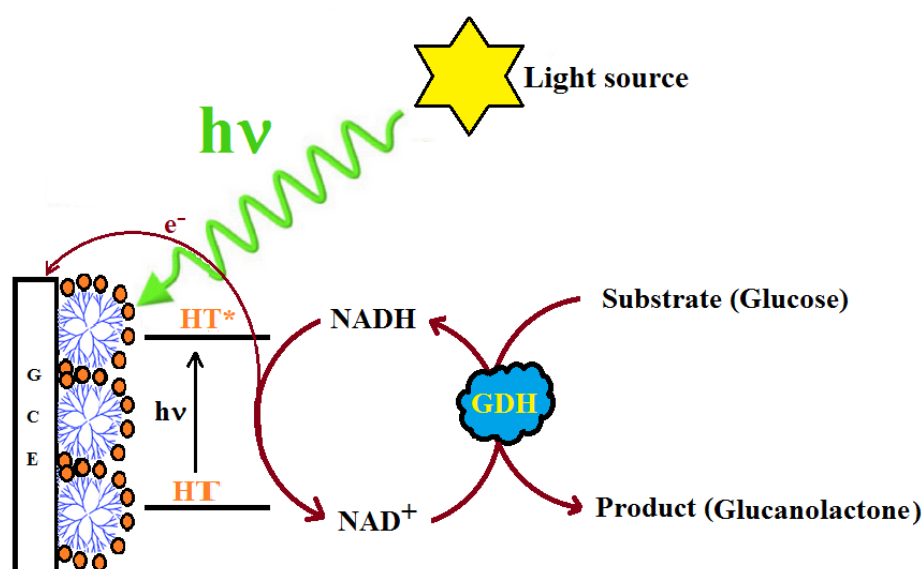


Figure 2.4. Schematic representation of the photoelectrochemical biosensor.

2.3.5.3. Photoelectrochemical biosensor studies in FIA system

The new home-made photoelectrochemical flow cell and FIA diagram, as shown in Figures 2.2B and 2.2A, were also used for studies of electrocatalytic and photoelectrocatalytic oxidation of glucose in FIA system. In all FIA experiments, 0.1 M PBS (pH 7.0) containing 0.1 M KCl was used as carrier solution. After GDH/poly-HT/PAMAM/GCE had been inserted into a flow cell, electrochemical and photoelectrochemical responses of glucose were monitored dependent on glucose concentration. For this, after a steady-state background current of supporting electrolyte under optimum conditions, which were optimized in the FIA procedure section, was obtained, the various concentrations of glucose containing 10 mM NAD⁺ were injected into the system and the current–time curves were recorded. The current–time curves were also recorded for the photoamperometric FIA study by irradiation of electrode surface throughout experiment. In all FIA experiments, three injections were made for each NADH standard solution. Same experiments were also repeated for bare GCE. All supporting electrolytes were deaerated by allowing highly pure argon to pass through for 5 min before the electrochemical experiments.

3. RESULTS AND DISCUSSION

3.1. Preparation of Modified Electrodes and Their Response towards Oxidation of NADH

All modified electrodes were prepared by electropolymerization of four different redox mediators (HT, MG, NR and MdB) onto GCE. In order to obtain the optimum modified electrode, which gives the best response for the electrocatalytic oxidation of NADH, the electropolymerization conditions such as pH of supporting electrolyte, monomer concentration, cycle number and especially anodic potential limit were optimized. In order to see the effect of each modified electrode on electrocatalytic oxidation of NADH, the cyclic voltammogram of NADH was recorded in 0.1 M PBS (pH 7.0) using each modified electrode obtained from optimization steps. Cyclic voltammograms were recorded a scan rate of 100 mVs^{-1} in all electropolymerization process, while a scan rate of 50 mVs^{-1} was used in the studies of electrocatalytic oxidation of NADH.

3.1.1. Poly-Hematoxylin modified glassy carbon electrode (Poly-HT/GCE)

In order to see the effect of used supporting electrolyte during the preparation of the modified electrode, poly-HT/GCEs were prepared in 0.1 M phosphate solutions containing 0.1 M NaNO_3 with various pH values (between 2 and 10). Then the cyclic voltammograms of NADH were recorded in 0.1 M PBS (pH 7.0) using each modified electrode. Figure 3.1A shows the typical cyclic voltammograms of the polymer film growth during the electropolymerization of 0.3 mM HT solution in 0.1 M PBS (pH 7.0) containing 0.1 M NaNO_3 . NaNO_3 was used as 0.1 M in the supporting electrolyte during all the electropolymerization process due to the catalytic effect of the NO_3^- anions on the electropolymerization process (Karyakin et al, 1999a). In the first cycle of cyclic voltammograms of HT (Figure 3.1A), one oxidation peak was observed at about +235 mV with a shoulder at +165 mV, which is attributed to the oxidation of monomeric catechol groups to quinone. In the second cycle, the current of this peak decreased. After the third cycle, the peak current began to grow slowly with increasing cycle numbers and peak potential was shifted to about +275 mV. Similar discussions were reported for electropolymerization of pyrogallol (Khoo and Zhu, 1998) and rutin (Jin et al., 2007), which are other catechol compounds.

Cathodic peak of HT at about -390 mV (Figure 3.1A) increased gradually with increasing scan cycles. These results demonstrated that the polymeric film of HT could be formed on GCE.

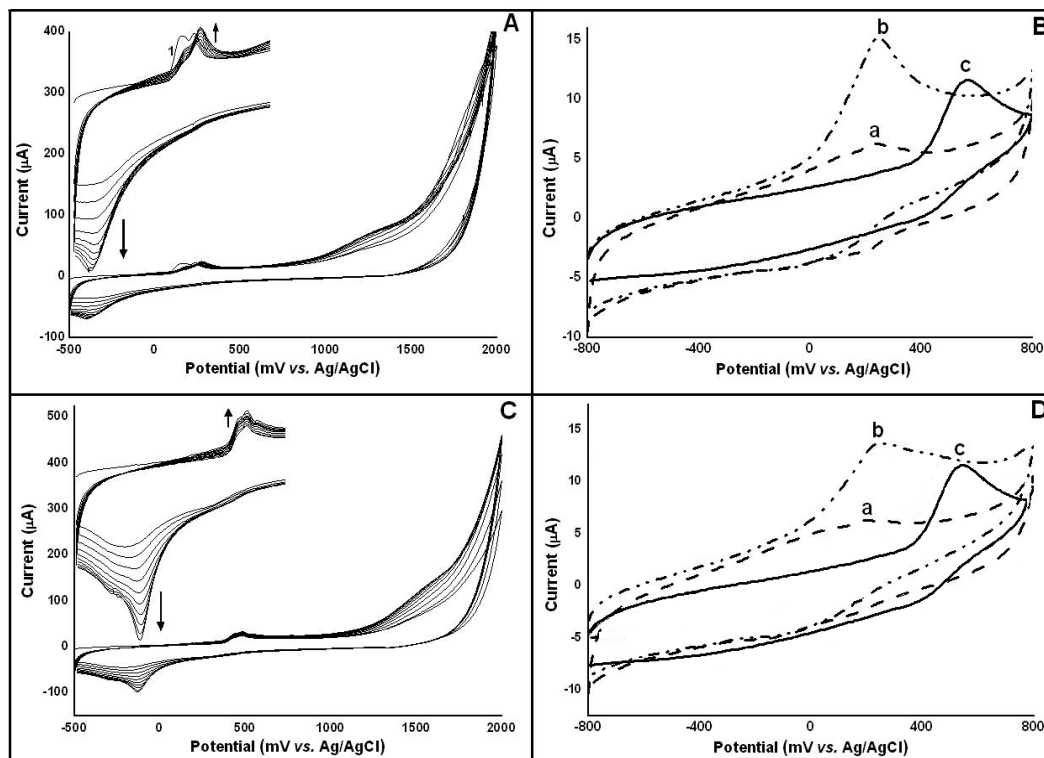


Figure 3.1. Repetitive cyclic voltammograms (10 cycles) of 0.3 mM HT at GCE in 0.1 M PBS with pH 7.0 (A) and pH 2.0 (C) containing 0.1 M NaNO₃ at 100 mVs⁻¹, in the potential range of -0.5 to +2.0 V vs. Ag/AgCl. B) and D) Cyclic voltammograms of poly-HT/GCE obtained from A and C respectively, in the absence (a) and in the presence (b) of 0.8 mM NADH c) the cyclic voltammograms of 0.8 mM NADH at bare GCE. Supporting electrolyte: 0.1 M PBS (pH 7.0); scan rate: 50 mVs⁻¹.

In the cyclic voltammogram of poly-HT/GCE in 0.1 M PBS (pH 7.0), two small reversible redox peaks were observed (Figure 3.1B, curve a). The formal potentials ($E^{\circ} = (E_{\text{an}} + E_{\text{cat}})/2$) of these pairs were found to be +120 mV and +225 mV. It can be concluded that these redox couples correspond to monomeric and polymeric form of HT, respectively. Before the response of poly-HT/GCE towards oxidation of NADH, the cyclic voltammogram of NADH was recorded at bare GCE. As shown in Figure 3.1B, the oxidation peak of NADH was observed at +550 mV at bare electrode (curve c) and this peak potential shifted to around +240 mV at poly-HT/GCE for 0.8 mM NADH (curve b). However, the cathodic peak current at +210 mV did not change in the presence of NADH. This mentioned potential shift can be explained that the oxidized form of HT on electrode surface reacts with NADH and increases the electron transfer rate of

NADH. During this process, while HT was converted to its reduced form, NADH was oxidized to NAD^+ . Finally, the reduced form of HT reoxidized. Thus it can be said that poly-HT/GCE had a good electrocatalytic effect on the NADH oxidation.

Electropolymerization of HT was also carried out in the phosphate solutions with various pH. Figure 3.1C shows the cyclic voltammograms of the polymer film growth during the successive potential scans of HT solution in 0.1 M PBS (pH 2.0) containing 0.1 M NaNO_3 . As can be seen, electropolymerization of HT was also observed in pH 2.0. However, increase in peaks attributed to the formation of polymeric form by increasing scan cycle was observed more clearly in pH 7.0 (Fig. 3.1A). Figure 3.1D shows the cyclic voltammogram relating to the electrocatalytic oxidation of NADH using poly-HT/GCE obtained from 0.1 M PBS (pH 2.0). The height of peak currents obtained from Figures 3.1B and 3.1D demonstrated that the response of modified electrode prepared at pH 7.0 towards NADH oxidation was better than that prepared at pH 2.0.

In order to find the optimum pH of supporting electrolyte during electropolymerization of HT, the cyclic voltammograms of 0.8 mM NADH were recorded at poly-HT/GCEs which were also prepared in the other phosphate solutions with various pH values. The electrocatalytic peak currents of NADH were calculated from difference between the anodic peak current of modified electrode in the absence and presence of 0.8 mM NADH (Appendix 1). The obtained electrocatalytic currents were plotted versus the pH (Figure 3.2A). As can be seen, the highest electrocatalytic current for NADH was obtained when poly-HT/GCE was prepared in pH 7.0 and also pH 8. Thus, PBS (pH 7.0) containing 0.1 M NaNO_3 was chosen as optimum supporting electrolyte for the electropolymerization of HT in the following experiments, because buffer capacity of pH 7.0 is higher than that of pH 8.

In addition, monomer concentration of HT and the cycle numbers during electropolymerization were also optimized for the electrocatalytic oxidation of NADH. The effect of monomer concentration and cycle numbers during electropolymerization of HT on electrocatalytic peak currents of NADH are given in Figures 3.2C and 3.2D, respectively. From these figures, the best response towards electrocatalytic oxidation of NADH was obtained, when electropolymerization of HT was performed in the presence of 0.3 mM HT monomer and 10 scan cycles (Appendix 1).

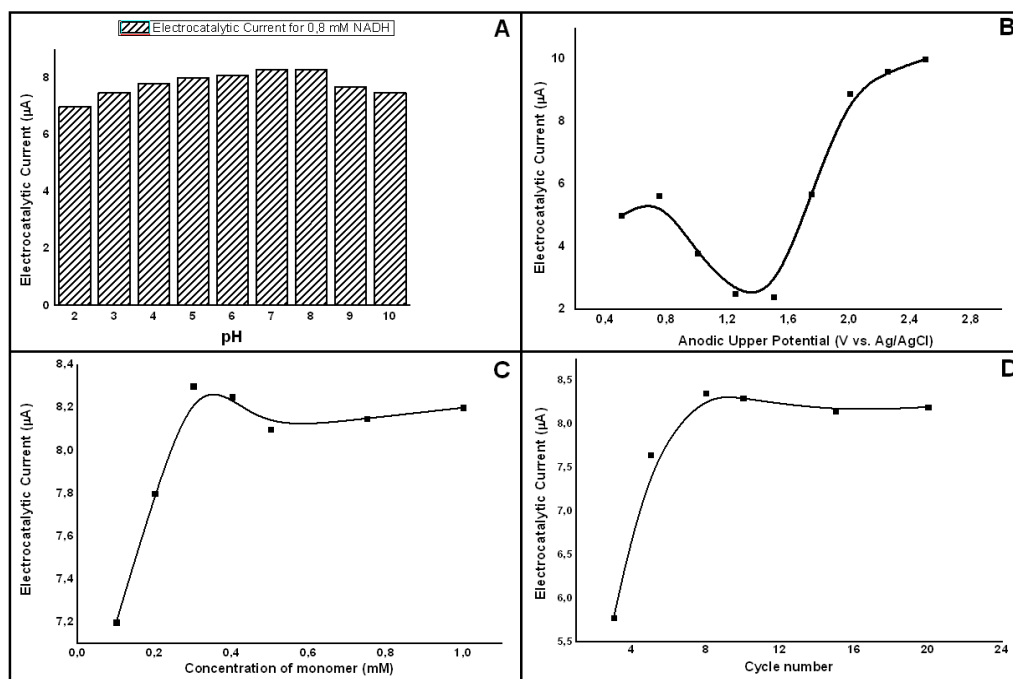


Figure 3.2. The effect of **A)** pH of supporting electrolyte, **B)** anodic potential limit, **C)** monomer concentration, and **D)** cycle number during the preparation of modified electrodes on the electrocatalytic oxidation of 0.8 mM NADH.

The potential scan range, especially the anodic potential limit, is one of the most important factors for the success of the electropolymerization process. The effect of anodic upper potential limit on electrocatalytic peak current of NADH, as well as its effect on starting of electropolymerization, is very important. In order to see the effect of potential range during the electropolymerization of HT on the electrocatalytic oxidation of NADH, firstly the modified electrodes were prepared in the different potential ranges and then the cyclic voltammograms in the presence of 0.8 mM NADH were recorded using these modified electrodes (Appendix 1). For this purpose, the anodic potential limit was varied between +0.5 and +2.5 V for the electropolymerization step. An initial potential of -0.5 V, a cyclic number of 10 cycles, monomer concentration of 0.3 mM and a scan rate of 100 mVs^{-1} were used in all electropolymerization steps. However, results obtained from only two potential ranges, -0.5 to 1.0 V and -0.5 to 1.75 V, were discussed (Figure 3.3) and the effect of potential range on electrocatalytic oxidation current of NADH was given in Figure 3.2B.

Figure 3.3A shows the successive cyclic voltammograms of HT in the potential range of -0.5 to +1.0 V. When the anodic upper potential limit was set to +1.0 V, the oxidation peak at +255 mV with a shoulder at +205 mV gradually

decreased by increasing the cycle number, while the reduction peak at +180 mV was not changed. When the anodic upper potential limit was fixed as 1.75 V, the new peaks attributed to polymeric form of HT were observed after third cycle (Figure 3.3C). However, this increase was not observed when the anodic potential limit was selected as +1.0 V. These results indicated that the potential scan in the range of -0.5 to +1.0 V was not enough for the electropolymerization of HT on GCE and the anodic upper potential should be at least 1.75 V for the starting of electropolymerization.

Cyclic voltammograms of prepared poly-HT/GCEs were recorded in the presence of 0.8 mM NADH. Figure 3.3B shows the cyclic voltammograms of poly-HT/GCE obtained from the potential scan in the range of -0.5 to +1.0 V and the electrocatalytic response of this electrode towards NADH was also not satisfactory. However, this response was found better when anodic potential limit was at least +1.75 V vs. Ag/AgCl (Figure 3.3D).

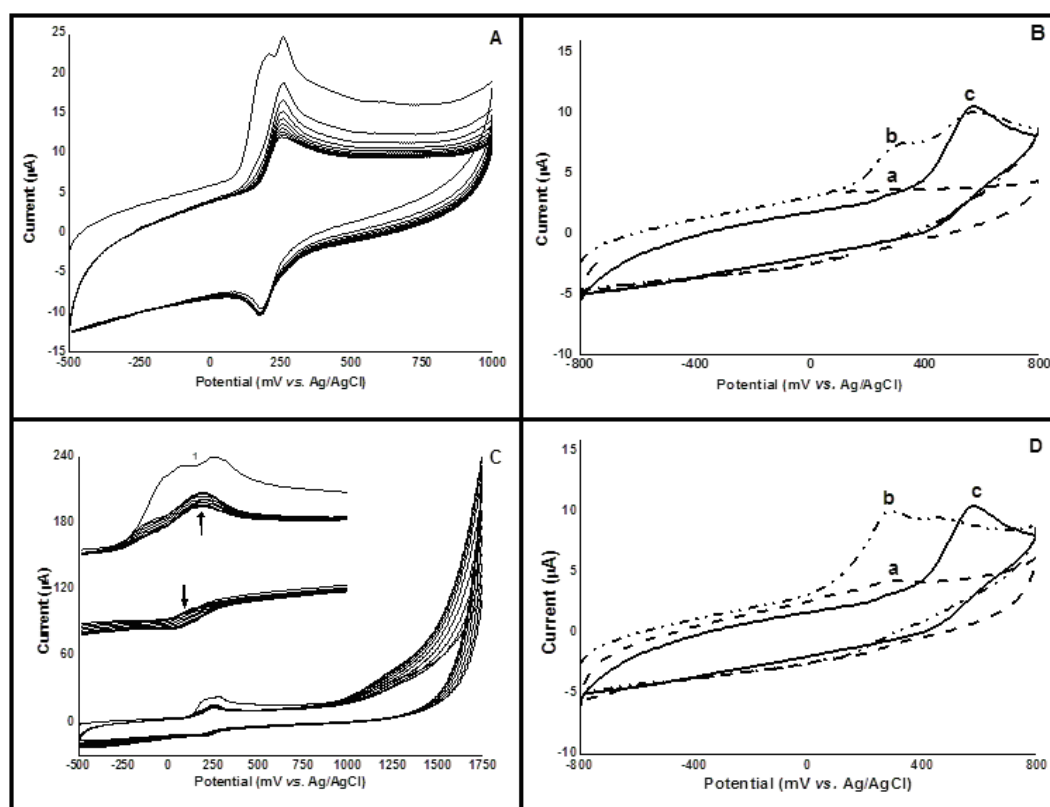


Figure 3.3. Repetitive cyclic voltammograms (10 cycles) of 0.3 mM HT at GCE in 0.1 M PBS (pH 7.0) containing 0.1 M NaNO₃ at 100 mVs⁻¹ in the potential range of A) -0.5 to 1.0 V and C) -0.5 to 1.75 V. B) and D): Cyclic voltammograms of a poly-HT/GCE obtained from A and C, respectively, in the absence (a) and in the presence (b) of 0.8 mM NADH, (c) cyclic voltammogram of 0.8 mM NADH at a bare GCE. Supporting electrolyte: 0.1 M PBS (pH 7.0); scan rate: 50 mVs⁻¹.

In order to see the best response of modified electrodes towards the electrocatalytic oxidation of NADH, the electrocatalytic peak currents of NADH were calculated from the difference between anodic peak currents of modified electrode in the absence and presence of 0.8 mM NADH. The obtained current values were plotted versus anodic potential limit during electropolymerization process (Figure 3.2B). This curve shows that the best electrocatalytic current was observed when anodic applied potential was fixed at 2.0 V during electropolymerization of HT on GCE. Cyclic voltammograms for the preparation of poly-HT/GCE in the potential range between -0.5 and 2.0 V and for its electrocatalytic response towards NADH oxidation, were previously given in Figure 3.1A and 3.1B, respectively.

As a result, in order to obtain the best electrocatalytic current for NADH oxidation, HT was electropolymerized by cycling (10 times) on GCE between -0.5 and +2.0 V vs. Ag/AgCl at a scan rate of 100 mVs^{-1} in 0.1 M PBS (pH 7.0) containing 0.3 mM monomer and 0.1 M NaNO_3 .

Electropolymerization mechanism of HT on GCE

Khoo and Zhu (1998) investigated the electropolymerization of pyrogallol by recording repetitive cyclic voltammograms of 10 mM pyrogallol at GCE in 0.1 M PBS (pH 7.0) at scan rate of 20 mVs^{-1} . They reported that the broad peak at +0.32 V attributed to monomer oxidation was observed in the first cycle; this peak drastically decreased and the peak potential was shifted to a more positive potential (+0.43 V) in the second cycle, and it was almost nonexistent in the third cycle. This behavior was explained by the passivation of electrode due to the formation of an insoluble polymer film. However, a small oxidation peak began to grow slowly with about the same potential as for the original oxidation of monomer. A similar result was also reported for the electropolymerization of catechol (Khoo and Zhu, 1999) and was also obtained in our studies for HT.

Moreover, it was reported that generally the electrochemical oxidation of phenolic compounds produces unstable phenoxy radicals that can be further oxidized to phenoxy or can react to form dimers, which readily polymerize into polyaromatic compounds (Khoo and Zhu, 1999; Andreescu et al., 2003). Especially, Jin et al., (2007) suggested the electropolymerization mechanism of

rutin on paraffin-impregnated graphite electrode. They emphasized that rutin undergoes electrochemical oxidation in two ways related to the two catechol hydroxyl groups and other two hydroxyl groups; the former not only can carry out a two-electrons two-proton reversible reaction, but it can also generally produce unstable phenoxy radicals that readily interact with each other or with another rutin monomer to form a strongly adherent film at bare electrode. In addition, Ryu et al., (2003) presented peroxidase catalyzed polymerization of phenols of three distinct reaction steps: initiation, radical-radical coupling and radical transfers. It was stated that phenol oxidized to phenoxy radicals in the presence of H_2O_2 and enzyme, then this radical delocalized to the aromatic structure and dimerization and also polymerization was formed via radical-radical (carbon-carbon) coupling and radical transfer and coupling reactions. The same polymerization mechanism was also proposed for 2-hydroxycarbazole (Bilici et al., 2010). It was reported that in the presence of H_2O_2 , Horseradish peroxidase can polymerize hydroxy-functionalized aromatic compounds to produce corresponding radicals. These radicals may couple together through radical coupling to form dimers, oligomers, and finally polymers. They gave possible coupling sites for 2-hydroxy carbazole.

In another study, Ferreira et al., (2006) investigated the electropolymerization of phenolic compounds such as phenol, m-cresol, 2,5-dimethylphenol and 2,3,5-trimethylphenol on Pt and Au electrodes. They indicated that phenoxy radicals were initially formed as intermediates during the oxidation of phenol to quinones, and then these radicals could be further oxidized to quinones or could react irreversibly to form dimeric forms through the C-O-C coupling or C-C coupling. Finally these dimers could be oxidized again to produce radicals, which could couple with phenoxy radical or with other dimeric radicals to produce the polymer.

We can suggest a similar mechanism for the electropolymerization of HT on GCE using these useful information and comments. Thus, firstly HT can produce a phenoxy radical during its oxidation, then this radical can be delocalized to the aromatic structure, and finally possible dimerization reactions can be formed through radical-radical (C-O-C or C-C) coupling (Figure 3.4). Following, the polymerization can be formed by increasing the scan cycle. This suggested electropolymerization mechanism was also used by Samide et al., (2013).

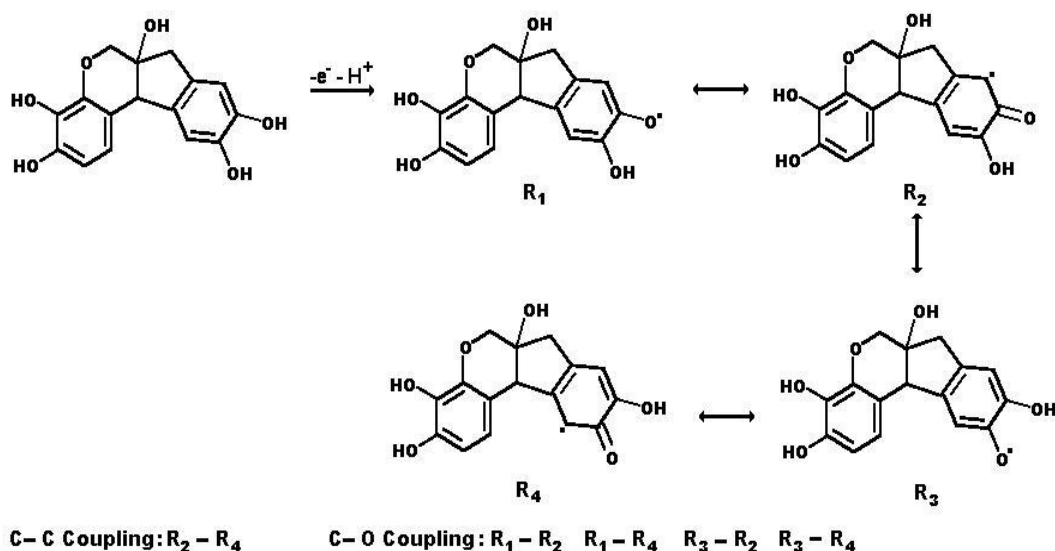


Figure 3.4. Electropolymerization mechanism of HT.

3.1.2. Poly-Methylene Green modified glassy carbon electrode (Poly-MG/GCE)

In order to see the effect of used supporting electrolyte during the preparation of modified electrode on the electrocatalytic oxidation of NADH, poly-MG/GCEs were also prepared in 0.1 M phosphate solutions containing 0.1 M NaNO_3 with various pH values (between 2 and 10). Then the cyclic voltammogram of NADH was recorded in 0.1 M PBS (pH 7.0) using each modified electrode. Figures 3.5A, 3.5C and 3.5E show the cyclic voltammograms of the polymer film growth during the electropolymerization of 0.5 mM MG in 0.1 M H_3PO_4 solution, 0.1 M PBS (pH 7.0) and pH 10.0 phosphate solution, respectively. As can be seen from Figure 3.5A, there are two anodic peaks at 250 mV and 650 V and two cathodic peaks at 125 mV and -140 mV in the first cyclic voltammogram. The pair of redox peaks (at 250 mV for anodic and 125 mV for cathodic) are attributed to the oxidation and reduction of monomeric form of MG. The anodic peak at about 650 mV is attributed to the formation of cationic radical species, while cathodic peak at -140 mV can be attributed to the reduction of protonated MG. Anodic peak at 250 mV increased, while two cathodic peaks at 125 mV and -140 mV decreased with successive scanning and a new cathodic peak appeared at about 250 mV. These results indicate that polymerization of MG was successfully obtained on GCE. The similar electropolymerization of MG on GCE was also obtained in the neutral (Figure 3.5C) and basic (Figure 3.5E) supporting electrolytes.

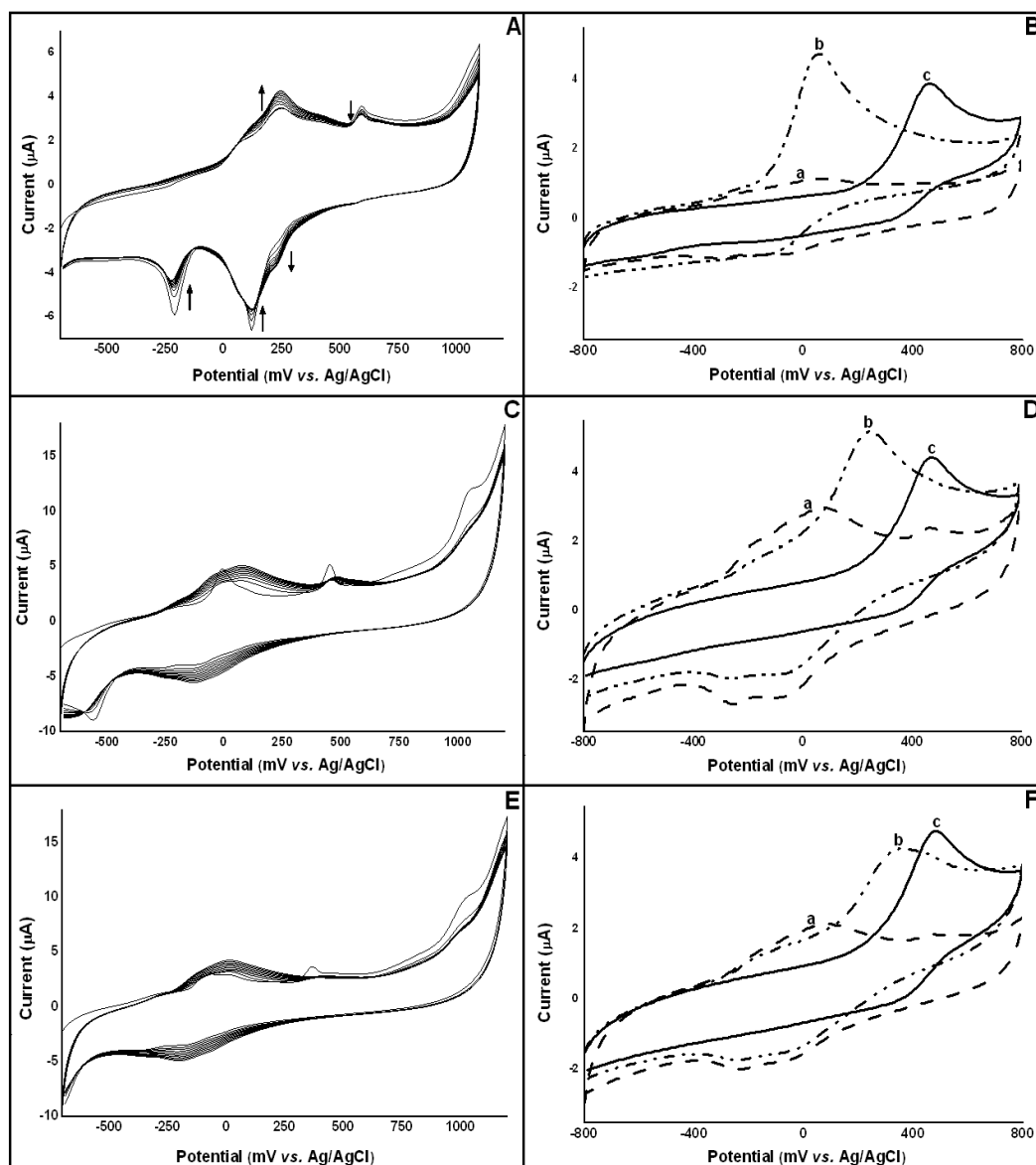


Figure 3.5. Repetitive cyclic voltammograms (10 cycles) of 0.5 mM MG at GCE in 0.1 M H_3PO_4 (A), and 0.1 M phosphate solutions with pH 7.0 (C) and pH 10.0 (E) containing 0.1 M NaNO_3 at 100 mVs^{-1} , in the range of -0.7 to $+1.1$ V vs. Ag/AgCl. B), D) and F) Cyclic voltammograms of poly-MG/GCE obtained from A, C and E respectively, in the absence (a) and in the presence (b) of 0.4 mM NADH c) the cyclic voltammograms of 0.4 mM NADH at bare GCE. Supporting electrolyte: 0.1 M PBS (pH 7.0); scan rate: 50 mVs^{-1} .

Figures 3.5B, 3.5D and 3.5F show the cyclic voltammograms of modified electrodes which were obtained from electropolymerization of MG in Figures 3.5A, 3.5C and 3.5E respectively, in the absence (curve a) and presence of 0.4 mM NADH (curve b). Moreover, curve c in these figures shows the cyclic voltammogram of 0.4 mM NADH using bare GCE. Electrocatalytic oxidation of NADH was also achieved by using poly-MG/GCE, because the oxidation peak

potential of NADH observed at +500 mV at bare electrode (Figure 3.5B, curves c) shifted to around +100 mV at poly-MG/GCE for 0.4mM NADH (Figure 3.5B, curve b). This potential shifting can be explained by the oxidized form of MG on electrode surface reacting with NADH and increasing the electron transfer rate of NADH. During this process, while MG converted to its reduced form, NADH oxidized to NAD^+ . Finally, the reduced form of MG reoxidized.

In order to find the optimum pH of used supporting electrolyte during electropolymerization of MG, the cyclic voltammograms of 0.4 mM NADH were recorded at poly-MG/GCEs which were prepared in phosphate solutions with various pH values. The electrocatalytic peak currents of NADH were calculated from the difference between anodic peak current of modified electrode in the absence and presence of 0.4 mM NADH. The obtained electrocatalytic currents were plotted versus the pH (Figure 3.6A). As can be seen, the highest electrocatalytic current for NADH was obtained when poly-MG/GCE was prepared in 0.1 M H_3PO_4 . Thus, the 0.1 M H_3PO_4 containing 0.1 M NaNO_3 was chosen as the optimum supporting electrolyte for the electropolymerization of MG in the following experiments. In addition, the monomer concentration of MG and cycle numbers were also optimized for electropolymerization process; the best response was obtained when the monomer concentration and cycle numbers used were as 0.5 mM and 10 cycles, respectively (Figures 3.6C and 3.6D).

In order to see the effect of potential range during the electropolymerization of MG on the electrocatalytic oxidation of NADH, firstly the modified electrodes were prepared in the different potential ranges and secondly the cyclic voltammograms of 0.4 mM NADH were recorded using these modified electrodes. For this purpose, the anodic potential limit was varied between +0.6 and +1.6 V for the electropolymerization step. An initial potential of -0.7 V, a cyclic number of 10 cycles, monomer concentration of 0.5 mM and a scan rate of 100 mVs^{-1} were used in all electropolymerization steps.

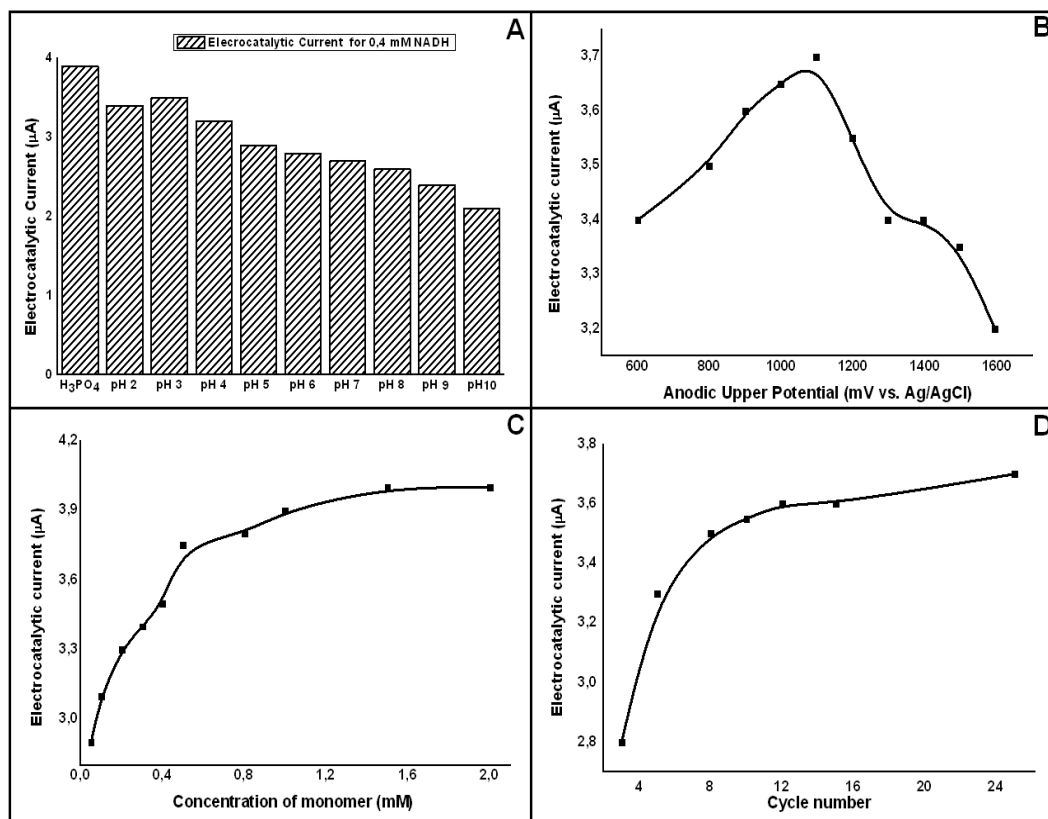


Figure 3.6. The effect of **A)** pH of supporting electrolyte, **B)** anodic potential limit, **C)** monomer concentration, and **D)** cycle number during the preparation of modified electrodes on the electrocatalytic oxidation of 0.4 mM NADH.

Figures 3.7A and 3.7C show the successive cyclic voltammograms of MG in the potential range of -0.7 to $+0.6$ V and -0.7 to 1.6 V, respectively. Electropolymerization was also observed when the anodic upper potential limit was set to $+0.6$ V, because this potential is near the potential for the formation of cationic radicalic species (650 mV). Figures 3.7B and 3.7D show the response of modified electrode obtained from Figures 3.7A and 3.7C, respectively, towards NADH oxidation. The electrocatalytic peak currents of NADH were calculated from difference between anodic peak currents of modified electrode in the absence and presence of 0.4 mM NADH. The obtained current values were plotted versus anodic potential limit (Figure 3.6B). This curve shows that the best electrocatalytic current was observed when anodic applied potential was fixed at 1.1 V during electropolymerization of MG on GCE. Cyclic voltammograms for the preparation of poly-MG/GCE in the potential range between -0.7 and 1.1 V and for its electrocatalytic response towards NADH oxidation were previously given in Figure 3.5A and 3.5B, respectively.

As a result, in order to obtain the best electrocatalytic current for NADH oxidation, MG was electropolymerized by cycling (10 times) on GCE between -0.7 and +1.1 V vs. Ag/AgCl at a scan rate of 100 mVs^{-1} in 0.1 M H_3PO_4 solution containing 0.5 mM monomer and 0.1 M NaNO_3 .

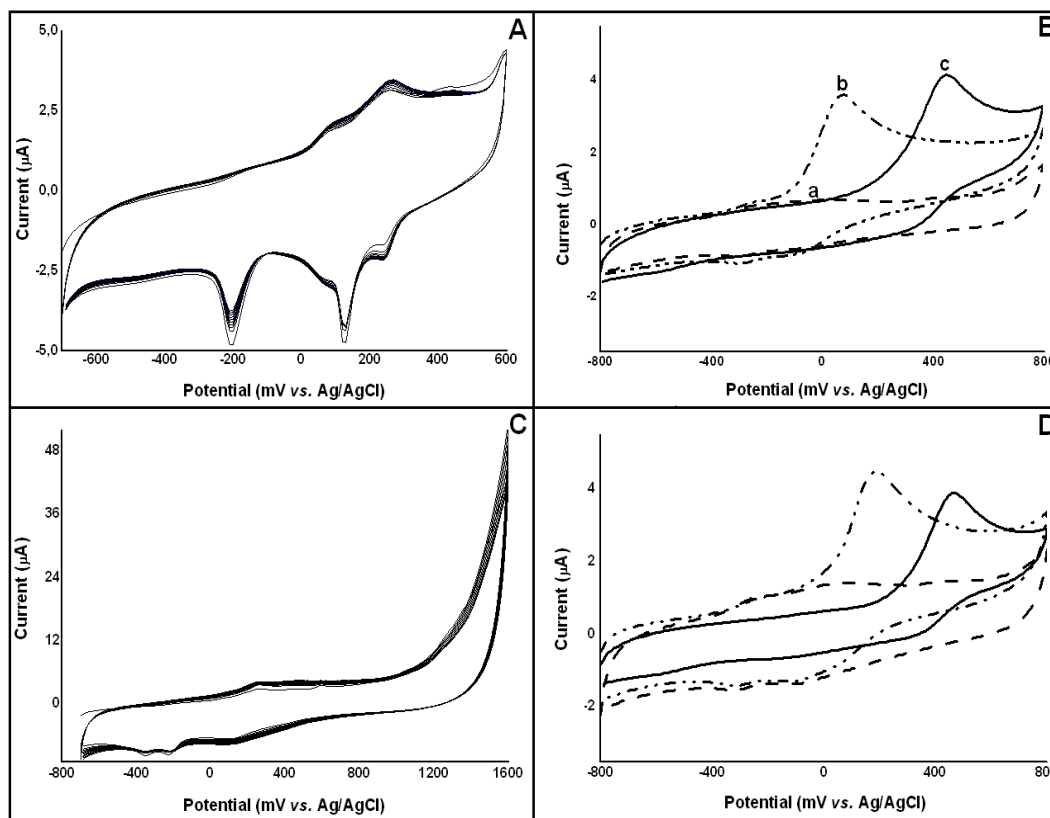


Figure 3.7. Repetitive cyclic voltammograms (10 cycles) of 0.5 mM MG at GCE in 0.1 M H_3PO_4 + 0.1 M NaNO_3 at 100 mVs^{-1} in the range of **A)** -0.7 to 0.6 V and **C)** -0.7 to 1.6 V. **B)** and **D)**: Cyclic voltammograms of a poly-MG/GCE obtained from A and C, respectively, in the absence (a) and in the presence (b) of 0.4 mM NADH, (c) cyclic voltammogram of 0.4 mM NADH at a bare GCE. Supporting electrolyte: 0.1 M PBS (pH 7.0); scan rate: 50 mVs^{-1} .

Electropolymerization mechanism of MG on GCE

Azine type dyes such phenothiazine, phenazine and phenoxazine mostly include primary or secondary amino groups as ring substituent and these groups can be oxidized between 600 and 1200 mV depending on supporting electrolyte. In the end of this oxidation step, cationic radicalic species, which are necessary for the electropolymerization process dependent on radical–radical coupling, are formed. Thus, the reaction mechanism for electropolymerization of MG, a phenothiazine dye, has been proposed by some authors (Barsan, et al., 2008; Karyakin 199b). The first step in the electropolymerization reaction sequence of

MG is the one-electron oxidation of the tertiary amino group in the monomer, ending up with the formation of a radical cation. In the second step, this radical is delocalized to the aromatic structure leading finally to the formation of possible dimerization reactions through radical–radical (carbon–nitrogen or carbon–carbon) coupling. More radicals were formed through the continuous potential cycling and an insoluble polymeric form (poly-MG) was gradually produced. All electropolymerization steps are given in Figure 3.8.

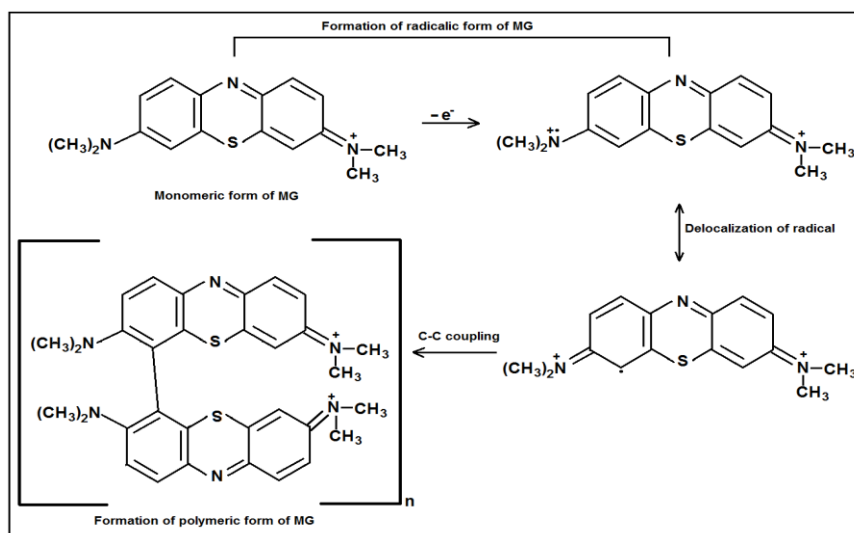


Figure 3.8. Electropolymerization mechanism of MG (Barsan et al., 2008).

3.1.3. Poly-Neutral Red modified glassy carbon electrode (Poly-NR/GCE)

The effect of supporting electrolyte, cycle number, monomer concentration and anodic upper potential used during NR electropolymerization process on electrocatalytic oxidation of NADH was also investigated for poly-NR/GCE by applying the procedure similar to the studies on preparation of poly-HT/GCE and poly-MG/GCE. Poly-NR/GCEs were prepared in different supporting electrolytes: 0.1 M H_2SO_4 , 0.1 M HCl and 0.1 M phosphate solutions with pH values between 2.0 and 10.0. In order to test the effect of supporting electrolyte on electrocatalytic oxidation of NADH, cyclic voltammograms were recorded in the absence and in the presence of 0.4 mM NADH, in 0.1 M PBS (pH 7.0) for modified electrodes obtained from every supporting electrolyte.

Fig. 3.9A presents the electropolymerization of NR in 0.1 M H_2SO_4 containing 0.05 mM NR and 0.1 M NaNO_3 at scan rate of 100 mVs^{-1} . In the first cycle, anodic and cathodic peaks were observed at -90 mV and at -150 mV,

respectively. These reversible peaks were attributed to monomeric form of NR. An irreversible peak observed at about +930 mV was attributed to the formation of radicalic cation of NR (Bauldreay and Archer, 1983; Chen and Gao, 2007a; Karyakin et al., 1995). A new anodic and cathodic peak at +460 mV and +370 mV, respectively, started to appear after the second potential scan. It was observed that the current of these redox peaks increased continuously by successive scanning, while the irreversible peak at +930 mV decreased. These results demonstrated that the amount of electroactive species increased and the polymerization of NR occurred on the GCE. Similar results were reported in literature (Bauldreay and Archer, 1983; Karyakin et al., 1999b).

Figure 3.9B (curve a) presents the cyclic voltammograms of poly-NR/GCE in PBS (pH 7.0), in the absence of NADH. Two small and reversible redox peaks were observed. The formal potentials ($E^{0'} = (E_a + E_c)/2$) of these redox peaks were found to be -455 mV and +80 mV, respectively. It can be concluded that these redox couples correspond to monomeric and polymeric form of NR, respectively. As shown in Fig. 3.9B (curve c), the oxidation peak of NADH was observed at +500 mV at unmodified GCE. However, electrochemical oxidation of NADH was observed at +140 mV in the case of the poly-NR/GCE (curve b). While the cathodic peak current of poly-NR/GCE observed at about +20 mV did not change, the anodic peak current increased in the presence of 0.4 mM NADH. It was found that compared with bare GCE (+500 mV), a 360 mV decrease in overpotential for NADH oxidation was observed at the present Poly-NR/GCE (+140 mV). Thus it can be concluded that poly-NR/GCE offers a good electrocatalytic effect towards the NADH oxidation. Similar electrocatalytic effect for NADH was also obtained for a composite electrode composed of ordered mesoporous carbon with polymeric NR on the GCE using electropolymerization procedure (Lu et al., 2010).

Figures 3.9C and 3.9E show the cyclic voltammograms of the polymer film growth through the electrocatalysis of 0.05 mM NR in pH 4.0 and pH 7.0 phosphate solutions, respectively. Although the electropolymerization process was also achieved in these media, the electrocatalytic response of this modified electrode towards NADH oxidation was not so high (Figures 3.9D and 3.9F).

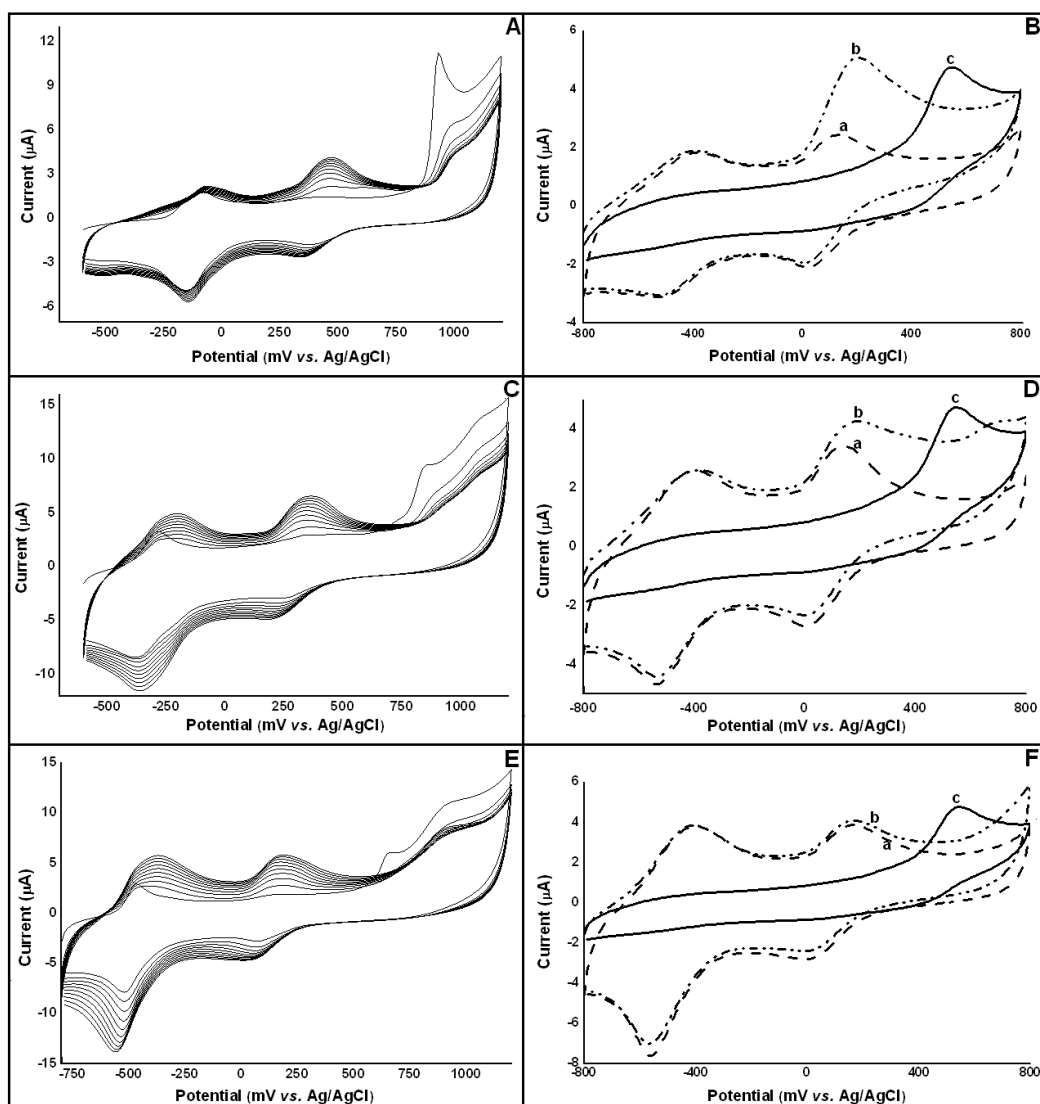


Figure 3.9. Repetitive cyclic voltammograms (10 cycles) of 0.05 mM NR at GCE in 0.1 M H₂SO₄ (A), and 0.1 M phosphate solutions with pH 4.0 (C) and pH 7.0 (E) containing 0.1 M NaNO₃ at 100 mVs⁻¹, in the range of -0.7 to +1.2 V vs. Ag/AgCl. (B), (D) and (F) Cyclic voltammograms of poly-NR/GCE obtained from A, B and C respectively, in the absence (a) and in the presence (b) of 0.4 mM NADH c) the cyclic voltammograms of 0.4 mM NADH at bare GCE Supporting electrolyte: 0.1 M PBS (pH 7.0); scan rate: 50 mVs⁻¹.

In order to find the optimum supporting electrolyte used in the electropolymerization of NR, electropolymerization process from Figure 3.9 was repeated in 0.1 M HCl, 0.1 M H₃PO₄, and 0.1 M phosphate solutions with different pH values (between 2.0 and 10.0) and the cyclic voltammograms of every prepared modified electrode were recorded in the absence and presence of 0.4 mM NADH in 0.1 M PBS (pH 7.0), at scan rate of 50 mVs⁻¹. The electrocatalytic peak currents of NADH were calculated from difference between the anodic peak current of modified electrode in the presence and absence of 0.4

mM NADH. The obtained electrocatalytic currents were plotted versus supporting electrolyte type and also the pH of phosphate solutions (Figure 3.10A). From obtained results, the highest electrocatalytic current for NADH oxidation was observed when poly-NR/GCE was prepared in H_2SO_4 . This phenomenon can be explained by formation of regular polymer growth of NR on electrode surface in acidic media. Chen and Gao reported that the electropolymerization from acidic aqueous solutions is generally preferable for formation of an electroactive polymer (Chen and Gao, 2007b). In some studies, strong acidic solutions were also used concerning the oxidative polymerization of NR (Chen and Gao, 2007a; 2007b; Chen and Lin, 2001; Broncová et al., 2004). In addition, in order to obtain the regular polymer growth in cyclic voltammetric conditions with a limited anodic switching potential requires acidic solutions (Chen and Gao, 2007b). Therefore, 0.1 M H_2SO_4 containing 0.1 M NaNO_3 was chosen as optimum supporting electrolyte for the electropolymerization of NR in the following experiments. In addition, the monomer concentration of NR and cycle numbers were also optimized for the electropolymerization process; the best response was obtained in the presence of 0.01 mM NR monomer and using 8 cycles (Figures 3.10C and 3.10D).

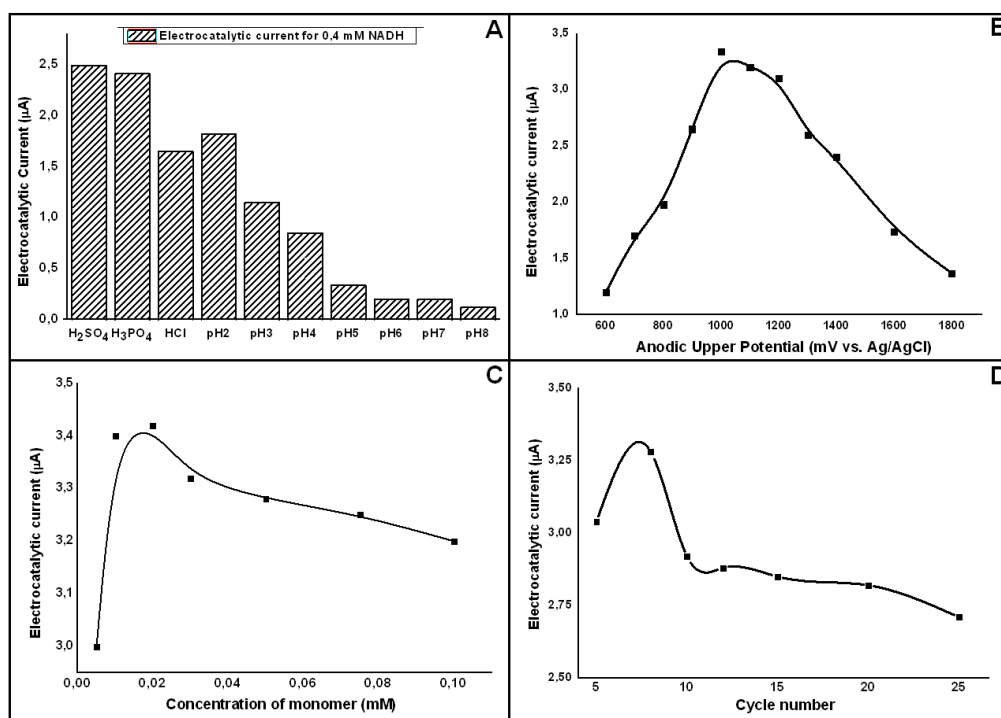


Figure 3.10. The effect of **A)** pH of supporting electrolyte, **B)** anodic potential limit, **C)** monomer concentration, and **D)** cycle number during the preparation of modified electrodes on the electrocatalytic oxidation of 0.4 mM NADH.

The effect of potential range used in the electropolymerization of NR on the electrocatalytic oxidation of NADH was also studied. For this purpose, the anodic potential limit was varied between +0.6 and +1.8 V for the electropolymerization step. An initial potential of -0.6 V, a cyclic number of 8 cycles, monomer concentration of 0.01 mM and a scan rate of 100 mVs⁻¹ were used in all electropolymerization steps. Figure 3.11A shows the successive cyclic voltammograms of NR in the potential range of -0.6 to +0.6 V. When the anodic upper potential limit was set to +0.6 V, the oxidation peak at -150 mV and cathodic peak at -190 mV gradually decreased by increasing the cycle number. As mentioned above, when the anodic upper potential limit was fixed as 1.1 V, new peaks attributed to polymeric form of NR were observed (Figure 3.9A), because the formation of cationic radicalic form of NR, which was observed at about 930 mV, is necessary for the initiating of electropolymerization of NR. The anodic upper potential of 0.6 V is not enough for the formation of cationic radicalic form. Figure 3.11B shows the cyclic voltammograms of poly-NR/GCE obtained from the potential scan in the range of -0.6 to +0.6 V; the electrocatalytic response of this electrode towards NADH was also not satisfactory. Figure 3.11C shows the successive cyclic voltammograms of NR in the potential range of -0.6 to 1.6 V. The electrocatalytic current of NADH decreased for the modified electrodes prepared at the anodic upper potential at 1.6 V (Figure 3.11D). This may depend on the electropolymerization, which can be damaged due to the formation of O₂ at high anodic potential.

The electrocatalytic peak currents of NADH were calculated from difference between anodic peak currents of modified electrode in the absence and presence of 0.4 mM NADH. The peak currents of NADH corresponding to each modified electrode were plotted versus anodic upper potential limit during electropolymerization process (Figure 3.10B). This curve showed that the applied potential during electropolymerization of NR should be chosen at least at 1.0 V, in order to obtain a good electrocatalytic current for NADH oxidation.

As a result, the optimum conditions used during the electropolymerization process of NR were established as being: supporting electrolyte, 0.1 M H₂SO₄ containing 0.1 M NaNO₃; monomer concentration, 0.01 mM; cycle numbers, 8; and potential range, -0.6 to +1.0 V vs. Ag/AgCl/KCl_{sat}.

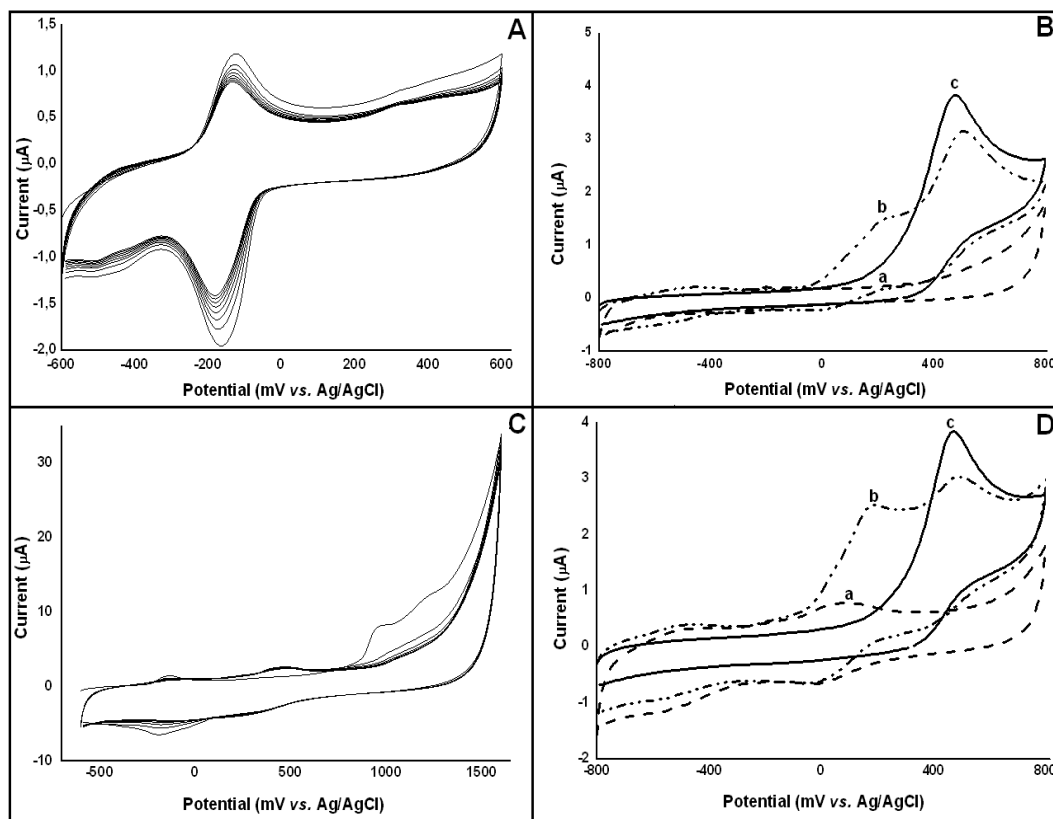


Figure 3.11. Repetitive cyclic voltammograms (10 cycles) of 0.01 mM NR at GCE in 0.1 M H₂SO₄ + 0.1 M NaNO₃ at 100 mVs⁻¹ in the range of **A)** -0.6 to 0.6 V **C)** and -0.6 to 1.6 V **B)** and **D)** Cyclic voltammograms of a poly-NR/GCE obtained from A and C, respectively, in the absence (a) and in the presence (b) of 0.4 mM NADH, (c) cyclic voltammogram of 0.4 mM NADH at a bare GCE. Supporting electrolyte: 0.1 M PBS (pH 7.0); scan rate: 50 mVs⁻¹.

Electropolymerization mechanism of NR

The electropolymerization mechanism of NR has been reported in some studies (Bauldreay and Archer, 1983; Chen and Gao, 2007a; Karyakin et al., 1995; 1999b; Barsan et al., 2008). The proposed mechanism for MG shown in Figure 3.8 can also be proposed for NR. The first step in the sequence of electropolymerization reactions of NR is the oxidation of -NH₂ group in the monomer and formation of a radical cation. Then, this radical can be delocalized to the aromatic structure and finally the radicalic dimerization can take place via carbon-nitrogen coupling. The formed dimers are strongly adsorbed on the electrode surface. It was reported in the above mentioned references, that more radicals were formed by continuously cycling of potential and thus the insoluble polymeric form of poly-NR was gradually produced.

3.1.4. Poly-Meldola Blue modified glassy carbon electrode (Poly-MdB/GCE)

MdB is another important redox mediator for electrocatalytic oxidation of NADH. The various electrode materials such as GCE, carbon paste electrode, especially graphite electrode, etc. were modified with this phenoxazine dye and these modified electrodes were used for electrocatalytic oxidation and also construction of biosensor dependent on NAD^+/NADH redox couple (Canevari, et al., 2011; Maroneze, 2008; Ladiu et al. 2007a; 2007b; 2005; Zhu, et al., 2007; Pereira, et al., 2006; Santos, et al., 2002b, 2003; Kubota, et al., 1996; Gorton et al., 1984). In this section, we also tried to use MdB modified electrode for electrocatalytic and also photoelectrocatalytic oxidation of NADH. For this aim, firstly the electropolymerization of MdB on the GCE was performed by recording cyclic voltammograms of 0.01 mM MdB in 0.1 M phosphate solutions containing 0.1 M NaNO_3 with various pH values (between 2 and 10) and then the cyclic voltammogram of NADH was recorded in PBS of pH 7.0, using each modified electrode. As a representative, Figure 3.12A shows the cyclic voltammograms of the polymer film growth of 0.01 mM MdB in 0.1 M pH 10.0 phosphate solutions. In the first cycle, one oxidation peak was observed at about -30 mV, which is attributed to the oxidation of monomeric MdB. In the second cycle, the current of this peak decreased. After the third cycle, the peak current began to grow slowly with increasing cycle numbers and peak potential was shifted to about +10 mV. Cathodic peak was observed at about -170 mV and increased slowly with increasing scan cycles. These results (Figure 3.12A) demonstrated that a good electropolymerization for MdB was not observed onto GCE.

In order to test electrocatalytic activity of poly-MdB/GCE towards NADH oxidation, cyclic voltammograms of modified electrode were recorded in the absence and in the presence of NADH. Figure 3.12B, curve a shows the cyclic voltammogram of poly-MdB/GCE in PBS (pH 7.0) at 50 mVs^{-1} in the absence of NADH. It can be seen that only an anodic peak and cathodic peak were observed at -150 mV and -280 mV, respectively. Figure 3.12B, curve b shows the cyclic voltammogram of poly-MdB/GCE in the presence of 0.5 mM NADH. While a part of the NADH oxidation was broadly observed at 170 mV, the other part of the NADH oxidation was observed at 550 mV, which is near the oxidation peak potential of NADH (about 500 mV) at bare GCE (Fig 6B, curve c). These results indicate poly-MdB/GCE does not have an efficient electrocatalytic effect towards NADH oxidation. Thus, photoelectrocatalytic oxidation of NADH with this

modified electrode was not tried. Although a few reports on electropolymerization of MB for sensor of some biologically important molecules such as dopamine, glucose and choline (Mao and Yamamoto, 2000; Yamaguchi, et al., 2006) have been discussed in the literature, our results show that electropolymerization of MdB on GCE was not successfully obtained. In addition, Karyakin et al., (1999a) reported that “Several attempts to electropolymerize MdB were done from different aqueous solutions in a wide range of pH. However, in every case only a minor amount of electroactive polymer was obtained. If we compare the chemical structures of MB and MdB, the latter contains only one benzene ring substituted with a tertiary amino group. The absence of a second similar aromatic ring substituent, able to delocalize the positive charge, could be a reason for the lack of electropolymerization observed.” (Karyakin, et al., 1999a). These comments also support our results.

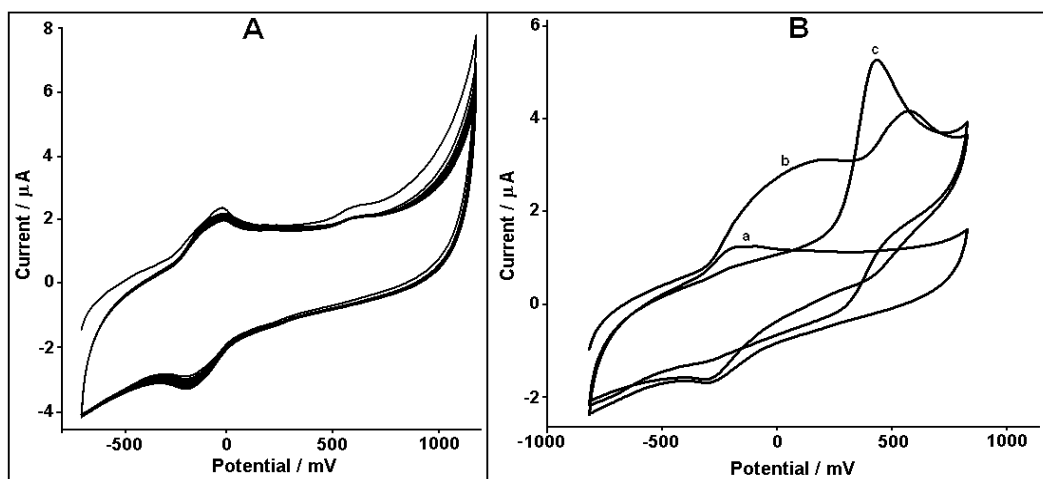


Figure 3.12. A) Repetitive cyclic voltammograms (10 cycles) of 0.01 mM MdB at GCE in 0.1 M phosphate solutions with pH 10 containing 0.1 M NaNO₃ at 100 mVs⁻¹, in the range of -0.7 to +1.2 V vs. Ag/AgCl. B) Cyclic voltammograms of poly-MdB/GCE obtained from A in the absence (a) and in the presence (b) of 0.4 mM NADH c) the cyclic voltammograms of 0.4 mM NADH at bare GCE. Supporting electrolyte: 0.1 M PBS (pH 7.0); scan rate: 50 mVs⁻¹.

3.2. Electrochemical Characterization of Prepared Modified Electrodes

3.2.1. Electrochemical behavior of poly-HT/GCE

The electrochemical behavior of the poly-HT modified GCE was investigated by recording cyclic voltammograms in a 0.1 M PBS (pH 7.0) at various scan rates (Figure 3.13A). Two redox pairs were observed in the cyclic voltammogram at low scan rates (Appendix 2). For example, the anodic and

cathodic peak potentials of polymeric form (Couple II) at 50 mVs^{-1} were clearly found to be +260 mV and +240 mV, respectively. However, the anodic and cathodic peaks of monomeric form (Couple I) were observed to be very small, at +170 mV and +110 mV, respectively. The anodic and cathodic peaks of these couples overlapped through increasing the scan rates. The anodic peak current (i_{pa}) and the cathodic peak current (i_{pc}) of Couple II corresponding to polymeric form of HT are linearly proportional to the scan rate (v) between $50\text{-}3200 \text{ mVs}^{-1}$ (Figure 3.13B). The equations and their regression coefficients for anodic and cathodic peaks of Couple II were found to be as follow:

$$i_{pa} = 0.032 v + 0.879 \quad (R^2 = 0.9976)$$

$$i_{pc} = -0.028 v + 1.54 \quad (R^2 = 0.9967)$$

These results indicated that surface reaction process occurred at poly-HT/GCE.

In order to determine the effect of pH on the formal standard potential, $E^{0'}$ of modified electrodes, the cyclic voltammograms of poly-HT/GCE were recorded in phosphate solutions of pH values between 2 and 9 at a 50 mVs^{-1} scan rate. The $E^{0'}$ value of polymeric form (Couple II) was calculated as the average of anodic and cathodic peak potentials ($E^{0'} = (E_{pa} + E_{pc})/2$) and was used as an approximation of the formal potential, $E^{0'}$ (Appendix 2). Figure 3.13C shows that the $E^{0'}$ value of redox couple dependent on pH and $E^{0'}$ values decreasing linearly with increasing of phosphate solution pH. The slope of this curve was found to be about -58.2 mV/pH unit at room temperature, which was equal to the anticipated Nernstian value for two electrons and two protons attending the electron transfer process.

In order to test the stability of poly-HT/GCE, the cyclic voltammograms of the modified electrode were recorded by successive scans (300 cycles) in 0.1 M PBS (pH 7.0), at a scan rate of 50 mVs^{-1} . Figure 3.13D shows the repetitive cyclic voltammograms of modified electrode with 300 cycles. At the first cycle, two redox pairs were observed. The anodic and cathodic peak potentials of the first couple were found to be +170 mV and +110 mV respectively, which can correspond to adsorbed monomeric form of HT. However, the anodic and cathodic peaks of the second couple were observed at +260 mV and +240 mV respectively, which can be attributed to polymeric form of HT. After a few scans (about five cycles), the peak currents of couples I and II decreased quickly on the continuous scanning. After 50 repetitive scans, change in height of the peaks became very small.

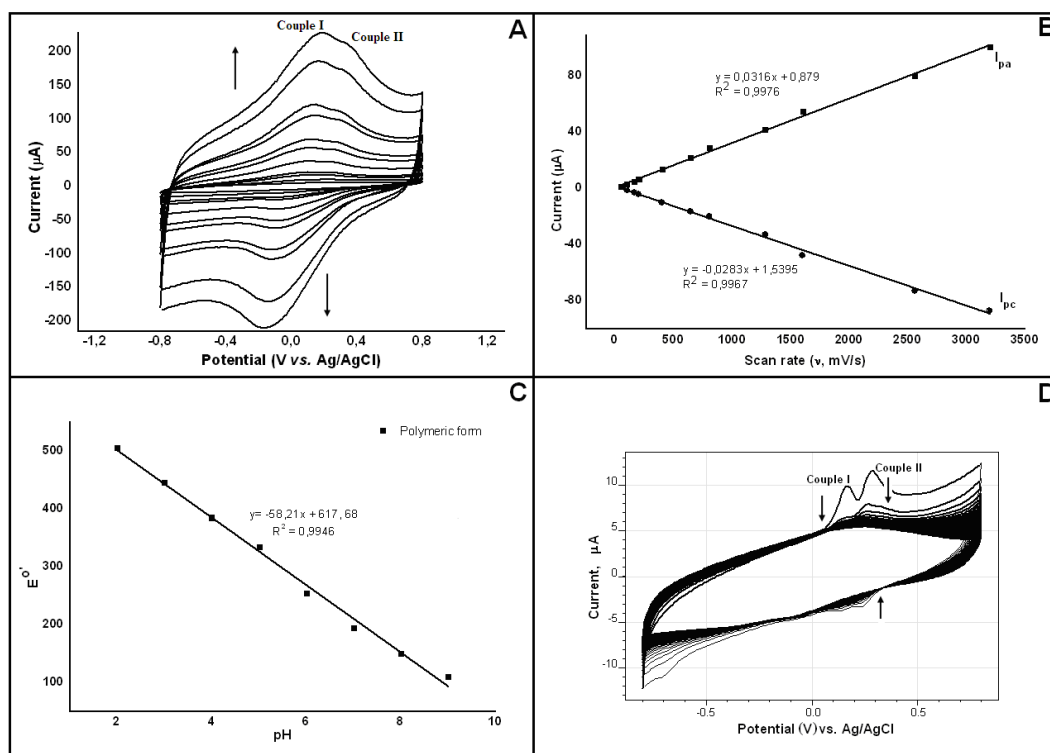


Figure 3.13. **A)** Cyclic voltammograms of poly-HT/GCE in 0.1 M PBS (pH 7.0) at a scan rates of 50, 100, 160, 200, 400, 640, 800, 1280, 1600, 2560, 3200 mVs^{-1} . **B)** The plot of the anodic (i_{pa}) and cathodic (i_{pc}) peak currents versus the scan rates for redox couple II. **C)** The plot of formal potential versus pH which was calculated from cyclic voltammograms of poly-HT/GCE recorded at 50 mVs^{-1} in the potential range of -0.8 to +0.8 V vs. Ag/AgCl. **D)** Repetitive cyclic voltammograms of poly-HT/GCE with 300 cycles in 0.1 M PBS (pH 7.0) at scan rate of 50 mVs^{-1} .

3.2.2. Electrochemical behavior of poly-MG/GCE

The electrochemical behavior of the poly-MG modified GCE was also investigated by recording its cyclic voltammograms in a 0.1 M PBS (pH 7.0) at various scan rates (Figure 3.14A). Two redox pairs were observed in the cyclic voltammogram at low scan rates. The anodic and cathodic peaks of these couples were overlapped through increasing of the scan rates. The anodic peak current (i_{pa}) and the cathodic peak current (i_{pc}) of Couple II corresponding to polymeric form of MG are linearly proportional to the scan rate (v) between 20-6400 mVs^{-1} (Figure 3.14B). The equations and their regression coefficients for anodic and cathodic peaks of polymeric form were found to be as follow:

$$i_{pa} = 0.0098 v + 0.6701 \quad (R^2 = 0.9985)$$

$$i_{pc} = -0.0087 v + 0.1006 \quad (R^2 = 0.9993)$$

These results indicated that surface reaction process occurred at poly-MG/GCE.

In order to determine the effect of pH on the formal standard potential, $E^{0'}$ of modified electrodes, the cyclic voltammograms of poly-MG/GCE were recorded in phosphate solutions of pH values between 2 and 10 at a 50 mVs^{-1} scan rate. Figure 3.14C shows that the $E^{0'}$ values of redox couples for polymeric and monomeric form of MG dependent on pH and these values decreased linearly with increasing of the pH. The slopes of these curves were found to be about -53.2 mV/pH and -56.9 mV/pH for polymeric and monomeric forms of MG, respectively which were equal to the anticipated Nernstian value for two electrons and two protons attending the electron transfer process for monomeric and polymeric forms.

In order to test the stability of poly-MG/GCE, the cyclic voltammograms of the modified electrode were recorded by successive scans (250 cycles) in 0.1 M PBS (pH 7.0) at a scan rate of 50 mVs^{-1} . Figure 3.14D shows the repetitive cyclic voltammograms of modified electrode with 250 cycles. At the first cycle, two redox pairs were observed. After about 100 repetitive scans, change in height of peaks became very small.

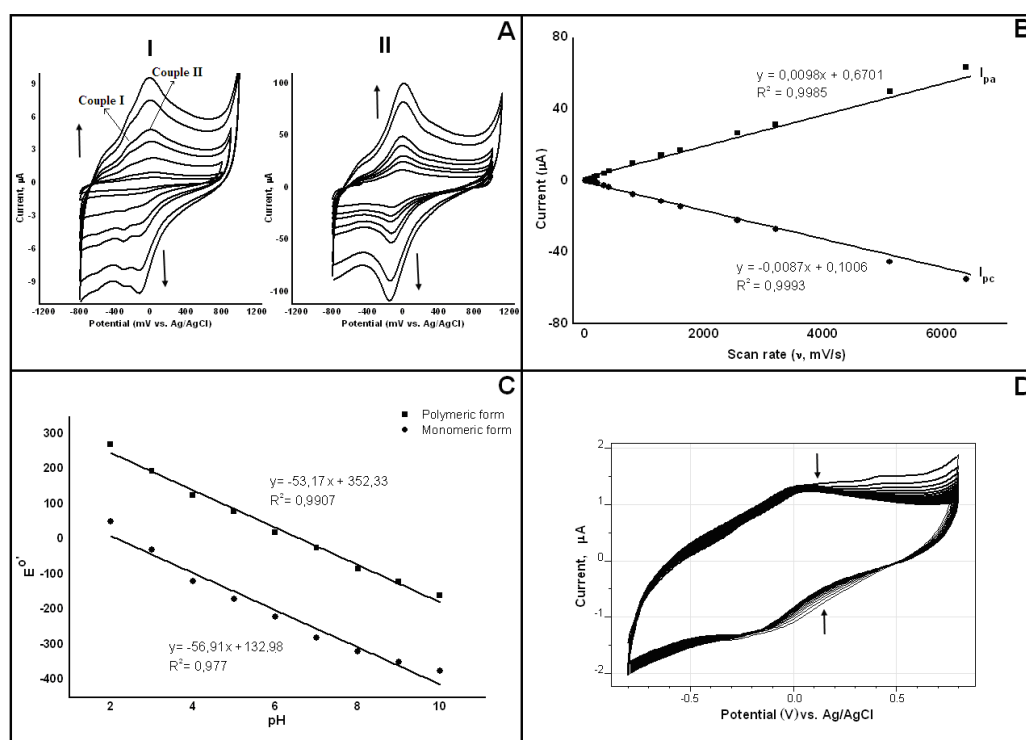


Figure 3.14. A) Cyclic voltammograms of poly-MG/GCE in 0.1 M PBS (pH 7.0) at a scan rates of **I**: 20, 50, 100, 160, 200, 400, 640; **II**: 800, 1280, 1600, 2560, 3200, 5120, 6400 mVs^{-1} , **B**) The plot of the anodic (i_{pa}) and cathodic (i_{pc}) peak currents versus the scan rates for redox couple II, **C**) The plot of formal potential versus pH which was calculated from cyclic voltammograms of poly-MG/GCE recorded at 50 mVs^{-1} in the potential range of -0.8 to $+0.8$ V vs. Ag/AgCl, **D**) Repetitive cyclic voltammograms of poly-MG/GCE with 250 cycles in 0.1 M PBS (pH 7.0) at scan rate of 50 mVs^{-1} .

3.2.3. Electrochemical behavior of poly-NR/GCE

The electrochemical behavior of the poly-NR modified GCE was also investigated by recording its cyclic voltammograms in a 0.1 M PBS (pH 7.0) at various scan rates (Figure 3.15A). Two redox pairs were observed in the cyclic voltammogram at low scan rates. The anodic and cathodic peaks of these couples were overlapped through increasing the scan rates. The anodic peak current (i_{pa}) and the cathodic peak current (i_{pc}) of Couple II corresponding to polymeric form of NR are linearly proportional to the scan rate (ν) between 20-6400 mVs^{-1} . (Figure 3.15B). The equations and their regression coefficients for anodic and cathodic peaks of polymeric form (Couple II) were found to be as follow:

$$i_{pa} = 0.0056 \nu + 0.3382 \quad (R^2 = 0.9965)$$

$$i_{pc} = -0.0053 \nu + 0.2115 \quad (R^2 = 0.9982)$$

These results indicated that surface reaction process occurred at poly-NR/GCE.

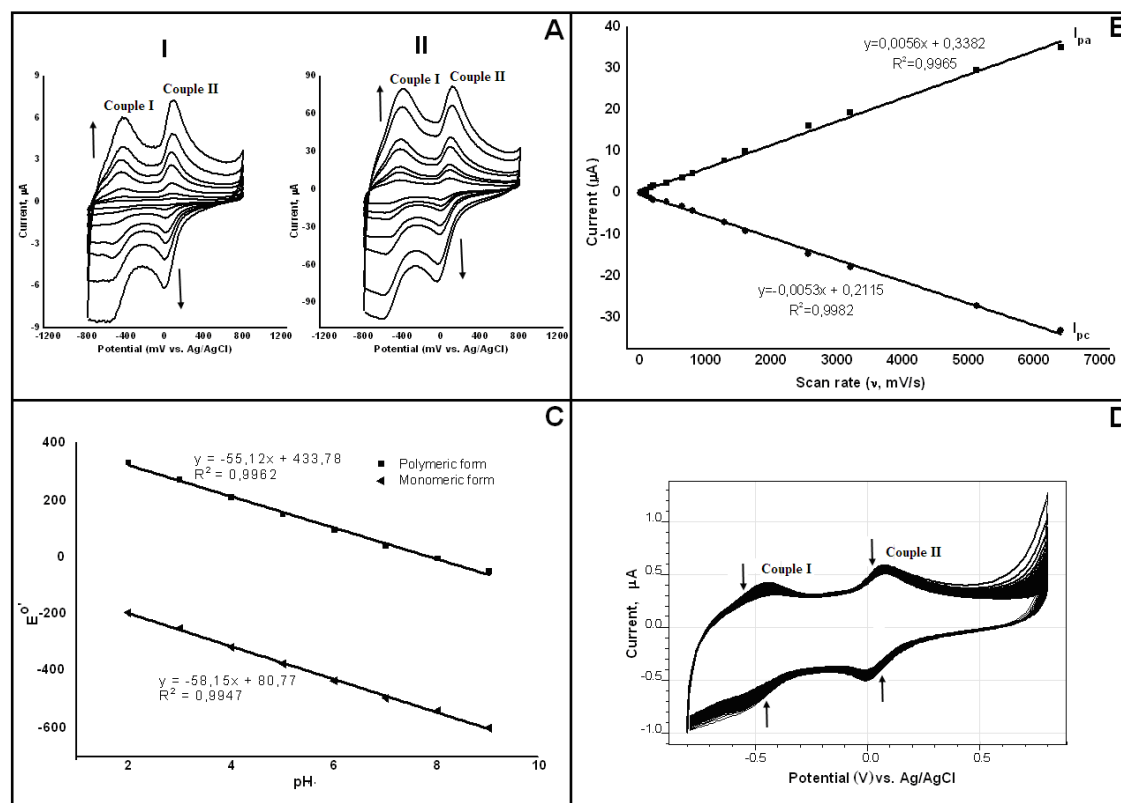


Figure 3.15. **A)** Cyclic voltammograms of poly-NR/GCE in 0.1 M PBS (pH 7.0) at a scan rates of **I:** 20, 50, 100, 160, 200, 400, 640; **II:** 800, 1280, 1600, 2560, 3200, 5120, 6400 mVs^{-1} . **B)** The plot of the anodic (i_{pa}) and cathodic (i_{pc}) peak currents versus the scan rates for redox couple II. **C)** The plot of formal potential versus pH which was calculated from cyclic voltammograms of poly-NR/GCE recorded at 50 mVs^{-1} in the potential range of -0.8 to +0.8 V vs. Ag/AgCl, **D)** Repetitive cyclic voltammograms of poly-NR/GCE with 200 cycles in 0.1 M PBS (pH 7.0) at scan rate of 50 mVs^{-1} .

In order to determine the effect of pH on the formal standard potential ($E^{0'}$) of modified electrodes, the cyclic voltammograms of poly-NR/GCE were recorded in phosphate solutions of pH values between 2 and 9 at a scan rate of 50 mVs⁻¹. Figure 3.15C shows that the $E^{0'}$ values of redox couple for polymeric and monomeric form of NR dependent on pH and these values decreased linearly with increasing pH. The slopes of these curves were found to be about -55.1 mV/pH and -58.2 mV/pH for polymeric and monomeric forms of MG, respectively which were equal to the anticipated Nernstian value for two electrons and two protons attending the electron transfer process for monomeric and polymeric forms.

In order to test the stability of poly-NR/GCE, the cyclic voltammograms of the modified electrode were recorded by successive scans (200 cycles) in 0.1 M PBS (pH 7.0) at a scan rate of 50 mVs⁻¹. Figure 3.15D shows that the repetitive cyclic voltammograms of modified electrode with 200 cycles. At the first cycle, two redox pairs were observed. After about 100 repetitive scans, change in height of peaks became very small.

3.3. Photoelectrocatalytic Studies

3.3.1. Photoelectrocatalytic oxidation of NADH using poly-HT/GCE

i. With cyclic voltammetry

Although the HT modified carbon paste electrode was found to be an active electron transfer mediator for the electrocatalytic oxidation of NADH (Zare et al., 2006a), poly-HT/GCE has not yet been reported for electrocatalytic and especially photoelectrocatalytic oxidation of NADH in the literature. Thus, it was expected that poly-HT/GCE can be used for the photoelectrocatalytic oxidation of NADH since the photoelectrocatalytic method has better sensitivity than electrocatalytic method for the determination of NADH (Dilgin et al., 2009; Gligor et al., 2009). In this context, a fiberoptic halogen lamp with 250 W was used for recording data during photoelectrochemical experiments.

Firstly, the effect of light on the poly-HT/GCE was examined prior to any experiments with photoelectrochemical oxidation of NADH. Cyclic voltammograms of the poly-HT/GCE were recorded with/without the irradiation of the electrode surface in the 0.1 M PBS (pH 7.0). When the surface of the poly-HT/GCE was

irradiated, a small increase in the peak currents was observed from the cyclic voltammograms (Figure 3.16 curves a and b).

It was found that poly-HT/GCE which prepared in the optimization conditions of electropolymerization process gives a good electrocatalytic response towards NADH (See Section 3.1.1). A similar result was also seen in Figure 3.16c₁ and c₂. If the peak potential of NADH at the unmodified GCE (about +550 mV, see Figure 3.1B) is compared with that of the poly-HT/GCE (about +230 mV, Figure 16c), it was observed that the overpotential for the electrochemical oxidation of NADH decreased by 320 mV. As can be seen in Figure 3.16, the electrocatalytic oxidation of NADH was observed at about +230 mV (Figure 3.16c₁) and the peak current decreased in the second cycle (Figure 3.16c₂). However, the peak current at +250 mV attributed to electrocatalytic oxidation of NADH increased with irradiation of electrode surface (Figure 3.16d₁) and especially, the peak current of second cycle (Figure 3.16d₂) was two times higher than that of obtained without irradiation for the same concentration of NADH (Figure 3.16c₂). The increase in the electrocatalytic peak current of NADH in the presence of light may depend on the excitation of the poly-HT on the electrode surface and its excited form can more rapidly react with NADH. Thus, it can be concluded that irradiation of the surface of poly-HT/GCE causes a faster photoelectrochemical oxidation of NADH than that of electrochemical.

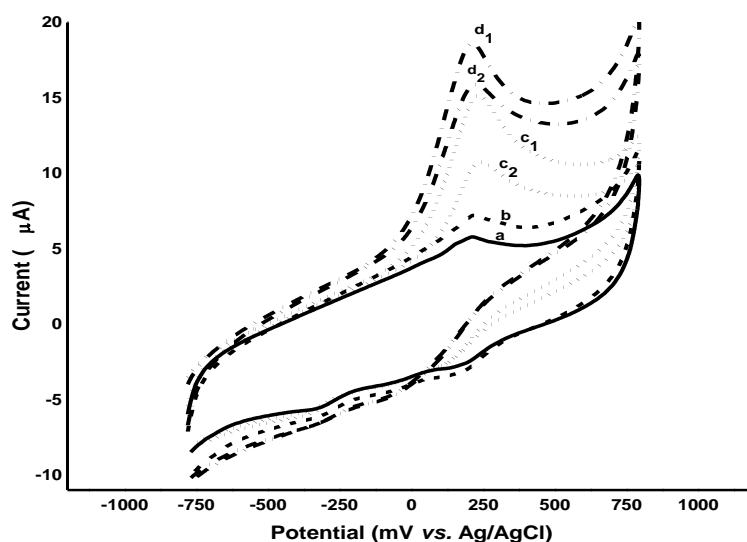
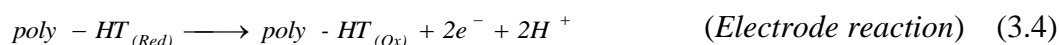
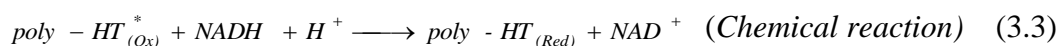
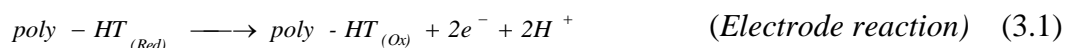


Figure 3.16. Cyclic voltammograms of poly-HT/GCE in the absence (a, b) and in the presence (c, d) of 0.8 mM NADH without (a, c) and with (b, d) irradiation of the electrode surface (in 0.1 PBS (pH 7.0); scan rate: 50 mVs⁻¹). c₁ and d₁: first cycle; c₂ and d₂: second cycle.

The mechanism of the photoelectrochemical oxidation of NADH with poly-TB modified GCE was explained by the fact that initially the oxidized redox mediator was excited by light, followed by the fact that the excited redox mediator rapidly reacts with NADH, and finally the obtained leuco form of the mediator was reoxidized at the electrode surface (Dilgin et al., 2007). This mechanism was firstly reported by Compton's research group for the electrocatalytic oxidation of ascorbic acid with TB and MB (Cooper et al., 1998, 1999). A similar photo ECE mechanism (Equations 3.1 - 3.4) can also be proposed for the photoelectrochemical oxidation of NADH with poly-HT/GCE.



ii. With amperometric methods

In order to perform amperometric studies, initially the optimum applied potential was optimized. For this aim, the current-time curves were recorded at various applied potential between 0 and 800 mV for 0.2 mM NADH in the 0.1 M PBS (pH 7.0) using GCE with and without irradiation of electrode surface. Same procedure was repeated for poly-HT/GCE at various applied potential between -100 and +600 mV.

Figure 3.17A shows the plot of amperometric and photoamperometric currents versus applied potential for 0.2 mM NADH at bare GCE. As can be seen in this figure, the maximum current of NADH oxidation was obtained at applied potential of 400-500 mV. It was seen that the currents obtained from the photoamperometric studies was higher two times than that from amperometric methods.

The current for NADH oxidation using bare GCE was monitored versus NADH concentration (Figure 3.17B) at 150 mV, which was generally found as the optimum applied potential for modified electrodes (Figure 3.17A).

According to this curve, the current values for NADH with various concentrations were found to be lower than that of modified electrodes, but the current also increased with irradiation of electrode surface. On the other hand, it was observed that the linearity range for bare electrode was very narrow.

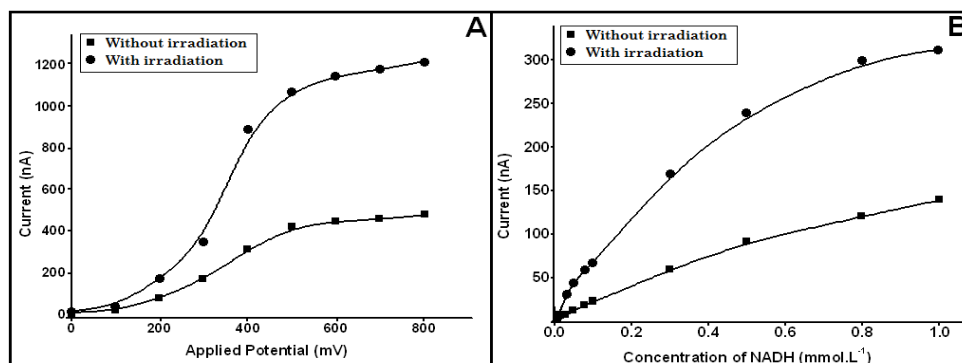


Figure 3.17. A) The plot of current for 0.2 mM NADH versus applied potential and B) the plot of current response versus the concentration of NADH at +150 mV applied potential in 0.1 M PBS (pH 7.0) using bare GCE with /without irradiation conditions.

Figure 3.18A shows the plot of electrocatalytic current versus applied potential for 0.2 mM NADH using poly-HT/GCE. As can be seen from this figure, the best response was obtained at applied potential of 200 mV. However, the photoamperometric current was 2.2 times higher than the amperometric current. Thus, the applied potential for both methods was selected as +200 mV for further investigations.

Current versus time responses for 0.2 mM NADH were recorded in 0.1 M PBS (pH 7.0) at 200 mV (Figure 3.18B). When the poly-HT/GCE surface was irradiated after obtaining a steady state background, a small current increase was observed. However, a large increase in the photoamperometric response was obtained when adding 0.2 mM NADH, which indicates that the electrochemical oxidation of NADH was greatly influenced by irradiation of the electrode surface.

Figure 3.18C shows the linear dependence of the electrocatalytic and photoelectrocatalytic current responses to concentrations of NADH in a 0.1 M PBS (pH 7.0). A linear calibration graph for NADH was obtained between 1.0×10^{-6} and 1.0×10^{-3} M for both methods. The linearity of these methods is described by the equations as follow:

$$i (\mu\text{A}) = 1.18 C (\text{mmolL}^{-1}) + 0.021 \quad (R^2 = 0.9926)$$

$$i (\mu\text{A}) = 2.66 C (\text{mmolL}^{-1}) + 0.034 \quad (R^2 = 0.9933)$$

for amperometric and photoamperometric studies, respectively, where i is current, C is the concentration of NADH and R is the regression coefficient. Although the steady state current increased with an increase in the NADH concentration for both the amperometric and the photoamperometric method, the slope of the current-NADH concentration curve of the photoelectrocatalytic procedure improved about 2.25 times compared with that obtained without irradiation.

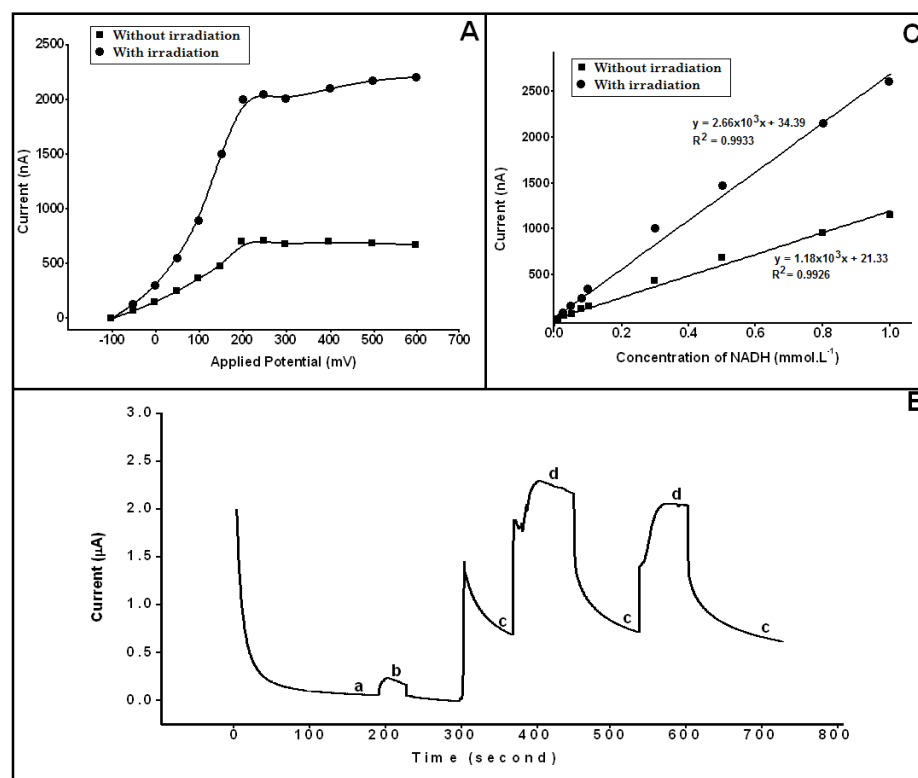


Figure 3.18. **A)** The plot of electrocatalytic and photoelectrocatalytic current for 0.2 mM NADH versus applied potential, **B)** Current versus time curve of a poly-HT/GCE in the absence (a, b) and in the presence (c, d) of 0.2 mM NADH without (a, c) and with (b, d) irradiation of the electrode surface in 0.1 M PBS (pH 7.0). Applied potential: +200 mV, **C)** Plot of electrocatalytic and photoelectrocatalytic current response vs. the concentration of NADH at +200 mV applied potential in 0.1 M PBS (pH 7.0) using poly-HT/GCE.

3.3.2. Photoelectrocatalytic oxidation of NADH using poly-MG/GCE

i. With cyclic voltammetry

Photoelectrocatalytic oxidation of NADH was also observed for poly-MG/GCE. The cyclic voltammograms of NADH using poly-MG/GCE with and without irradiation of electrode surface are given in Figure 3.19. This figure shows that irradiation of the surface of poly-MG/GCE causes a faster

photoelectrochemical oxidation of NADH than that of electrochemical. The photoelectrocatalytic oxidation mechanism can be explained a photo ECE mechanism, was already discussed in the section of 3.3.1.

If the peak potential of NADH at the unmodified GCE (about +500 mV, see Figure 3.5B) is compared with that of the poly-MG/GCE (about +80 mV, Figure 3.19c), it was observed that, the overpotential for the electrochemical oxidation of NADH decreased by 420 mV. However, the peak current at 20 mV attributed to electrocatalytic oxidation of NADH increased with irradiation of electrode surface (Figure 3.19d) and peak current was two times higher than that of obtained without irradiation for the same concentration of NADH (Figure 3.19c).

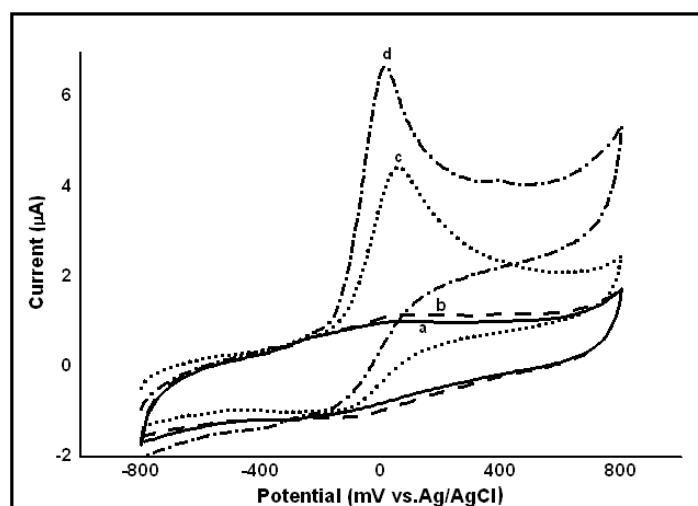


Figure 3.19. Cyclic voltammograms of a poly-MG/GCE in the absence (a, b) and in the presence (c, d) of 0.4 mM NADH without (a, c) and with (b, d) irradiation of the electrode surface. Supporting electrolyte: 0.1 M PBS (pH 7.0); scan rate: 50 mVs⁻¹.

ii. With amperometric methods

Figure 3.20A shows the plot of electrocatalytic current versus applied potential for 0.2 mM NADH using poly-MG/GCE. As can be seen from this figure, the best response was obtained at applied potential of +100 mV. The photoamperometric current was 2 times higher than the amperometric current. Thus, the applied potential for both methods was selected as +100 mV for further investigations.

Current versus time responses for 0.2 mM NADH were recorded in 0.1 M PBS (pH 7.0) at +100 mV (Figure 3.20B). When the poly-MG/GCE surface was irradiated after obtaining a steady state background, a small current increase was

observed. However, a large increase for the photoamperometric response was obtained when adding 0.2 mM NADH, which indicates that the electrochemical oxidation of NADH was highly influenced by irradiation of the electrode surface.

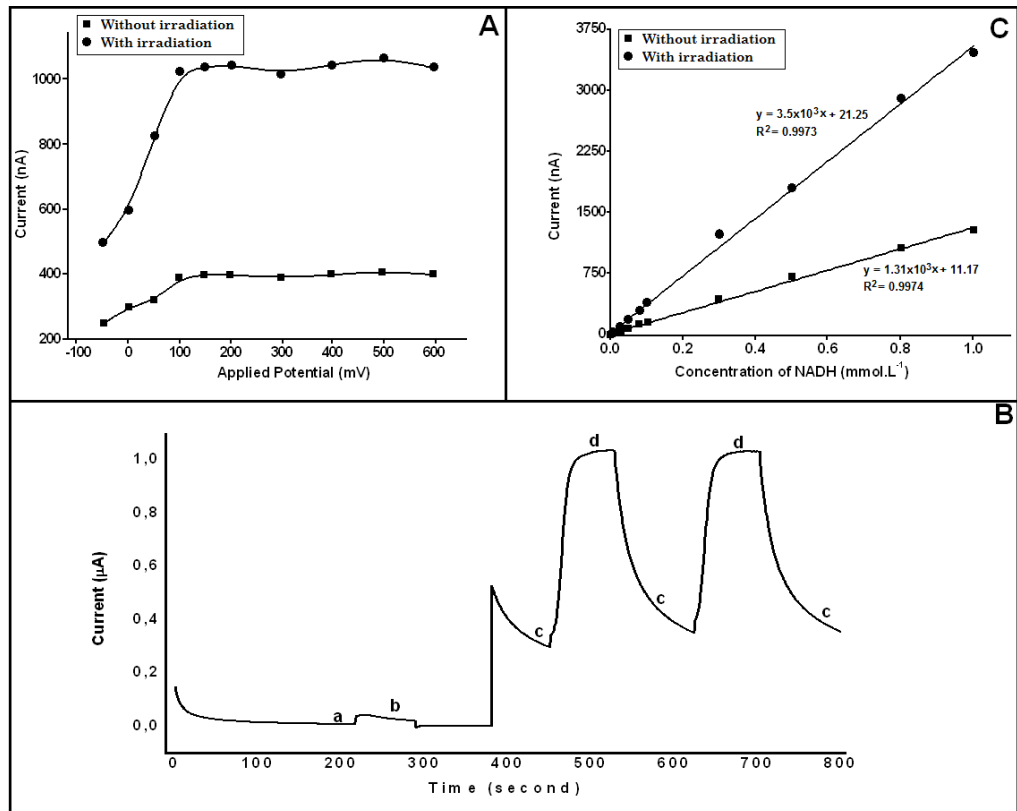


Figure 3.20. **A)** The plot of electrocatalytic and photoelectrocatalytic current for 0.2 mM NADH versus applied potential, **B)** Current versus time curve of a poly-MG/GCE in the absence (a, b) and in the presence (c, d) of 0.2 mM NADH without (a, c) and with (b, d) irradiation of the electrode surface in 0.1 M PBS (pH 7.0). Applied potential: +100 mV, **C)** Plot of electrocatalytic and photoelectrocatalytic current response vs. the concentration of NADH at +100 mV applied potential in 0.1 M PBS (pH 7.0) using polyMG/GCE.

Figure 3.20C shows the linear dependence of the electrocatalytic and photoelectrocatalytic current responses to the concentrations of NADH in a 0.1 M PBS (pH 7.0). A linear calibration graph for NADH was obtained between 1.0×10^{-6} and 1.0×10^{-3} M for both methods. The linearity of these methods is described by the equations as follow:

$$i (\mu\text{A}) = 1.31 C (\text{mmolL}^{-1}) + 0.011 \quad (R^2 = 0.9973)$$

$$i (\mu\text{A}) = 3.50 C (\text{mmolL}^{-1}) + 0.021 \quad (R^2 = 0.9974)$$

for amperometric and photoamperometric studies, respectively, where i is current, C is the concentration of NADH and R is the regression coefficient. Although the

steady state current increased with an increase in the NADH concentration for both the amperometric and the photoamperometric method, the slope of the current-NADH concentration curve of the photoelectrocatalytic procedure improved by about 2.67 times compared with that obtained without irradiation.

As previously mentioned, the mechanism of the photoelectrochemical oxidation of NADH was explained by the fact that initially the oxidized redox mediator was excited by light, followed by the fact that the excited redox mediator rapidly reacts with NADH, and finally the formed leuco form of the mediator was reoxidized at the electrode surface (Cooper et al. 1998; Cooper et al. 1999; Dilgin et al. 2007).

3.3.3. Photoelectrocatalytic oxidation of NADH using poly-NR/GCE

i. With cyclic voltammetry

Although NR modified electrodes were used as an active electron transfer mediator for the electrocatalytic oxidation of NADH (Barsan et al., 2008; Karyakin et al., 1999b), our literature search demonstrated that poly-NR/GCE had not yet been used for photoelectrocatalytic oxidation of NADH. Photoelectrocatalytic oxidation of NADH was also investigated for poly-NR/GCE. Firstly, the cyclic voltammograms of poly-NR/GCE electrodes were recorded with and without irradiation of electrode surface. When the electrode surface was irradiated, a small increase of peak currents was observed (Figure 3.21 a, b).

For studying the photoelectrocatalytic properties of poly-NR/GCEs towards NADH oxidation, cyclic voltammograms were recorded in the presence of 0.4 mM NADH, with and without irradiation of electrode surface. If the peak potential of NADH at the unmodified GCE (about +500 mV, see Figure 3.9B) is compared with that of the poly-NR/GCE (about +140 mV, Figure 3.21c), it was observed that the overpotential for the electrochemical oxidation of NADH decreased by 360 mV. However, the peak current at +120 mV attributed to electrocatalytic oxidation of NADH, increased with irradiation of electrode surface (Figure 3.21d) and peak current was two times higher than that obtained without irradiation for the same concentration of NADH (Figure 3.21c). It can be stated that the rate of reaction between NADH and poly-NR increases when the

irradiation of electrode surface takes place. As a conclusion, the irradiation of poly-NR/GCE surface leads to the photoelectrochemical oxidation of NADH.

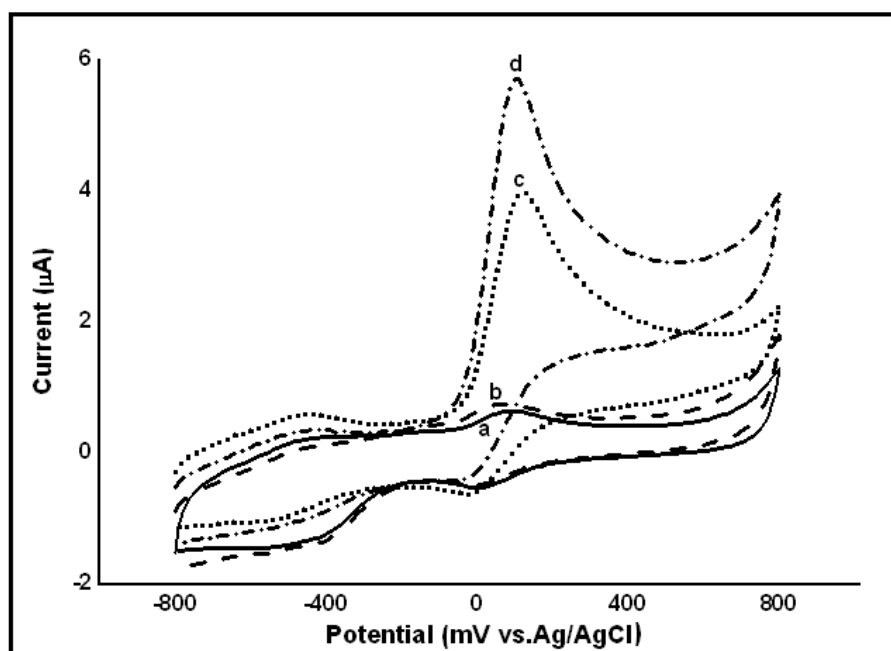


Figure 3.21. Cyclic voltammograms of a poly-NR/GCE in the absence (a, b) and in the presence (c, d) of 0.4 mM NADH without (a, c) and with (b, d) irradiation of the electrode surface Supporting electrolyte: 0.1 M PBS (pH 7.0); scan rate: 50 mVs⁻¹.

ii. With amperometric methods

Figure 3.22A shows the plot of electrocatalytic current versus applied potential for 0.2 mM NADH using poly-NR/GCE. As can be seen from this figure, the best response was obtained at applied potential of +150 mV. The photoamperometric current was 2 times higher than the amperometric current. Thus, the applied potential for both methods was selected as +150 mV for further investigations.

Current versus time responses for 0.2 mM NADH were recorded in 0.1 M PBS (pH 7.0) at +150 mV (Figure 3.22B). When the poly-NR/GCE surface was irradiated after obtaining a steady state background a small current increase was observed. However, a large increase for the photoamperometric response was obtained when adding 0.2 mM NADH, which indicates that the electrochemical oxidation of NADH was greatly influenced by irradiation of the electrode surface.

Figure 3.22C shows the linear dependence of the electrocatalytic and photoelectrocatalytic current responses to concentrations of NADH in a 0.1 M PBS (pH 7.0). A linear relationship between the NADH concentration and the peak current was obtained over the concentration range $1.0 \times 10^{-6} - 1.0 \times 10^{-3}$ M by the photoamperometric and amperometric method at the poly-NR/GCE. The linearity of these methods is described by the equations as follow:

$$i (\mu\text{A}) = 2.99C (\text{mmolL}^{-1}) + 0.037 \quad (R^2 = 0.994)$$

$$i (\mu\text{A}) = 1.50C (\text{mmolL}^{-1}) + 0.003 \quad (R^2 = 0.998)$$

for photoamperometric and amperometric studies, respectively, where i is the peak current and C is the concentration of NADH. When these equations are compared in terms of their slopes, it is clear that the sensitivity of the photoelectrocatalytic procedure is better than that of the amperometric method and the ratio of improvement is about two times more.

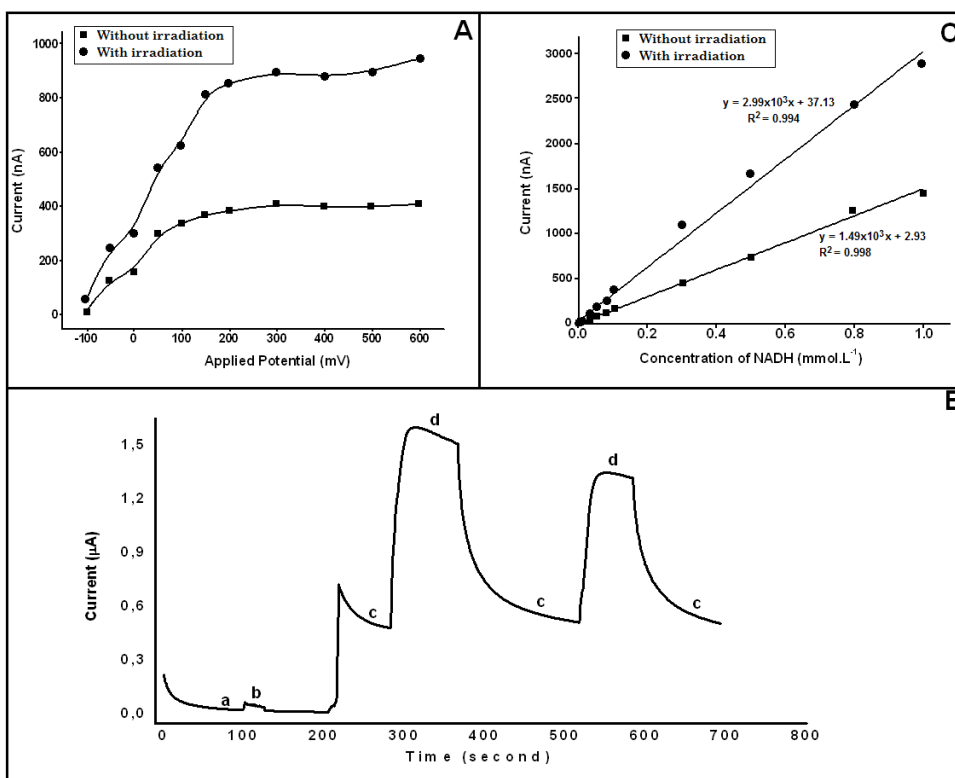


Figure 3.22. A) Plot of electrocatalytic and photoelectrocatalytic current for 0.2 mM NADH versus applied potential, B) Current versus time curve of a poly-NR/GCE in the absence (a, b) and in the presence (c, d) of 0.2 mM NADH without (a, c) and with (b, d) irradiation of the electrode surface in 0.1 M PBS (pH 7.0). Applied potential: +150 mV, C) Plot of electrocatalytic and photoelectrocatalytic current response vs. the concentration of NADH at +150 mV applied potential in 0.1 M PBS (pH 7.0) using poly-NR/GCE.

3.4. Photoelectrocatalytic Studies in Flow Injection Analysis System

3.4.1. Photoamperometric detection of NADH using poly-HT/GCE in FIA

In order to obtain the best amperometric and photoamperometric response of poly-HT/GCE towards NADH in FIA system, the effect of the applied potential, flow rate, sample loop and tubing length on the current of 0.1 mM NADH were investigated by recording current-time curves. Firstly, the applied potential was optimized in the conditions of 1.3 mL min⁻¹ flow rate, 100 μ L sample loop, 25 cm tubing length and 0.1 M PBS (pH 7.0) containing 0.1 M KCl as carrier stream. Thus, the current-time curves were recorded at various applied potentials using both poly-HT/GCE and also bare GCE. After a steady background current was obtained, 0.1 mM NADH solution was injected into the carrier stream.

By using amperometric and photoamperometric methods the obtained electrocatalytic and photoelectrocatalytic currents were individually measured from current-time curves obtained at various applied potential at poly-HT/GCE (Figure 3.23) and bare GCE (Figure 3.24). Figure 3.25 shows the plot of electrocatalytic and photoelectrocatalytic currents versus the applied potential. The response currents for electrocatalytic and photoelectrocatalytic oxidation of NADH in FIA system became apparent at 400 mV and reached a maximum value at about 650 mV at bare electrode (Figure 3.25 a and b). However, at poly-HT/GCE, the currents became apparent at -100 mV and reached a maximum value at about 300 mV (Figure 3.25 c and d). In addition, the current values obtained at the same potential values from the photoamperometric method were higher about by 50-40% than that obtained from amperometric method. Thus an applied potential of +300 mV was selected as optimum applied potential.

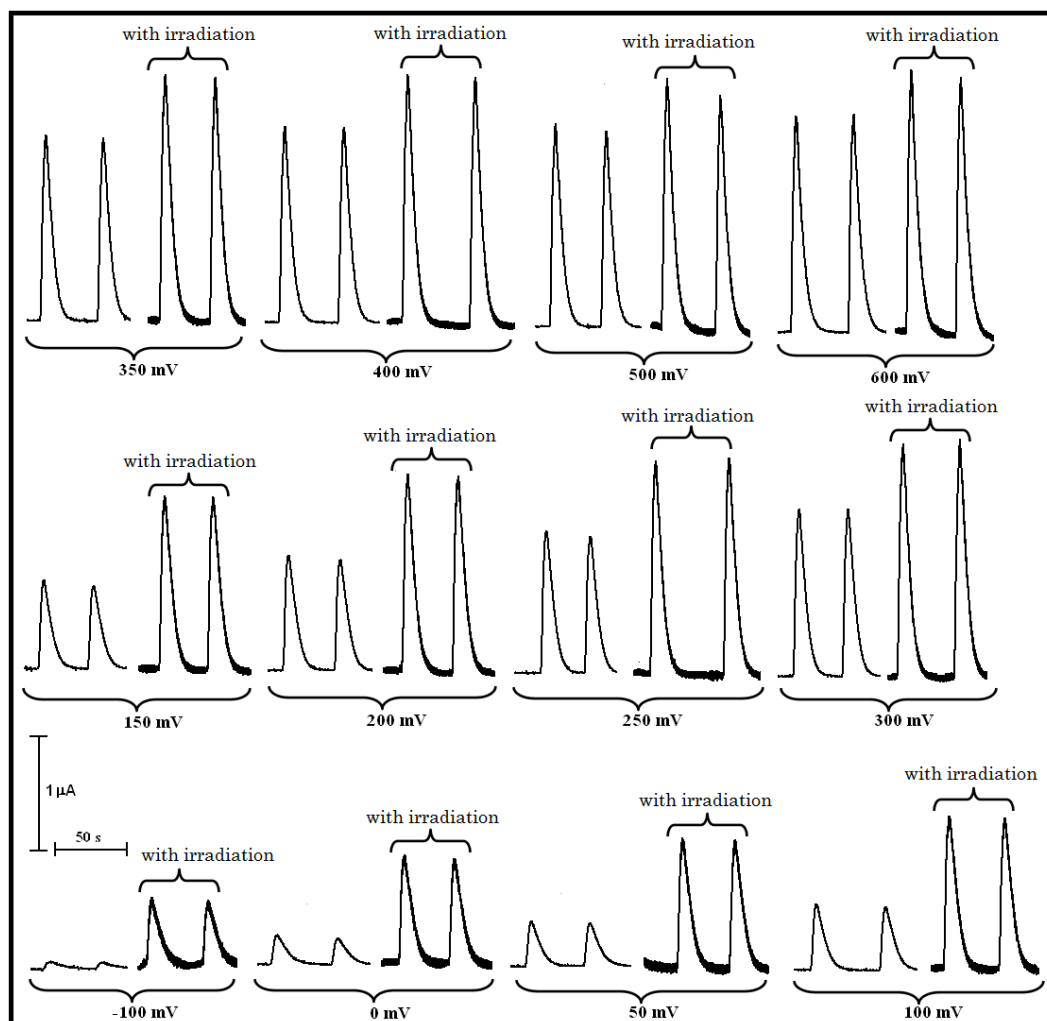


Figure 3.23. The fiagrams of 0.1 mM NADH at various applied potential using Poly-HT/GCE.

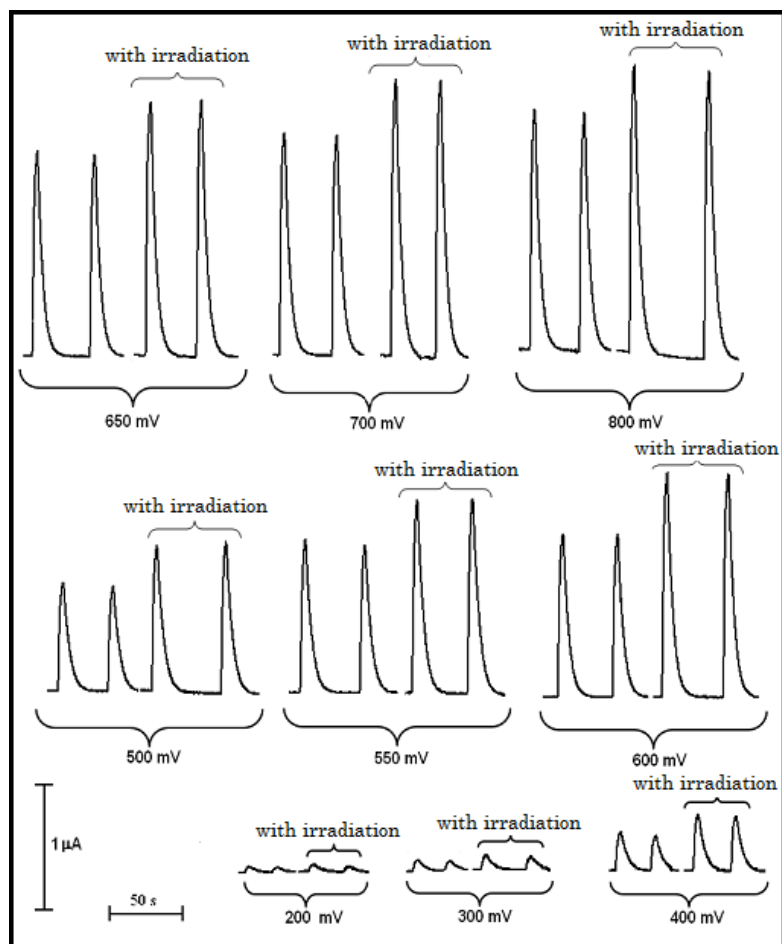


Figure 3.24. The diagrams of 0.1 mM NADH at various applied potential using bare GCE.

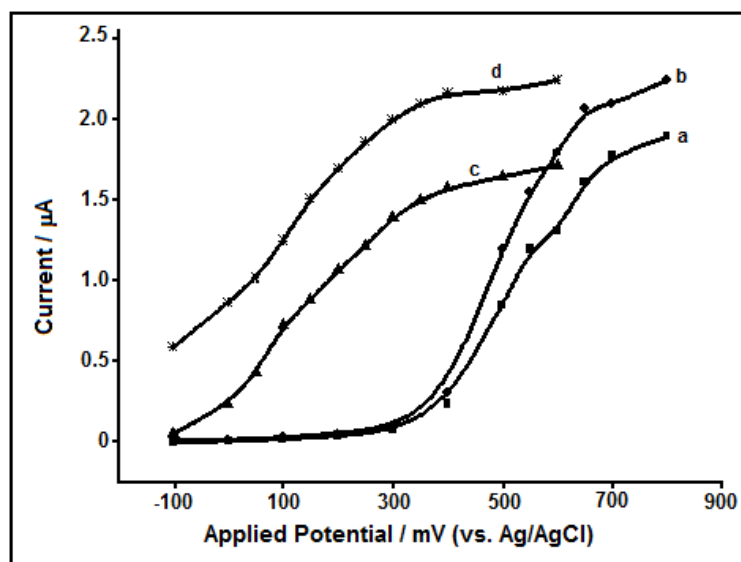


Figure 3.25. The effect of applied potential on a) amperometric and b) photoamperometric peak currents obtained diagrams using bare GCE and c) amperometric and d) photoamperometric peak currents obtained diagrams using poly-HT/GCE. Injected: 0.1 mM NADH solution.

Secondly, the effect of flow rate on electrocatalytic and photoelectrocatalytic currents was investigated. For this purpose, the current-time curves were recorded at various flow rates using poly-HT/GCE in 0.1 M PBS (pH 7.0) containing 0.1 M KCl using 100 μL sample loop and 25 cm tubing length. Figure 3.26 shows the plot of the electrocatalytic and photoelectrocatalytic currents of 0.1 mM NADH versus flow rate. The peak currents were increased by increasing the flow rate from 0.3 mL min^{-1} to 1.3 mL min^{-1} . After the flow rate of 1.3 mL min^{-1} , the peak currents slowly decreased by increasing flow rates. However, the decrease in the photoamperometric currents (Figure 3.26b) was higher than amperometric currents (Figure 3.26a) at high flow rates. This can be attributed to the fact that time is not enough for the interaction between injected NADH and the excited mediator on the electrode surface.

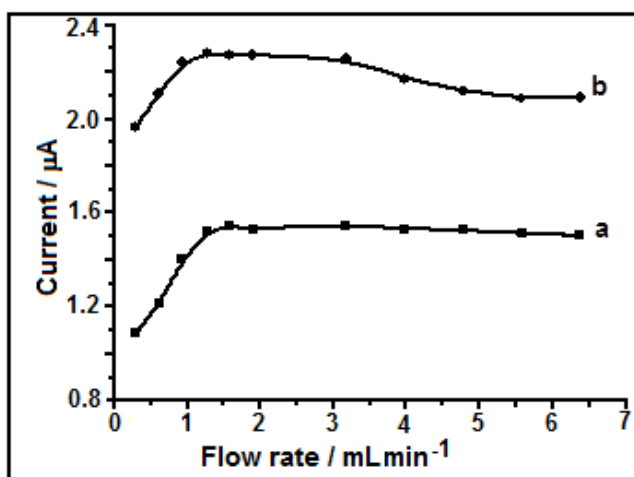


Figure 3.26. The effect of flow rate on a) amperometric, and b) photoamperometric peak currents of 0.1 mM NADH obtained diagrams using poly-HT/GCE.

In addition, the peak height increased linearly by increasing the sample volume (20, 50, 100 μL) while the peak width was broadened. The effect of transmission tube length on currents was also examined. The smallest transmission tube length was used (10 cm) because there was no chemical reaction in the tube and the dispersion of injected NADH must be limited along the tube. When the transmission tube length was increased, both photoamperometric and amperometric current peaks were broadened, therefore sample frequency was decreased.

From optimization studies, the applied potential, the flow rate, the sample volume, and the transmission tube length were determined as +300 mV vs. Ag/AgCl, 1.3 mL min^{-1} , 100 μL and 10 cm, respectively.

Both amperometric and photoamperometric currents versus various concentration of NADH were recorded using poly-HT/GCE in these optimum conditions. Figure 3.27 shows the current-time curves for amperometric and photoamperometric FI responses for various concentrations of NADH. Although the peak current increased depending on NADH concentration for both the amperometric and the photoamperometric methods, the responses of photoamperometric method were higher than that of amperometric method in all concentrations (Appendix 3).

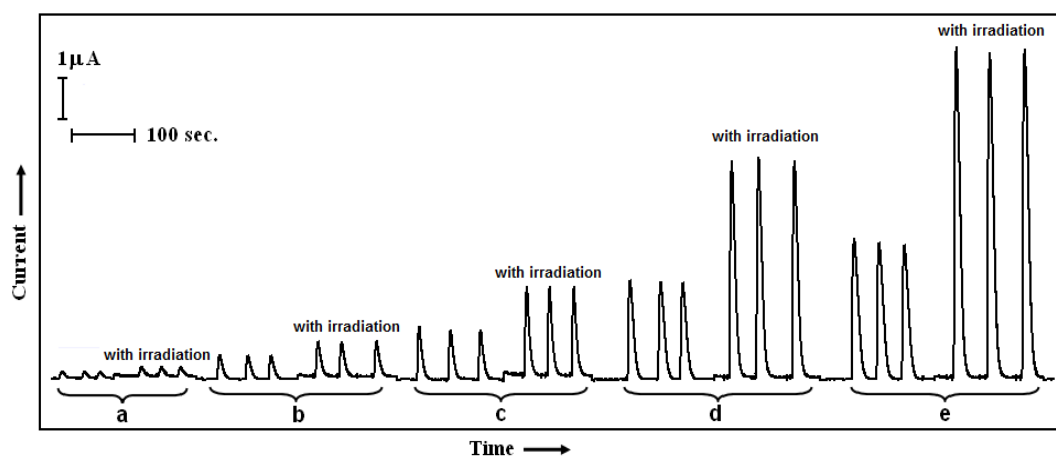


Figure 3.27. Current-time curves of NADH with different concentrations a) 10, b) 40, c) 100, d) 400, e) 1000 μM NADH using poly-HT/GCE in FIA system (Carrier stream: 0.1 M PBS (pH 7.0) containing 0.1 M KCl, Applied potential: +300 mV; Flow rate: 1.3 mL min^{-1} , sample loop: $100 \mu\text{L}$; transmission tubing length: 10 cm).

Figure 3.28 shows a plot of catalytic current versus NADH concentration (Appendix 3). A linear relationship between the NADH concentration and the peak current was obtained over the concentration range $2.0 \times 10^{-7} - 1.5 \times 10^{-4} \text{ M}$ by amperometric FIA and $2.0 \times 10^{-7} - 2.5 \times 10^{-4} \text{ M}$ by the photoamperometric FIA methods at the poly-HT/GCE. The linearity of these methods is described by the equations as follow:

$$i (\mu\text{A}) = 11.96 C (\text{mM}) + 0.029 \quad (R^2 = 0.9908)$$

$$i (\mu\text{A}) = 18.51 C (\text{mM}) + 0.048 \quad (R^2 = 0.9956)$$

for amperometric and photoamperometric studies, respectively, where i is the peak current and C is the concentration of NADH. When these equations are compared in terms of their slopes, it is clear that the sensitivity of the photoelectrocatalytic FIA procedure is better than that of the amperometric method and the ratio of improvement is about 55%.

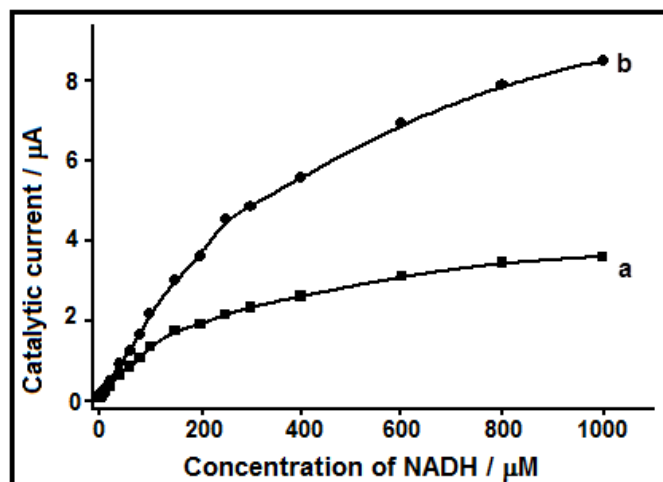


Figure 3.28. Dependence of the catalytic currents on NADH concentration for a) amperometric and b) photoamperometric analysis of NADH using poly-HT/GCE in FIA system. (Carrier stream: 0.1 M PBS (pH 7.0) containing 0.1 M KCl, applied potential: +300 mV; flow rate: 1.3 mL min⁻¹; sample loop: 100 μL ; transmission tubing length: 10 cm).

The repeatability of the method was investigated by repeated injections ($n = 8$, 100 μL) of the 6.0×10^{-5} M NADH and the relative standard deviation (RSD) was found to be 2.2% and 4.3% for the amperometric and photoamperometric FIA method, respectively. These results show that the proposed methods have acceptable repeatability because obtained RSD values were lower than 10%. The limit of detection (LOD) values were found to be 4.0×10^{-8} and 3.0×10^{-8} M (signal/noise = 3) and the limit of quantification (LOQ) value were found to be 1.2×10^{-7} and 1.0×10^{-7} M (signal/noise = 3) for amperometric and photoamperometric determination of NADH in FIA system, respectively.

The electrocatalytic oxidation of NADH was reported by Zare et al. (2006a) using HT modified carbon paste electrode. A decrease in overpotential of NADH was found to be ca. 280 mV, while in present study it was found to be 310 mV. They reported that the limit of detection was estimated to be order of 0.08 μM , which was obtained from differential pulse voltammetric determination. However, in photoamperometric FIA method using poly-HT/GCE the detection limit was found to be 0.03 μM . Thus, it can conclude that the sensitivity for NADH determination was significantly improved in the present study.

3.4.2. Photoamperometric detection of NADH using poly-MG/GCE in FIA

In order to obtain the best amperometric and photoamperometric response of poly-MG/GCE towards NADH in FIA system, the effect of the applied potential, flow rate, sample loop and tubing length on the current of 0.1 mM

NADH was also investigated by recording current-time curves. Firstly, the applied potential was optimized under the conditions of 1.3 mL min^{-1} , flow rate, $100 \text{ }\mu\text{L}$ sample loop, 10 cm tubing length and 0.1 M PBS (pH 7.0) containing 0.1 M KCl as carrier stream. Thus, the current-time curves were recorded at various applied potentials using both poly-MG/GCE and bare GCE. After a steady background current was obtained, 0.1 mM NADH solution was injected into the carrier stream. The electrocatalytic and photoelectrocatalytic currents were measured from current-time curves obtained at various applied potential using poly-MG/GCE (Figure 3.29).

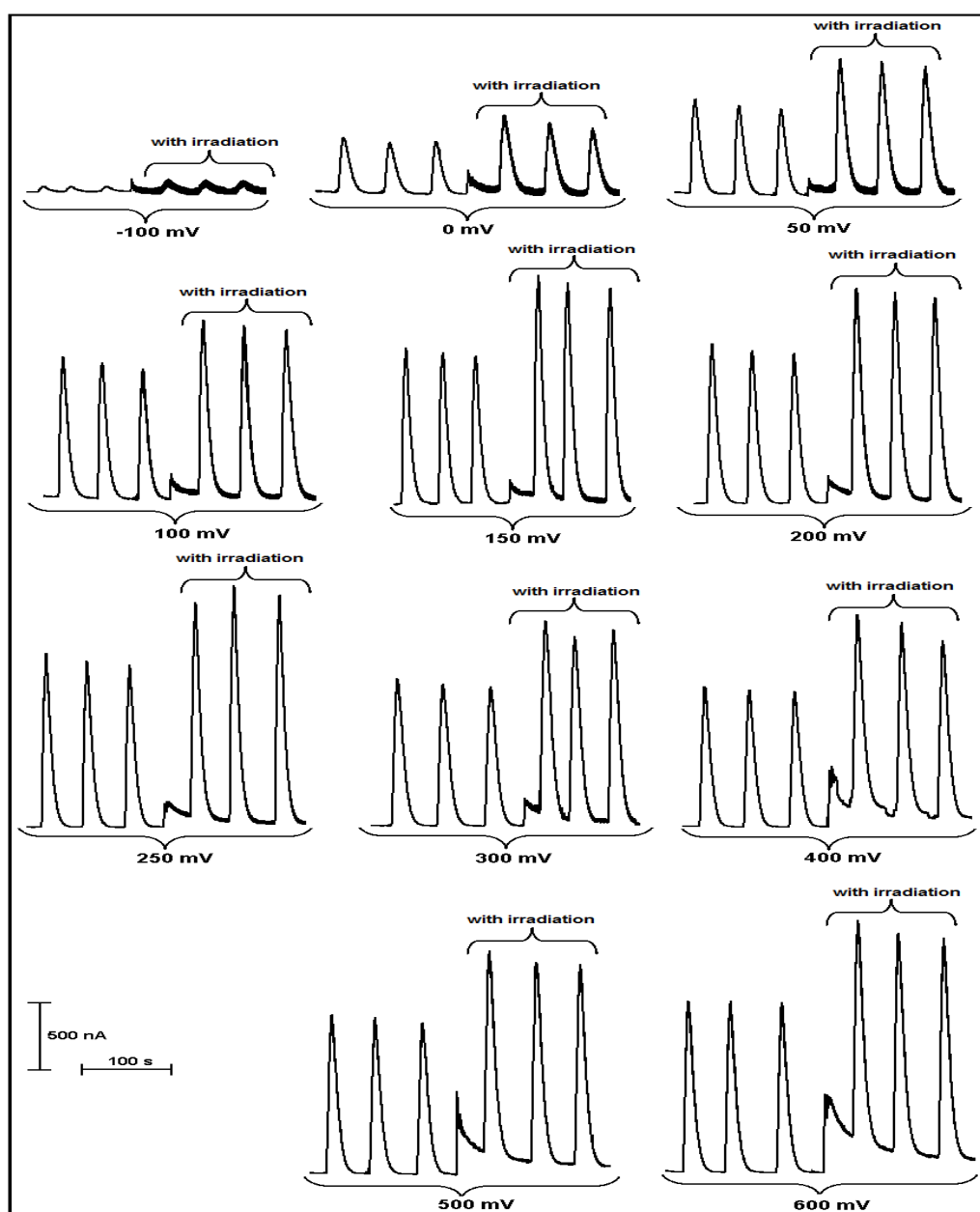


Figure 3.29. The diagrams of 0.1 mM NADH at various applied potential using poly-MG/GCE.

Figure 3.30 shows the plot of electrocatalytic and photoelectrocatalytic currents versus the applied potential. As above mentioned, the response currents for electrocatalytic and photoelectrocatalytic oxidation of NADH in FIA system became apparent at 400 mV and reached a maximum value at about 650 mV at bare electrode (See Figure 3.25 a and b). However, at poly-MG/GCE, the currents became apparent at -100 mV and reached a maximum value at about 150 mV (Figure 3.30 a and b). In addition, the current values obtained from the photoamperometric method were higher by about 30% than those obtained from amperometric method. Thus an applied potential of +150 mV was selected as optimum applied potential.

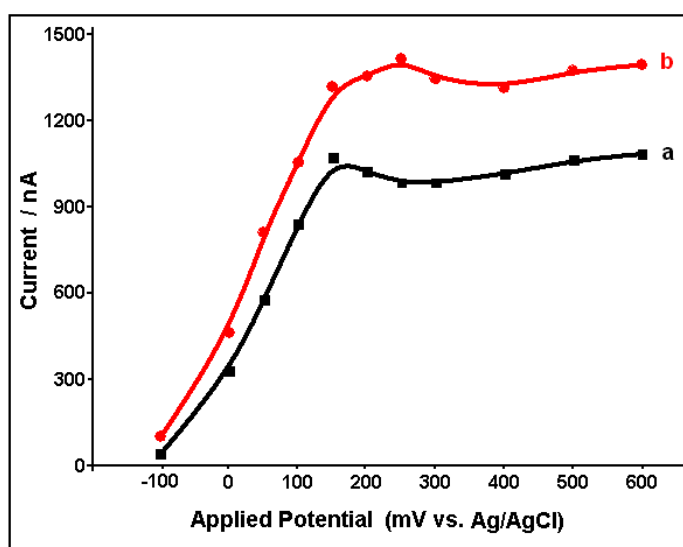


Figure 3.30. The effect of applied potential on a) amperometric and b) photoamperometric peak currents obtained using poly-MG/GCE. Injected: 0.1 mM NADH solution.

Secondly, the effect of flow rate on electrocatalytic and photoelectrocatalytic currents was investigated. For this purpose, the current-time curves were recorded at various flow rates using poly-MG/GCE in 0.1 M PBS (pH 7.0) containing 0.1 M KCl using 100 μL sample loop and 25 cm tubing length. Figure 3.31 shows the plot of the electrocatalytic and photoelectrocatalytic currents of 0.1 mM NADH versus flow rate. The peak currents increased by increasing the flow rate from 0.3 mL min^{-1} to 1.3 mL min^{-1} . After the flow rate of 1.3 mL min^{-1} , the peak currents slowly decreased by increasing flow rates. However, the decrease in the photoamperometric currents (Figure 3.31b) was higher than amperometric currents (Figure 3.31a) at high flow rates. This can be attributed to the fact that time was not enough for the interaction between injected NADH and the excited mediator on the electrode surface.

In addition; the peak height increased linearly by increasing the sample volume (20, 50, 100 μL) while the peak width was broadened. The effect of transmission tube length on currents was also examined. The smallest transmission tube length was used (10 cm) because there was no chemical reaction in the tube and the dispersion of injected NADH must be limited along the tube. When the transmission tube length was increased, both photoamperometric and amperometric current peaks were broadened, therefore sample frequency was decreased.

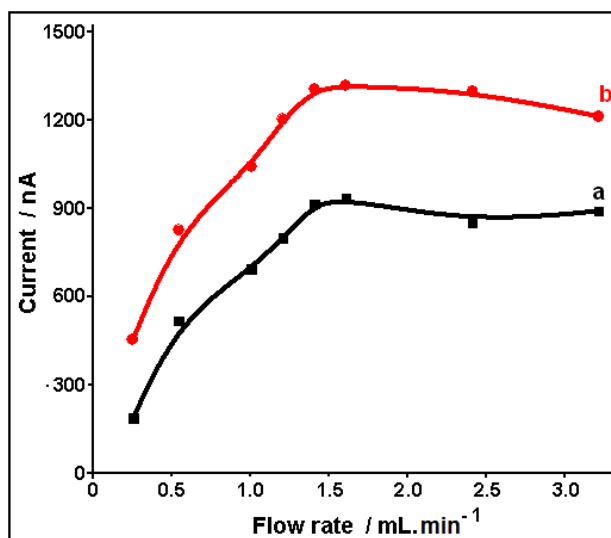


Figure 3.31. The effect of flow rate on a) amperometric b) photoamperometric peak currents of 0.1 mM NADH obtained diagrams using poly-MG/GCE.

From optimization studies, the applied potential, the flow rate, the sample volume, and the transmission tube length were determined as +150 mV, 1.3 mLmin⁻¹, 100 μL and 10 cm, respectively.

Both amperometric and photoamperometric currents versus various concentration of NADH were recorded using poly-MG/GCE in these optimum conditions. Figure 3.32 shows the current-time curves for amperometric and photoamperometric FI responses to various concentrations of NADH. Although the peak current increased depending on NADH concentration for both the amperometric and the photoamperometric methods, the responses of photoamperometric method were higher than that of amperometric in all concentrations.

Figure 3.33 shows a plot of catalytic current versus NADH concentration. From this figure, a linear relationship between the NADH concentration and the

peak current was obtained over the concentration range $5.0 \times 10^{-7} - 5 \times 10^{-4}$ M by the photoamperometric and also amperometric FIA method at the poly-MG/GCE.

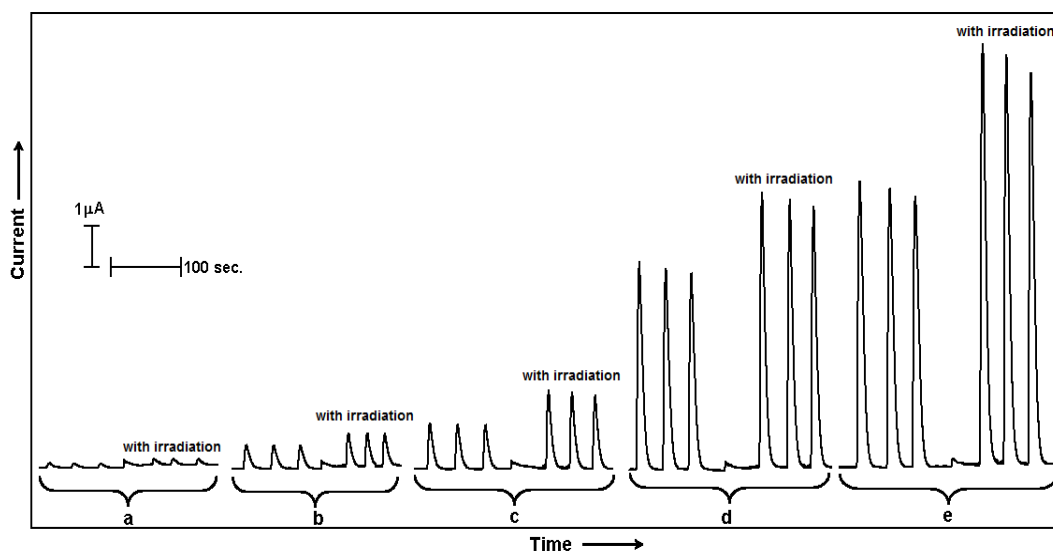


Figure 3.32. Current- time curves of NADH with different concentrations a) 10, b) 50, c) 100, d) 500, e) 1000 μM NADH using poly-MG/GCE in FIA system (Carrier stream: 0.1 M PBS (pH 7.0) containing 0.1 M KCl, Applied potential: +150 mV; Flow rate: 1.3 mL min^{-1} , sample loop: 100 μL ; transmission tubing length: 10 cm).

The linearity of these methods is described by the following equations:

$$i (\mu\text{A}) = 9.82 C (\text{mM}) + 0.015 \quad (R^2 = 0.999)$$

$$i (\mu\text{A}) = 12.39 C (\text{mM}) + 0.074 \quad (R^2 = 0.998)$$

for amperometric and photoamperometric studies, respectively, where i is the peak current and C is the concentration of NADH. Linearity criteria were also satisfied for the proposed methods since R-squared values of calibration curves were better than 0.995. When these equations are compared in terms of their slopes, it is clear that the sensitivity of the photoelectrocatalytic FIA procedure is better than that of the amperometric method and the ratio of improvement is about 26%.

The repeatability of the method was investigated by repeated injections ($n = 8$, 100 μL) of the 1.0×10^{-4} M NADH and the RSD was found to be 3.4% and 5.6% for the amperometric and photoamperometric FIA method, respectively. These results show that the proposed methods have acceptable repeatability because obtained RSD values were lower than 10%. LODs were found to be 3.0×10^{-7} and 2.5×10^{-7} M (signal/noise = 3) and LOQs were found to be 9×10^{-7} and 8×10^{-7} M for amperometric and photoamperometric determination of NADH in FIA system, respectively.

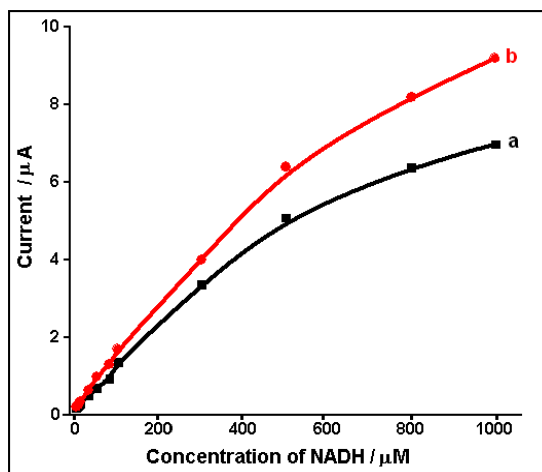


Figure 3.33. Dependence of the catalytic currents on NADH concentration for a) amperometric and b) photoamperometric analysis of NADH using poly-MG/GCE in FIA system. (Carrier stream: 0.1 M PBS (pH 7.0) containing 0.1 M KCl, applied potential: +150 mV; flow rate: 1.3 mL min⁻¹; sample loop: 100 μL ; transmission tubing length: 10 cm).

The electrocatalytic oxidation of NADH and alcohol biosensor dependent on NADH/NAD⁺ was reported by Dai et al. (2008) using MG modified GCE. They reported that the limit of detection was estimated to be in the order of 3.8 μM , which was obtained from amperometric method. However, in photoamperometric FIA method using poly-MG/GCE, the detection limit was found to be 0.3 μM . Thus, it can conclude that the sensitivity for NADH determination was improved more than ten times in the present study.

Also noting that the obtained results at the poly-HT/GCE were better than those of obtained at the poly-MG/GCE using the photoamperometric FIA method. In other words, the sensitivity of FIA procedure increased about 1.55-fold at the poly-HT/GCE with irradiation but increased 1.26-fold at the poly-MG/GCE. For this reason, it was decided to use the poly-HT/GCE in the biosensor studies.

3.5. Biosensor and Photoelectrochemical Biosensor Studies

3.5.1. Cyclic voltammetric studies

Electrocatalytic and photoelectrocatalytic oxidation of glucose at GDH based poly-HT modified GCEs were investigated using cyclic voltammetric techniques. Firstly, the electrochemical and photoelectrochemical response of dehydrogenase immobilized GCE (GDH/GCE without poly-HT) and PAMAM modified GCE (GDH/PAMAM/GCE without poly-HT) to glucose was investigated by recording cyclic voltammograms. For this, cyclic voltammograms

of GDH/GCE and GDH/PAMAM/GCE were recorded in 0.1 M PBS (pH 7.0) containing 10 mM NAD^+ in the absence and in the presence of 10 mM glucose at 5 mVs^{-1} scan rate, respectively. The obtained cyclic voltammograms are given in Figures 3.34 and 3.35.

In the first voltammograms (Fig. 3.34a and Fig. 3.35a), no peak was observed because the supporting electrolyte did not include any substrate (glucose). When the substrate was added to supporting electrolyte, a reversible peak at about +800 mV at GDH/GCE (Fig. 3.34b) and at about +760 mV at GDH/PAMAM/GCE (Fig. 3.35b) was observed, which was attributed to the oxidation of enzymatically produced NADH to NAD^+ at bare and PAMAM modified GCEs (Reactions 3.6 and 3.7). When the electrode surface was irradiated with the light source, the peak current increased a little for both electrodes (Figures 3.34c and 3.35c).

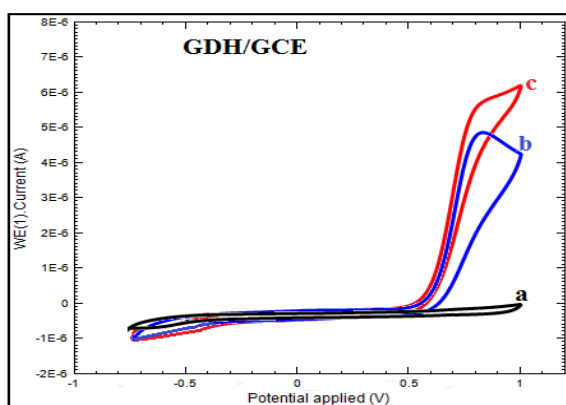


Figure 3.34. Cyclic voltammograms of GDH/GCE in the presence of 10 mM NAD^+ and a) in the absence, b) in the presence of 10 mM glucose without irradiation and c) b with irradiation. Supporting electrolyte: 0.1 M PBS (pH 7.0); scan rate: 5 mVs^{-1} .

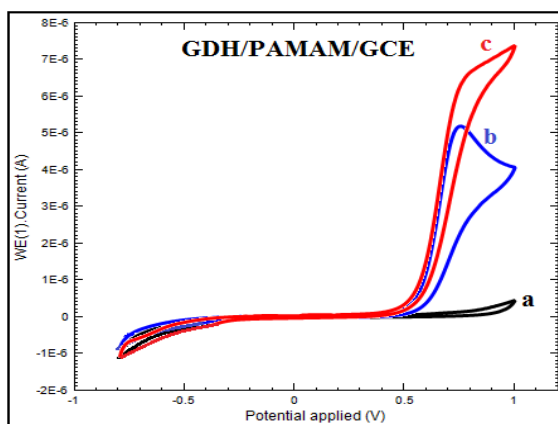
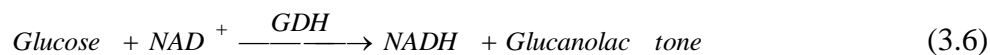


Figure 3.35. Cyclic voltammograms of GDH/PAMAM/GCE in the presence of 10 mM NAD^+ and a) in the absence, b) in the presence of 10 mM glucose without irradiation and c) b with irradiation. Supporting electrolyte: 0.1 M PBS (pH 7.0); scan rate: 5 mVs^{-1} .



In order to see the effect of mediator, HT was electropolymerized onto GCE and PAMAM/GCE (electropolymerization conditions: HT monomer concentration, 0.3 mM; cycle numbers, 20; scan rate, 100 mVs⁻¹; potential range, (-0.5) – (+2.1) V; supporting electrolyte, 0.1 M PBS (pH 7.0) containing 0.1 M NaNO₃). Then GDH was immobilized onto those electrode surfaces after they were washed with water and dried in argon atmosphere. Before the response of modified electrodes towards glucose, some parameters such as cycle numbers during electropolymerization of HT and scan rate during recording cyclic voltammograms of glucose which especially affect the cyclic voltammograms with irradiation. Firstly, the cyclic voltammograms of glucose were recorded at various scan rates using GDH/poly-HT/PAMAM/GCE (Fig. 3.36) which was prepared by electropolymerization of HT with 10 cycles. Fig. 3.36 showed that the electrocatalytic oxidation peak current of enzymatically produced NADH not increased by increasing of scan rate in the irradiation of electrode surface. Therefore, a scan rate of 5 mVs⁻¹ was selected an optimum value for recording cyclic voltammograms of glucose with and without irradiation. In order to see the effect of cycle number during electropolymerization of HT on glucose response, poly-HT/PAMAM/GCEs were prepared at various cycle numbers such as 10, 20 and 30 cycles and the cyclic voltammograms of glucose were recorded by using these electrodes with and without irradiation (Fig. 3.37). While scan cycle was optimized as 10 cycle for electrocatalytic oxidation of NADH (see Section 3.1.1), cyclic voltammograms of glucose in Fig. 3.37 showed that poly-HT/PAMAM/GCE with 20 scan cycles offered the best response to glucose detection for biosensing studies. Obtained cyclic voltammograms with 20 cycles for electropolymerization process on GCE and PAMAM/GCE are shown in Figures 3.38 and 3.39, respectively. As can be seen in these figures, the oxidation peak at +385 mV with a shoulder at +285 mV and reduction peak at about -480 mV observed in the first scan cycle were gradually increased by increasing the scan cycle after the second cycle. Electropolymerization mechanism was proposed in Section 3.1.1. However, it was observed that increase of monomeric peaks by increasing the scan cycle at PAMAM/GCE was found to be better than at GCE. This result shows that PAMAM dendrimer has a good surface for electropolymerization of HT.

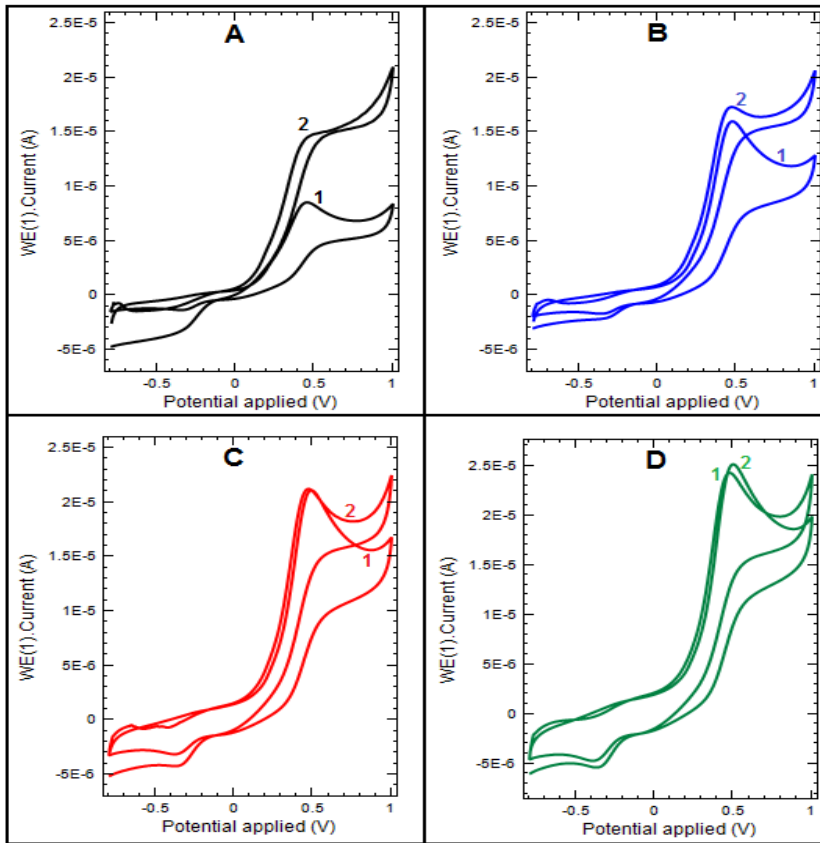


Figure.3.36. Cyclic voltammograms of GDH/poly-HT/PAMAM/GCE, which obtained from electropolymerization of HT on PAMAM/GCE using 10,cycles, in the presence of 10 mM NAD^+ and 10 mM glucose without irradiation (1) and with irradiation (2) at various scan rates A) 5 B) 10, C) 20 and D) 50 mVs^{-1} . Supporting electrolyte: 0.1 M PBS (pH 7.0).

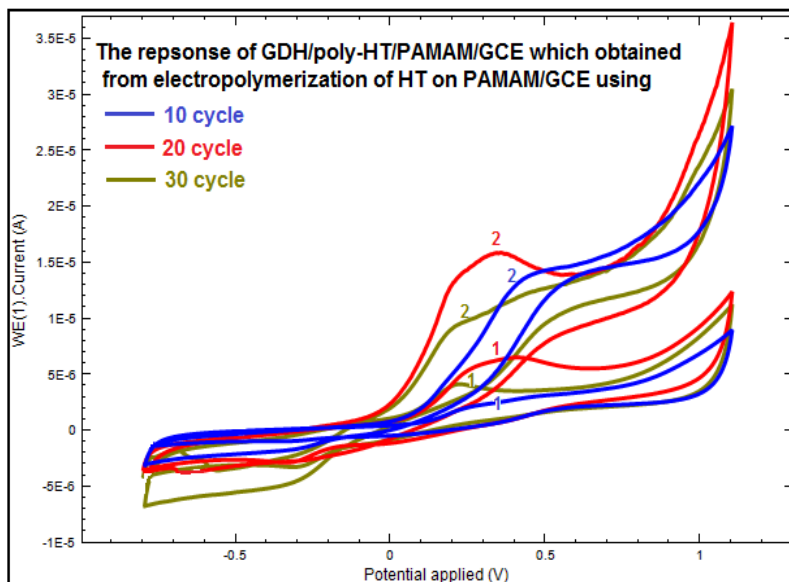


Figure 3.37. Cyclic voltammograms of GDH/poly-HT/PAMAM/GCE, which obtained from electropolymerization of HT on PAMAM/GCE using 10, 20 and 30 cycles, in the presence of 10 mM NAD^+ and 10 mM glucose without (1) and with (2) irradiation. Supporting electrolyte: 0.1 M PBS (pH 7.0); scan rate: 5 mVs^{-1} .

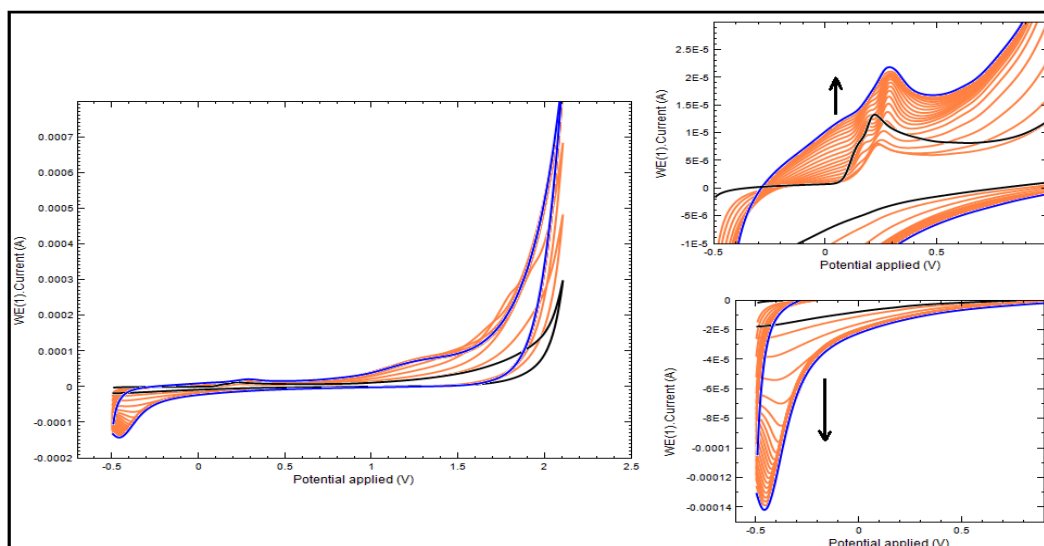


Figure 3.38. Repetitive cyclic voltammograms (20 cycles) of 0.3 mM HT at GCE in 0.1 M PBS (pH 7.0) containing 0.1 M NaNO_3 at 100 mVs^{-1} , in the range of -0.5 to +2.1 V vs. Ag/AgCl.

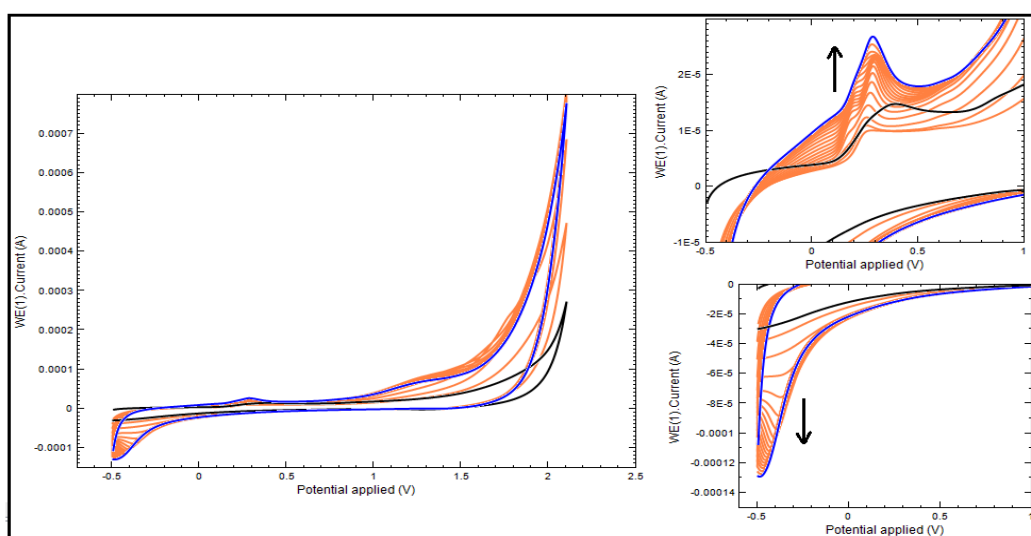


Figure 3.39. Repetitive cyclic voltammograms (20 cycles) of 0.3 mM HT at PAMAM/GCE in 0.1 M PBS (pH 7.0) containing 0.1 M NaNO_3 at 100 mVs^{-1} , in the range of -0.5 to +2.1 V vs. Ag/AgCl.

After polymerization, GDH was immobilized onto these electrodes (poly-HT/GCE and poly-HT/PAMAM/GCE). The electrochemical and photoelectrochemical response of both electrodes to glucose was investigated by cyclic voltammetric technique. The above mentioned (for GDH/GCE and GDH/PAMAM/GCE) cyclic voltammetric procedures for biosensing and photobiosensing of glucose were also repeated for these electrodes. The obtained cyclic voltammograms are given in Figures 3.40 and 3.41 for GDH/Poly-HT/GCE and GDH/Poly-HT/PAMAM/GCE, respectively.

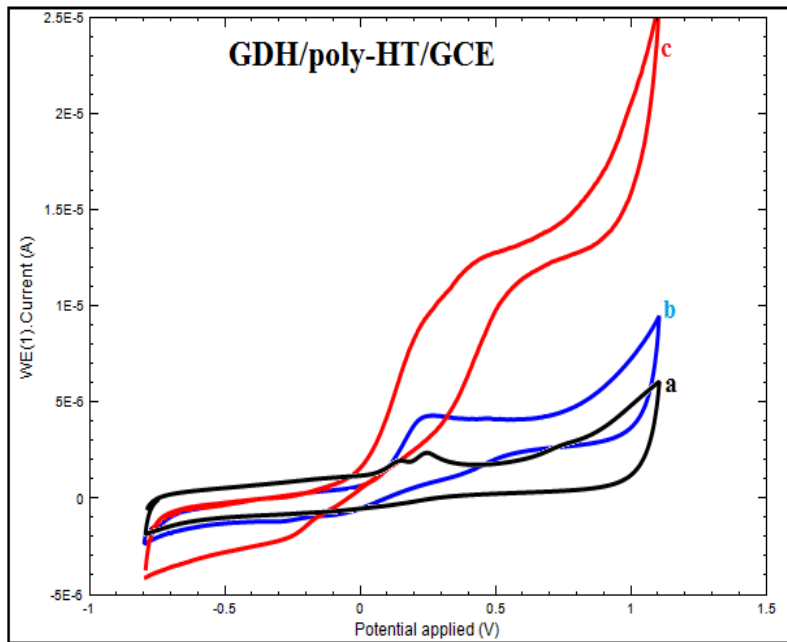


Figure 3.40 Cyclic voltammograms of GDH/poly-HT/GCE in the presence of 10 mM NAD^+ and a) in the absence, b) in the presence of 10 mM glucose without irradiation and c) b with irradiation. Supporting electrolyte: 0.1 M PBS (pH 7.0); scan rate: 5 mVs^{-1} .

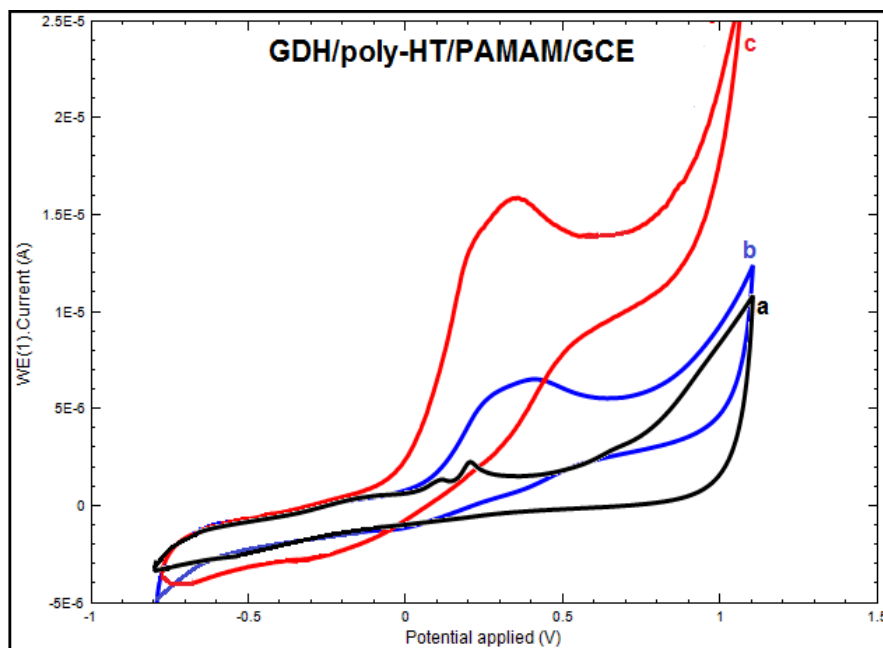
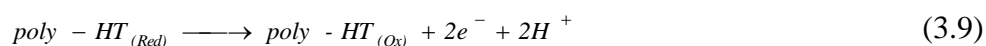
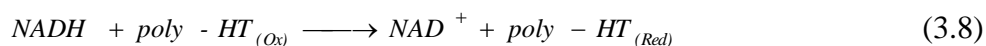


Figure 3.41. Cyclic voltammograms of GDH/poly-HT/PAMAM/GCE in the presence of 10 mM NAD^+ and a) in the absence, b) in the presence of 10 mM glucose without irradiation and c) b with irradiation. Supporting electrolyte: 0.1 M PBS (pH 7.0); scan rate: 5 mVs^{-1} .

In the first cyclic voltammograms of both electrodes, only an anodic peak at about +210 mV with a shoulder at +120 mV was observed in the presence of NAD^+ (Fig. 3.40a and 3.41a). These peaks can be attributed to oxidation of

polymeric form of HT. In the presence of glucose, the current of this peak increased at both electrodes, which is attributed to the electrocatalytic oxidation of enzymatically produced NADH to NAD^+ (Figures 3.40b and 3.41b). When the electrode surfaces were irradiated with the light source, a large enhancement in this peak current was observed for both electrodes (Figures 3.40c and 3.41c). However, increase in peak current of glucose at GDH/Poly-HT/PAMAM/GCE with irradiation of electrode surface was observed to be better than that at GDH/poly-HT/GCE.

If it was compared the peak potential of glucose at GDH/GCE (about +800 mV, see Figure 3.34b) and GDH/PAMAM/GCE (about 760 mV, see Figure 3.35b) with that of the GDH/poly-HT/GCE (about +250 mV, Figure 3.40b) and GDH/poly-HT/PAMAM/GCE (about 300 mV, Figure 3.41b), the overpotential for the electrochemical oxidation of NADH produced by enzymatic reaction of glucose decreased by 550 mV and 360 mV at GDH/poly-HT/GCE and GDH/poly-HT/PAMAM/GCE, respectively. Moreover, the peak current at 300 mV (GDH/poly-HT/PAMAM/GCE) and 250 mV (GDH/poly-HT/GCE) attributed to electrocatalytic oxidation of NADH increased with irradiation of electrode surface (Figure 3.40c and 3.41c). However, the peak shape and increase in peak current of NADH related to glucose concentration at GDH/Poly-HT/PAMAM/GCE with irradiation of electrode surface was observed to be better than that at GDH/poly-HT/GCE. The increase in the electrocatalytic peak current of NADH with light depends on excitation of poly-HT on the electrode surface and its excited form can more rapidly react with NADH. Thus, it can be concluded that irradiation of the surface of poly-HT/GCE causes a faster photoelectrochemical oxidation of NADH than that of electrochemical. The mechanism can be explained by reactions between 3.6 and 3.9. These results showed that the photoelectrochemical biosensor dependent on NAD^+/NADH redox couple and dehydrogenase enzyme can be constructed for glucose detection. A similar result was also obtained for thionine modified multiwalled carbon nanotube and gold nanoparticle functionalized indium tin oxide electrode (Deng et al, 2008). However, in this cited study FIA system was not used. As distinct from this, the proposed method in present study also includes photoelectrochemical biosensor in FIA system.



3.5.2. Amperometric studies in FIA system

3.5.2.1. Optimization of the Experimental Parameters

After the investigation of biosensing and photoelectrochemical biosensing of glucose using cyclic voltammetric technique, it was also investigated using amperometric techniques in FIA system. However, only GDH/Poly-HT/PAMAM/GCE was used in FIA amperometric studies. In order to obtain the best amperometric and photoamperometric response of GDH/Poly-HT/PAMAM/GCE towards glucose in FIA system, the effect of the applied potential and flow rate on the current of 0.8 mM glucose containing 10 mM NAD^+ was investigated by recording fiagrams. Firstly, the applied potential was optimized under the conditions of 1.1 mL min^{-1} flow rate, $100 \text{ }\mu\text{L}$ sample loop, 10 cm tubing length and 0.1 M PBS (pH 7.0) containing 0.1 M KCl as carrier stream. Then, the current-time curves were recorded at various applied potential. After a steady background current was obtained, 0.8 mM glucose containing 10 mM NAD^+ was injected into the carrier stream. The amperometric and photoamperometric currents were measured from current-time curves obtained at various applied potential (Appendix 4). Figure 3.42 shows the current-time curves of GDH/Poly-HT/PAMAM/GCE for 0.8 mM glucose containing 10 mM NAD^+ obtained at various applied potential.

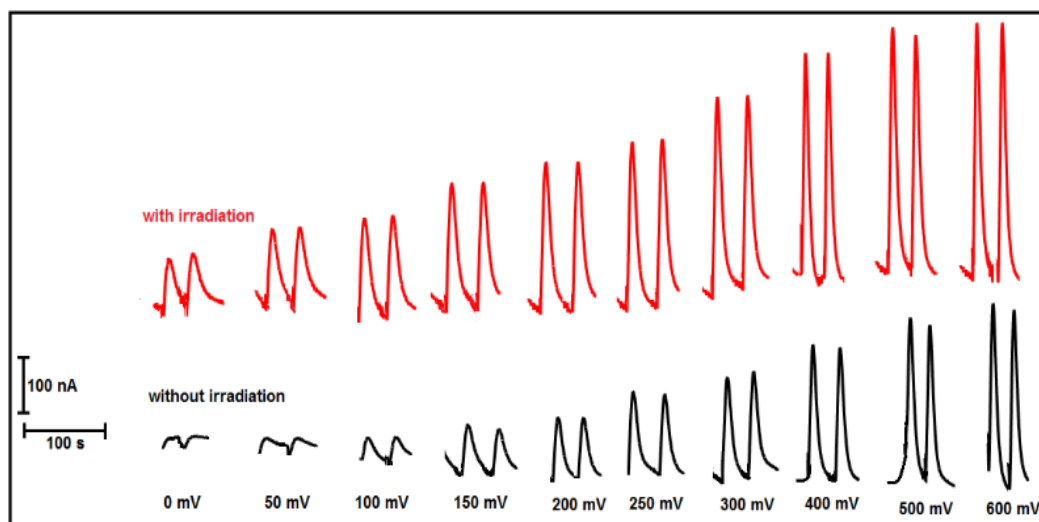


Figure 3.42. Current-time curves of 0.8 mM glucose containing 10 mM NAD^+ at various applied potential using GDH/Poly-HT/PAMAM/GCE. (Carrier stream: 0.1 M PBS (pH 7.0) containnig 0.1 M KCl; flow rate: 1.1 mLmin^{-1} ; sample loop: $100 \text{ }\mu\text{L}$; tubing length:10 cm).

Figure 3.43 shows the plot of electrocatalytic and photoelectrocatalytic currents of glucose versus the applied potential (Appendix 4). The best currents for electrocatalytic and photoelectrocatalytic oxidation of NADH produced by enzymatic reaction of glucose in FIA system were found at about 300 mV. In addition, the current values obtained from the photoamperometric method were about 50-40% higher than that obtained from amperometric method. Thus an applied potential of +300 mV was selected as optimum in order to minimize interference effects.

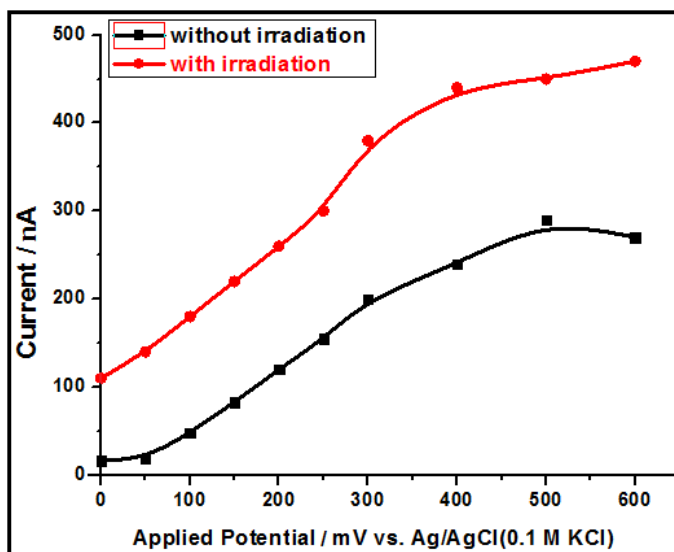


Figure 3.43. The effect of applied potential on ■) amperometric and ●) photoamperometric peak currents obtained diagrams using GDH/Poly-HT/PAMAM/GCE. Injected: 0.8 mM glucose containing 10 mM NAD^+ .

In the second optimization step, the effect of flow rate on electrocatalytic and photoelectrocatalytic currents of glucose was investigated. For this purpose, the current-time curves were recorded at various flow rates using GDH/Poly-HT/PAMAM/GCE in 0.1 M PBS (pH 7.0) containing 0.1 M KCl using 100 μL sample loop and 10 cm tubing length. Figure 3.44 shows the diagrams of GDH/Poly-HT/PAMAM/GCE for 0.8 mM glucose containing 10 mM NAD^+ obtained at various flow rates. Figure 3.45 shows the plot of the electrocatalytic and photoelectrocatalytic currents of 0.8 mM glucose containing 10 mM NAD^+ versus flow rate (Appendix 5). As can be seen in this figure, the maximum peak current was observed at the lowest flow rate, 0.125 mL, because, biosensors and photoelectrochemical biosensors could find enough time for the occurrence of enzymatic reaction and also photoexcitation of mediator in the low flow rate. The peak currents decreased by increasing the flow rate from 0.125 mL min^{-1} to 2.2 mL min^{-1} . Thus, the lowest flow rate, 0.125 mL min^{-1} was selected as optimum flow rate even though sample frequency is very low.

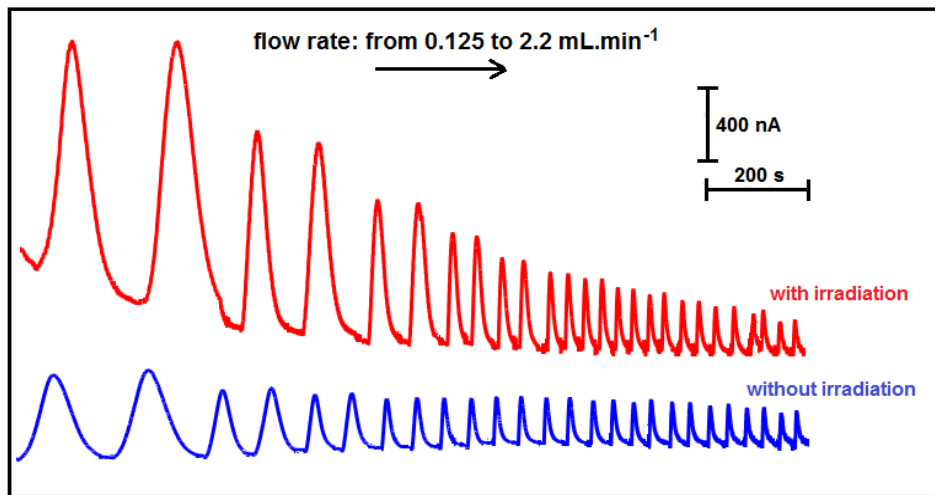


Figure 3.44. The diagrams of 0.8 mM glucose containing 10 mM NAD^+ at various flow rate using GDH/Poly-HT/PAMAM/GCE. (Carrier stream: 0.1 M PBS (pH 7.0) containing 0.1 M KCl; applied potential: 300 mV; sample loop: 100 μL ; tubing length: 10 cm).

The effect of other parameters such as the sample volume, and the transmission tube length on electrocatalytic and photoelectrocatalytic currents of glucose was also similarly investigated. From all these studies, the applied potential, the flow rate, the sample volume, and the transmission tube length were determined as +300 mV, 0.125 mL min^{-1} , 100 μL and 10 cm, respectively. Both amperometric and photoamperometric currents versus various concentration of glucose were recorded using GDH/Poly-HT/PAMAM/GCE in these optimum conditions.

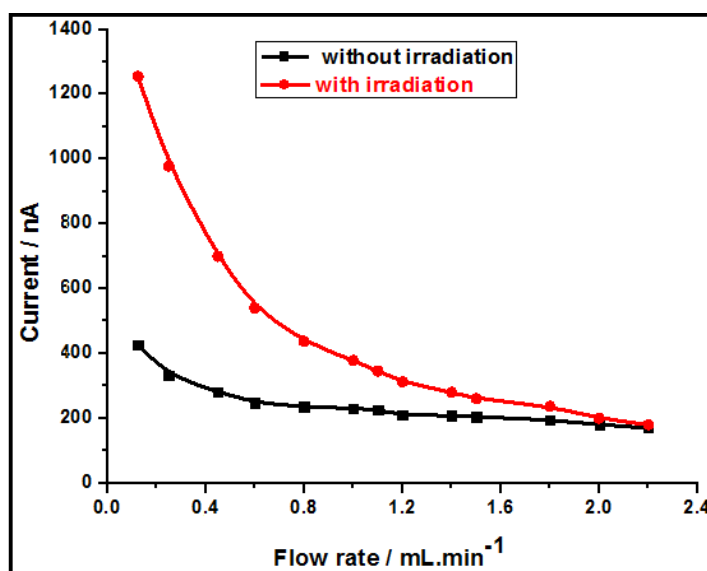


Figure 3.45. The effect of flow rate on ■) amperometric and ●) photoamperometric peak currents obtained diagrams using GDH/Poly-HT/PAMAM/GCE. Injected: 0.8 mM glucose containing 10 mM NAD^+ .

3.5.2.2. Calibration curve and amperometric response in FIA

To establish that a reliable analytical response could be achieved for the glucose, under optimized conditions using a GDH/Poly-HT/PAMAM/GCE, a calibration study was carried out over the range 5×10^{-6} – 1×10^{-2} M glucose concentration, with two injections of each concentration being made via a 100 μ L sample loop. Figure 3.46 shows the fiagrams for amperometric and photoamperometric FI responses to various concentrations of glucose. Although the peak currents increased depending on glucose concentration for both the amperometric and the photoamperometric methods, the responses of photoamperometric method were higher than those of amperometric in all concentrations.

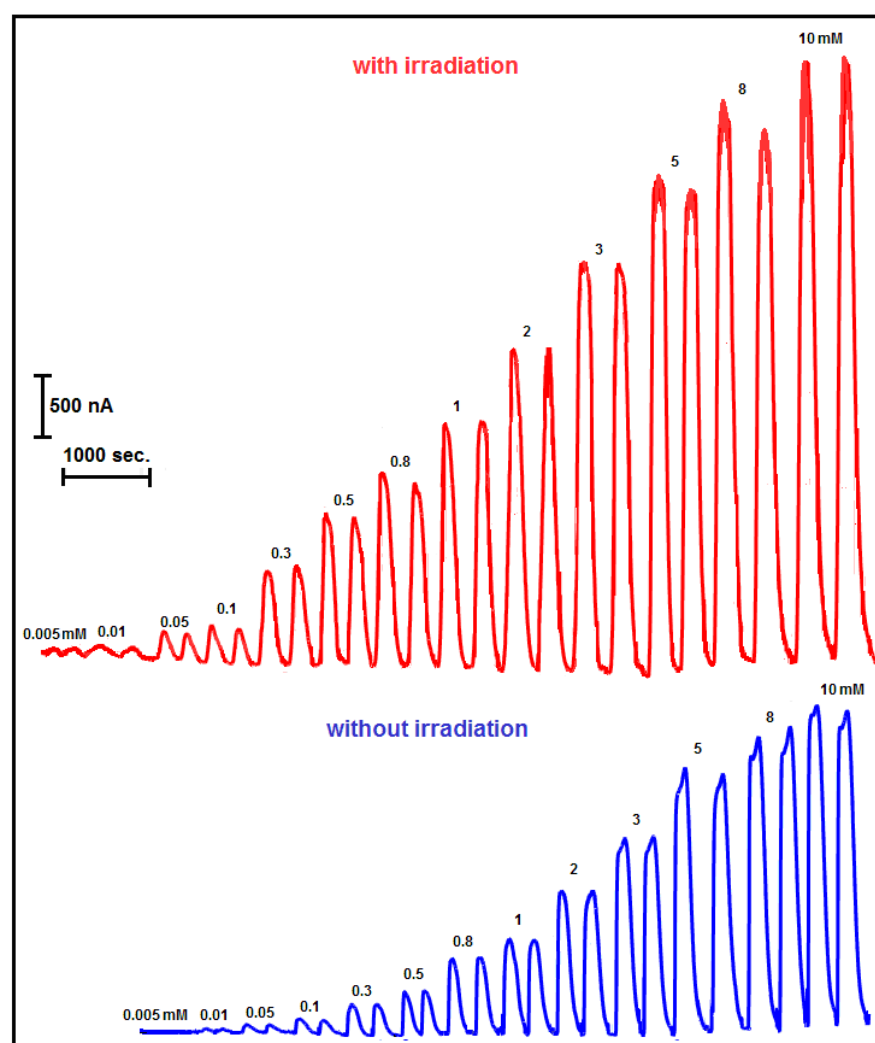


Figure 3.46. Current-time curves of glucose with different concentrations in the range from 0.005 mM to 10 mM glucose containing 10 mM NAD^+ using GDH/Poly-HT/PAMAM/GCE in FIA system (Carrier stream: 0.1 M PBS (pH 7.0) containing 0.1 M KCl, applied potential: +300 mV; Flow rate: 0.125 mL min^{-1} ; sample loop: 100 μ L; transmission tubing length: 10 cm).

Both amperometric and photoamperometric currents versus various concentrations of glucose were also recorded using GDH/PAMAM/GCE (without HT) in the optimized conditions. Figure 3.47 shows current-time curves obtained from GDH/PAMAM/GCE for various glucose concentrations. No enzymatically produced NADH oxidation peaks were observed until 8 mM glucose concentration. Only small peaks were observed up to 8 mM glucose.

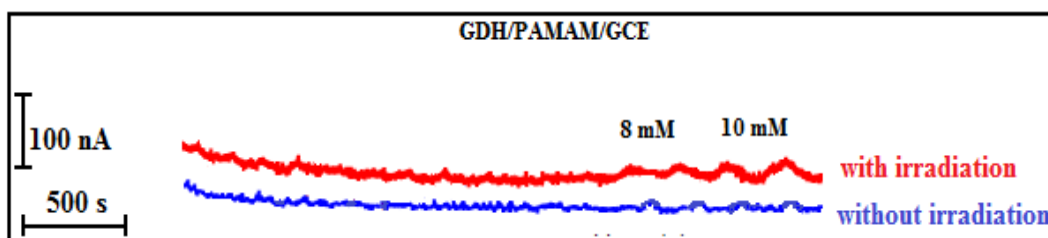


Figure 3.47. Current-time curves of glucose with various concentrations containing 10 mM NAD^+ using GDH/PAMAM/GCE in FIA system (Carrier stream: 0.1 M PBS (pH 7.0) containing 0.1 M KCl; applied potential: +300 mV; flow rate: $0.125 \text{ mL min}^{-1}$; sample loop: $100 \mu\text{L}$; transmission tubing length: 10 cm).

Figure 3.48A shows a plot of catalytic current versus glucose concentration (Appendix 6). From this figure, a linear relationship between the glucose concentration and the peak current was obtained over the concentration range $1.0 \times 10^{-5} - 1.0 \times 10^{-3} \text{ M}$ and $5 \times 10^{-6} - 1 \times 10^{-3} \text{ M}$ by the photoamperometric FIA and amperometric FIA method, respectively, at the GDH/Poly-HT/PAMAM/GCE (Figure 3.48B). The linearity of these methods is described by the following equations:

$$i (\mu\text{A}) = 0.76 C (\text{mM}) + 0.0035 \quad (R^2 = 0.995)$$

$$i (\mu\text{A}) = 1.90 C (\text{mM}) + 0.0027 \quad (R^2 = 0.998)$$

for amperometric and photoamperometric studies, respectively, where i is the peak current and C is the concentration of glucose. When these equations are compared in terms of their slopes, it is clear that the sensitivity of the photoelectrocatalytic FIA procedure is better than that of the amperometric method and the ratio of improvement is about 2.5. The limit of detection (LOD) was calculated as 3×10^{-6} and $1.5 \times 10^{-6} \text{ M}$ glucose for amperometric and photoamperometric glucose biosensors, respectively, based on $3s_b/m$ where s_b is the standard deviation of the blank response and m is the slope of the calibration curve. Limit of quantification (LOQ) was calculated as 1×10^{-5} and $5 \times 10^{-6} \text{ M}$ glucose for amperometric and photoamperometric glucose biosensors, respectively, based on $10s_b/m$.

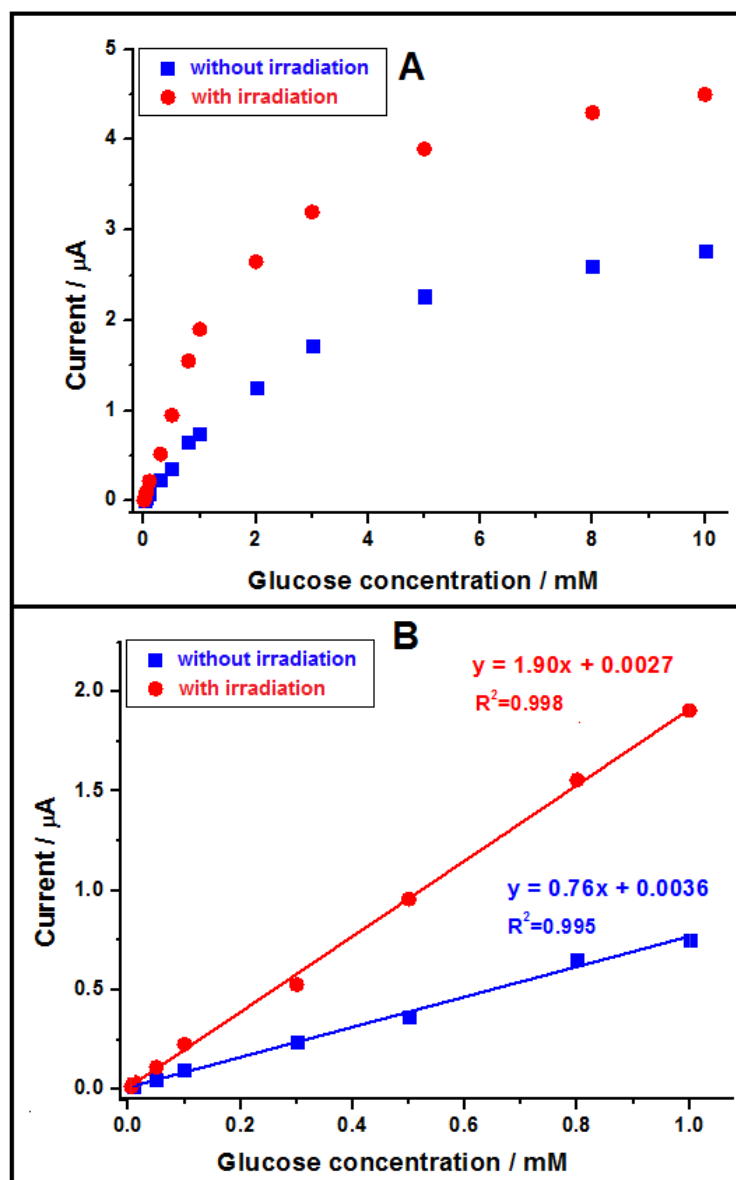


Figure 3.48. A) Dependence of the catalytic currents on glucose concentration, B) calibration curve for ■) amperometric and ●) photoamperometric analysis of glucose using GDH/Poly-HT/PAMAM/GCE in FIA system. (Carrier stream: 0.1 M PBS (pH 7.0) containing 0.1 M KCl, applied potential: +300 mV; flow rate: $0.125 \text{ mL min}^{-1}$; sample loop: $100 \mu\text{L}$; transmission tubing length: 10 cm).

The precision of electrochemical and photoelectrochemical biosensor was investigated by making 5 repeat injections of 3×10^{-4} and 1×10^{-3} M glucose solution. The obtained diagram was shown in Figure 3.49. The RSD for electrochemical and photoelectrochemical biosensors were calculated to be 1.8% and 2.3% for 3.0×10^{-4} and 1.4% and 3.5% for 1×10^{-3} M, respectively. These results indicate GDH/Poly-HT/PAMAM/GCE has very good repeatability for electrochemical and photoelectrochemical biosensing of glucose.

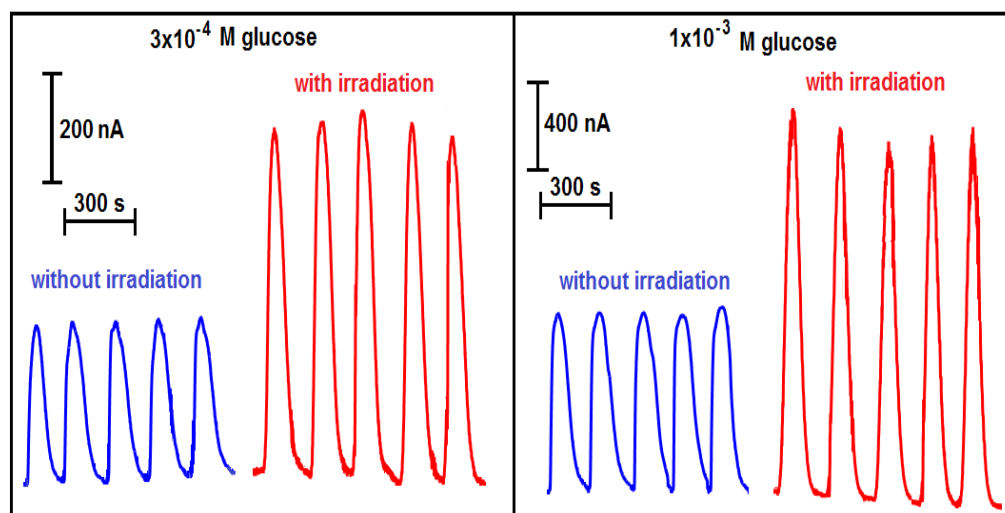


Figure 3.49. Repeat injections of 3×10^{-4} and 1×10^{-3} M glucose using the proposed biosensor in with and without irradiation. (Carrier stream: 0.1 M PBS (pH 7.0) containing 0.1 M KCl, applied potential: +300 mV; flow rate: $0.125 \text{ mL min}^{-1}$; sample loop: $100 \mu\text{L}$; transmission tubing length: 10 cm).

3.5.2.3. Investigation of interfering substances

There are various species that interfere with glucose detection in the real samples, including ascorbic acid (AA), dopamine (DA), uric acid (UA), L-cysteine (L-Cyst) and other monosaccharides such as galactose, saccharose, and fructose. With this aim, the diagrams of glucose in the presence of these interfering compounds without irradiation were recorded in the optimum conditions. Figure 3.50 shows the obtained diagram of 3×10^{-4} M glucose in the presence of possible interfering compounds with various concentrations. As can be seen, in the presence of AA, DA, UA and L-Cyst, serious interferences were occurred with the amperometric enzyme glucose sensors because the oxidation potentials of their were close to that of glucose (300 mV at GDH/Poly-HT/PAMAM/GCE). It was reported that generally, using the Nafion membrane effectively removes the interference of AA because it is negatively charged and repels negatively charged organic species, such as AA (Kim et al., 2013). However, it is difficult to remove the interference caused by neutral or positively charged, very small organics, such as DA and UA, etc. These interfering species cannot be removed using only a Nafion membrane. Another possible way to eliminate the interference effect of AA, is to use ascorbate oxidase (Pariente, et al., 1997; Tzang et al., 2001). While ascorbate is selectively oxidized to dehydroascorbate in the presence of ascorbate oxidase and molecular oxygen, NADH produced by enzymatic reaction was not influenced by this medium.

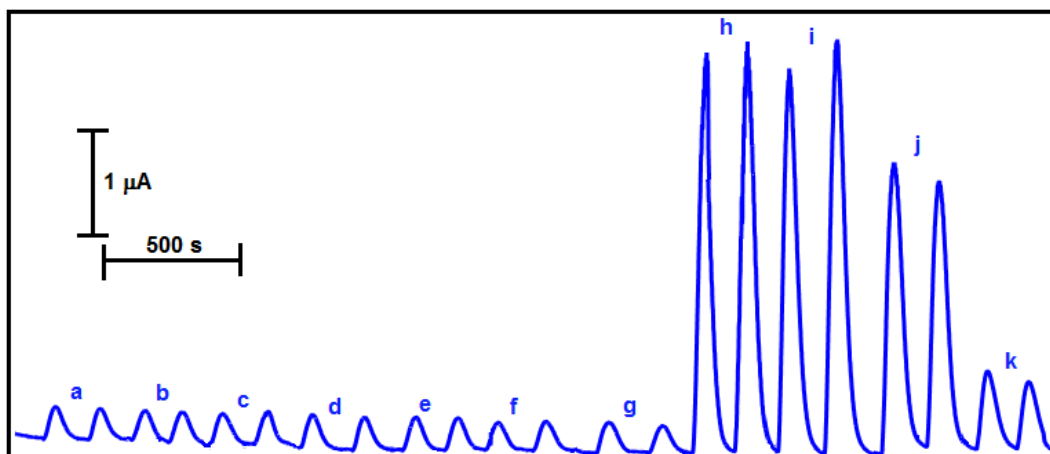


Figure 3.50. Electrochemical biosensing of 3×10^{-4} M glucose (a) in the presence of 3×10^{-4} M fructose (b), galactose (c), saccharose (d); 3×10^{-2} M fructose (e), galactose (f), saccharose (g) and 3×10^{-4} M ascorbic acid (h), dopamine (i), uric acid (j) and L-cysteine (k). (Carrier stream: 0.1 M PBS (pH 7.0) containing 0.1 M KCl, applied potential: +300 mV; flow rate: $0.125 \text{ mL min}^{-1}$; sample loop: $100 \text{ } \mu\text{L}$; transmission tubing length: 10 cm).

In order to remove the interfering effect of these compounds, very small amount of lead(IV) acetate as an oxidizing agent can be added to Nafion layer due to preoxidation reaction of these interfering compounds before they reach the electrode surface (Kim et al., 2013). Moreover, no interference in the presence of other monosaccharides including galactose, saccharose and fructose was observed because the GDH is very selective for glucose against other monosaccharides. In order to reduce the interfering effect of AA, DA, UA and L-Cyst, the fiagrams of 3×10^{-4} M glucose were also recorded in the absence and in the presence of these interfering compounds at applied potential of 100 mV. Although interference effect of UA and L-Cyst was reduced, the reducing of interfering effect of AA and DA has not been achieved in this potential also. On the other hand, the peak current of glucose at 100 mV decreased about two folds in comparison with 300 mV.

3.5.2.4. Storage stability of the biosensor

The storage stability of the biosensor has been studied over a period of 15 days. The sensor was stored in 0.1 M PBS (pH 7.0) at 4°C when not in use. The catalytic current response with and without irradiation could maintain about 15% and 50% of the initial signal, respectively. The first reason of decrease in photoelectrochemical biosensor responses was the effect of light on dehydrogenase enzyme. The other reason was defects and deformations occurring on modified electrodes day by day.

4. CONCLUSION

In this thesis, it was aimed investigation of electrocatalytic and photoelectrocatalytic oxidation of NADH and construction of electrochemical and photoelectrochemical biosensor using modified GCEs. The thesis experiments consist of seven steps i) preparation of modified electrodes, ii) voltammetric behavior of modified electrodes, iii) electrocatalytic and photoelectrocatalytic oxidation of NADH at these modified electrodes using cyclic voltammetric technique, iv) amperometric and photoamperometric detection of NADH at these modified electrodes, v) amperometric and photoamperometric detection of NADH in FIA system, vi) construction of electrochemical and photoelectrochemical biosensor dependent on NAD⁺/NADH-dehydrogenase enzyme, vii) electrochemical and photoelectrochemical biosensor in FIA system.

i) Preparation of modified electrodes: In the preparation of modified electrodes, four different dyes, HT, MG, NR and MdB, were selected as redox mediator. Because quinolic and especially azine type dyes show a good electrocatalytic effect towards the oxidation of NADH. In the modification procedure, electropolymerization of these redox mediators onto GCE was carried out because electropolymerized modified electrodes has some advantages high stability and reproducibility, good electrocatalytic effect etc. in comparison with other modification procedures. Electropolymerization conditions for each modified electrode such as pH of supporting electrolyte, monomer concentration, cycle number and especially anodic potential limit were optimized dependent on their optimum response for the electrocatalytic oxidation of NADH. All optimized parameters are shown in Table 2.1 for each mediator. Electropolymerization of MdB has not been succeeding due to its chemicals structure which hinders its electropolymerization, although MdB is very efficient mediator for electrocatalytic oxidation of NADH. The most important parameter is anodic upper potential because the formation of cationic radicalic species which initiate electropolymerization of mediators is dependent on this potential value.

ii) Voltammetric behavior of modified electrodes: In the investigation of electrochemical behavior of each modified electrode, their cyclic voltammograms were recorded dependent on scan rate in 0.1 M PBS (pH 7.0) and pH. In addition, 200-300 repetitive cyclic voltammograms of each modified electrode were recorded for their stability. The anodic peak current (i_{pa}) and the cathodic peak

current (i_{pc}) of polymeric form of all modified GCEs are linearly proportional to the scan rate (v) (Table 3.1) indicated that surface reaction process occurred at electropolymerized modified electrodes surface. $E^{0'}$ value of redox couple of polymeric form of all modified electrodes dependent on pH and $E^{0'}$ values decreasing linearly with increasing of supporting electrolyte pH. The slope of curves (Table 3.1) was found to near the anticipated Nernstian value indicated that two electrons and two protons attend the electron transfer process of all mediators. In addition, after about 50 or 100 repetitive scans, change in height of peaks of polymeric form of all modified electrodes became very small indicating the good stability of electrodes.

Table 3.1. Equations obtained from the current-scan rate (v) and the formal potential-pH curves for the polymeric form of modified GCEs with different redox mediators.

Electrode	Equations from $i - v$ curves			Equations from $E^{0'} - \text{pH}$ curves $2 \leq \text{pH} \leq 10$
	Scan rate (mVs^{-1})	Anodic Peak (μA)	Cathodic peak (μA)	
Poly-HT/GCE	50-3200	$i_{pa} = 0.032v + 0.879$ $R^2 = 0.9976$	$i_{pc} = -0.028v + 1.54$ $R^2 = 0.9967$	$E^{0'} = -58.21\text{pH} + 617.68$ $R^2 = 0.9946$
Poly-MG/GCE	20-6400	$i_{pa} = 0.0098v + 0.6701$ $R^2 = 0.9985$	$i_{pc} = -0.0087v + 0.1006$ $R^2 = 0.9993$	$E^{0'} = -53.17\text{pH} + 352.33$ $R^2 = 0.9907$
Poly-NR/GCE	20-6400	$i_{pa} = 0.0056v + 0.3382$ $R^2 = 0.9965$	$i_{pc} = -0.0053v + 0.2115$ $R^2 = 0.9982$	$E^{0'} = -55.12\text{pH} + 433.78$ $R^2 = 0.9962$

iii) Electrocatalytic and photoelectrocatalytic oxidation of NADH at these modified electrodes using cyclic voltammetric technique: In order to see the electrocatalytic and photoelectrocatalytic oxidation of NADH, cyclic voltammograms of each modified electrode were recorded in 0.1 M PBS (pH 7.0) in the absence and in the presence of NADH with and without irradiation of electrode surface. Peak currents of modified electrodes in the absence of NADH were slightly increased with irradiation. When the peak potential of NADH at the unmodified GCE (about +500 - 550 mV,) is compared with that of modified electrodes, it was observed that the overpotential for the electrochemical oxidation of NADH shifted to negative direction (between 50 and 200 mV dependent on mediator type). However, the peak current attributed to electrocatalytic oxidation

of NADH increased with irradiation of electrode surface. The increase in the electrocatalytic peak current of NADH in the presence of light may depend on the excitation of redox mediators on the electrode surface and its excited form can more rapidly react with NADH. Thus, it can be concluded that the irradiation of the surface of modified electrodes causes faster photoelectrochemical oxidation of NADH than that of electrochemical.

iv) Amperometric and photoamperometric detection of NADH at these modified electrodes: In order to perform amperometric and photoamperometric studies the current-time curves of each modified electrodes were recorded dependent on NADH concentration with and without irradiation of electrode surface at an applied potential which was optimized for each electrode. Obtained results were summarized in Table 3.2. As can be seen, the slope of concentration curve (for NADH) of the photoelectrocatalytic procedure improved by about 2-3 times compared with that obtained without irradiation for all modified electrodes. In addition, the best result among the slope ratios of photoamperometric curves to amperometric curves was obtained for poly-HT/GCE (about 2.67).

Table 3.2. Analytical characteristics of modified electrodes for amperometric and photoamperometric determination of NADH.

Modified electrode	Applied Potential (mV)	Linear concentration range (M)	Equation of calibration curve*	m_{II}/m_I **
Poly-HT/GCE	+200	$1 \times 10^{-6} - 1 \times 10^{-3}$	I : $i(\mu A) = 1.18C(mM) + 0.021$ $R^2 = 0.9926$ II: $i(\mu A) = 2.66C(mM) + 0.034$ $R^2 = 0.9933$	2.25
Poly-MG/GCE	+100	$1 \times 10^{-6} - 1 \times 10^{-3}$	I : $i(\mu A) = 1.31C(mM) + 0.011$ $R^2 = 0.9973$ II: $i(\mu A) = 3.50C(mM) + 0.021$ $R^2 = 0.9974$	2.67
Poly-NR/GCE	+150	$1 \times 10^{-6} - 1 \times 10^{-3}$	I : $i(\mu A) = 1.50C(mM) + 0.003$ $R^2 = 0.998$ II: $i(\mu A) = 2.99(mM) + 0.037$ $R^2 = 0.994$	2.00

*I and II equation of amperometric and photoamperometric curves, respectively.

** m_I and m_{II} , slope of amperometric and photoamperometric curves, respectively.

m_I/m_{II} represents improvement in calibration sensitivity

v) Amperometric and photoamperometric detection of NADH in FIA system:

FIA experiments were performed using a new home-made flow cell in which only working electrode surface was irradiated with the light source. After some parameters such as flow arte, applied potential, sample loop and tubing length were optimized, the current–time curves in FIA (fiagrams) were recorded dependent on NADH concentration with and without irradiation of electrode surface. In this step, only poly-HT/GCE and poly-MG/GCE was used because the stable results were not obtained at poly-NR/GCE. The obtained results were given in Table 3.3. As can be seen, the sensitivity of the photoelectrocatalytic FIA procedure is better than that of the amperometric method. In addition, the results obtained from poly-HT/GCE are better than that from poly-MG/GCE.

Table 3.3. Analytical characteristics of poly-HT/GCE and poly-MG/GCE for amperometric and photoamperometric detection of NADH in FIA system.

	Poly-HT/GCE	Poly-MG/GCE
Applied Potential (mV)	+300	+150
Linear concentration range (M)	I* : $2.0 \times 10^{-7} - 1.5 \times 10^{-4}$ II*: $2.0 \times 10^{-7} - 2.5 \times 10^{-4}$	I : $5.0 \times 10^{-7} - 5.0 \times 10^{-4}$ II: $5.0 \times 10^{-7} - 5.0 \times 10^{-4}$
LOD/LOQ (M)	I : $4.0 \times 10^{-8} / 1.2 \times 10^{-7}$ II: $3.0 \times 10^{-8} / 1.0 \times 10^{-7}$	I : $3.0 \times 10^{-7} / 9.0 \times 10^{-7}$ II: $2.5 \times 10^{-7} / 8.0 \times 10^{-7}$
Equation of calibration curve	I : $i(\mu\text{A}) = 11.96C(\text{mM}) + 0.029$ $R^2 = 0.9908$ II: $i(\mu\text{A}) = 18.51C(\text{mM}) + 0.048$ $R^2 = 0.9956$	I : $i(\mu\text{A}) = 9.82C(\text{mM}) + 0.015$ $R^2 = 0.999$ II: $i(\mu\text{A}) = 12.39C(\text{mM}) + 0.074$ $R^2 = 0.998$
Improvement in calibration sensitivity (m_{II}/m_I^{**})	1.55	1.26

*I and II equation of amperometric and photoamperometric curves, respectively.

** m_I and m_{II} : slope of amperometric and photoamperometric curves, respectively.

vi) Construction of electrochemical and photoelectrochemical biosensor dependent on NAD^+ /NADH-dehydrogenase enzyme: For the biosensor studies, HT, which was selected more stable redox mediator for electrocatalytic oxidation of NADH, was electropolymerized onto PAMAM-modified GCE and then GDH was immobilized onto poly-HT/PAMAM/GCE by the cross-linking method using glutaraldehyde. PAMAM dendrimer represents a friendly environment for the

immobilization of enzymes as well as for the good electropolymerization of HT. When the peak potential of enzymatically produced NADH at the GDH/PAMAM (about +800 V) GDH/PAMAM/GCE (about +760 mV) is compared with that of GDH/poly-HT/PAMAM/GCE (about 300 mV), it was observed that the overpotential for the electrochemical oxidation of NADH shifted to negative direction. While direct oxidation of NADH at bare electrode was observed at about 500 mV, the oxidation of the enzymatically produced NADH was observed at 800 mV. It can be dependent on the decreasing effect of GDH on the conductivity of electrode surface. When the enzyme modified electrode surface was irradiated with the light source, the peak current attributed to electrocatalytic oxidation of enzymatically produced NADH increased about two times. This results show that photoelectrochemical biosensor can be constructed using mediator and enzyme modified electrodes.

vii) Electrochemical and photoelectrochemical biosensor in FIA system:

The most important part of this thesis is the constructing photoelectrochemical biosensor in FIA system. Although, photoelectrochemical biosensor dependent on NAD^+/NADH redox couple-dehydrogenase enzymes (Deng et al., 2008; Schubert et al., 2009) has been reported, according to our search of the literature, photoelectrochemical biosensor in FIA system have not been reported, yet. Therefore, photoelectrochemical biosensing of glucose in the FIA system using GDH/Poly-HT/PAMAM/GCE was proposed for the first time in this thesis.

After some parameters such as flow rate, applied potential, sample loop and tubing length were optimized, fiagrams were recorded dependent on glucose concentration with and without irradiation of electrode surface. When the electrochemical biosensor was performed, the anodic current increased linearly with the glucose concentration over the range from 0.01 to 1.0 mM with the sensitivity of $0.76 \mu\text{A mM}^{-1}$ and detection limit $3.0 \mu\text{M}$. After the irradiation, the linear range of the photoelectrochemical biosensor was from 5×10^{-3} to 1.0 mM with the sensitivity of $1.90 \mu\text{A mM}^{-1}$ and detection limit $1.5 \mu\text{M}$. The sensitivity increased nearly 2.5 folds while the detection limit decreased 2.0 folds, in contrast to the reaction without irradiation. The various analytical detection parameters such as detection potential of glucose, linearity ranges and calculated LOD were compared with other modified electrodes in previously published reports for the biosensing of glucose. The results are illustrated in Table 3.4.

Table 3.4. Comparison of analytical parameters obtained from GDH/poly-HT/PAMAM/GCE with different electrodes in the literature for electrochemical biosensing of glucose dependent on NAD^+ /NADH redox couple and dehydrogenase enzyme.

Electrode type	Method	DP	LR	LOD	References
FePhenTPy modified SPCE	AMP	0.55 V vs. C electrode	30-600 g/dL (17-330 μM)	12 mg/dL (6.7 μM)	Kim et al., 2013.
MdB modified SPCE	FIA AMP	0.05 V vs. Ag/AgCl	0.075-30 mM	-	Piano et al., 2010a.
CNTP modified with Os-redox polymers	AMP	0.2 V vs. Ag/AgCl	Upto 0.8 mM	10 μM	Antiochia and Gorton, 2007.
Au modified SWCNT-a nonothin PPF	AMP	0.2 V vs. Ag/AgCl	4.9-19 mM	-	Hoshino et al., 2012b.
CNTs-IL/GCE	CV	0.25 V vs. Ag/AgCl	0.02-1.0 mM	9 μM	Bai et al., 2012.
NB SWCNT modified GCE	AMP	0 V vs. SCE	0.1-1.7 mM	0.3 μM	Saleh et al., 2011.
Poly-NB modified SWCNT/GCE	AMP	0.05 V vs. Ag/AgCl	0.01-8.5 mM	5 μM	Du et al., 2008.
Poly- MB on Au	FIA AMP	0.02 V vs. Ag/AgCl	1.0-4.0 mM	-	Silber et al., 1996
Poly-TB on graphite electrode	AMP	-	0.05-3.0 mM	-	Zhou et al., 1998.
Th cross-linked MWCNTs and Au NPs multilayer functionalized ITO electrode	AMP	0.2 V vs. Ag/AgCl	0.01-2.56 mM	5 μM	Deng et al., 2008.
	AMP under irradiation		1×10^{-3} -3.250 mM	0.7 μM	
GDH/poly-HT/PAMAM/GCE	FIA AMP	0.3 V vs. Ag/AgCl	0.01-1.0 mM	3 μM	This work
	FIA AMP under irradiation		5×10^{-3} -1.0 mM	1.5 μM	

FePhenTPy: 5-[2,5-di (thiophen-2-yl)-1H-pyrrol-1-yl]-1,10-phenanthroline iron(III) chloride, PPF: Plasmon polymerized film, SPCE: Screen printed carbon electrode, LR: linearity range, DP: Detection potential, LOD: Limit of detection, CNTP: Carbon nanotube paste, AMP: Amperometry, NB: Nile Blue, SWCNT: Single walled carbon nanotube, IL Ionic liquid, TB: Tolidine blue, ITO: Indium tin oxide, NPs: Nanoparticles, GDH: Glucose dehydrogenase,

As can be seen, the electrocatalytic detection potential of glucose (DP) at the GDH/poly-HT/PAMAM/GCE was better than DP of 5-[2,5-di (thiophen-2-yl)-1H-pyrrol-1-yl]-1,10-phenanthroline iron(III) chloride modified screen printed carbon electrode (SPCE). Although the DP results for the modified electrodes

were better than the GDH/poly-HT/PAMAM/GCE, the LOD and linearity range of proposed electrode was better than that of the compared modified electrodes.

In the study, linearity criteria were satisfied for the proposed methods since R-squared values of calibration curves were better than 0.995 in general and the calculated RSD values were lower than 10%.

As a result, this thesis represented the successful dehydrogenase-based electrochemical and photoelectrochemical biosensors in FIA system at GDH/poly-HT/PAMAM/GCE. The biocatalytical performance of the biosensor was greatly improved by the photovoltaic effect of the dye using as mediator.

REFERENCES

- Al-Jawadi, E., Poller, S., Haddad, R. and Schuhmann, W.,** 2012, NADH oxidation using modified electrodes based on lactate and glucose dehydrogenase entrapped between an electrocatalyst film and redox catalyst-modified polymers, *Microchim. Acta*, 177(3-4):405-410 pp.
- Alvarez, N.L.S., Ortea, P.M., Paneda, A.M., Castanon, M.J.L., Ordieres, A.J.M. and Blanco, P.T.,** 2001, A comparative study of different adenine derivatives for the electrocatalytic oxidation of β -nicotinamide adenine dinucleotide, *J. Electroanal. Chem.*, 502(1-2):109-117 pp.
- Alvarez, N.L.S., Castanon, M.J.L., Ordieres, A.J.M., Blanco, P.T. and Abruna, H.D.,** 2005, 5-Hydroxytryptophan as a precursor of a catalyst for the oxidation of NADH, *Anal. Chem.*, 77:2624-2631 pp.
- Andreescu, S., Andreescu, D. and Sadik, O.A.,** 2003, A new electrocatalytic mechanism for the oxidation of phenols at platinum electrodes, *Electrochem. Commun.* 5:681-688 pp.
- Antiochia, R. and Gorton, L.,** 2007, Development of a carbon nanotube paste electrode osmium polymer-mediated biosensor for determination of glucose in alcoholic beverages, *Biosens. Bioelectron.*, 22:2611-2617 pp.
- Arechederra, M.N., Jenkins, C., Rincón, R.A., Artyushkova, K., Atanassov, P. and Minteer, S.D.,** 2010, Chemical polymerization and electrochemical characterization of thiazines for NADH electrocatalysis application, *Electrochim. Acta*, 55(22):6659-6664 pp.
- Arechederra, M.N., Add, P.K. and Minteer, S.D.,** 2011, Poly(neutral red) as a NAD^+ reduction catalyst and a NADH oxidation catalyst: Towards the development of a rechargeable biobattery, *Electrochim. Acta*, 56(3):1585-1590 pp.
- Arvinte, A., Sesay, A.M., Virtanen, V. and Bala, C.,** 2008, Evaluation of Meldola blue-carbon nanotube-sol-gel composite for electrochemical NADH sensors and their application for lactate dehydrogenase-based biosensors, *Electroanalysis*, 20(21):2355-2362 pp.
- Arvinte, A., Rotariu, L., Bala, C. and Gurban, A.M.,** 2009, Synergistic effect of mediator-carbon nanotube composites for dehydrogenases and peroxidases based biosensors, *Bioelectrochem.*, 76:107-114 pp.

REFERENCES (continued)

- Aydogdu, G., Zeybek, D.K., Zeybek, B. and Pekyardimci, S.,** 2013, Electrochemical sensing of NADH on NiO nanoparticles-modified carbon paste electrode and fabrication of ethanol dehydrogenase-based biosensor, *J. Appl. Electrochem.*, 43(5):523-531 pp.
- Bai, J., Bo, X.J., Qi, B. and Guo, L.P.,** 2010, A Novel polycatechol/ordered mesoporous carbon composite film modified electrode and its electrocatalytic application, *Electroanalysis*, 22(15):1750-1756 pp.
- Bai, L., Wen, D., Yin, J., Deng, L., Zhu, C., Dong, S.,** 2012, Carbon nanotubes-ionic liquid nanocomposites sensing platform for NADH oxidation and oxygen, glucose detection in blood, *Talanta*, 91:110-115.
- Balamurugan, A., Ho, K.C., Chen, S.M. and Huang, T.Y.,** 2010, Electrochemical sensing of NADH based on Meldola Blue immobilized silver nanoparticle-conducting polymer electrode, *Colloids and Surfaces A-Physicochemical and Engineering Aspects*, 362(1-3):1-7 pp.
- Barsan, M.M., Pinto, E.M. and C. M. A. Brett,** 2008, Electrosynthesis and electrochemical characterisation of phenazine polymers for application in biosensors, *Electrochim. Acta*, 53(11):3973-3982 pp.
- Bartlett, P.N. and Simon, E.,** 2000, Poly(aniline)-poly(acrylate) composite films as modified electrodes for the oxidation of NADH, *Physical Chemistry Chemical*, 2(11):2599-2606.
- Bartlett, P.N., Simon, E. and Toh, C.S.,** 2002, Modified electrodes for NADH oxidation and dehydrogenase-based biosensors, *Bioelectrochem.*, 56(1-2):117-122 pp.
- Baskar, S., Chang, J.L. and Zen, J.M.,** 2012, Simultaneous detection of NADH and H₂O₂ using flow injection analysis based on a bifunctional poly(thionine)-modified electrode, *Biosens. Bioelectron.*, 33(1):95-99 pp.
- Bauldreay, J.M. and Archer, M.D.,** 1983, Mediated redox reactions at the 1-aminophenazine-modified rotating-disk electrode, *Electrochim. Acta*, 28:1515-1522 pp.
- Belenky P., Bogan, K.L. and Brenner, C.,** 2007, NAD⁺ metabolism in health and disease, *Trends Biochem. Sci.*, 32(1):12-19 pp.

REFERENCES (continued)

- Biellmann, J.F., Lapinte, C., Haid, E. and Weimann, G.,** 1979, Structure of lactate dehydrogenase inhibitor generated from coenzyme, *Biochemistry*, 18(7):1212-1217 pp.
- Bilici, A., Kaya, I., Yildirim M. and Doğan F.,** 2010, Enzymatic polymerization of hydroxy-functionalized carbazole monomer, *J. Mol. Catal. B: Enzym.*, 64 (1-2):89-95 pp.
- Birkmayer, G.D., Kay, G.G. and Vurre, E.,** 2002, Stabilized NADH improves jet lag-induced cognitive performance deficit, *Wien Med. Wochenschr.*, 152(17-18):450-454 pp.
- Birkmayer, J.G., Nadlinger, K.F. and Hallstrom, S.,** 2004, On the safety of reduced nicotinamide adenine dinucleotide (NADH), *J. Environ. Pathol. Toxicol. Oncol.*, 23(3):179-194 pp.
- Blaedel, W. J. and Jenkins, R.A.,** 1975, Electrochemical oxidation of reduced nicotinamide adenine dinucleotide, *Anal. Chem.*, 47(8):1337-1343 pp.
- Borgo, C.A., Lazarin, A.M. and Gushikem, Y.,** 2002, Methylene blue-zirconium phosphate-cellulose acetate hybrid membrane film attached to a platinum electrode and its application in electrocatalytic oxidation of NADH, *Sens. Actuators B: Chem.*, 87:498-505 pp.
- Broncová, G., Shishkanova, T.V., Matejka, P., Volf, R. and Král, V.,** 2004, Citrate selectivity of poly(neutral red) electropolymerized films, *Anal. Chim. Acta*, 511:197-205 pp.
- Cai, C-X., Ju, H-X. and Chen H.Y.,** 1995, Cobalt hexacyanoferrate modified microband gold electrode and its electrocatalytic activity for oxidation of NADH, *J. Electroanal. Chem.*, 397:185-190 pp.
- Cai, C-X. and Xue, K-H.,** 1997a, Electrocatalysis of NADH oxidation with electropolymerized films of Nile blue A, *Anal. Chim. Acta*, 343:69-77 pp.
- Cai, C-X. and Xue, K-H.,** 1997b, Electrocatalysis of NADH oxidation with electropolymerized films of Azure I, *J. Electroanal. Chem.*, 427:147-153 pp.
- Cai, C-X. and Xue, K-H.,** 1998, Electrochemical polymerization of toluidine blue O and its electrocatalytic activity toward NADH oxidation, *Talanta*, 47:1107-1119 pp.

REFERENCES (continued)

- Canevari, T.C., Vinhas, R.C.G., Landers, R. and Gushikem, Y.,** 2011, SiO₂/SnO₂/Sb₂O₅ microporous ceramic material for immobilization of Meldola's blue: Application as an electrochemical sensor for NADH, *Biosens. Bioelectron.*, 26(5):2402-2406 pp.
- Chakraborty, S. and Raj, C.R.,** 2007, Amperometric biosensing of glutamate using carbon nanotube based electrode, *Electrochem. Commun.*, 9:1323-1330 pp.
- Chen, H-Y., Zhou, D-M., Xu, J-J. and Fang, H-Q.,** 1997, Electrocatalytic oxidation of NADH at a gold electrode modified by thionine covalently bound to self-assembled cysteamine monolayers, *J. Electroanal. Chem.*, 422:21-25 pp.
- Chen, S.M. and Lin, K.C.,** 2001, The electrocatalytic properties of polymerized neutral red film modified electrodes, *J. Electroanal. Chem.*, 511(1-2):101-114 pp.
- Chen, Y.L., Yuan, J.H., Tian, C.X. and Wang, X.Z.,** 2004, Flow-injection analysis and voltammetric detection of NADH with a poly-toluidine blue modified electrode, *Anal. Sci.*, 20(3):507-511 pp.
- Chen, C.X. and Gao, Y.H.,** 2007a, Electrochemical polymerization of neutral red in the presence of sulfoferrocenecarboxylic acid, *Polymer*, 48:5572-5580 pp.
- Chen, C.X. and Gao, Y.H.,** 2007b, Electrosyntheses of poly(neutral red), a polyaniline derivative, *Electrochim. Acta*, 52:3143-3148 pp.
- Chi, Q. and Dong, S.,** 1994, Electrocatalytic oxidation and flow injection determination of reduced nicotinamide coenzyme at a glassy carbon electrode modified by a polymer thin film, *Analyst*, 119:1063-1066 pp.
- Cooper, J.A., Wu, M. and Compton, R.G.,** 1998, Photoelectrochemical analysis of ascorbic acid, *Anal. Chem.*, 70(14):2922-2927 pp.
- Cooper, J.A., Woodhouse, K.E., Chippindale A.M. and Compton, R.G.,** 1999, Photoelectrochemical Determination of Ascorbic Acid Using Methylene Blue Immobilized in α -Zirconium Phosphate, *Electroanalysis*, 11(17):1259-1265 pp.

REFERENCES (continued)

- Cosnier, S. and Lous, K.L.**, 1996, A new strategy for the construction of amperometric dehydrogenase electrodes based on laponite gel-methylene blue polymer as the host matrix, *J. Electroanal. Chem.*, 406:243-246 pp.
- Cosnier, S., and Karyakin A.A.**, 2010, Electropolymerization Concepts, Materials and Applications, *Wiley-VCH Verlag GmbH & Co. KGaA*
- Cox, J.A., Tess, M.E. and Cummings T.E.**, 1996, Electroanalytical methods based on modified electrodes: A review of recent advances, *Rev. Anal. Chem.*, 15(3):173-223 pp.
- Dai, Z.H., Liu, F.X., Lu, G.F. and Bao, J.C.**, 2008, Electrocatalytic detection of NADH and ethanol at glassy carbon electrode modified with electropolymerized films from methylene green, *J. Solid State Electrochem.*, 12(2):175-180.
- Dai, H., Xu, H., Lin, Y., Wu, X. and Chen, G.**, 2009, A highly performing electrochemical sensor for NADH based on graphite/poly(methylmethacrylate) composite electrode, *Electrochem. Commun.*, 11:343-346 pp.
- Dawson, R.B.**, 1985, Data for Biochemical Research (3rd ed.). Oxford: Clarendon Press. 122p.
- De Lucca, A.R., Santos, A.D., Pereira, A.C. and Kubota, L.T.**, 2002, Electrochemical behavior and electrocatalytic study of the methylene green coated on modified silica gel, *J. Colloid Interf. Sci.*, 254(1):113-119 pp.
- Deng, L., Wang, Y., Shang, L., Wen, D. and Wang, F.**, 2008, A sensitive NADH and glucose biosensor tuned by visible light based on thionine bridged carbon nanotubes and gold nanoparticles multilayer, *Biosens. Bioelectron.*, 24(4):951-957 pp.
- Dicu, D., Munteanu, F.D., Popescu, I.C. and Gorton, L.**, 2003, Indophenol and O-quinone derivatives immobilized on zirconium phosphate for NADH electro-oxidation, *Anal. Lett.*, 36(9):1755-1779
- Dilgin Giray, D., Gligor, D., Gökçel, H.İ., Dursun, Z. and Dilgin, Y.**, 2010, Photoelectrocatalytic oxidation of NADH in a flow injection analysis system using a poly-hematoxylin modified glassy carbon electrode, *Biosens. Bioelectron.*, 26(2):411-417 pp.

REFERENCES (continued)

- Dilgin Giray, D., Gligor, D., Gökçel, H.İ., Dursun, Z. and Dilgin, Y.,** 2011, Glassy carbon electrode modified with poly-Neutral Red for photoelectrocatalytic oxidation of NADH, *Microchim. Acta*, 173(3-4):469-476 pp.
- Dilgin, Y., Dursun, Z. and Nişli, G.,** 2003, Flow injection amperometric determination of ascorbic acid using a photoelectrochemical reaction after immobilization of methylene blue on muscovite, *Turk. J. Chem.*, 27:167-180 pp.
- Dilgin, Y.,** 2004, The Uses of Modified Muscovite at Photoelectrochemical Reactions and The Application to New Techniques, (PhD Thesis) *Ege Univ. Grad. Sc. Nat. Appl. Sci.*
- Dilgin, Y., Dursun, Z., Nişli, G. and Gorton, L.,** 2005, Photoelectrochemical investigation of methylene blue immobilised on zirconium phosphate modified carbon paste electrode in flow injection system, *Anal. Chim. Acta*, 542(2):162-168 pp.
- Dilgin, Y. and Nişli, G.,** 2006, Flow Injection Photoamperometric Investigation of Ascorbic Acid Using Methylene Blue Immobilized on Titanium Phosphate, *Anal. Lett.*, 39(3):451-465 pp.
- Dilgin, Y., Gorton, L. and Nişli, G.,** 2007, Photoelectrocatalytic oxidation of NADH with electropolymerized toluidine blue O, *Electroanalysis*, 19(2-3):286-293 pp.
- Dilgin, Y., Dilgin Giray, D., Dursun, Z., Gökçel, H.İ., Gligor, D., Bayrak, B. and Ertek, B.,** 2011, Photoelectrocatalytic determination of NADH in a flow injection system with electropolymerized methylene blue, *Electrochim. Acta*, 56(3):1138-143 pp.
- Dilgin, Y., Kızılkaya B., Ertek, B., Işık, F. and Dilgin Giray, D.,** 2012a, Electrocatalytic oxidation of sulphide using a pencil graphite electrode modified with hematoxylin, *Sens. Actuators B: Chem.*, 171-172:223-229 pp.
- Dilgin, Y., Ertek, B., Kızılkaya, B., Dilgin Giray, D. and Gökçel, H.İ.,** 2012b, Electrocatalytic oxidation of NADH using a pencil graphite electrode modified with hematoxylin, *Sci. Advanced Mat.*, 4(9):920-927pp.

REFERENCES (continued)

- Dilgin, Y., Kızılkaya, B., Dilgin Giray, D., Gökçel, H.İ. and Gorton, L.,** 2013, Electrocatalytic oxidation of NADH using a pencil graphite electrode modified with quercetin, *Colloid. Surf. B*, 102:816-82 pp.
- Dong, D., Zheng, D., Wang, F.Q., Yang, X.Q., Wang, N., Li, Y.G., Guo, L.H. and Cheng, J.,** 2004, Quantitative photoelectrochemical detection of biological affinity reaction: biotin-avidin, *Anal. Chem.*, 76(2):499-501 pp.
- Dos Santos Silva, F.A., Lopes C.B., Costa, E.O., Lima, P.R., Kubota, L.T., Goulart, M.O.F.,** 2010, Poly-xanthurenic acid as an efficient mediator for the electrocatalytic oxidation of NADH, *Electrochem. Commun.*, 12:450-454 pp.
- Du, P., Liu, S., Wu, P. and Cai, C.,** 2007, Single-walled carbon nanotubes functionalized with poly(nile blue A) and their application to dehydrogenase-based biosensors, *Electrochim. Acta*, 53:1811-1823 pp.
- Du, P., Wu, P. and Cai, C.,** 2008, A glucose biosensor based on electrocatalytic oxidation of NADPH at single-walled carbon nanotubes functionalized with poly(nile blue A), *J. Electroanal. Chem.*, 624(1-2):21-26 pp.
- Dursun, Z. and Nişli, G.,** 2001, The importance of chemically modified electrodes in voltammetry and flow system, *Journal of Faculty of Science Ege University*, 24:25-36 pp.
- Fang, J., Qi, B., Yang, L. and Guo, L.,** 2010, Ordered mesoporous carbon functionalized with poly-azure B for electrocatalytic application, *J. Electroanal. Chem.*, 643(1-2):52-57 pp.
- Ferreira, M., Varela, H., Toressi, R.M. and Tremiliosi-Filho, G.,** 2006, Electrode passivation caused by polymerization of different phenolic compounds, *Electrochim. Acta*, 52:434-442 pp.
- Florou, A.B., Prodromidis, M.I., Karayannis, M.I. and Tzouwara-Karayanni, S.M.,** 1998, Electrocatalytic oxidation of NADH in flow analysis by graphite electrode modified with 2,6-dichlorophenolindophenol salts, *Electroanalysis*, 10(18):1261-1268 pp.
- Forsyth, L.M., Preuss, H.G., MacDowell, A.L., Chiazze, L.J., Birkmayer, G.D. and Bellanti, J.A.,** 1999, Therapeutic effects of oral NADH on the symptoms of patients with chronic fatigue syndrome, *Ann. Allergy Asthma Immunol.*, 82(2):185-191 pp.

REFERENCES (continued)

- Fotouhi, L., Raei, F., Heravi, MM. and Nematollahi, D.,** 2010, Electrocatalytic activity of 6,7-dihydroxy-3-methyl-9-thia-4,4a-diazafluoren-2-one/multi-wall carbon nanotubes immobilized on carbon paste electrode for NADH oxidation: Application to the trace determination of NADH, *J. Electroanal. Chem.*, 639(1-2):15-20 pp.
- Gao, Q., Cui, X.Q., Yang, F., Ma, Y. and Yang, X.R.,** 2003, Preparation of poly(thionine) modified screen-printed carbon electrode and its application to determine NADH in flow injection analysis system, *Biosens. Bioelectron.*, 19(3):277-282 pp.
- Gao, Q., Wang, W.D., Ma, Y. and Yang, X.R.,** 2004, Electrooxidative polymerization of phenothiazine derivatives on screen-printed carbon electrode and its application to determine NADH in flow injection analysis system, *Talanta*, 62(3):477-482 pp.
- Gao, Q., Sun, M., Peng, P., Qi, H. and Zhang, C.,** 2010, Electro-oxidative polymerization of phenothiazine dyes into a multi layer-containing carbon nanotube on a glassy carbon electrode for the sensitive and low-potential detection of NADH, *Microchim. Acta*, 168:299-307 pp.
- Ge, B., Tan, Y., Xie, Q., Ma, M. and Yao, S.,** 2009, Preparation of chitosan–dopamine-multiwalled carbon nanotubes nanocomposite for electrocatalytic oxidation and sensitive electroanalysis of NADH, *Sens. Actuators B: Chem.*, 137:547-554 pp.
- Gilmartin, M.A.T. and Hart, J.P.,** 1995, Sensing with chemically and biologically modified carbon electrodes: A review, *Analyst*, 120:1029-1045 pp.
- Gligor D., Dilgin Y., Popescu I.C. and Gorton L.,** 2009, Photoelectrocatalytic oxidation of NADH at graphite electrode modified with a new polymeric phenothiazine, *Electroanalysis*, 21(3-5):360-367 pp.
- GlobalFIA,** 2013, <http://www.globalfia.com/> (Date accessed: 10 January 2014)
- Golabi, S.M. and Irannejad, L.,** 2005, Preparation and electrochemical study of fisetin modified glassy carbon electrode. Application to the determination of NADH and ascorbic acid, *Electroanalysis*, 17:985-996 pp.

REFERENCES (continued)

- Gong, J., Wang, X., Li, X. and Wang, K.,** 2012, Highly sensitive visible light activated photoelectrochemical biosensing of organophosphate pesticide using biofunctional crossed bismuth oxyiodide flake arrays, *Biosens. Bioelectron.*, 38(1):43-49 pp.
- Gorton, L., Torstensson, A., Jaegfeldt, H. and Johansson, G.,** 1984, Electrocatalytic oxidation of reduced nicotinamide coenzymes by graphite electrodes modified with an adsorbed phenoxazinium salt, meldola blue, *J. Electroanal. Chem. Interfacial Electrochem.*, 161(1):103-120 pp.
- Gorton, L.,** 1995, Carbon-Paste electrodes modified with enzymes, tissues and cells, *Electroanalysis*, 7(1):23-45 pp.
- Gorton, L. and Dominguez, E.,** 2002a, Encyclopedia of Electrochemistry edited by Allen J. Bard and Martin Stratmann, Bioelectrochemistry edited by George S. Wilson, Wiley WCH Verlag, 9: 69p.
- Gorton, L. and Dominguez, E.,** 2002b, Electrocatalytic oxidation of NAD(P)H at mediator-modified electrodes, *Rev. Mol. Biotechnol.*, 82(4):371-392.
- Gözükara, E.,** 2001, Biochemistry, Volume 2, 4th edition, 680-682 pp.
- Greef, R., Peat, R., Peter, L.M., Pletcher, D. and Robinson, J.,** 1985, Instrumental Methods in Electrochemistry, Ellis Horwood Limited.
- Hansen, E.H.,** 1996, Principles and applications of flow injection analysis in biosensors, *J. Mol. Recognit.*, 9(5-6):316-325 pp.
- Hasebe, Y., Wang, Y. and Fukuoka, K.,** 2011, Electropolymerized poly(Toluidine Blue)-modified carbon felt for highly sensitive amperometric determination of NADH in flow injection analysis, *J. Environ. Sci.-China*, 23(6):1050-1056 pp.
- Ho, Y.H., Periasamy, A.P. and Chen, S.M.,** 2011, Photoelectrocatalytic regeneration of NADH at poly(4,4-diaminodiphenyl sulfone)/nano TiO₂ composite film modified indium tin oxide electrode, *Sens. Actuators B: Chem.*, 156:84-94 pp.
- Hoshino, T. and Muguruma, H.,** 2012a, Selective detection of NADH with neutral red functionalized carbon nanotube/plasma-polymerized film composite electrode, *Electrochemistry*, 80(2):85-87 pp.

REFERENCES (continued)

- Hoshino, T., Sekiguchi, S.I. and Mugurama, H.,** 2012b, Amperometric biosensor based on multilayer containing carbon nanotube, plasma-polymerized film, electron transfer mediator phenothiazine, and glucose dehydrogenase, *Bioelectrochem.*, 84:1-5 pp.
- Hua, E., Wang, L., Jing, X.Y., Chen, C.T. and Xie, G.M.,** 2013, One-step fabrication of integrated disposable biosensor based on ADH/NAD(+)/meldola's blue/graphitized mesoporous carbons/chitosan nanobiocomposite for ethanol detection, *Talanta*, 111:163-169 pp.
- IUPAC,** IUPAC Recommendations, 1997, Chemically Modified Electrodes: Recommended Terminology and Definitions, *Pure Appl. Chem.*, 69:1317-1323 pp.
- Jaegfeldt, H.,** 1980, Adsorption and electrochemical oxidation behavior of NADH at a clean platinum-electrode, *J. Electroanal. Chem.*, 110(1-3): 295-302 pp.
- Jameson, D.M., Thomas, V. and Zhou, D.M.,** 1989 Time-resolved fluorescence studies on NADH bound to mitochondrial malate dehydrogenase, *Biochim. Biophys. Acta*, 994(2):187-190 pp.
- Jaraba, P., Agui, L., Yanez-Sedeno, P. and Pingarron, J.M.,** 1998, NADH amperometric sensor based on poly(3-methylthiophene)-coated cylindrical carbon fiber microelectrodes: application to the enzymatic determination of L-lactate, *Electrochim. Acta*, 43(23):3555-3565 pp.
- Jiang, X., Zhu, L., Yang, D., Mao, X. and Wu, Y.,** 2009, Amperometric ethanol biosensor based on integration of alcohol dehydrogenase with Meldola[1]s blue/ordered mesoporous carbon electrode, *Electroanalysis*, 21(14):1617-1623 pp.
- Jin, G.P., Chen, Q.Z., Ding, Y.F. and He, J.B.,** 2007, Electrochemistry behaviour of adrenalin, serotonin and ascorbic acid at novel poly rutin modified paraffin-impregnated graphite electrode, *Electrochim. Acta*, 52:2535-2541 pp.
- Ju, H.X., Dong, L. and Chen, H.Y.,** 1996, Amperometric determination of lactate dehydrogenase based on a carbon fiber microcylinder electrode modified covalently with toluidine blue O by acylation, *Talanta*, 43:1177-1183 pp.

REFERENCES (continued)

- Karyakin, A.A., Bobrova, O. A. and Karyakina, E. E.**, 1995, Electroreduction of NAD⁺ to enzymatically active NADH at poly (neutral red) modified electrodes, *J. Electroanal. Chem.*, 399(1-2):179-184 pp.
- Karyakin, A.A., Karyakina, E.E., Schuhmann W. and Schmidt, H.L.**, 1999a, Electropolymerized azines: Part II. In a search of the best electrocatalyst of NADH oxidation, *Electroanalysis*, 11(8):553-557 pp.
- Karyakin, A.A., Karyakina, E.E., and Schmidt, H.L.**, 1999b, Electropolymerized azines: A new group of electroactive polymers, *Electroanalysis*, 11(3):149-155 pp.
- Karyakin, A.A., Ivanova, Y.N., Revunova, K.V. and Karyakina, E.E.**, 2004, Electropolymerized flavin adenin dinucleotide as an advanced NADH transducer, *Anal. Chem.* 76(7):2004-2009 pp.
- Kasimova, M.R., Grigiene, J., Krab K, Hagedorn, P.H., Flyvbjerg, H., Andersen, P.E. and Møller, I.M.**, 2006, The free NADH concentration is kept constant in plant mitochondria under different metabolic conditions, *Plant Cell*, 18(3):688-698 pp.
- Katakis, I. and Dominguez, E.**, 1997, Catalytic electrooxidation of NADH for dehydrogenase amperometric biosensors, *Microchim. Acta*, 126:11-32 pp.
- Khoo, S.B. and Zhu, J.**, 1998, Poly(pyrogallol) film on glassy carbon electrode for selective preconcentration and stripping voltammetric determination of Sb(III), *Anal. Chim. Acta*, 373:15-27 pp.
- Khoo, S.B. and Zhu, J.**, 1999, Poly(catechol) film modified glassy carbon electrode for ultratrace determination of Cerium (III) by differential pulse anodic stripping voltammetry, *Electroanalysis*, 11:546-552 pp.
- Kim, D.M., Kim, M.Y., Reddy, S.S., Cho, J., Cho, C.H., Jung, S. and Shim, Y.B.**, 2013, Electron-transfer mediator for a NAD-glucose dehydrogenase-based glucose sensor, *Anal. Chem.*, 85(23):11643-11649 pp.
- Koyuncu, D., Erden, P.E., Pekyardımcı, Ş. and Kılıç, E.**, 2007, A new amperometric carbon paste enzyme electrode for ethanol determination, *Anal. Lett.*, 40:1904-1922 pp.
- Kubota, L.T. and Gorton, L.**, 1999, Electrochemical study of flavins, phenazines, phenoxazines and phenothiazines immobilized on zirconium phosphate, *Electroanalysis*, 11(10-11):719-728 pp.

REFERENCES (continued)

- Kubota, L.T., Gouvea, F., Andrade, A.N., Milagres, B.G. and Neto, G.O.,** 1996, Electrochemical sensor for NADH based on Meldola's blue immobilized on silica gel modified with titanium phosphate, *Electrochim. Acta*, 41:1465-1469 pp.
- Kumar, S.A. and Chen, S-M.,** 2007, Fabrication and characterization of Meldola's blue/zinc oxide hybrid electrodes for efficient detection of the reduced form of nicotinamide adenine dinucleotide at low potential, *Anal. Chim. Acta*, 592:36-44 pp.
- Kumar, S.A. and Chen, S.M.,** 2008, Electroanalysis of NADH using conducting and redox active polymer/carbon nanotubes modified electrodes-A review, *Sensors*, 8:739-766 pp.
- Ladiu, C.I., Popescu, I.C. and Gorton, L.,** 2005, Electrocatalytic oxidation of NADH at carbon paste electrodes modified with Meldola Blue adsorbed on zirconium phosphate: effect of Ca^{2+} and polyethyleneimine, *J. Solid State Electrochem.*, 9, 296-303 pp.
- Ladiu, C.I., Garcia, R., Popescu, I.C. and Gorton, L.,** 2007a, NADH electrocatalytic oxidation at glassy carbon paste electrodes modified with Meldola blue adsorbed on alpha-titanium phosphate, *Revista De Chimie*, 58, 465-469 pp.
- Ladiu, C.I., Garcia, R., Popescu, I.C. and Gorton, L.,** 2007b, NADH electrocatalytic oxidation at glassy carbon paste electrodes modified with meldola blue adsorbed on acidic alpha-zirconium phosphate, *Revue Roumaine De Chimie*, 52, 67-74 pp.
- Lakowicz, J.R., Szmecinski, H., Nowaczyk, K. and Johnson, M.L.,** 1992, Fluorescence lifetime imaging of free and protein-bound NADH, *Proc. Natl. Acad. Sci. U.S.A.*, 89(4):1271-1275 pp.
- Lane, R.F. and Hubbard, A.T.,** 1973, Electrochemistry of chemisorbed molecules. I. Reactants connected to electrodes through olefinic substituents, *J. Phy. Chem.*, 77:1401-1410 pp.
- Lawrence, N.S. and Wang, J.,** 2006, Chemical adsorption of phenothiazine dyes onto carbon nanotubes: Towards the low potential detection of NADH, *Electrochem. Commun.*, 8(1):71-76 pp.

REFERENCES (continued)

- Li, N.B., Duan, J.P. and Chen, G.N.**, 2003, Electrochemical polymerization of Azure Blue II and its electrocatalytic activity toward NADH oxidation, *Chin. J. Chem.*, 523: 93-105 pp.
- Li, Y., Shi, L., Ma, W., Li, D-W., Kraatz, H-B. and Long, Y-T.**, 2011, 6-Vinyl coenzyme Q₀: Electropolymerization and electrocatalysis of NADH oxidation exploiting poly-*p*-quinone-modified electrode surfaces, *Bioelectrochem.*, 80(2):128-131 pp.
- Li, H.Z., Wen H. and Barton, S.C.**, 2012, NADH oxidation catalyzed by electropolymerized azines on carbon nanotube modified electrodes, *Electroanalysis*, 24(2):398-406 pp.
- Li, Z., Huang, Y., Chen, L., Qin, X.L., Huang, Z., Zhou, Y.P., Meng, Y., Li, J., Huang, S.Y., Liu, Y., Wang, W., Xie, Q.J. and Yao, S.Z.**, 2013a, Amperometric biosensor for NADH and ethanol based on electroreduced graphene oxide-polythionine nanocomposite film, *Sens. Actuators B: Chem.*, 181:280-287 pp.
- Li, L., Lu, H.M. and Deng, L.**, 2013b, A sensitive NADH and ethanol biosensor based on graphene-Au nanorods nanocomposites, *Talanta*, 113:1-6 pp.
- Liang, M.M., Liu, S.L., Wei, M.Y. and Guo, L.H.**, 2006, Photoelectrochemical oxidation of DNA by ruthenium tris(bipyridine) on a tin oxide nanoparticle electrode, *Anal. Chem.*, 78(2):621-623 pp.
- Lin, K.C., Lin, Y.C. and Chen, S.M.**, 2012, Electrocatalytic reaction of hydrogen peroxide and NADH based on poly (neutral red) and FAD hybrid film, *Analyst*, 137:186-194 pp.
- Lin, KC., Li, YS. and Chen, SM.**, 2013, Electrochemical determination of nicotinamide adenine dinucleotide and hydrogen peroxide based on poly(xanthurenicacid), flavin adenine dinucleotide and functionalized multi-walled carbon nanotubes, *Sens. Actuators B: Chem.*, 184:212-219 pp.
- Liu, Y., Zhang, H.L., Lai, G.S., Yu, A.M., Huang, Y.M. and Han, D.Y.**, 2010, Amperometric NADH biosensor based on magnetic chitosan microspheres/poly(thionine) modified glassy carbon electrode, *Electroanalysis*, 22(15):1725-1732 pp.

REFERENCES (continued)

- Liu, S.Q., Dai, G.P., Yuan, L. and Zhao, Y.P.**, 2012, A NADH sensor based on 1,2-naphththoquinone electropolymerized on multi-walled carbon nanotubes modified glassy carbon electrode, *J.Chin. Chem. Soc.*, 59(11):1409-1414 pp.
- Lobo, M.J., Miranda, A.J. and Tunon, P.**, 1996a, Flow-injection analysis of ethanol with an alcohol dehydrogenase-modified carbon past electrode, *Electroanalysis*, 8(10):932-937 pp.
- Lobo, M.J., Miranda, A.J. and Tunon, P.**, 1996b, A comparative study of some phenoxazine and phenothiazine modified carbon paste electrodes for ethanol determination, *Electroanalysis*, 8:591-596 pp.
- Lobo, M.J., Miranda, A.J. and Tunon, P.**, 1997, Amperometric biosensor based on NAD(P) dependent dehydrogenase enzymes, *Electroanalysis*, 9(3):191-202 pp.
- Lu, B.P., Bai, J., Bo, X.J., Yang, L. and Guo, L.P.**, 2010, Electrosynthesis and efficient electrocatalytic performance of poly(neutral red)/ordered mesoporous carbon composite, *Electrochim. Acta*, 55(15):4647-4652 pp.
- Mai, N., Liu, X., Zeng, X., Xing, L., Wei, W. and Luo, S.**, 2010, Electrocatalytic oxidation of the reduced nicotinamide adenine dinucleotide at carbon ionic liquid electrode modified with polythionine/multi-walled carbon nanotubes composite, *Microchim. Acta*, 168:215-220 pp.
- Maleki, A., Nematollahi, D., Clausmeyer, J., Henig, J., Plumere, N. and Schuhmann, W.**, 2012, Electrodeposition of catechol on glassy carbon electrode and its electrocatalytic activity toward NADH oxidation, *Electroanalysis*, 24:1932-1936 pp.
- Malinauskas, A., Niaura, G., Bloxham, S., Ruzgas, T. and Gorton, L.**, 2000, Electropolymerization of preadsorbed layers of some azine redox dyes on graphite, *J. Colloid Interf. Sci.*, 230(1):122-127 pp.
- Malinauskas, A., Ruzgas T. and Gorton, L.**, 2001, Electrochemical study of glassy carbon electrodes modified with zirconium phosphate and some azine-type redox dyes *J. Solid State Electrochem.*, 5:287-292 pp.

REFERENCES (continued)

- Manesh, K.M., Santhosh, P., Gopalan, A. and Lee, K.P.**, 2008, Electrocatalytic oxidation of NADH at gold nanoparticles loaded poly(3,4-ethylenedioxythiophene)-poly(styrene sulfonic acid) film modified electrode and integration of alcohol dehydrogenase for alcohol sensing, *Talanta*, 75(5):1307-1314 pp.
- Mano, N. and Kuhn, A.**, 1999a, Immobilized nitro-fluorenone derivatives as electrocatalysts for NADH oxidation, *J. Electroanal. Chem.*, 477(1):79-88 pp.
- Mano, N. and Kuhn, A.**, 1999b, Ca²⁺ enhanced electrocatalytic oxidation of NADH by immobilized nitro-fluorenes, *Electrochem. Commun.* 1(10):497-501 pp.
- Mano, N. and Kuhn, A.**, 2001, Cation induced amplification of the electrocatalytic oxidation of NADH by immobilized nitro-fluorenone derivatives, *J. Electroanal. Chem.*, 498(1-2):58-66 pp.
- Mao, L.Q. and Yamamoto, K.**, 2000, Glucose and choline on-line biosensors based on electropolymerized Meldola's blue, *Talanta*, 51, 187-195 pp.
- Mao, X., Wu, Y., Xu, L., Cao, X.J., Cui, X.J. and Zhu, L.**, 2011, Electrochemical biosensors based on redox carbon nanotubes prepared by noncovalent functionalization with 1,10-phenanthroline-5,6-dione, *Analyst*, 136:293-298 pp.
- Maroneze, C.M., Arenas, L.T., Luz, R.C.S., Benvenuti, E.V., Landers, R. and Gushikem, Y.**, 2008, Meldola Blue immobilized on a new SiO₂/TiO₂/graphite composite for electrocatalytic oxidation of NADH, *Electrochim. Acta*, 53:4167-4175 pp.
- Maroneze, C.M., Luz, R.C.S., Landers, R. and Gushikem, Y.**, 2010, SiO₂/TiO₂/Sb₂O₅/graphite carbon ceramic conducting material: preparation, characterization, and its use as an electrochemical sensor, *J. Solid State Electrochem.*, 14:115-121 pp.
- Mayer, M. and Ruzicka, J.**, 1996, Flow injection based renewable Electrochemical sensor system, *Anal. Chem.*, 68:3808-3814 pp.
- McKelvie, I.D.**, 1999, Flow Injection Analysis, *Analytical Testing Technology*, 20:20-24 pp.

REFERENCES (continued)

- Meng, L., Wu, P., Chen, G.X., Cai, C.X., Sun, Y.M. and Yuan, Z.H.,** 2009, Low potential detection of glutamate based on the electrocatalytic oxidation of NADH at thionine/single-walled carbon nanotubes composite modified electrode, *Biosens.Bioelectron.*, 24(6):1751-1756 pp.
- Meredith, M.T., Giround, F. and Minteer, S.D.,** 2012, Azine/hydrogel/nanotube composite-modified electrodes for NADH catalysis and enzyme immobilization, *Electrochim. Acta*, 72:207-214 pp.
- Miyake, T., Oike, M., Yoshino, S., Yatagawa, Y., Haneda, K., Kaji, H. and Nishizawa, M.,** 2009, Biofuel cell anode: NAD⁺/glucose dehydrogenase-coimmobilized ketjenblack electrode, *Chem. Phys. Lett.*, 480(1-3):123-126 pp.
- Moiroux, J. and Elving, P. J.,** 1978, Effect of adsorbtion, electrode material, operational variables on the oxidation dihydronicotinamide adenine dinucleotide at carbon electrodes, *Anal. Chem.*, 50(8):1056-1062 pp.
- Moses, P.R., Wier, L. and Murray, R.W.,** 1975, Chemically modified tin oxide electrode, *Anal. Chem.*, 47(12):1882-1886.
- Mousty, C.,** 2004, Sensors and biosensors based on clay-modified electrodes-new trends, *Applied Clay Science*, 27(3-4):159-177 pp.
- Mousty, C.,** 2010, Biosensing applications of clay-modified electrodes: A Review, *Anal. Bioanal. Chem.*, 396(1):315-325 pp.
- Mu, S., Zhang, Y. and Zhai, J.,** 2009, Electrocatalysis of NADH oxidation by nanostructured poly(aniline-co-2-amino-4-hydroxybenzenesulfonic acid) and experimental evidence for the catalytic mechanism, *Electrochem. Commun.*, 11:1960-1963 pp.
- Munteanu, F.D., Okamoto, Y. and Gorton, L.,** 2003, Electrochemical and catalytic investigation of carbon paste modified with toluidine blue O covalently immobilised on silica gel, *Anal. Chim. Acta*, 476:43-54 pp.
- Munteanu, F.D., Mano, N., Kuhn, A. and Gorton, L.,** 2004, NADH electrooxidation using carbon paste electrodes modified with nitrofluorenone derivatives immobilized on zirconium phosphate, *J. Electroanal.Chem.*, 564(1-2):167-178 pp.

REFERENCES (continued)

- Murray, R.W., Ewing, A.G. and Durst, R.A., 1987**, Chemically modified electrodes molecular design for electroanalysis, *Anal. Chem.*, 59(5):379A-390A pp.
- Nassef, H.M., Radi, A-E. and Q'Sullivan, C.K., 2006**, Electrocatalytic sensing of NADH on a glassy carbon electrode modified with electrografted o-aminophenol film, *Electrochem. Commun.*, 8:1719-1725 pp.
- Navratilova, Z. and Kula, P., 2003**, Clay modified electrodes: Present applications and prospects, *Electroanalysis*, 15(10):837-846 pp.
- Nesakumar, N., Sethuraman, S., Krishnan, U.M. and Rayappan J.B.B., 2013**, Fabrication of lactate biosensor based on lactate dehydrogenase immobilized on cerium oxide nanoparticles, *J. Colloid Interf. Sci.*, 410:158-164 pp.
- Nesakumar, N., Thandavan, K., Sethuraman, S., Krishnan, U.M. and Rayappan J.B.B., 2014**, An electrochemical biosensor with nanointerface for lactate detection based on lactate dehydrogenase immobilized on zinc oxide nanorods, *J. Colloid Interf. Sci.*, 414:90-96 pp.
- Pariente, F., Tobalina, F., Darder, M., Lorenzo, E. and Abruna, H.D., 1996**, Electrodeposition of redox-active films of dihydroxybenzaldehydes and related analogs and their electrocatalytic activity toward NADH oxidation, *Anal. Chem.*, 68(18):3135-3142 pp.
- Pariente, F., Tobalina, F., Moreno, G., Hernandez, L., Lorenzo, E. and Abruna, H.D., 1997**, Mechanistic studies of the electrocatalytic oxidation of NADH and ascorbate at glassy carbon electrodes modified with electrodeposited films derived from 3,4-dihydroxybenzaldehyde, *Anal. Chem.*, 69(19):4065-4075 pp.
- Parikh, A., Patel, K., Patel, C. and Patel B.N., 2010**, Flow injection: A new approach in analysis, *J. Chem. Pharm. Res.*, 2(2):118-125 pp.
- Pelzmann, B., Hallström, S. and Koidl, B., 2003**, NADH supplementation decreases pinacidil-primed I K ATP in ventricular cardiomyocytes by increasing intracellular ATP. *Br. J. Pharmacol.*, 139 (4):749-754 pp.
- Pereira, A.C., Macedo, D.V., Santos, A.S. and Kubota, L.T., 2006**, Amperometric biosensor for lactate based on Meldola's blue adsorbed on silica gel modified with niobium oxide, *Electroanalysis*, 18:1208-1214 pp.

REFERENCES (continued)

- Pessoa, C.A., Gushikem, Y., Kubota, L.T. and Gorton, L.,** 1997, Preliminary electrochemical study of phenothiazines and phenoxazines immobilized on zirconium phosphate, *J. Electroanal. Chem.*, 431:23-27 pp.
- Piano, M., Serban, S., Biddle, N., Pittson, R., Drago, G.A. and Hart, J.P.,** 2010a, A flow injection system, comprising a biosensor based on a screen-printed carbon electrode containing Meldola's Blue-Reinecke salt coated with glucose dehydrogenase, for the measurement of glucose, *Anal. Biochem.*, 396(2):269-274 pp.
- Piano, M., Serban, S., Pittson, R., Drago, G.A. and Hart, J.P.,** 2010b, Amperometric lactate biosensor for flow injection analysis based on a screen-printed carbon electrode containing Meldola's Blue-Reinecke salt, coated with lactate dehydrogenase and NAD(+), *Talanta*, 82(1):34-37 pp.
- Pinczewska, A., Sosna, M., Bloodworth, S., Kilburn J.D. and Bartlett, P.N.,** 2012, High-throughput synthesis and electrochemical screening of a library of modified electrodes for NADH oxidation, *J. Am. Chem. Soc.*, 134(43):18022-18033 pp.
- Pollak, N., Dölle, C. and Ziegler, M.,** 2007, The power to reduce: pyridine nucleotides-small molecules with a multitude of functions, *Biochem. J.*, 402(2):205-218 pp.
- Popescu, I.C., Dominguez, E., Narvaez, A., Pavlov, V. and Katakis, I.,** 1999, Electrocatalytic oxidation of NADH at graphite electrodes modified with osmium phenanthroline-dione, *J. Electroanal. Chem.*, 464(2):208-214 pp.
- Prieto-Simon, B., Macanas, J., Munoz, M. and Fabregas, E.,** 2007, Evaluation of different mediator-modified screen-printed electrodes used in a flow system as amperometric sensors for NADH, *Talanta*, 71(5):2102-2107 pp.
- Qi, B., Peng, X., Fang, J. and Guo, L.,** 2009, Ordered mesoporous carbon functionalized with polythionine for electrocatalytic application, *Electroanalysis*, 21:875-880 pp.
- Qin, X., Xiang-Ya, H. and Shi-Rong, H.,** 2011, Electrochemical sensors based on electropolymerized films: electropolymerization, Dr. Ewa Schab Balcerzak (Ed.) ISBN: 978-953-307-693-5, In-Tech.
- Radoi, A. and Compagnone, D.,** 2009, Recent advances in NADH electrochemical sensing design, *Bioelectrochem.*, 76(1-2):126-134 pp.

REFERENCES (continued)

- Raj, C.R., Gobi, K.V. and Ohsaka, T.,** 2000, Electrocatalytic oxidation of NADH at the self-assembled monolayer of nickel II macrocycle on gold electrode, *Bioelectrochem.*, 51:181–186 pp.
- Ramesh, P., Sivakumar, P. and Sampath, S.,** 2003, Phenoxazine functionalized, exfoliated graphite based electrodes for NADH oxidation and ethanol biosensing, *Electroanalysis*, 15:1850-1858 pp.
- Ramirez-Molina, C., Boujtita, M. and El Murr, N.,** 2003, New strategy for dehydrogenase amperometric biosensors using surfactant to enhance the sensitivity of diaphorase/ferrocene modified carbon paste electrodes for electrocatalytic oxidation of NADH, *Electroanalysis*, 15(13):1095-1100 pp.
- Ren, X., Chen, D., Meng, X., Tang, F., Hou, X., Han, D. and Zhang, L.,** 2009, Zinc oxide nanoparticles/glucose oxidase photoelectrochemical system for the fabrication of biosensor, *J. Colloid Interf. Sci.*, 334(2):183-187 pp.
- Ricci, F., Amine, A., Moscone, D. and Palleschi, G.,** 2007, A probe for NADH and H₂O₂ amperometric detection at low applied potential for oxidase and dehydrogenase based biosensor applications, *Biosens. Bioelectron.*, 22(6):854-862 pp.
- Rotariu, L., Istrate, O-M. and Bala, C.,** 2014, Poly(allylamine hydrochloride) modified screen-printed carbon electrode for sensitive and selective detection of NADH, *Sens. Actuators B: Chem.*, 191:491-497 pp.
- Ruzicka, J. and Hansen, E.H.,** 1975, Flow injection analysis. Part I. A new concept of fast continuous flow analysis, *Anal. Chim. Acta*, 78:145-14 pp.
- Ruzicka, J. and Hansen, E.H.,** 1988, Flow Injection Analysis, Second Edition, *John Wiley&Sons*, 62:15-86 pp.
- Ruzicka, J. and Hansen, E.H.,** 2000, Peer reviewed: flow injection analysis: from beaker to microfluidics, *Anal. Chem.* 72 (5):212A-217A pp.
- Ryu, K., McEldoon, J.P., Pokora, A.R., Cyrus, W. and Dordick, J.,** 1993, Numerical and Monte Carlo simulations of phenolic polymerizations catalyzed by peroxidase, *Biotechnol. Bioeng.*, 42:807-814 pp.
- Saleh, F.S., Rahman, M.R., Kitamura, F., Okajima, T., Mao, L.Q. and Ohsaka, T.,** 2011, A Simple and effective way to integrate Nile blue covalently onto functionalized SWCNTs modified GC electrodes for sensitive and selective electroanalysis of NADH, *Electroanalysis*, 23(2):409-416 pp.

REFERENCES (continued)

- Salimi, A., Hallaj, R. and Ghadermazi, M.,** 2005, Modification of carbon ceramic electrode prepared with sol-gel technique by a thin film of chlorogenic acid: application to amperometric detection of NADH, *Talanta*, 65(4):888-894 pp.
- Samide, A., Tutunaru, B., Bratulescu, G. and Ionescu, C.,** 2013, Electrochemical synthesis and characterization of new electrodes based on poly-hematoxylin films, *J. Appl. Polymer Sci.*, 130(1):687-697 pp.
- Santiago, M.B., Velez, M.M., Borrero, S., Diaz, A., Casillas, C.A., Hofmann, C., Guadalupe, A.R. and Colon, J.L.,** 2006, NADH electrooxidation using bis(1,10-phenanthroline-5,6-dione) (2,2'-bipyridine) ruthenium(II)-exchanged zirconium phosphate modified carbon paste electrodes, *Electroanalysis*, 18(6):559-572 pp.
- Santos, A.S., Gorton, L. and Kubota, L.T.,** 2002a, Nile blue adsorbed onto silica gel modified with niobium oxide for electrocatalytic oxidation of NADH, *Electrochim. Acta*, 47:3351-3360 pp.
- Santos, A.S., Gorton, L. and Kubota, L.,** 2002b, Electrocatalytic NADH oxidation using an electrode based on Meldola blue immobilized on silica coated with niobium oxide, *Electroanalysis*, 14:805-812 pp.
- Santos, A.S., Freire, R.S. and Kubota, L.T.,** 2003, Highly stable amperometric biosensor for ethanol based on Meldola's blue adsorbed on silica gel modified with niobium oxide, *J. Electroanal. Chem.*, 547:135-142 pp.
- Santos, A.S., Pereira, A.C., Duran, N., Kubota, L.T.,** 2006, Amperometric biosensor for ethanol based on co-immobilization of alcohol dehydrogenase and meldola's blue on multi-wall carbon nanotube, *Electrochim. Acta*, 52:215-220 pp.
- Schubert, K., Khalid, W., Yue, Z., Parak, W.J. and Lisdat, F.,** 2010, Quantum-Dot-modified electrode in combination with NADH-dependent dehydrogenase reactions for substrate analysis, *Langmuir*, 26(2):1395-1400 pp.
- Sha, Y.F., Gao, Q., Qi, B. and Yang, X.R.,** 2004, Electropolymerization of azure B on a screen-printed carbon electrode and its application to the determination of NADH in a flow injection analysis system, *Microchim. Acta*, 148(3-4):335-341 pp.

REFERENCES (continued)

- Sharifi, E., Salimi, A. and Shams, E.,** 2013, Electrocatalytic activity of nickel oxide nanoparticles as mediatorless system for NADH and ethanol sensing at physiological pH solution, *Biosens. Bioelectron.*, 45:260-266 pp.
- Shi, H., Zhao, G., Liu, M. and Zhu, Z.,** 2011, A novel photoelectrochemical sensor based on molecularly imprinted polymer modified TiO₂ nanotubes and its highly selective detection of 2,4-dichlorophenoxyacetic acid, *Electrochem. Commun.* 13(12):1404-1407 pp.
- Silber, A., Hampp, N. and Schuhmann, W.,** 1996, Poly(methylene blue)-modified thick film gold electrodes for the electrocatalytic oxidation of NADH and their application in glucose biosensors, *Biosens. Bioelectron.* 11:215-223 pp.
- Silva Luz R.C., Damos, F.S. and Atsushi, A.,** 2008, Electrocatalytic activity of 2,3,5,6-tetrachloro-1,4-benzoquinone/multi-walled carbon nanotubes immobilized on edge plane pyrolytic graphite electrode for NADH oxidation, *Electrochim. Acta*, 53:4706–4714 pp.
- Simon, E. and Bartlett, P.N.,** 2003, Biomolecular Films, Design, Function and Applications. Ed: Rusling, J.F., Marcel Dekker, New York, 499p.
- Smyth, M.R. and Vos, J.G.,** 1992, Analytical Voltammetry, *Elsevier*, 27: 1st Edition.
- Sun, J., Zhu, Y., Yang, X. And Li, C.,** 2009, Photoelectrochemical glucose biosensor incorporating CdS nanoparticles, *Particuology*, 7(5):347-352 pp.
- Teymourian, H., Salimi, A. and Hallaj, R.,** 2012, Low potential detection of NADH based on Fe₃O₄ nanoparticles/multiwalled carbon nanotubes composite: Fabrication of integrated dehydrogenase-based lactate biosensor, *Biosens. Bioelectron.*, 33(1):60-68 pp.
- Thevenot, D.R., Toth, K., Durst, R.A. and Wilson, G.S.,** 2001, Electrochemical biosensors:Recommended definitions and classification, *Anal. Lett.*, 34:635-659 pp.
- Tiwari, I. and Gupta, M.,** 2014, Neutral red interlinked gold nanoparticles/multiwalled carbon nanotubes hybrid nanomaterial and its application for the detection of NADH, *Materials Research Bulletin*, 49:94-101 pp.

REFERENCES (continued)

- Tse, D.C.S. and Kuwana, T.**, 1978, Electrocatalysis of dihydronicotinamid adenosine diphosphate with quinones and modified quinone electrode, *Anal. Chem.*, 50:1315-1318 pp.
- Tu, X., Xie, Q., Huang, Z., Yang, Q. and Yao, S.**, 2007, Synthesis and characterization of novel quinone-amine polymer/carbon nanotubes composite for sensitive electrocatalytic detection of NADH, *Electroanalysis*, 19(17):1815-1821 pp.
- Tzang, C.H., Yuan, R., and Yang, M.**, 2001, Voltammetric biosensors for the determination of formate and glucose-6-phosphate based on the measurement of dehydrogenase-generated NADH and NADPH, *Biosens. Bioelectron.*, 16(3): 211–219 pp.
- Unden, G. and Bongaerts, J.**, 1997, Alternative respiratory pathways of *Escherichia coli*: energetics and transcriptional regulation in response to electron acceptors, *Biochim. Biophys. Acta*, 1320(3):217–234 pp.
- Van Staden, J.F. and Van Staden, R.I.C.**, 2012, Flow-injection analysis systems with different detection devices and other related techniques for the in vitro and in vivo determination of dopamine as neurotransmitter. A review, *Talanta*, 102:34-43 pp.
- Vasantha, V.S. and Chen, S-H.**, 2006, Synergistic effect of a catechin-immobilized poly(3,4-ethylenedioxythiophene)-modified electrode on electrocatalysis of NADH in the presence of ascorbic acid and uric acid, *Electrochim. Acta*, 52:665-674 pp.
- Vasilescu, A., Andreescu, S., Bala, C., Litescu, S.C., Noguer, T. and Marty, J-L.**, 2003a, Screen-printed electrodes with electropolymerized meldola blue as versatile detectors in biosensors, *Biosens. Bioelectron.*, 18:781-790 pp.
- Vasilescu, A., Noguer, T., Andreescu, S., Calas-Blanchard, C., Bala, C. and Marty, J-L.**, 2003b, Strategies for developing NADH detectors based on Meldola Blue and screen-printed electrodes: a comparative study, *Talanta*, 59:751-765 pp.
- Villamil, M.J.F., Ordieres, A.J.M. and Blanco, P.T.**, 1997, Immobilized enzyme electrode for the determination of L-lactate in food samples, *Anal. Chim. Acta*, 345:37-43 pp.

REFERENCES (continued)

- Walcarius, A.**, 1998, Analytical applications of silica-modified electrodes, A comprehensive review, *Electroanalysis*, 10(18):1217-1235 pp.
- Walcarius, A.**, 1999, Zeolite-modified electrodes in electroanalytical chemistry, *Anal. Chim. Acta*, 384(1):1-16 pp.
- Wang, E., Ji, H. and Hou, W.**, 1991, The use of chemically modified electrodes for liquid chromatography and flow-injection analysis, *Electroanalysis*, 3(1):1-11 pp.
- Wang, J.**, 2006, Analytical Electrochemistry, Third Edition, *John Wiley&Sons*, New York.
- Wang, G.L., Xu, J.J. and Chen H.Y.**, 2009a, Dopamine sensitized nanoporous TiO₂ film on electrodes: photoelectrochemical sensing of NADH under visible irradiation, *Biosens. Bioelectron.*, 24(8):2494-2498 pp.
- Wang, G.L., Xu, J.J. and Chen, H.Y.** 2009b, Progress in the studies on photoelectrochemical sensors, *Sci. China Ser. B-Chem.*, 52:1789-1800 pp.
- Wang, K., Wu, j., Liu, Q., Jin, Y., Yan, J., Cai, J.**, 2012a, Ultrasensitive photoelectrochemical sensing of nicotinamide adenine dinucleotide based on graphene-TiO₂ nanohybrids under visible irradiation, *Anal. Chim. Acta*, 745:131-136 pp.
- Wang, W., Bao, L., Lei, J., Tu, W. and Ju, H.**, 2012b, Visible light induced photoelectrochemical biosensing based on oxygen-sensitive quantum dots, *Anal. Chim. Acta*, 744:33-38 pp.
- Wang, P., Dai, W., Ge, L., Yan, M., Ge, S., Yu, J.**, 2013a, Visible light photoelectrochemical sensor based on Au nanoparticles and molecularly imprinted poly(o-phenylenediamine)-modified TiO₂ nanotubes for specific and sensitive detection chlorpyrifos, *Analyst*, 138(3):939-945 pp.
- Wang, Z., Etienne, M., Urbanova, V., Kohring, G.-W. and Walcarius, A.**, 2013b, Reagentless D-sorbitol biosensor based on D-sorbitol dehydrogenase immobilized in a sol-gel carbon nanotubes-poly(methylene green) composite, *Anal. Bioanal. Chem.*, 405(11):3899-3906 pp.
- Windholz, M.**, 1983, The Merck Index: An Encyclopedia of chemicals, drugs, and biologicals (10th ed.), Rahway, N.J., US:Merck. 909p.

REFERENCES (continued)

- Wring, S.A. and Hart, J.P.**, 1992, Chemically modified, carbon-based electrodes and their application as electrochemical sensors for the analysis of biologically important compounds - A review, *Analyst*, 117(8):1215-1229 pp.
- Wu, Q., Maskus, M., Pariente, F., Tobalina, F., Fernandez, V.M., Lorenzo, E. and Abruna, H.D.**, 1996, Electrocatalytic oxidation of NADH at glassy carbon electrodes modified with transition metal complexes containing 1,10-phenanthroline-5,6-dione ligands, *Anal. Chem.*, 68(20):3688-3696 pp.
- Yamaguchi, T., Komura, T., Hayashi, S., Asano, M., Niu, G.Y. and Takahashi, K.**, 2006, Electrocatalytic activity of electropolymerized Meldola's blue toward oxidation of dopamine, *Electrochemistry*, 74 (1):32-41 pp.
- Yan, Y.M., Yehezkeli, O. and Willner, I.**, 2007, Integrated, electrically contacted NAD(P)⁺-dependent enzyme-carbon nanotube electrodes for biosensors and biofuel cell applications, *Chem. Eur. J.*, 13:10168-10175 pp.
- Yang, D.W. and Liu, H.H.**, 2009, Poly(brilliant cresyl blue)-carbonnanotube modified electrodes for determination of NADH and fabrication of ethanol dehydrogenase-based biosensor, *Biosens. Bioelectron.*, 25(4):733-738 pp.
- Yogeswaran, U. and Chen S. M.**, 2008, Recent trends in the application of carbon nanotubes-polymer composite modified electrodes for biosensors: A Review, *Anal. Lett.*, 41(2):210-243 pp.
- You, JM. and Jeon, S.**, 2011, Electrocatalytic oxidation of NADH on a glassy carbon electrode modified with MWCNT-Pd nanoparticles and poly 3,4-ethylenedioxyppyrole, *Electrochim. Acta*, 56(27):10077-10082 pp.
- Zaitseva, G., Gushikem, Y., Ribeiro, E.S. and Rosatto, S.S.**, 2002, Electrochemical property of methylene blue redox dye immobilized on porous silica-zirconia-antimonia mixed oxide, *Electrochim. Acta*, 47:1469-1474 pp.
- Zare, HR. and Golabi, SM.**, 1999, Electrocatalytic oxidation of reduced nicotinamide adenine dinucleotide (NADH) at a chlorogenic acid modified glassy carbon electrode, *J. Electroanal. Chem.*, 464(1):14-23 pp.
- Zare, HR. and Golabi, SM.**, 2000, Caffeic acid modified glassy carbon electrode for electrocatalytic oxidation of reduced nicotinamide adenine dinucleotide (NADH), *J. Solid State Electrochem.*, 4(2):87-94 pp.

REFERENCES (continued)

- Zare, H.R., Nasirizadeh, N., Ardakani, M.M. and Namazian, M.,** 2006a, Electrochemical properties and electrocatalytic activity of hematoxylin modified carbon paste electrode toward the oxidation of reduced nicotinamide adenine dinucleotide (NADH), *Sens. Actuators B: Chem.*, 120(1):288-294 pp.
- Zare, H.R., Nasirizadeh, N., Golabi, S.M., Namazian, M., Ardakani, M.M. and Nematollahi, D.,** 2006b, Electrochemical evaluation of coumestan modified carbon paste electrode: Study on its application as a NADH biosensor in presence of uric acid, *Sens. Actuators B: Chem.*, 114(2):610-617 pp.
- Zare, H.R., Samimi, R., Nasirizadeh, N. and Mazloum-Ardakani, M.,** 2010, Preparation and electrochemical application of rutin biosensor for differential pulse voltammetric determination of NADH in the presence of acetaminophen, *J. Serbian Chem. Soc.*, 75(10):1421-1434 pp.
- Zen, J.M., Kumar, A.S. and Tsai, D.,** 2003, Recent updates of chemically modified electrodes in analytical chemistry, *Electroanalysis*, 15(13):1073-1087 pp.
- Zeng, J., Wei, W., Wu, L., Liu, X., Liu, K. and Li, Y.,** 2006, Fabrication of poly(toluidine blue O)/carbon nanotube composite nanowires and its stable low-potential detection of NADH, *J. Electroanal. Chem.*, 595:152-160 pp.
- Zeng, Y.L., Huang, Y.F., Jiang, J.H., Zhang, X.B., Tang, C.R., Shen, G.L. and Yu, R.Q.,** 2007, Functionalization of multi-walled carbon nanotubes with poly(amidoamine) dendrimer for mediator-free glucose biosensor, *Electrochem. Commun.*, 9:185-190 pp.
- Zhai, X., Li, Y., Liu, G., Cao, Y., Gao, H., Yue, C. and Sheng, N.,** 2013, Electropolymerized toluidine blue O functionalized ordered mesoporous carbon-ionic liquid gel-modified electrode and its low-potential detection of NADH, *Sens. Actuators B: Chem.*, 178:169-175 pp.
- Zhang, B., Guo, L.H. and Greenberg, M.M.,** 2012, Quantification of 8-OxidGuo lesions in double-stranded DNA using a photoelectrochemical DNA sensor, *Anal. Chem.*, 84(14):6048-6053 pp.
- Zhang, Z.X. and Zhao, C.Z.,** 2013, Progress of photoelectrochemical analysis and sensors, *Chin. J. Anal. Chem.*, 41(3):436-444 pp.

REFERENCES (continued)

- Zheng, M., Cui, Y., Li, X., Liu, S. and Tang, Z.,** 2011, Photoelectrochemical sensing of glucose based on quantum dot and enzyme nanocomposites, *J. Electroanal. Chem.*, 656(1-2):167-173 pp.
- Zhou, D-M., Fang, H-Q., Chen, H-Y., Ju, H-X. and Wang, Y.,** 1996, The electrochemical polymerization of methylene green and its electrocatalysis for the oxidation of NADH, *Anal. Chim. Acta*, 329:41-48 pp.
- Zhou, D-M., Sun, J-J., Chen, H-Y. and Fang, H-Q.,** 2008, Electrochemical polymerization of toluidine blue and its application for the amperometric determination of b-D-glucose, *Electrochim. Acta*, 43:1803-1809 pp.
- Zhu, L., Zhai, J., Yang, R., Tian, C. and Guo, L.,** 2007, Electrocatalytic oxidation of NADH with Meldola's blue functionalized carbon nanotubes electrodes, *Biosens. Bioelectron.*, 22:2768-2773 pp.
- Zhu, L., Yang, R., Jiang, X. and Yang, D.,** 2009, Amperometric determination of NADH at a Nile blue/ordered mesoporous carbon composite electrode, *Electrochem. Commun.*, 11(3):530-533 pp.

CIRRICULUM VITAE**Personal Details**

Name : Didem GİRAY DİLGİN
Date and Place of Birth : March 7th 1979, İzmir Turkey
Address : Çanakkale Onsekiz Mart Univ.
E-mail address : didemgiray79@hotmail.com
Nationality : Turkey
Civil Status : Married
Academic Degree : PhD

**Education**

PhD : Graduate School of Natural and Applied Sciences, Ege University, Turkey, 2014.
PhD thesis : Preparation and Applications of Modified Electrodes with Redox Mediators for Photoelectrocatalytic Systems
Master : Graduate School of Natural and Applied Sciences, Ege University, Turkey, 2004.
Master Thesis : Determination of heavy metal contents of UV digested vinegar samples by potentiometric stripping analysis.
Graduated : Faculty of Science, Department of Chemistry, Ege University, Turkey, 2000.

PUBLICATIONS

- 1 Dilgin, Y., Kizilkaya, B., **Dilgin, D.G.**, Gökçel, H.İ., Gorton, L.,
“Electrocatalytic oxidation of NADH using a pencil graphite electrode modified with quercetin” *Colloids and Surfaces B: Biointerfaces*, 102, (2013) 816-821.
- 2 Dilgin, Y., Ertek, B., Kizilkaya, B., **Dilgin, D.G.**, Gokcel, H.I.,
“Electrocatalytic Oxidation of NADH Using a Pencil Graphite Electrode Modified with Hematoxylin” *Science of Advanced Materials*, 4(9) (2012) 920-927.
- 3 Dilgin, Y., Kızılkaya B., Ertek, B., Işık, F., **Dilgin, D.G.**, “Electrocatalytic oxidation of sulphide using a pencil graphite electrode modified with hematoxylin” *Sensors and Actuators B: Chemical*, 171-172 (2012) 223-229.
- 4 Dilgin, Y., Kızılkaya, B., Ertek, B., Eren, N., **Dilgin, D.G.**, “Amperometric determination of sulfide based on its electrocatalytic oxidation at a pencil graphite electrode modified with quercetin” *Talanta*, 89 (2012) 490-495.
- 5 **Dilgin, D.G.**; Gligor, D., Gokcel, H.I., Dursun, Z., Dilgin, Y., “Glassy carbon electrode modified with poly-Neutral Red for photoelectrocatalytic oxidation of NADH” *Microchimica Acta*, 173 (2011) 469-476 (**from this thesis**).
- 6 Dilgin, Y., **Dilgin D.G.**, Dursun, Z., Gökçel, H.İ., Giligor, D., Bayrak, B., Ertek, B., “Photoelectrocatalytic Determination of NADH in a Flow Injection System with Electropolymerized Methylene Blue” *Electrochimica Acta*, 56 (2011) 1138-1143
- 7 **Dilgin D.G.**, Gligor D., Gökçel H.İ., Dursun Z., Dilgin Y., “Photoelectrocatalytic oxidation of NADH in a flow injection analysis system using a poly-hematoxylin modified glassy carbon electrode” *Biosensors & Bioelectronics*, 26(2): 411-417 (2010) (**from this thesis**).
- 8 Dilgin, Y., Koparir, M., Çetin, A., Cansız, A., Yilmaz, S., **Giray, D.**,
“Electrochemical Behaviour of 5-Benzyl-4-(4'-Methylphenyl)-4h-1,2,4-Triazole-3-Thiol By Voltammetry” *Journal of The Indian Chemical Society*, 84 1024-1025 (2007).
- 9 **Dilgin, D.G.**, Gökçel, H.İ. “Photoelectrochemical biosensing of glucose in flow injection analysis based on poly-hematoxyline mofied glassy carbon electrode coated with glucose dehydrogenase” will be submitted to *Biosensor and Bioelectronics* in 2014)

PAPERS PRESENTED AT MEETINGS AND SYMPOSIA (INTERNATIONAL)

- 1 Çakın, A., **Dilgin, D.G.**, “Dilgin, Y., “Electrocatalytic oxidation of NADH at poly-neutral red modified pencil graphite electrode” *10th International Electrochemistry Meeting in TURKEY*, 4-8 September 2013, page:139, Konya/TURKEY (Poster)
- 2 Dilgin, Y., Kizilkaya, B., **Dilgin, D.G.**, Gökçel, H.İ., Gorton, L., “Electrocatalytic Oxidation of NADH using a pencil graphite electrode modified with quercetin” *9th International Electrochemistry Meeting in TURKEY*, 25-29 September 2011, page:123, Çeşme İzmir/TURKEY(Poster).
- 3 Ertek, B., Eren, N., Dilgin, Y., Kizilkaya, B., **Dilgin, D.G.**, “Amperometric Determination of Sulphide depend on its electrocatalytic oxidation at apencil graphite electrode modified with quercetin, Electrocatalytic Oxidation of NADH using a pencil graphite electrode modified with quercetin” *9th International Electrochemistry Meeting in TURKEY*, 25-29 September 2011, page:124, Çeşme İzmir/TURKEY (Poster).
- 4 Bayrak B., Ertek B., **Dilgin D.G.**, Gökçel H.İ., Kızilkaya B., Dilgin Y., "Photoelectrocatalytic oxidation of NADH at a poly-methylene blue modified glassy carbon electrode" 8th International Electrochemistry Meeting, October 8-11, 2009 page:209, Side-Antalya/TURKEY (Poster).
- 5 **Dilgin D.G.**, Gökçel H.İ., Dursun Z., Dilgin Y., Gligor D.M., "Photoelectrocatalysis of NADH at a poly-neutral red/glassy carbon electrode" *8th International Electrochemistry Meeting*, October 8-11, 2009, page:47, Side-Antalya/TURKEY (Oral Presentation).
- 6 Dilgin, Y., Kaya, İ., **Giray, D.**, Gökçel, H.İ., Dursun, Z., “Electropolymerization of hematoxylin for electrocatalytic oxidation of NADH” *6th Aegean Analytical Chemistry Days*, 9-12 October 2008, Denizli-TURKEY (Poster).

PAPERS PRESENTED AT MEETINGS AND SYMPOSIA (NATIONAL)

- 1 **Dilgin D.G.**, Gökçel H.İ., Ertek E., Dilgin Y., “The construction of biosensor depend on NADH by using electrodes modified with azin type dyes” *I. National Chemistry Student Congress*, Uludağ University, 7-10 April 2010 Bursa/TURKEY (Oral presentation).
- 2 **Dilgin D.G.**, Ertek E., Dönmez E., Bayrak, B., Gökçel H.İ., Dursun Z., Dilgin Y., “Photoelectrocatalytic oxidation of NADH using methylene green modified glassy carbon electrode” *I. National Chemistry Student Congress*, Uludağ University, 7-10 April 2010 Bursa/TURKEY (Poster).
- 3 Dilgin, Y., **Giray, D.**, Gligor, D., Gorton, L., “Photoelectrocatalytic oxidation of NADH with modified electrodes” *4th National Analytical Chemistry Congress*, 25-27 June 2008 Elazığ/TURKEY (Oral presentation).
- 4 Gökçel, H.İ., Ertaş, F.N., **Giray, D.**, Tural, H., “Heavy Metal Analysis in Vinegar decomposed with Uv using potentiometric stripping technique” *19th National Chemistry Congress*, 30th September- 4th October 2005 Kuşadası/TURKEY (Poster).

APPENDICES

Appendix 1 Data for Figure 3.2A, B, C and D

Appendix 2 Data for Figure 3.13B and C

Appendix 3 Data for Figure 3.28

Appendix 4 Data for Figure 3.43

Appendix 5 Data for Figure 3.45

Appendix 6 Data for Figure 3.48

Some data obtained in the study were given in this section as a table according to figure number. However, only data for HT were presented because the biosensor studies were performed by using HT modified electrodes.

Appendix 1. Data for Figure 3.2A, B, C and D

3.2A		3.2B		3.2C		3.2D	
pH	Current* (μA)	Anodic upper potential (V)	Current* (μA)	Monomer concentration (mM)	Current* (μA)	Cycle number	Current* (μA)
2	7.0	0.50	5.0	0.10	7.2	3	5.8
3	7.5	0.75	5.6	0.20	7.8	5	7.7
4	7.8	1.00	3.8	0.30	8.3	8	8.4
5	8.0	1.25	2.5	0.40	8.2	10	8.3
6	8.1	1.50	2.4	0.50	8.1	15	8.2
7	8.3	1.75	5.7	0.75	8.2	20	8.2
8	8.3	2.00	8.9	1.00	8.2		
9	7.7	2.25	9.6				
10	7.5	2.50	10.0				

* : Electrocatalytic current for 0.8 mM NADH

Appendix 2. Data for Figure 3.13B and C

3.13B			3.13C	
Scan rate (mVs^{-1})	Anodic peak current (μA)	Catodic peak current (μA)	pH	Formal potential (mV)
50	1.3		2	505
100	2.8	-1.5	3	445
160	4.8	-2.8	4	385
200	6.5	-4.1	5	335
400	13.5	-10.0	6	255
640	21.7	-16.2	7	195
800	29.0	-19.7	8	150
1280	41.7	-32.7	9	110
1600	54.6	-47.4		
2560	80.1	-72.6		
3200	100.8	-86.8		

Appendix 3. Data for Figure 3.28

Concentration of NADH (μM)	Current for electrocatalytic oxidation (nA)	
	Without irradiation	With irradiation
0.2	3	4
0.4	6	8
0.6	8	11
0.8	12	18
1	16	24
2	32	47
4	64	92
6	94	136
8	131	187
10	156	221
20	298	408
40	596	857
60	799	1212
80	1011	1621
100	1316	2140
150	1700	2980
200	1870	3620
250	2122	4536
300	2306	4880
400	2586	5602
600	3091	6990
800	3435	7973
1000	3590	8590

Appendix 4. Data for Figure 3.43

Applied Potential	Current (nA) for 0.8 mM glucose	
	Without irradiation	With irradiation
0	17	110
50	19	140
100	48	180
150	83	220
200	120	260
250	155	300
300	190	360
400	240	440
500	290	450
600	270	470

Appendix 5. Data for Figure 3.45

Flow rate (mL min ⁻¹)	Current (nA) for 0.8 mM glucose	
	Without irradiation	With irradiation
0.125	427	1255
0.25	332	978
0.45	282	700
0.6	248	540
0.8	235	437
1.0	231	378
1.1	225	346
1.2	211	312
1.4	208	280
1.5	204	260
1.8	195	237
2.0	180	200
2.2	170	180

Appendix 6. Data for Figure 3.48

Glucose concentration (mM)	Current (μA)	
	Without irradiation	With irradiation
0.005	-	0.007
0.01	0.007	0.03
0.05	0.04	0.11
0.1	0.09	0.22
0.3	0.23	0.52
0.5	0.36	0.95
0.8	0.65	1.55
1.0	0.75	1.90
2.0	1.26	2.70
3.0	1.73	3.20
5.0	2.27	3.90
8.0	2.60	4.30
10.0	2.78	4.50